TECHNISCHE UNIVERSITÄT MÜNCHEN
Lehrstuhl für Proteomik und Bioanalytik

Identifying small molecule probes for kinases by chemical proteomics

Maria Reinecke

Vollständiger Abdruck der von der Fakultät Wissenschaftszentrum Weihenstephan für Ernährung, Landnutzung und Umwelt der Technischen Universität München zur Erlangung des akademischen Grades eines

Doktors der Naturwissenschaften

genehmigten Dissertation.

Vorsitzende:	Prof. Angelika Schnieke, Ph.D.
Prüfer der Dissertation:	1. Prof. Dr. Bernhard Küster 2. Prof. Dr. Stefan Knapp 3. apl. Prof. Dr. Philipp J. Jost

Die Dissertation wurde am 20.04.2020 bei der Technischen Universität München eingereicht und durch die Fakultät Wissenschaftszentrum Weihenstephan für Ernährung, Landnutzung und Umwelt am 05.08.2020 angenommen.

Abstract

Protein and lipid kinases are involved in almost every cellular signalling pathway, and alterations in their catalytic activity largely affect cellular homeostasis which can lead to the development of human diseases. Over the past two decades thousands of small molecule kinase inhibitors have been developed to target aberrant activated kinases. The majority of such compounds target the ATP binding pocket of the kinase domain which is highly conserved, rendering the development of selective compounds challenging. Hence, thorough evaluation of the target space of small molecule kinase inhibitors is essential to fully understand a drug's mode of action and to evaluate potential application areas. Small molecule kinase inhibitors can be used either for medical applications as molecular targeting agents or in basic research as chemical probes to investigate the cellular function of a certain kinase. Despite the high value of kinase inhibitors, a large part of the human kinome still lacks highly selective inhibitors. Here, a chemical proteomic approach (Kinobeads) was harnessed to elucidate the target space of over 1,200 kinase inhibitors in order to identify potential new chemical probes and to shed light on their mechanisms of action.

Initially, a new Kinobeads matrix was developed that extended the kinome coverage to phosphatidylinositol 3-kinases (PI3Ks) and PI3K-related kinases (PIKKs). Together with an optimized cell lysate mixture, more than 300 kinases are now accessible for Kinobeads selectivity profiling. In addition, optimization of the experimental workflow and the mass spectrometric measurement method led to a drastic reduction of sample preparation and data acquisition time enabling large scale selectivity profiling of more than thousand small molecule kinase inhibitors.

Following the method optimization, the target landscape of 1,232 tool compounds (published kinase inhibitor set (PKIS), PKIS2, kinase chemogenomic set and Roche library) were determined to find new selective kinase inhibitors and compounds for the hitherto undruggable kinome. Several hundred new potential chemical probes were found that target 73 different kinases, many of which were missing a chemical probe. Examples of highly selective inhibitors for the kinases CK2 and SYK were further validated with functional assays. Moreover, compounds targeting the understudied kinase PKN3 were discovered and utilized for functional phosphoproteomic studies to identify potential downstream substrates of PKN3. Overall, the generated dataset proved to be a valuable resource for drug discovery in order to find new chemical probes.

In addition, the Kinobeads technology was used to survey 55 clinical kinases inhibitors for their target space. Here, the selectivity of the panel ranged from broad spectrum kinase inhibitors to highly selective inhibitors. Special emphasis was put on the profiling of clinical mTOR and PI3K inhibitors which was made possible by the new Kinobeads affinity matrix. Selectivity profiling revealed an interesting off-target (DCK) of the designated mTOR inhibitor TG100-115. In addition, an adapted Kinobeads workflow enabled distinguishing between reversible and irreversible off-targets of five covalent BTK inhibitors. Moreover, it was shown that ATP supplementation of the lysate prior to Kinobeads enrichment resulted in a shift of affinities for some kinases.

In summary, the presented work highlights the usability of chemical proteomics (Kinobeads) for elucidating the target space of kinase inhibitors, in order to discover new chemical probes. This thesis offers a large resource for the scientific community for further drug discovery and drug development.

Zusammenfassung

Protein- und Lipid-Kinasen sind an nahezu jedem zellulären Signalweg beteiligt. Eine abnormale katalytische Aktivität von Kinasen beeinflusst das zelluläre Gleichgewicht und kann zur Entstehung von Krankheiten führen. Innerhalb der letzten zwei Jahrzehnte wurden zahlreiche niedermolekulare Kinaseinhibitoren entwickelt, die Kinasen mit abnormaler Aktivität hemmen. Die meisten dieser Verbindungen zielen auf die strukturell konservierte ATP-Bindungstasche in der Kinasedomäne ab, so dass die Entwicklung selektiver Inhibitoren oft eine Herausforderung darstellt. Eine gründliche Charakterisierung des Zielraums von niedermolekularen Kinase-inhibitoren ist daher unerlässlich, um die Wirkungsweise eines Inhibitors vollständig zu verstehen. Kinaseinhibitoren können entweder für medizinische Anwendungen als zielgerichtete Medikamente oder in der Grundlagenforschung als chemische Sonden zur Untersuchung der zellulären Funktion einer Kinase eingesetzt werden. Obwohl Kinaseinhibitor sehr nützlich sind, fehlt einem großen Teil des menschlichen Kinoms noch immer ein hochselektiver Inhibitor. In dieser Arbeit wurde ein chemisch-proteomischer Ansatz (Kinobeads Methode) genutzt, um den Zielraum von über 1.200 Kinaseinhibitoren aufzuklären, damit neue chemische Sonden gefunden werden können und der Wirkmechanismus der Inhibitoren besser verstanden werden kann.

Zunächst wurde eine neue Kinobeads-Matrix entwickelt, die die Kinomabdeckung auf Phosphatidylinositol-3-Kinasen (PI3Ks) und PI3K-verwandte Kinasen (PIKKs) erweiterte. Zusammen mit einem optimierten Zelllysatgemisch können nun mehr als 300 Kinasen mit Kinobeads angereichert werden. Darüber hinaus führte die Optimierung des experimentellen Arbeitsablaufs und der massenspektrometrischen Messmethode zu einer drastischen Reduzierung der Probenpräparationszeit und der Datenerfassungszeit.

Im Anschluss an die Methodenoptimierung wurden die Zielproteine von 1.232 Verbindungen (aus: Published kinase inhibitor set (PKIS), PKIS2, kinase chemogenomic set und einer Roche-Bibliothek) bestimmt, um neue selektive Kinaseinhibitoren zu finden. Es wurden mehrere hundert neue selektive Inhibitoren gefunden, die 73 verschiedene Kinasen binden, wobei vielen von diesen ein hochselektiver Inhibitor fehlte. Beispiele für selektive Inhibitoren für die Kinasen CK2 und SYK wurden mit funktionalen Assays validiert. Darüber hinaus wurden Verbindungen für die wenig untersuchte Kinase PKN3 gefunden, welche für funktionelle Phosphoproteom-Experimente verwendet wurden, um nachgeschaltete Substrate von PKN3 zu identifizieren. Insgesamt ist der generierte Datensatz eine wertvolle Ressource, um neue chemische Sonden zu finden.

Darüber hinaus wurden mit der Kinobeads-Technologie 55 klinische Kinaseinhibitoren auf ihre Zielproteine hin untersucht. Dabei reichte die Selektivität der Inhibitoren von Breitspektrum-Kinaseinhibitoren bis hin zu hochselektiven Inhibitoren. Besonderes Augenmerk wurde auf die Profilierung der klinischen mTOR- und PI3K-Inhibitoren gelegt, was durch die neue Kinobeads-Affinitätsmatrix erst ermöglicht wurde. Die Selektivitätsprofilierung ergab ein interessantes bis dato unbekanntes Zielprotein (DCK) des designierten mTOR-Inhibitors TG100-115. Darüber hinaus ermöglichte ein angepasster Kinobeads Workflow die Unterscheidung zwischen reversiblen und irreversiblen Zielproteinen von fünf kovalenten BTK-Inhibitoren. Zusätzlich wurde gezeigt, dass die Zugabe von ATP zum Zelllysat vor der Kinobeads-Anreicherung zu einer Verschiebung der Affinitäten für einige Kinasen führte.

Zusammenfassend unterstreicht diese Arbeit, wie nützlich die chemische Proteomik für die Aufklärung der Zielproteine von Kinase-Inhibitoren ist, um damit neue chemische Sonden zu entdecken. Diese Arbeit bietet der wissenschaftlichen Gemeinschaft eine nützliche Ressource für die weitere Arnzneimittelentwicklung.

Table of contents

Introduction

Table of contents

1 Human Protein and Lipid Kinases

1.1 Kinases in Cellular Signaling

The human kinome. Human protein and lipid kinases are key players in nearly all aspects of cellular function and orchestrate the activity of almost all cellular processes. They are organized in signaling cascades and transmit external and internal stimuli to regulate growth, division, development and death of a cell by changing the activity of effector proteins and lipids.[1] Protein and lipid kinases are enzymes that catalyze the transfer of the terminal phosphate group of adenosine triphosphate (ATP) to a protein or lipid resulting in the formation of a phosphate ester linkage through a nucleophilic substitution reaction (Figure 1A).[2] During this process that is known as phosphorylation, the phosphoanhydride bond between the β- and γ-phosphate of ATP is cleaved and 8-12 kcal/mol of free energy is released which is the driving force of this reaction.[3]

Protein and lipid phosphorylation requires a tight interplay between kinases and phosphatases catalyzing dephosphorylation (Figure 1A) to enable a flexible and rapid response to diverse extra- and intracellular stimuli and to fine-tune cellular signaling networks.[4] Protein phosphorylation as a regulatory mechanism performed by protein kinases was first discovered by Krebs and Fischer in the late 1950s. The importance of phosphorylation in cellular signaling is reflected by the fact that around 2 % of the human genome encodes for kinases.[5] Due to its reversibility and versatility, protein phosphorylation is a key posttranslational modification that introduces a negative charge to a serine, threonine or tyrosine residue of a protein. This in turn can affect the conformation of a protein, alter protein activity and stability or modulate protein-protein interactions as well as sub-cellular localization.[3] As the name suggests, lipid kinases phosphorylate lipids in the plasma membrane and on the membranes of organelles, thereby changing their localization and reactivity.[6]

The first comprehensive study of all human kinases was done in 2002 by Manning and coworkers who identified 518 protein kinases and classified them into nine distinct groups according to their sequence similarity.[5] The absolute number of protein kinases in the human genome however is still under debate, since some kinases were recharacterized as member of another protein family and some phosphorylate non-protein substrates. In a recent publication, the super family of human kinases, also known as the human kinome, comprises 555 members that can be grouped into a main class of 497 eukaryotic protein kinases (ePKs) and, due to the lack of sequence similarity in a class of 58 atypical protein kinases (aPKs) that include the lipid kinases.[7] Despite the lack in sequence similarity, some of the atyptical kinases reveal structural similarities to ePK and share the prototypical ePK fold. Hence, 26 out of the 58 aPKs were further classified as protein kinase like (PKL).[8] The group of ePKs can be further subdivided into nine groups according to the sequence of their catalytic domain and their biological function: AGC family containing PKA PKG and PKC, calcium/calmodulin dependent kinase (CAMK), casein kinases 1 (CK1), a group of cyclin dependent kinases, MAP kinases, glycogen synthase kinase and casein kinase (CMGC), receptor guanylate cyclases (RGC), sterile 20 kinases (STE), tyrosine kinases (TK) and tyrosine kinase like (TKL) and others.[5,9]

Approximately 10 % of the protein kinases lack key catalytic residues and hence catalytic activity. These kinases, termed pseudokinases, can still have important regulatory functions like cell trafficking and allosteric regulation of other proteins as well as scaffolding functions.[10] Regardless of which class a kinase belongs to, almost all of them play a decisive role in cellular signal transduction. As an example of the way kinases forward external and internal stimuli via a complex signaling cascade to reach a cellular response, the PI3K/AKT/mTOR signaling pathway is described in more detail hereafter.

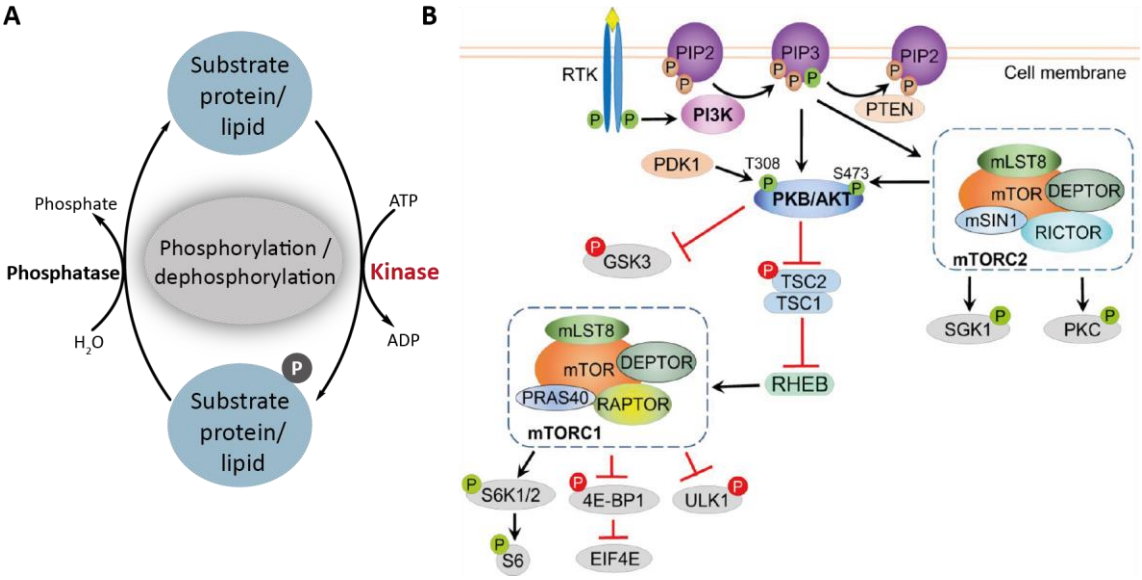

Figure 1 | Role of kinases in cellular signaling. (A) Schematic representation of phosphorylation. Proteins and lipids are phosphorylated by kinases under consumption of ATP. Dephosphorylation is carried out by phosphatases. (B) Schematic representation of the PI3K/AKT/mTOR signaling cascade. The signaling network with all nodes, activating and inhibiting interaction partners as well as downstream effectors are depicted. Red circles indicate inhibitory phosphorylation and green circles activating phosphorylation. Phosphorylation marked in brown is not induced by this signaling network. Adapted from Yu and Cui.[11]

The PI3K/AKT/mTOR pathway. The phosphatidylinositol-3-kinases (PI3K), the protein kinase B (PKB), also known as RAC-alpha serine/threonine-protein kinase (AKT), and the mammalian target of rapamycin (mTOR) are key players of the PI3K/AKT/mTOR signaling pathway.[11] PI3Ks belong to the family of lipid kinases and have the capability to phosphorylate phosphatidylinositol-(4,5)-bisphosphate (PIP_2) to phosphatidylinositol-(3,4,5)-triphosphate (PIP_3) (Figure 1B). The PI3K family can be divided into three subclasses of which class I, including the α-, β-, γ- and δ-isoforms, is the best studied class.[12] Through activation of receptor tyrosine kinases or G protein coupled receptors (GPCR) by external stimuli like growth factors such as EGF or insulin, PI3K is recruited to the membrane where it gets activated.[13,14] After phosphorylation of PIP_2, PIP_3 recruits AKT together with phosphoinositide-dependent kinase 1 (PDK1) and mTOR to the membrane. mTOR is part of the PI3K related kinase (PIKK) family[15] and forms two distinct complexes, mTORC1 and mTORC2, which can be distinguished by their composition, substrate specificity and sensitivity to rapamycin.[16] The complex phosphorylating AKT at the membrane is mTORC2 which consists of mTOR, DEP domain-containing mTOR-interacting protein (DEPTOR)[17], target of rapamycin complex subunit LST8 (mLST8)[18], stress-activated map kinase-interacting protein 1 (mSIN1)[19],

proline-rich protein 5 (PROTOR)[20] and the rapamycin insensitive companion of mTOR (RICTOR). Substrates of mTORC2 are AKT and SGK1.[16,21]

After recruitment to the membrane, AKT gets doubly phosphorylated at Thr-309 and Ser-473 by PDK1 and mTORC2, respectively.[11] The AKT kinase belongs to the AGC kinase family and after activation, mediates cell growth and cell survival by phosphorylation of several downstream proteins.[22] The main downstream effector protein complex of AKT is mTORC1 which consist of mTOR, DEPTOR[17], mLST8[18], Proline-rich AKT1 substrate (PRAS40, also known as AKT1S1)[23] and regulatory associated protein of mTOR (RAPTOR)[24]. The main substrates are the eukaryotic translation initiation factor 4E (eIF-4E) binding protein (4EBP1) and the ribosomal S6 kinase (S6K) which respectively phosphorylate the eukaryotic translation initiation factor 4E (eiF-4E) and ribosomal protein S6 (Figure 1 B). The PI3K/AKT/mTOR pathway regulates cell processes like cell proliferation, cell growth and cell metabolism.[11,14,25] The signaling cascade is antagonized at different steps by several proteins including the tumor suppressor phosphatase and tensin homolog (PTEN) which is able to dephosphorylate PIP_3 to PIP_2 and thereby leads to inactivation of AKT.[11]

1.2 Structure of Human Protein and Lipid Kinase Domains

Despite overall low sequence similarity, the structure of the catalytic domain is highly conserved between ePKs and aPKs, notably the PKL class, which was revealed by the first aPK X-ray crystallographic structure solved by Walker and coworkers in 1999.[26,27] Up to date, 268 ePK and 15 aPK X-ray structures have been solved giving an insight into the structure and the different conformational states of ePKs and aPKs.[7] The catalytic kinase domain is highly dynamic and flexible and allows the binding of ATP and the substrate in the active state.[28] During the process of phosphorylation the kinase domain switches between two different states, the active and the inactive conformation.[29] In between the two extreme states the kinase domain performs different movements which are together referred as kinase domain “breathing”.[30] The active conformation is highly conserved within the kinase family because they all catalyze the same reaction, while the inactive state can vary greatly between the different kinase classes.[29]

The basic structure of the kinase domain consists of two structurally different loops connected by a flexible hinge region (Figure 2). The N-lobe comprises five stranded β sheets and a prominent α helix also known as αC helix while the larger C-lobe comprises only α helices.[7] The ATP molecule and the substrate can bind in the cleft between these two lobes. Overall, the kinase domain features several conserved regions most of which are very flexible and can adopt different conformations. A key signature of every active kinase is the formation of a regulatory hydrophobic spine, known as R-spine which consists of four key residues (RS1-RS4). The four residues are the histidine in the HDR motif of the catalytic loop, the phenylalanine in the DFG motif of the activation loop and two aliphatic residues in the αC helix and the β4 strand.[31,32] The assembly of the R-spine, mediated by well-organized events, leads to an active conformation of the kinase.

The DFG (aspartic acid, phenylalanine, glycine) motif is a key player in the activation of the kinase. This conserved motif can rotate and flip between the DFG-in conformation that is characteristic for an active kinase (R-spine formation) and DFG-out conformation that is characteristic for an

inactive kinase (disordered R-spine). In the active state of the kinase, the aspartate is pointing towards the ATP binding pocket where it interacts with bound ATP while the phenylalanine orients towards the hydrophobic pocket which leads to R-spine formation.[9]

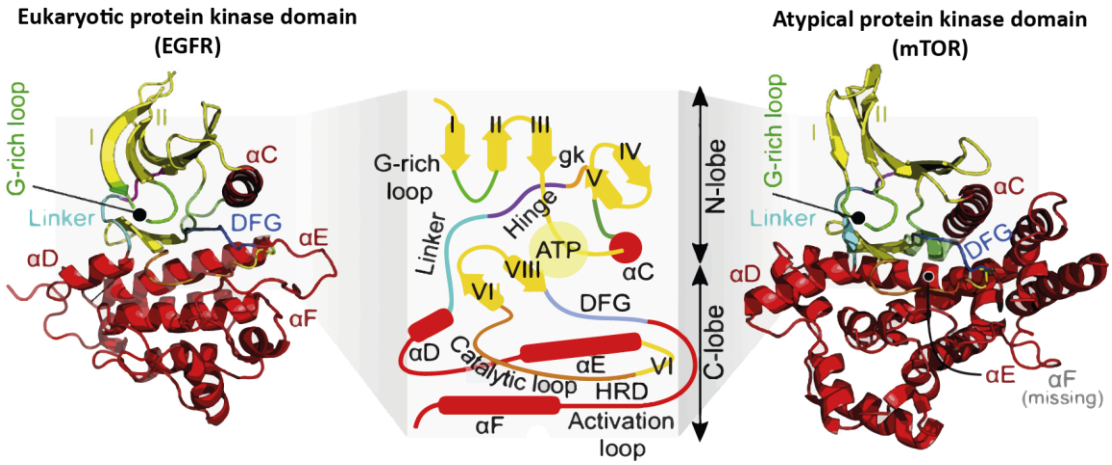

Figure 2 | Structure of eukaryotic protein kinase (ePK) domain and atypical protein kinase (aPK) domains. The ePK domain exemplified by EGFR (left panel) and aPK domain exemplified by mTOR (right panel) are structured into a N-lobe and C-lobe. Several catalytic motifs that are involved in the transfer of the γ-phosphate of ATP to the substrate are conserved between ePKs and aPKs (middle panel). Adapted with permission from Kanev *et al*.[7]

Many but not all kinases are activated upon phosphorylation of the activation loop which is a loop of 20-30 residues C-terminal of the DFG motif.[33] This leads to an interaction between the negatively charged phosphate in the activation loop and the positively charged arginine of the HRD (histidine, arginine, aspartate) motif in ePKs. The HRD motif is mirrored in aPKs (DRH) suggesting that the histidine rather than the aspartic acid serves as catalytic base.[7,34] Upon phosphorylation of the activation loop, ATP is able to bind in the cleft between the two lobes and sits next to a highly conserved loop that connects β1 and β2 sheets. This loop is known as G-rich loop as it contains a glycin rich motif (GxGxxG) that makes the loop very flexible. This motif allows the G-rich loop to approach the phosphate of ATP very closely to position ATP within the pocket.[29] The glycine rich motif of the G-rich loop is highly conserved within the ePKs while it is missing in the G-rich loop (often referred to as p-loop for aPKs) of aPKs.[7]

The G-rich loop also positions another conserved region in the kinase domain, the AxK motif, that forms a salt bridge with a glutamate in the αC helix in the active state and thus aligns ATP in the pocket.[30] After ATP binds, the catalytic spine (C-spine) is completed that consists of a series of hydrophobic residues positioned in the N-lobe and C-lobe and allows the two lobes to close.[31] For the enzymatic reaction to occur, the substrate has to bind to the kinase in close proximity to ATP. After the catalytic cycle has been completed ADP and the phosphorylated substrate are released.

In order to become fully active, some kinases are dependent on interaction partners. One prominent example are the cyclin dependent kinases (CDKs) which require the formation of a cyclin/CDK complex to establish a catalytically active ATP binding pocket.[35] While the binding sites are structurally highly conserved between ePKs and aPKS, regions outside the binding sites differ considerably as exemplified by absence of the αF-helix in most aPKs (Figure 2).[7]

1.3 Kinases in Human Diseases

Kinases are molecular switches whose catalytic activity is stringently regulated and tightly controlled.[36] Aberrant kinase activity caused by mutations, chromosomal rearrangements or gene amplification leads to altered phosphorylation states of cellular proteins which in turn alter signaling transduction.[37,38] Therefore kinases play a major role in various human pathologies like cancer[37], immunological[39], neurological[40] and inflammatory[39] diseases and over the last two decades have become one of the most important drug targets in pharmaceutical research.[38] For instance, the Janus kinase (JAK) - signal transducer and activator of transcription protein (STAT) pathway, the Burton tyrosine kinase (BTK)-spleen tyrosine kinase (SYK) pathway and the mitogen-activated protein kinase (MAPK) are associated with the development of autoimmune and inflammatory diseases.[39,41]

Especially in the field of cancer, kinases play a crucial role. Cancer is a group of proliferative human diseases with the capability to invade neighboring tissue and to spread over other parts of the body. During the development of cancer, the cancer cell can accumulate several malignant molecular features including abnormal kinase activity that have many diverse functions. However, the growth and survival of cancer cells can be dependent on the activation of a single critical oncogene responsible for the malignant phenotype.[42] This concept is known as “oncogene addiction” and provides the rational for molecular targeted therapy.[43] By inhibiting the activity of this single oncogene with antibodies or small molecules, the growth of cancer cells can be restrained and ideally the patient survival can be prolonged.[44] The first oncogene to be discovered was the Rous sarcoma virus transforming factor (v-Src) which was identified as a protein kinase.[45] Notorious kinase oncogenes comprise BRAF, which is often mutated (V600E mutation) in malignant melanoma[46], the oncogenic BCR-ABL fusion gene in chronic myeloid leukemia (CML)[47] and the PI3K family. Oncogenic mutations in the catalytic subunit of PIK3CA indeed are found in approximately 40 % of all breast cancers[48] while the PI3K/AKT/mTOR signaling pathway (see Introduction Chapter 1.1) is one of the most frequently dysregulated pathways in cancer. Besides PI3K, various other components of the signaling cascade like AKT[49] can be mutated and result in a radical disturbance in the control of cell growth and survival.[50]

Sustained cell growth and proliferation as well as resistance to cell death and activation of migration and invasion are only three of the six postulated hallmarks of cancer that can be caused by dysregulated kinase signaling.[51] Oncogenic kinase mutations and fusion proteins like BRAF V600E or BCR-ABL can be targeted by molecular targeting agents (MTA) like small molecules or antibodies. Next generation sequencing (NGS) enables the identification of such oncogenic kinase mutations in tumor samples from patients and open up the opportunity to treat the patient with an appropriate MTA that blocks the activity of mutated or dysregulated kinases. This allows patient to be treated more precisely and with ideally less side effect than standard chemotherapy. This concept is known as precision medicine and is quickly gaining popularity especially in the field of oncology.

2 Targeting Kinases with Small Molecules

Due to their pivotal role in cellular signalling, kinases play an essential role in nearly all disease areas (see Introduction Chapter 1). Therefore, targeting kinases with aberrant expression or activation has moved into the focus of drug discovery over the last two decades. With the raising popularity of targeted therapies over traditional chemotherapy, two major molecular approaches have emerged for targeting kinases: antibodies and small molecules.[52] Antibodies are large biomolecules that bind to the extracellular domain of receptor tyrosine kinases, thereby preventing the binding of the ligand that activates the kinase. In contrast, small molecules can penetrate the cells and therefore inhibit also intracellular kinases downstream of receptor tyrosine kinases.[53] Since small molecule kinase inhibitors have been the focus of my work, this chapter provides a more detailed introduction to this class of therapeutics.

2.1 Different Binding Modes of Kinase Inhibitors

Different binding types of reversible small molecule kinase inhibitors. As stated above (see Introduction Chapter 1.2), the kinase domain has high structural flexibility and can adapt different conformations. Small molecule inhibitors can bind to various kinase conformations and are classified according to the activation state their kinase target exhibits during binding and to the pocket of the kinase to which they bind. Several classification categories have been developed in the past decade.[54,55] For instance, Dar and Shokat categorized small molecule kinase inhibitors into three classes that either target the active kinase conformation (type I), the inactive conformation (type II) or bind to an allosteric site of the kinase (type III).[54] Then, Zuccotto further subdivided type I inhibitors into two distinct classes (type I and type I½).[55] The currently most acknowledged classification system based on Roskoski[56]work divides kinase inhibitors into the following classes: type I, I½, III, IV, and V (Figure 3).[56]

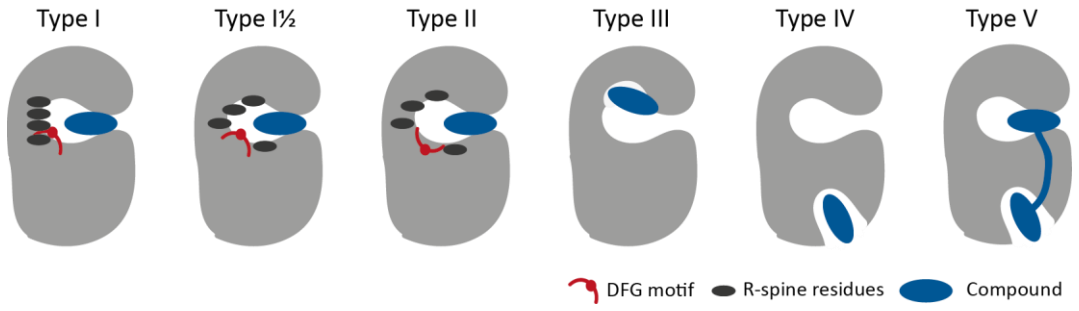

Figure 3 | Binding modes of small molecule kinase inhibitors. Kinase inhibitors are categorized into type I, I½, II, III, IV, and V inhibitors. Type I, I ½ and II molecules bind to the ATP binding site and are distinguished by the inactive or active conformation of the kinase. Type III inhibitors target the neighboring phospho-acceptor site of the kinase and type IV an allosteric site remote from the catalytic center. Bivalent inhibitors targeting both the ATP pocket and an allosteric binding site are categorized into type V.

Type I, I½ and II inhibitors are ATP competitive and bind the adenosine binding pocket while forming hydrogen bonds with the hinge region of the kinase.[56] The vast majority of kinase inhibitors engage their target kinase at the active site and compete with the high concentration of ATP in the cells (intracellular concentration of 1-5 mM). Several structural elements in the kinase domain are taken into account to classify ATP competitive inhibitors into the three different classes. Type I inhibitors target the kinase when it is fully active meaning that the DFG-Asp and the Cα are pointing into the ATP binding pocket and the R spine is ordered and active. As described by Zuccotto, the DFG-Asp is pointing into the pocket but the Cα is pointing out and the R spine is disordered for type I½ inhibitors.[55] In contrast, type II inhibitors bind to the fully inactive kinase where the DFG-Asp and Cα point out of the pocket. The cleft between the two lobes of the kinase domain can be divided into the front cleft, the gate area and the back cleft.[57,58] These defined regions are used to further classify ATP competitive inhibitors into an A subclass and a B subclass.[56] Inhibitors of subclass A bind in the front cleft, the back cleft and near the gatekeeper residue while subclass B inhibitors only bind in the front cleft and the gate area and do not reach the back pocket.[56]

Since the active conformation of the kinase is more conserved than the inactive conformation, it had long been inferred that type II inhibitors are more selective than type I and I½ inhibitors.[59] However recent systematic profiling work of our group has disproven this assumption.[60] The whole classification of kinase inhibitors depending on which activity state of the kinase they bind, is not exclusive meaning that one inhibitor can bind to different activation states. One example is Dasatinib which is a type I inhibitor for ABL and type I½ inhibitor for LYN.[56] Type III inhibitors bind to the phospho-acceptor site next to the ATP binding pocket. A prominent example is Trametinib, a MEK1/2 inhibitor that binds in the pocket near the ATP binding site of the kinase and blocks the kinase in its inactive state.[61] Type IV inhibitors are also non ATP competitive inhibitors and bind to an allosteric site remote from the ATP binding pocket. For example, some of the clinically approved mTOR inhibitors (Everolimus, Rapamycin and Temsirolimus) are type IV inhibitors and not ATP competitive.[56] Bivalent inhibitors that bind to two regions of the kinase domain are summarized as type V inhibitors. Examples are recently developed CK2 inhibitors that target a cryptic pocket of CK2 and the ATP binding pocket.[62]

Covalent small molecule kinase inhibitors. In contrast to all the other inhibitor types, type VI inhibitors bind covalently to their targets, typically via Michael addition of a cysteine.[56,63,64] This covalent bond can be either reversible (e.g. with unstable Michael adducts) or irreversible.[65] Prominent examples of irreversible clinical kinase inhibitors are Acalabrutinib[66] and Ibrutinib[67] targeting BTK or Afatinib[68] and Neratinib[69] inhibiting EGFR. These inhibitors contain a reactive electrophilic functionality in the parent structure that reacts with nucleophilic cysteine residues within or close to the binding site of the small molecule to the kinase domain. The inhibitory mechanism of covalent inhibitors occurs in two steps.[70] First, the compound binds non-covalently to the target protein and places its moderately reactive electrophile close to the cysteine residue of the kinase. The resulting complex then undergoes specific bond formation, typically via Michael addition, which forms the inhibiting complex. Accordingly, it has to be noted that designated type VI inhibitors can engage off-targets as non covalent inhibitors. Ibrutinib for instance forms a covalent bond with its intended target BTK but can also bind reversibly to several kinases that lack the reactive cysteine in the active site.

A covalent mechanism of drug-target binding provides pharmacological advantages over reversible binding in terms of prolonged duration of action. For the irreversible inhibitors, uncoupling of the pharmacodynamics of a drug from its pharmacokinetics is achieved. Here, target inhibition persists after drug clearance and is dependent on target protein turnover (degradation and synthesis rate). This allows for less frequent dosing and lower drug doses. The potency and selectivity of covalent inhibitors is dependent on the affinity of the initial non-covalent complex formation and the rate of subsequent bond formation. To minimize off-target effects, inhibitors should ideally target a nucleophile that is unique to the specific kinase.

2.2 Promiscuity of Kinase Inhibitors

Selectivity versus polypharmacology. When designing new small molecule kinase inhibitors for drug or probe discovery, achieving selectivity is a major challenge.[71] Most of the small molecules developed today are targeting the ATP binding pocket that is highly conserved within the human kinome, because allosteric inhibiting sites are rare. Accordingly, designing highly selective ATP competitive kinase inhibitors is a challenging task.[72] Especially in basic research where chemical probes (see Introduction Chapter 2.3) are used to study kinase function in cellular signaling, the imperious necessity arises to have access to selective compounds with known target profiles. Indeed, high selectivity and potency are a prerequisite for compounds to be classified as chemical probes.[73] Only when the function of a single kinase is pharmacologically disrupted can the cellular effect unambiguously be assigned to the specific kinase. In addition, if the survival and proliferation of a cancer cell is dependent on a single overactivated kinase, inhibition of this kinase has dramatic biological and clinical effects. In this case a highly selective inhibitor for this kinase would be beneficial and would minimize off-target effects.

In contrast, cancer cells that rely on the dysregulation of several kinases or even several pathways, would be inhibited more effectively if a multi-kinase inhibitor or a combination of selective inhibitors are administered.[74] From a clinical perspective, simultaneous targeting of the dysregulated kinase(s) and known resistance driver(s) (like MET or EPHA2 in case of EGFR inhibitor resistant tumors[75,76]) can also be favorable for the patient survival. In practice, compounds with multiple targets and polypharmacological features are often tolerable or even beneficial for the treatment of diseases with multiple genetic alterations like cancer.[74] Various clinically approved kinase inhibitors to date are broad spectrum kinase inhibitors like Dasatinib or Bosutinib targeting 67 and 45 proteins, respectively.[60] Additionally, inhibitor promiscuity can open up new opportunities by repositioning approved drugs for other diseases.[77] A prime example for kinase drug repositioning is Imatinib which was approved in 2001 as a BCR-ABL inhibitor for treating chronic myelogenous leukemia. The discovery of KIT as another target of Imatinib led to subsequent approval of Imatinib as a KIT inhibitor for treating gastro-intestinal stromal tumors.[77] Despite these advantages, unselective inhibitors can fail clinical evaluation because they elicit off-target toxic or adverse side effects for the patient.[78] Overall, drug discovery has much to gain from knowing the full target profile and the selectivity of small molecule kinase inhibitors which allow to better estimate risks and opportunities of off-target engagement.

Different approaches for selectivity calculation. Determining the selectivity of a compound, however, is a very challenging task. Depending on how selectivity is defined and computed, the compound can be perceived differently. For example, the compound selectivity can be either computed to get a global, target-independent view on the selectivity, or to characterize the ability of a compound to selectively hit a specific enzyme.[79] Additionally, experimental factors can influence the quantification of selectivity such as the assay technology (binding assay or activity assay), the experimental design (single dose or dose response measurement) and the enzyme source (recombinant, in lysate or in cell) that is used for profiling, which may lead to different selectivities of the same compound. In the past decades various approaches have been developed to calculate the selectivity of a compound namely entropy[80,81], selectivity score[59,82], Gini coefficient[83], partition index[84] and CATDS[60,85] (concentration- and target-dependent-selectivity). Compared to the first four approaches, CATDS provides more versatility and works for variable panel sizes. CATDS measures the target engagement of a specific protein at a certain drug concentration relative to the target engagement of all targets at that drug concentration and hence approches selectivity in a concentration- and target-dependent manner.[60] With the CATDS score one dataset can be utilized to answer different selectivity questions. For instance, the $CATDS_{target}$ calculates the selectivity of a compound towards a particular target whereas $CATDS_{multi-target}$ computes the selectivity for a group of proteins.

2.3 Small Molecule Kinase Inhibitors for Clinical Use and Basic Research

Small molecule kinase inhibitors for clinical use. Over the past 30 years protein kinases have been subjected to extensive drug development efforts. By the end of 2019, 55 small molecule kinase inhibitors have been approved by the U.S. Food and Drug Administration (FDA) mainly for the treatment of cancer and inflammation (http://www.icoa.fr/pkidb/).[86] Overall, cancer is by far the largest therapeutic area of small molecule kinase inhibitors but recently drug discovery programs have expanded their focus towards new therapeutic areas.[41] Small molecule kinase inhibitors are nowadays also used for the treatment of autoimmune and inflammatory diseases. For example the JAK inhibitor Baricitinib is approved for the treatment of rheumatoid arthritis and the SYK inhibitor Fostamatinib is used for chronic immune thrombocytopenia.[87] The foundation of the clinical success of kinase inhibitors was laid in 2001 with the approval of Imatinib for the treatment of chronic myelogenous leukemia (Figure 4).[88] By inhibiting the oncogenic fusion protein BCR-ABL that is causing the disease, Imatinib blocks proliferation and induces apoptosis of the cancer cells. Out of the 55 approved molecules, 39 are designated tyrosine kinases inhibitors and thus form the largest category of kinase drugs. The group of tyrosine kinases inhibitors can be recognized by the suffix –tinib in the compound name. The first non-tyrosine kinase inhibitor was approved in 2005: the BRAF inhibitor Sorafenib is administered in advanced renal cell carcinoma and hepatocellular carcinoma (Figure 4).[89,90] The first inhibitor targeting an atypical protein kinase was Idelalisib which was approved in 2014 for the treatment of three types of leukemia: relapsed/refractory chronic lymphocytic leukemia, relapsed follicular lymphoma and relapsed small lymphocytic lymphoma.[91] Idelalisib is orally effective and targets the delta isoform of PI3K. To date, four inhibitors targeting aPKs are approved and several others are in clinical phases I-III.

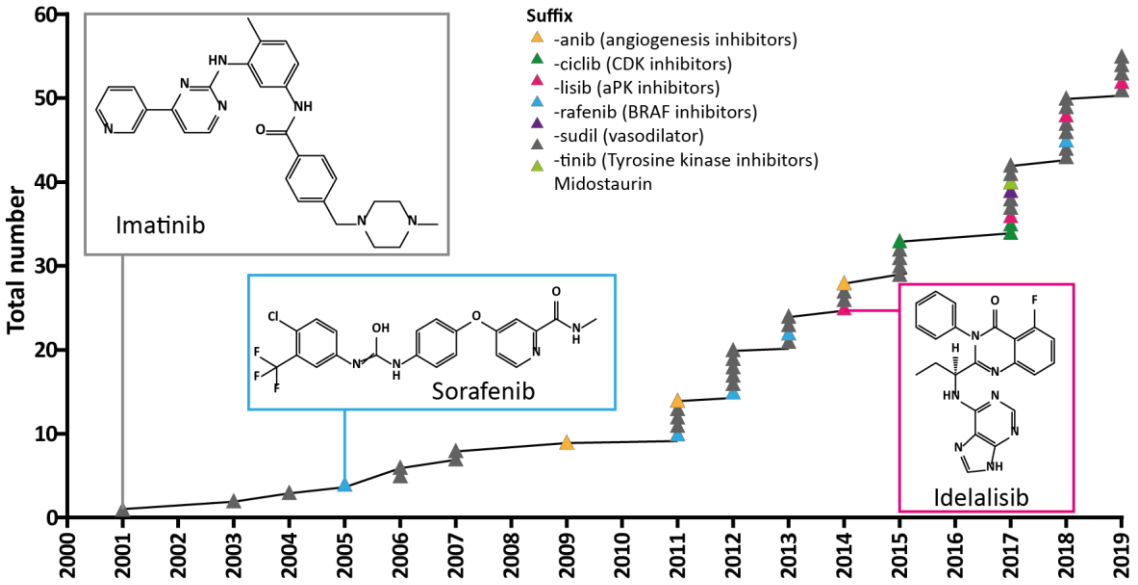

Figure 4 | Approved small molecule kinase inhibitors. Time line of FDA approved small molecule kinase inhibitors are shown as black line. The suffix of the drug name is linked to the mechanism of action or class of primary targets as indicated by different colors. Tyrosine kinases represent the most targeted kinase subfamily. Adapted from Kanev et al.[7]

Rapamycin and its analogues are the first generation of inhibitors of the atypical protein kinase mTOR but are not categorized as classical ATP-competitive small molecule kinase inhibitors due to their mode of action (Introduction Chapter 2.1). In 1999, Rapamycin was approved for immunosuppression after organ transplants.[92] In 2007 and 2009 Temsirolimus and Everolimus followed, two derivatives of Rapamycin that were approved by the FDA for the treatment of advanced renal cell carcinoma.[93] Several second generation ATP-competitive mTOR inhibitors are currently in clinical trials for various indications. In addition to the 55 approved kinase inhibitor, several hundred are currently in clinical trials for a variety of human diseases (www.clinicaltrials.gov).

Small molecule kinase inhibitors for basic research. Apart from pharmaceutical research, small molecule kinase inhibitors also play a major role in basic research for exploring the function of a kinase in a defined biological context. To be qualified as chemical probe, a compound must meet stringent criteria that were recently debated within the chemical biology community (Figure 5).[94-97] First of all the compounds should address the designated target with sufficient potency (<100 nM in biochemical assays and <1 µM in cellular assays) and must be able to penetrate into the cell to engage the target intracellularly.[94] Furthermore, the chemical probe must be highly selective (>30-fold selectivity within the subfamily) such that the cellular effect can be exclusively assigned to the designated target. Besides the target-related criteria, physicochemical properties are also considered. Chemical probes should be soluble in aqueous or organic solvents and should be chemically stable. Additionally, control compounds such as inactive analogs would be beneficial for experimental testing. The compound itself should have no pan-assay interference compounds (PAINS)[98] elements in its chemical structure.

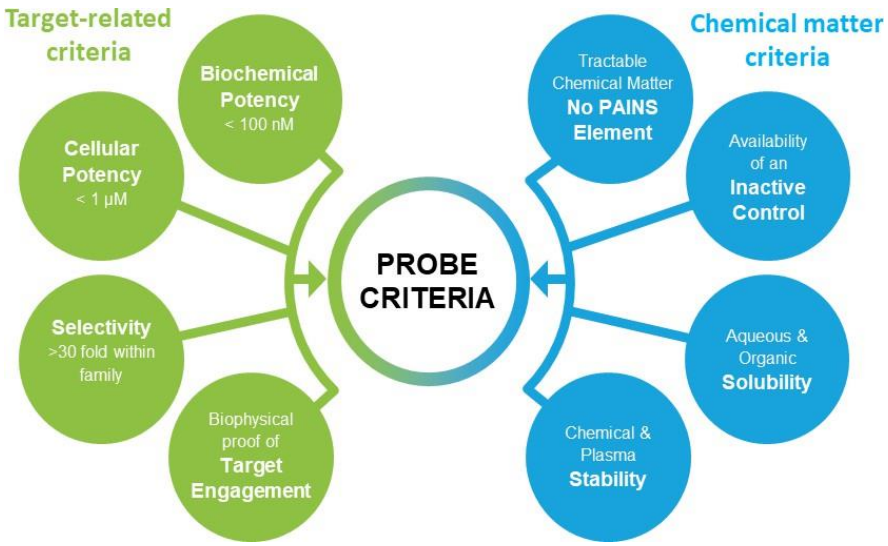

Figure 5 | Stringent selection criteria for chemical probes. To be qualified as chemical probes, compounds must meet predefined target-related and chemical matter criteria. Here are criteria shown that are applied by the structural genomics consortium. Adapted from Mueller et al.[94]

The highly selective compounds that meet these criteria facilitate the functional annotation of the human proteome/genome and help to understand physiological and pathological processes in the cell.[96] They are highly complementary to genetic tools like RNA interference (RNAi) or CRISPR since chemical probes can be used to only modulate the function of a protein rather than removing the whole protein.[97] Currently, 77 chemical probes for 102 different protein kinases and two probes for lipid kinases are listed in www.chemicalprobes.org, a portal for scientists to find suitable chemical probes. It should be noted that not all compounds in the portal meet the strict probe criteria, but are listed due to the lack of a better probe. Hence more than 80 % of the kinome still lack an appropriate chemical probe that full all probe criteria.

2.4 Progress in Targeting the Untargeted Kinome

More than ten years ago, 75 % of all research was focused on only 10 % of the kinome.[99,100] Today, the so called Harlow-Knapp (not peer-reviewed in[101]) effect is still relevant for kinase research. Although approximately 85 % of the human kinome is associated with at least one disease as revealed by disease-gene association databases, cancer mutation data, text mining and genome-wide association studies, industrial and academic pharmaceutical research mainly focus on a few well-studied kinases with known functions in cellular signaling.[102] Especially tyrosine kinases and a few other kinases, that are important for cell survival and proliferation, are of great interest for most research groups. From this perspective, it is not surprising that the function of approximately one third of the kinome is still poorly understood or completely unknown.[103] The most studied kinases are members of the MAP kinase and PI3K/AKT/mTOR pathways such as mTOR with more than 32,000 PubMed entries at the end of 2019.

In addition to the kinases involved in these pathways the spleen tyrosine kinase (SYK) is another well studied kinase which acts downstream of various transmembrane receptors including classical immunoreceptors and plays a crucial role in a variety of biological processes including adaptive and innate immunity, cellular adhesion, osteoclast maturation and vascular development.[104] In tumorigenesis, SYK can act as tumor promoter as in the case of many hematopoietic malignancies, but also as tumor suppressor in the case of non-immune cells, where SYK restricts cell migration and increases cell-cell interations.[105]

In contrast to this, many kinases are still poorly investigated and the function and their pharmaceutical potential is often unknown. Approximately half of the kinome accounts for only 5 % of all research publications on kinases in general.[102] The serine/threonine kinase N3 (PKN3) is one of the poorly investigated kinases with only 26 research publications in PubMed for a keyword search of the gene name until end of 2019. According to mechanistic studies, PKN3 acts downstream of PI3K and has been functionally linked to metastasis, invasion and tumor growth.[106,107] An emerging field in basic research represents the non-enzymatic members and non-catalytic scaffolding functions of the kinome. Pseudokinases like HER2 as prominent example, are associated with diseases when mutated or overexpressed although they lack the catalytic activity.[108]

The imbalance in kinase research focusing only on a small subset of the human kinome is also reflected in the availability of small molecule kinase inhibitors for different kinases. The 55 approved kinase inhibitors to date are designed to target around 20 different protein kinases and the hundreds of drugs currently in clinical trials are made for an additional 15-20 kinases.[87] Although many kinase inhibitors have been developed already, most of them are very promiscuous[60] and hundreds of kinases still lack a selective inhibitor (www.chemicalprobes.org). Selective and potent small molecule kinase inhibitors are however necessary as powerful tools to study the function and biology of a specific kinase in dose and time dependent manner in various cells and animal models.[94] Therefore, kinases without a chemical probe tend to be less studied as it is costlier to study a kinase without an available reagent and their pharmaceutical potential is ignored.

To functionalize the kinome and help validate new kinase targets for therapeutic intervention, the structural genomics consortium (SGC) has endeavored to develop chemical probes for the entire kinome. [109,110] The consortium is an open access public-private partnership of several research groups supported by eight companies and public funders. The SGC distributed a library of 367 small molecules, namely the protein kinase inhibitor set (PKIS), in order to crowdsource the discovery of novel chemical starting points for the development of new chemical probes.[110,111] The compounds were provided by GlaxoSmithKline (GSK) and selected based on the following criteria: i) the compound structures have been published, ii) compounds were screened against a limited number of kinases, iii) GSK has the compounds physically in stock and vi) compounds have balanced chemical and biological diversity.[110] The 367 compounds of the PKIS library can be grouped into 31 chemotypes and target more than 200 kinases as determined in a recombinant kinase activity assay.[112] After the success of the PKIS library, the SGC compiled a second library called PKIS2 comprising 645 small molecule kinase inhibitors representing 86 chemotypes that were provided by GSK, Pfizer, and Takeda.[113] Overall, PKIS and PIKS2 were distributed to over 300 laboratories and were mainly used for phenotypic screenings.[110]

The ultimate goal of the SGC is to build a chemogenomic set that contain chemical probes for all human kinases. As described by Jones and Bunnage, a chemogenomic set is a collection of well characterized selective small molecules.[114] As of November 2018, the kinase chemogenomic set (KCGS) assembled by the SGC is a collection of 188 selective small molecule kinase inhibitors that were derived from PKIS, PKIS2, compounds from the scientific literature and compounds donated from SGC members.[115] To be included in the KCGS, compounds should demonstrate an activity on the designated target below 100 nM in a recombinant kinase activity or binding assay and target less than 5 % of the tested kinases. These criteria are less stringent than the chemical probe criteria (Introduction Chapter 2.3). Overall, the 188 compounds that meet this criteria target 212 distinct kinases demonstrating that still a lot of kinases are lacking an selective kinase inhibitor.[110]

3 Methodologies to Elucidate Drug-Protein Interactions

Knowing the entire target space of a small molecule kinase inhibitor is indispensable in drug discovery to fully understand the compounds mode of action and to assess its utility as potential therapeutic agent or chemical probe. Especially after phenotypic screening where the compound is tested for a specific biological response, target deconvolution is essential in order to understand the molecular mechanism that causes the phenotypic effect.[116] To elucidate the target space of small molecule kinase inhibitors, various different technologies are available today which all have their merits and drawbacks and can differ greatly from each other.[41] For example, some technologies require structural modification of the compound in order to implement an immobilization or enrichment handle which is often time and cost intensive, whereas other strategies do not modify the compound at all. Additionally, the input material (kinase resource) varies strongly between different approaches. On the one hand, there are activity assays or binding assays that utilize recombinantly expressed full length kinases or only the kinase domain for compound profiling. On the other hand, other technologies make use of cell lysates as native protein source and some techniques even identify drug targets in living cells. Furthermore, the different approaches can vary greatly in their throughput capability from only very few compounds to thousands of compounds that are tested in parallel. In order to give a closer look on the different approaches, some of the technologies to elucidate the target spectrum of small molecule kinase inhibitors are explained in more detail in the following section.

3.1 *In-vitro* and *In-vivo* Profiling Assays

***In vitro* enzymatic and binding assays.** High-throughput screening platforms have proven to be beneficial in the discovery of kinase inhibitors because large compound libraries can be easily screened against a kinase in a short period of time to determine compound potency. Nowadays, large kinase panels even offer the possibility to screen compounds against many kinases to assess the compounds selectivity as comprehensive as possible.[117] Over time many different screening technologies suitable for high throughput screening have been developed. In general, the technologies can be classified in two different formats, activity based assays (also known as enzymatic assays) and binding based assays.[118] Both assay formats use either the kinase domain or the full length kinases. The usage of isolated protein kinase domains or recombinantly expressed full length kinases facilitates high throughput and yields robust and reproducible results, but does not accomplish close-to-physiological conditions because the kinase is completely disentangled from its cellular environment.[79]

Activity assays are preferentially used by the drug discovery community and directly or indirectly measure the quantity of product production such as the consumption of ATP, the production of ADP, or the amount of phosphorylated or non-phosphorylated substrate.[119] Typical detection methods of activity assays are radioactivity, fluorescence and luminescence.[118,119] Among the various activity assays, the radiometric assay remains the gold standard due to its high sensitivity. In this assay, the kinase is incubated with the substrate, cofactors and radioisotope-labeled ATP.[119]

During the reaction, the radiolabeled phosphate of ATP is transferred to the substrate which is subsequently quantified. To increase the throughput of this method, Reaction Biology has developed the HotSpotSM technology, a miniaturized version of this activity assay.[119] Another example of an activity based assay is the Nanosyn technology that is based on the microfluidic mobility shift platform of PerkinElmer (former Caliper) (Figure 6).[112,119] The electrophoretic mobility shift assay makes use of the fact that phosphorylated peptides are more negatively charged than their unphosphorylated counterpart and hence the substrate and the product can be separated via differences in their mobility. The active and purified kinase is incubated with ATP, the inhibitor that has to be tested and a fluorescence-labeled substrate. After the reaction has taken place, the mixture of phosphorylated product and unphosphorylated substrate are separated by electrophoresis and both the substrate and the product fluorescences are measured to increase the precision of the assay.[112,118] This assay type has successfully been applied to delineate the target space of the PKIS library (367 compounds; see Introduction Chapter 2.4) by Elkins *et al*.[112]

An alternative to activity assays are binding based assays that are capable of measuring the binding of a small molecule towards a kinase. Although binding does not necessarily mean that the activity of the kinase is inhibited, Rudolf and coworkers showed that there is a good correlation between measurements of compound binding and enzymatic activity inhibition for reversible compounds.[118] An example of a binding assay is the KinomeScan™ technology developed by Ambit and later licensed by DiscoverX.[119] This binding assay requires DNA tagged kinases and immobilized standard kinase inhibitors on Streptavidin-coated magnetic beads. The DNA tagged kinase is combined with an inhibitor of interest which will prevent its target kinases from binding to the beads. The quantity of bead bound protein is analyzed by qPCR and compared between the control and the test sample. The KinomeScan technology has been used for target annotation of the PKIS2 library.[113]

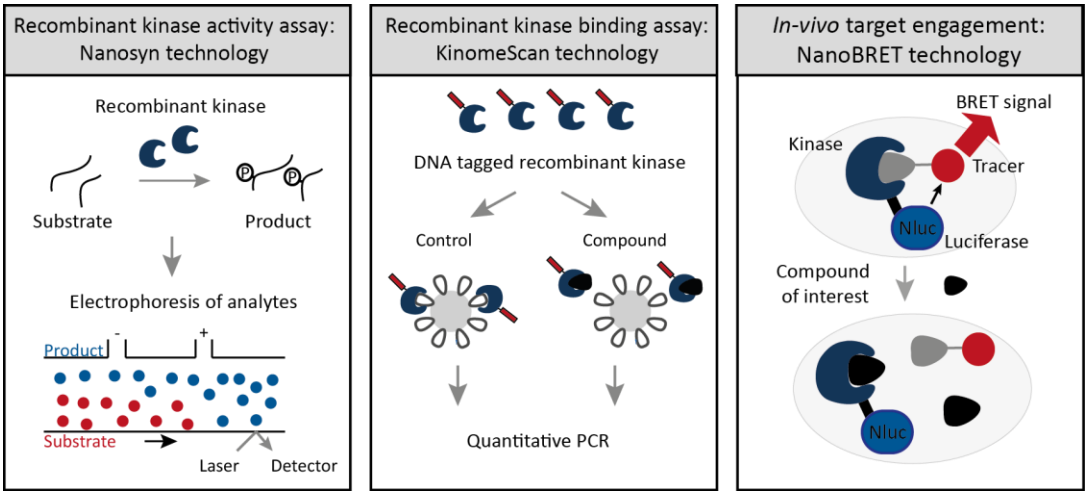

Figure 6 | Activity assay, binding assay and in-vivo assay for drug target deconvolution. The Nanosyn technology separates substrate and product based on their different charge (phosphorylation adds a negative charge to the substrate). The fluorescence of product and substrate are measured. The KinomeScan technology is a competitive binding assay where the free compounds and beads compete for binding to the kinase. Bead bound kinases are subsequently quantified by qPCR. NanoBRET technology measures target engagement in cells by detecting a BRET signal upon tracer binding to the kinase. Free inhibitor prevent tracer binding and lead to a reduced BRET signal.

***In-vivo* target engagement.** Biochemical assays such as the ones described above help to identify possible targets of the kinase inhibitors but do not consider cellular features like posttranslational modifications, complex partners, target localization, cellular compartments or intracellular ATP concentration. Knowledge of the kinases which the inhibitor is able to bind to in cells is crucial to understand the drug's mode of action. Additionally, *in-vitro* assays do not measure the cell permeability of the compound. Therefore, cellular assays are necessary to identify and validate target engagement in cells and to measure binding affinities of kinase inhibitors in cells. In 2018, Vasta and coworkers published a technology that utilizes a bioluminescence resonance energy transfer (NanoBRET) technique.[120] Here the full-length kinase is tagged with a 19-kDa luciferase (NanoLuc, Nluc)[121] and is used as BRET donor. The BRET acceptor is a cell-permeable fluorescent energy transfer probe (tracer) which was developed based on broad selective kinase inhibitors. By adding the energy transfer probe to the cells expressing the full-length kinase NanoLuc fusion protein, the probe is entering the cell and can bind to the fusion protein. When the BRET donor and acceptor are in close proximity, a BRET signal is quantified. If the cells are pre-incubated with the energy transfer probe, compound binding to the targeted kinase results in a competitive displacement of the tracer. Upon binding of the unlabeled compound, the BRET signal is decreased dose dependently which is then used for intracellular affinity calculation.[120] This technology enables determination of cell permeability, intracellular target engagement and affinity of ATP competitive kinase inhibitors under intracellular ATP concentrations. But the NanoBRET assay also requires cloning of cells to express a fusion gene under maybe artificial concentrations which reduces throughput.

3.2 Mass Spectrometry Based (Chemical) Proteomics for Target Deconvolution

Since kinases do not act in isolation but are intertwined in complex signaling cascades, proteomics approaches in the relevant biological background are highly eligible to get an unbiased view on the selectivity and potency of small molecule kinase inhibitors.[122-124] Mass spectrometry based quantitative proteomics has emerged as a powerful tool for studying drug-protein interactions and technological advances over the past two decades enable the identification of thousands of proteins in a single experiment with higher throughput and less input material. The following section will give an overview of several proteomic based drug target deconvolution approaches that have been developed so far, which allow for kinase inhibitor profiling.

Global proteomics approaches. Since the catalytic action of protein kinases is the phosphorylation of proteins, inhibition of kinases by small molecules leads to an altered phosphorylation state in a cell. Analysis of the phosphorylation status of cellular substrate proteins upon inhibitor treatment can therefore be used to elucidate the drug's mode of action and to indirectly determine drug-protein interactions (Figure 7).[60,125] If the phosphorylation of a kinase cognate substrate is reduced, it can be concluded that the activity of the responsible kinase is inhibited by the compound. Traditionally Western Blots have been used to monitor such inhibition and validate a target hypothesis. The multiplexing capacity of mass spectrometry has led to the emergence of

phosphoproteomics as a powerful tool to investigate perturbed signaling pathways upon inhibitor treatment in a hypothesis-free and global manner.[126] Because phosphorylated proteins tend to be of lower abundance and phosphorylation of a particular site tends to be substoichiometric[127], enrichment of the phosphoproteome is necessary to achieve enough analytical depth. One common strategy to enrich phosphopeptides is immobilized metal affinity chromatography (IMAC) where negatively charged phosphopeptides interact with positively charged metal ions (e.g. Fe^{3+}).[128] Despite the advances in phosphoproteomics technologies, the function of many phosphosites and the kinases responsible for their phosphorylation are unknown making it challenging to investigate the drug's mode of action.[129] Additionally, substrates can be phosphorylated by more than one specific kinase leading to potential compensation mechanisms upon inhibition of one kinase. Nevertheless, many studies have already shown that monitoring changes in phosphoproteomes after administration of a kinase inhibitor can help to better understand the drug's mode of action.[60,125]

Another global proteomics based approach is thermal proteome profiling (TPP) that directly identifies drug-protein interactions in living cells (Figure 7).[130,131] TPP is a combination of a cellular thermal shift assay (CETSA)[132] developed by Nordlund and colleagues and multiplexed quantitative mass spectrometry.[131] CETSA is based on the assumption that upon drug binding the heat-stability of a protein is altered (stabilization or destabilization). Hence a liganded protein exhibits a shifted melting temperature in comparison to the unliganded form, which can be evidenced by performing a temperature-dependent unfolding and precipitation experiment. Initially, results of a CETSA experiment were read out by Western Blotting as a hypothesis-driven technique. Combining CETSA with quantitative mass spectrometry allows the determination of protein thermal stability on a proteome level enabling hypothesis-free target deconvolution.[130] A variant of CETSA is the isothermal dose response assay (ITDR) where the temperature is kept constant and the cells are treated with different inhibitor concentrations.[132] With increasing concentrations a drug-protein complex stability might be altered which enables the calculation of binding affinities. The advantage of TPP is the measurement of drug-protein interactions in the physiological environment of the cell. However, not all proteins are subjected to measurable thermal shifts upon inhibitor binding, resulting in false negatives as relevantly demonstrated for multikinase inhibitors.[131,133]

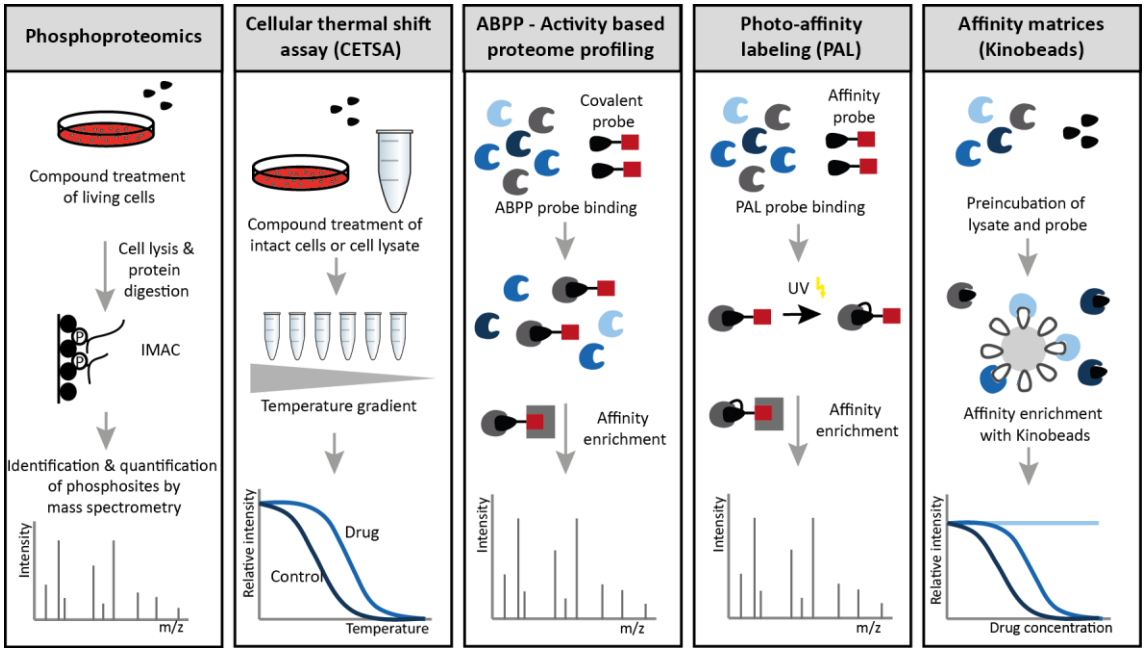

Figure 7 | Schematic representation of different proteomic based approaches for drug target identification. The phosphoproteomic approach measures the abundance of phosphosites after drug or control treatment of cells. The cellular thermal shift assay (CETSA) measures thermal stability of proteins with or without inhibitor treatment. Activity based proteome profiling utilizes a covalent probe that reacts with the target protein which can be subsequently enriched by an affinity enrichment tag. Photo-affinity labeling makes use of a probe that reversibly binds to its target protein first and covalently reacts with it upon irradiation in a second step. Affinity matrices like the Kinobeads enrich the fraction of target proteins from cell lysates that are not bound by the inhibitor of interest. Modified from Heinzlmeir.[134]

Probe-based chemoproteomics approaches. The term "chemoproteomics" describes a research area at the interface of medicinal chemistry, biochemistry and cell biology that utilizes chemical probes to gain insights into the mode of action of small molecules.[135,136] Several probe-based chemoproteomics techniques have been developed to date that generally utilize a small molecule as bait to capture target proteins present in cell extracts or intact cells. Binding of the bait to its targets can be either covalent (activity-based profiling) or noncovalent (affinity based profiling).[136] Cravatt and coworkers pioneered the activity-based protein profiling (ABPP) approach (Figure 7).[137-139] Here active-site directed chemical probes targeting whole enzyme families, like proteases[139] and hydrolases[137], were developed. The chemical probes consist of at least two elements, a reactive group that covalently binds to a catalytic residue of the enzyme and a reporter group to enable protein enrichment with beads. Competition with an investigated small molecule results in reduced binding of the chemical probe and thus decreased enrichment. Recently, Taunton and colleagues have developed a sulfonyl fluoride probe (XO44) that is capable of binding covalently to the catalytic lysine of up to 133 endogenous kinases.[140] This technology allows kinase drug target profiling within cells. However, due to the covalent nature of the probe, which disturbs the binding equilibrium between inhibitor and protein, it is difficult to determine true binding affinities of mostly reversible kinase inhibitors. Another chemical proteomic strategy to identify drug protein interaction is photo-affinity labeling (PAL) (Figure 7).[141-143] Here, the compound is functionalized with a photoreactive moiety (e.g. trifluoromethylphenyl diazirine) and an enrichment tag (e.g. biotin). After the compound has entered the cell and bound reversibly to

its targets, irradiation with a specific wavelength of light leads to the formation of a proximity-based covalent bond with the nearest molecule, in the best case the targeted protein. Upon enrichment through the affinity handle, targeted proteins can be identified by mass spectrometry. In a competition set up, PAL allows target deconvolution of an inhibitor of interest.

In classical affinity based chemoproteomic experiments, a linkable version of the investigated bioactive compound is directly immobilized on a matrix and targets are pulled out of cell extracts.[122,144] If the compound is lacking a reactive group for immobilization, an immobilizable version has to be synthesized. Analysis of the structure-activity relationship of the compound prior synthesis help to choose a linkage position for the reactive group. Comparison of the activity of the linkable molecule and its parent compound in a relevant functional assay validates the engagement of the same main target. Additionally due to the complexity of cell extracts, unspecific binding can make it challenging to distinguish between background binding and true binders. This can be in parts avoided by adjusting the linker lengths and coupling density of the compound on the beads.[144] But in order to distinguish between true targets and background binding, competitive pulldown experiments have to be performed. Nevertheless, the modified version of the compound is often optimized towards binding to the designated target (if known) which does not take potential off-targets into account and may lead to false negatives. To alleviate these limitations and to increase throughput, the affinity matrix should be designed in a way that allows the affinity enrichment of a complete subproteome and not only the targets of the compound under investigation.[123] A prerequisite for such a defined affinity matrix is a conserved and druggable binding site of the targeted subproteome. This is for instance the case for histone deacetylases and kinases. For these two subproteomes, affinity matrices have been developed.[145-147]

Competition binding assays for target deconvolution of kinase inhibitors. In 2007, Bantscheff *et al* introduced the concept of Kinobeads to profile ATP-competitive small molecule kinase inhibitors (Figure 7).[145] The Kinobeads affinity matrix originally consisted of seven ATP competitive broad spectrum kinase inhibitors immobilized on Sepharose beads that were able to enrich 183 protein kinases from K-562 cell lysates. To increase kinome coverage of Kinobeads, the probes and the cell lysates were further improved. A cell lysate mixture of four cell lines (K-562, MV-4-11, SK-N-BE(2), Colo205) and a combination of three broad selective (Purvalanol B, linkable PD-173955, Compound19) and two more specific probes (linkable Vandetanib, Compound 15) were found to be an optimal combination.[147] Coupled to quantitative mass spectrometry, the technology enabled the simultaneous identification and quantification of 253 kinases and several other ATP-binding proteins in their native background.[60] In a competitive set up, targets of reversible ATP-competitive kinase inhibitors can be deconvoluted. Lysates are pre-treated with increasing inhibitor concentrations leading to a competition between the free drug and Kinobeads for the active site of the kinase. Reduced enrichment of the protein target by Kinobeads results in a dose dependent intensity reduction in the subsequent mass spectrometry readout. The Kinobeads technology was recently used to annotate the target landscape of 243 clinical kinase inhibitor identifying novel and to some extent surprising drug-protein interactions.[60] Within this study using Kinobeads, ferrochelatase (FECH) was identified as a common off-target of several small molecule kinase inhibitors that can be associated with side effects observed during treatment of patients with kinase inhibitors.[148]

A similar approach is the KiNativ technology that utilizes biotinylated ATP. The labeled ATP transfers the biotin covalently to the conserved AxK lysine of the active site of kinases and other ATP-binding proteins. Preincubation with a compound of interest prevents the biotinylated ATP from binding to the protein. Subsequent enrichment with Streptavidin beads and MS analysis allows the identification and quantification of targeted proteins.[149,150] While Kinobeads are designed to enrich mainly kinases, the KiNativ approach enriches a large number of other ATP-binding proteins.[151] Lysate based technologies like the Kinobeads and KiNativ approach enable target deconvolution in close-to-physiological conditions. Complex cell extracts contain endogenously expressed full length proteins that carry all necessary post translational modifications, cofactors and binding partners. Additionally, such experiments can be performed using any kind of cell or tissue lysate enabling tissue or cell line specific target deconvolution even in non-human material.[79]

Considerations when performing a competition binding assay. Binding of a compound to a protein is determined by the basic concepts of thermodynamics and kinetics. While kinetics expresses how fast the association/dissociation of a complex happens, thermodynamics describes how tightly two complex partner interact with each other. Both concepts are important to understand the interaction between a compound and the protein and the interaction between the protein and the affinity matrix.

Common thermodynamic measures for compound protein interactions are the half maximal inhibitor concentration (IC_{50}), the half maximal effective concentration (EC_{50}) and the dissociation constant at equilibrium (K_d). The IC_{50} value describes the concentration of the compound where 50 % of the protein is inhibited, whereas EC_{50} values report the concentration at which 50 % of the maximal effect is observed. While EC_{50} and IC_{50} are assay dependent, the K_d value is assay independent and describes the tendency of the compound-protein complex to dissociate into its individual complex components. The dissociation constant describes the concentration of the compound that is needed to occupy half of the targeted protein and can be calculated by the following equation, where L is the ligand (the inhibitor), P is the protein and PL is the ligand-protein complex.

$$\text{dissociation constant } \mathrm{K_d} = \frac{[\mathrm{L}] * [\mathrm{P}]}{[\mathrm{PL}]} \ \#(1) \qquad (1)$$

Experimental determination of the dissociation constant with a competition binding assay, like the Kinobeads technology, requires considerations of several assay-dependent aspects.[79,145] First of all, the protein concentration must be lower than the estimated K_d values. If this prerequisite is not met and the compound concentration is much higher, the experimental K_d would always be half of the concentration of the protein regardless of the actual affinity of the compound to the target. Since kinases are generally of low abundance in cell extract, the assumption can be considered as fair in most cases. Exceptions can arise when a kinase is overexpressed in a specific cell line, such as EGFR in A549 cells.

Additionally, the affinity matrix should ideally not influence the equilibrium between the compound and the targeted protein which is not the case for Kinobeads. During a competitive Kinobeads pulldown experiment, first an equilibration between the free compound and its targets is established. By adding Kinobeads to the cell extracts, kinases and other ATP-binding proteins are captured by the affinity matrix leading to a three membered equilibrium between the protein, the compound and the affinity matrix. Proteins captured by the affinity matrix are taken out of the equilibrium between the compound and its targets which results in a distortion of the compound-target equilibrium. This effect is known as protein depletion and induces a shift of determined affinity values toward higher concentrations. For this reason, not the K_d but an assay-dependent EC_{50} value is measured. The extent of protein depletion depends on i) the affinity of the protein to the immobilized probe, ii) the concentration of the immobilized probe and iii) the concentration of the protein in the lysate. All these parameters are usually unknown and impossible to calculate in a classical chemoproteomic experiment. In general, assay conditions should be selected in a way that protein depletion is less than 10 %. This can be partially achieved by using sub-micromolar concentrations of the affinity matrix and a large excess of lysate. Nevertheless, protein depletion cannot be completely eliminated and a depletion factor is required to correct for this effect. Sharma et al[152] introduced a concept to convert assay dependent EC_{50} values into independent K_d values which was slightly modified for Kinobeads.[151] Therefore, two consecutive pulldowns of the vehicle control are performed. At best, a negligible amount of protein is captured by the beads in the first pulldown so that in the second pulldown the same quantity of protein can be enriched again. This should lead to almost identical protein intensities of the first and second pulldown in the mass spectrometry readout. If a larger fraction of a protein is depleted from the cell extract, less protein can bind to the affinity matrix in the second pulldown resulting in lower intensities. The depletion factor, also known as correction factor, can be calculated by dividing the intensity of the second pulldown by the intensity of the first pulldown as shown in equation 2.

$$\mathrm{r} = \frac{\text{incubation (PD2)}}{\text{incubation (PD1)}} = \frac{\text{intensity (PD2)}}{\text{intensity (PD1)}} = \frac{fraction\ f\ (P - f(P))}{fraction\ f(P)} \tag{2}$$

Considering the equation developed by Cheng and Prusoff[153] to convert experimental EC_{50} values into K_d values, the correction factor concept described above as well as the binding equilibrium between Kinobeads and proteins, EC_{50} values can be converted into K_d values with the following equations:[151]

$$K_d(probe) = \frac{[probe] * [P]}{[probe * P]} = [probe] * \frac{r}{1 - r} \tag{3}$$

$$K_d(ligand) = \frac{K_{d(probe)}}{K_{d(probe)} + [probe]} * EC_{50} \tag{4}$$

With (3) in (4):

$$K_d(ligand) = \frac{[probe] * \frac{r}{1-r}}{[probe] * \frac{r}{1-r} + [probe]} * EC_{50} = \frac{\frac{r}{1-r}}{\frac{r}{1-r} + r} * EC_{50} \quad (5)$$

$$\mathbf{K_d = depletion\ factor\ r * EC_{50}} \quad (6)$$

Furthermore, entropy and enthalpy affect the experimental outcome of a competitive binding assay. Immobilization of a probe onto a solid matrix reduces the degree of freedom compared to the non-immobilized compound. This leads to a decrease of entropy which in turn increases the binding affinity of the immobilized probe. Therefore, proteins have in general higher affinities which can translate into longer residence times on the beads compared to the free compound. Taken together, the entropy and residence time alterations upon compound immobilization make it inevitable to allow the establishment of the thermodynamic equilibrium between the free compound and its target proteins by preincubation of the cell extract before the addition of the affinity matrix. Nevertheless, some proteins can display short residence times on the beads which may lead to the loss of bead-bound proteins during washing of the beads. Overall, the Kinobeads technology is more suitable to detect rather strong compound-protein interactions in the nano to low micromolar range.

Although kinetic parameters, represented by the association (k_{on}) and dissociation (k_{off}) rates, strongly influence the success of the competitive binding assay they are not directly measured by a competitive binding assay. The residence time is the reciprocal of k_{off} and decribes the period of time in which the protein is occupied by the compound.[154] To evaluate a drug's effect *in vivo* it is crucial to know not only the affinity and selectivity of a compound but also the residence time. In an open system like the human body, where the drug is constantly distributed, absorbed or metabolized, it might be advantageous to have a long residence time at the target protein to increase the effect of the drug and therefore improve the therapeutic outcome. A special case are irreversible covalent inhibitors that have infinite residence times. How long the inhibitory effect last, mainly depends on the turnover of the protein (synthesis and degradation rate) rather than on the pharmacokinetic properties of the inhibitor.[63]

3.3 Basic Principles of Bottom-up Proteomics

Because mass spectrometry allows to simultaneously measure the abundance of thousands of proteins in a sample, it has evolved to the standard readout of proteomics-based experiments such as Kinobeads assays. Generally speaking, mass spectrometry is an analytical technique that measures the mass to charge ratio of an analyte. Mass spectrometry has become the workhorse of proteomics, able to accurately identify and quantify proteins within complex biological samples. Mass spectrometry based proteomics can be divided into two main fields, the top-down approach[155,156], that measures intact proteins, and the bottom-up approach that measures peptides. This study relied on the nowadays primarily used bottom-up proteomic approach which is experimentally and computationally more advantageous and evolved than top-down proteomics and is therefore discussed in more detail below.[157]

Experimental procedure of a bottom-up proteomic experiment. A common bottom-up proteomics workflow (Figure 8) starts with the extraction of proteins from their cellular context which can be either done under native or denaturing conditions depending on whether the native protein structure is required for further analysis or not.[158] If necessary, proteins can then be fractionated or enriched, for example by affinity enrichment with Kinobeads.[147,159] Prior to digestion, proteins are reduced and cysteines are alkylated (e.g. carbamidomethylation) to unfold the proteins and ensure the accessibility of digestion enzyme to all cleavage sites. Proteins are enzymatically digested to peptides using a sequence-specific protease. Here, trypsin is predominantely used that enzymatically cleaves C-terminally after the amino acids arginine and lysine.[160] To increase sequence coverage, other proteases like chymotrypsin, LysC, LysN, AspN, GluC and ArgC can be used.[161] At this point, a fractionation step or an enrichment step of peptides, e.g. carrying posttranslational modifications, can be added to the workflow.[162] Immobilized metal affinity chromatography (IMAC), for instance, is a common technique to enrich phosphopeptides that are usually of low abundance.[128] The processed samples are highly complex, containing thousands of peptides which will exceed the analytical capacity of a mass spectrometer. Therefore, an ion-pair reverse phase liquid chromatography (RP-LC) system is coupled online to a mass spectrometer to enable temporal distribution of the peptide analytes and reduce the sample complexity at a given time of the measurement.[163,164] Hereby, peptides are separated by their hydrophobicity over time, which improves the accessibility of the peptide to the mass spectrometer. Upon elution, the peptide gets ionized and the mass and intensity of the ion is measured in the mass spectrometer.

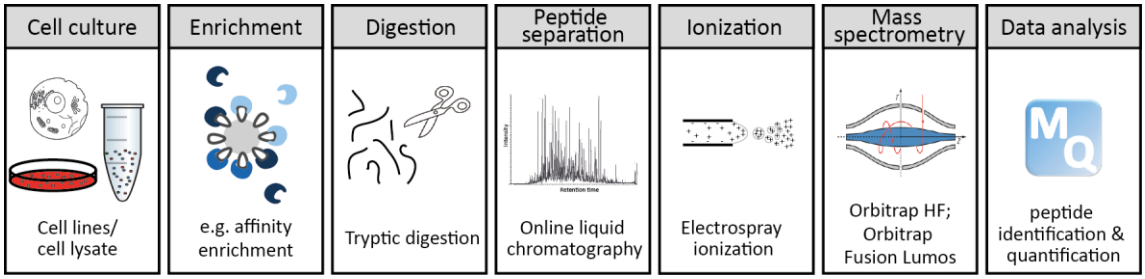

Figure 8 | Typical bottom up proteomics workflow. Proteins are lyzed under native or denaturating conditions. Prior to protein digestion using trypsin, proteins can be enriched by affinity matrices like Kinobeads. After digestion peptides are separated by online liquid chromatography and subsequently ionized. Mass to charge ratios of peptides and fragments are measured by tandem mass spectrometry. Identification and quantification of peptide and fragment spectra is performed by specialized software like MaxQuant. Modfied from Steen and Mann.[165]

Mass spectrometry. Generally speaking, a mass spectrometer is a molecular balance that measures the response of a charged analyte to electric and magnetic forces.[166] A mass spectrometer can be roughly subdivided into three parts: an ion source, a mass analyzer and a detector. Since the mass to charge ratio is measured, the analyte needs to get ionized before subjecting it to the mass spectrometer. The main ionization method used in proteomics to charge the analyte and transfer it into the gas-phase is electrospray ionization (ESI).[167] Upon elution from the RP-LC, the analyte passes through a thin emitter to which high voltage is applied resulting in a charged liquid. The electric potential at the emitter leads to the formation of a Taylor cone. When the potential reaches a specific limit, a jet of small droplets is emitted from the cone. Further evaporation of the solvent and fission into smaller droplets ultimatively results in charged analytes. ESI is a soft ionization technique that produces multiple charged analytes and can be coupled to liquid chromatography.[168,169]

The ion optics are composed of several multipoles and lenses that focus and propel the ions under vacuum from the ion source to the mass analyzer by a direct current voltage gradient.[166] Common mass analyzers that are used to measure the response of a charged analyte to electric and magnetic forces are quadrupole, ion trap and orbitrap. Their performance is characterized by their resolution, accuracy, sensitivity and scan speed.[166,170] A quadrupole possesses four rod-shaped electrodes.[171] The two opposite rods always share the same polarity (for example they are both positive) while the other two rods share the opposite polarity (both negative). By oscillating electrical fields, the quadrupole selectively stabilizes or destabilizes the trajectories of ions with specific mass to charge ratios that move through the quadrupole. Therefore, the quadrupole is mainly used as mass filter in hybrid instruments. The linear ion trap is composed of a quadrupole framed by two electrodes.[172] The quadrupole as described above confines ions radially while the static electrodes on the end trap the ions axially. The linear ion trap, as the name indicates, is able to collect and store ions leading to high sensitivity of the mass analyzer. The orbitrap mass analyzer consists of a spindle-shaped central electrode surrounded by an outer electrode.[173] By applying voltage to the electrodes, tangential injected ions oscillate along the z-axis and rotate around the central electrode. Since the frequency of the oscillation only depends on the mass to charge ratio and an instrument specific constant k, the recorded image current can be deconvoluted by Fourier transformation into a mass spectrum (relative intensity over m/z values).[173-175]

Hybrid mass spectrometer combining two or three of the mass analyzer mentioned above have emerged as the leading platform in proteomics. One commonly used instrument is the Q Exactive™ HF Hybrid Quadrupole-Orbitrap™ mass spectrometer (Thermo Fisher Scientific) that combines a quadrupole and an orbitrap and was mainly used for this study (Figure 9).[176] Here the charged analyte is transferred via the ion optics including an improved injection flatapole to the quadrupole. Filtered ions are forwarded to the C-trap which focuses the ions before further injection into the orbitrap. Other commonly used types of instruments are the newer generation Orbitrap Fusion™ Lumos™ Tribrid™ that features three mass analyzer (linear ion trap, quadrupole and orbitrap) and the older generation Orbitrap Elite (both Thermo Fisher Scientific) that combines a linear ion trap and an orbitrap mass analyzer.[177,178]

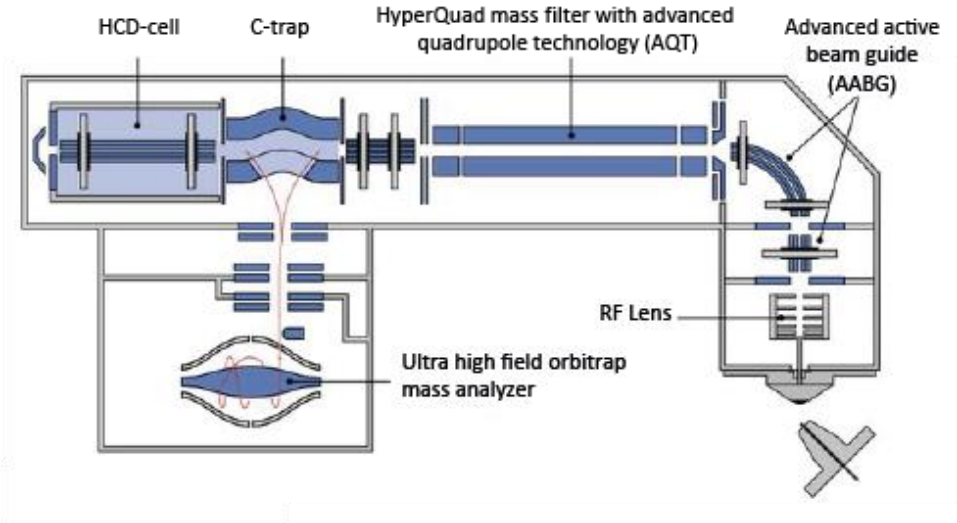

Figure 9 | The Q Exactive™ HF Hybrid Quadrupole-Orbitrap™ mass spectrometer. After ionization, peptide ions are focused and propelled through the ion optics. The quadrupole mass analyzer acts as mass filter. Ions are subsequently analyzed in the ultrahigh field orbitrap. Adapted from Thermo Fisher Scientific.

Tandem mass spectrometry. A mass spectrum (MS1 spectrum, Figure 10 A) contains information about the monoisotopic mass and the charge of the peptide (precursor) which is not enough information to unambiguously identify the sequence of the peptide. Therefore, tandem mass spectrometry is required to enable identification of the peptide sequence (Figure 10 A).[179 180] Here, a single precursor ion is selected based on the mass to charge ratio and the intensity. The selected precursor peptide is collected in the C-trap before it is transferred to the higher energy collision induced dissociation (HCD) cell.[181] In the HCD cell, the precursor peptides are accelerated by a current offset and fragmented by collision with an inert gas. In addition to HCD, there are other fragmentation methods all of which lead to different cleavage within the peptide bonds. HCD fragmentation results in a breakage of the peptide bond between the carbonyl and the nitrogen (Figure 10 B). This fragmentation method mainly produces b- (N-terminus) and y-ions (C-terminus) according to the nomenclature of Roepstorff, Fohlman and Biemann (Figure 10 B).[182] Subsequently, fragment ions are read out in the mass analyzer. Ideally, the mass of the different fragment ions should differ by only one amino acid to determine the full amino acid sequence of the precursor ion by m/z differences of the individual fragments. After a precursor is selected for

sequencing in MS2, it is excluded for a predefined time from further selection to avoid multiple sequencing of the very same peptides. During a data dependent acquisition mode the mass spectrometer automatically switches between MS1 and MS2 scans where several MS2 scan (depending on the applied method) are acquired after one MS1 scan.[183-185] The Orbitrap Fusion Lumos instrument type is able to operate in a MS3 based mode where fragment ions of the MS2 scan are selected and again fragmented and measured. Acquisition of MS3 spectra is beneficial for TMT-based quantification (see below).[186]

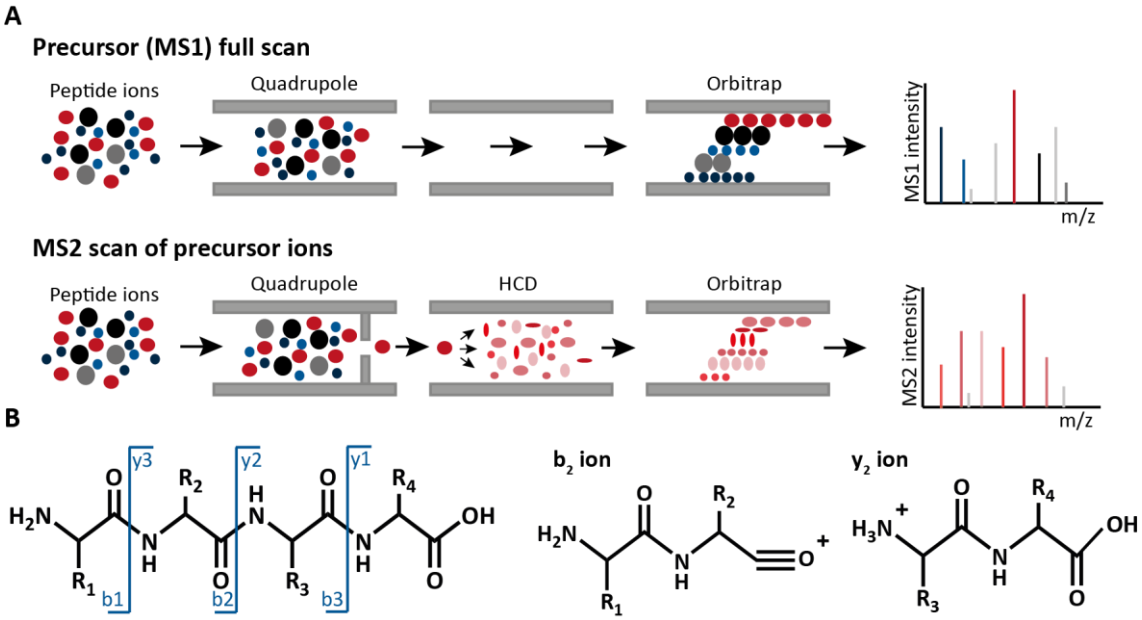

Figure 10 : Tandem mass spectrometry. (A) Basic principle of tandem mass spectrometry. To generate a precursor (MS1) full scan, all ions are transferred via the quadrupole to the orbitrap and the mass to charge ratios (m/z) of all ions eluting at that time are recorded in the orbitrap. After acquiring a MS1 spectrum, a precursor ion is selected in the quadrupole and fragmented in the HCD cell. m/z values and the corresponding intensities of fragment ions are recorded in the orbitrap and an MS2 spectrum is acquired. (B) Fragmentation of peptides via HCD leads to the formation of b- and y-ions.

Protein identification. Following data acquisition, the amino acid sequence of the analyzed peptides can be derived from MS2 spectra. Modern mass spectrometers generate thousands of spectra (MS1 and MS2) within one hour making it impossible to manually annotate the spectra. Therefore, several peptide sequencing algorithms have been developed to automatically identify amino acid sequences from MS2 spectra.[187] One approach is de novo sequencing that identifies the amino acid sequence directly from the peaks of the MS2 spectra without resource of any protein database.[188] MS2 spectra are inherently deficient making de novo sequencing much more difficult. The most commonly used approach is peptide matching which relies on database search algorithms, such as Mascot[189] and Andromeda[190] (implemented in MaxQuant).[189,191] Hereby, a predefined protein sequence database previously generated by genomics data is digested in silico and the possible m/z values of all theoretical peptide fragment spectra are calculated. Then, m/z values of both the experimentally determined and the theoretical spectra are matched and a score is calculated for each pair (peptide-spectrum-match, PSM) that described how similar the experimental and theoretical spectra are. The PSM with the highest score is then reported as the

identified peptide. However, matching thousands of experimental spectra to theoretical spectra generated by large databases can lead to erroneous matching, especially for low quality MS spectra. One mechanism to control the false discovery rate (FDR) is the target-decoy approach.[192,193] Here, experimental spectra are searched additionally against a decoy database that contains reverse versions of the original theoretical spectra of the database. Since the reversed decoy peptide sequences do not occur in nature, each match to the decoy database is false by definition. The assumption is that random hits in the target database occur at the same rate as the decoy hits, allowing for the identification of a score cutoff at which the list of PSMs contains a controllable amount of false-positives. Common FDR cutoffs in proteomics datasets are 1 %. Since proteins are measured indirectly through measuring peptides derived from tryptic digestion in bottom-up proteomics, subsequent protein inference from peptide sequence data becomes necessary. However, the sequence of each peptide can often not be assigned to a single protein because isoforms or closely related proteins share the amino acid sequence. If no unique peptide can be assigned to a protein, proteins that share the same peptides are grouped together (protein groups).

Protein quantification. Typically not only the identity of a peptide or protein in a sample is of interest but also its quantity in relation to other proteins (absolute quantification), or other samples (relative quantification) which is primarily done in most proteomic studies.[194,195] The intensity measured by a mass spectrometer does not qualify inherently for quantification because the intensity of a peptide is dependent on its physicochemical properties (length, charge and hydrophobicity) and its ionization efficiency.[195,196] But the peptides should behave similarly between different measurements facilitating relative quantification between different samples. In mass spectrometry based proteomics two different strategies can be distinguished: label free and label based quantification. For label free quantification (LFQ), the intensities of a precursor ion in consecutive MS1 scans are plotted against the retention time of the peptide from the chromatography column. The area under the curve of the extracted ion chromatogram (XIC) is integrated and results in the LFQ intensity of the peptide. The MaxQuant software that is commonly used in academia for identification and quantification of peptides and proteins, features an algorithm called MaxLFQ that additionally normalizes the relative intensities between different samples.[197,198] LFQ quantification allows comparison of an unlimited number of samples and covers a broader dynamic range compared to label based approaches. A shortcoming of LFQ is the missing value problem that leads to missing quantification or missing identification of peptides within a sample.[199] This can be overcome in part by using an algorithm called match between runs that aligns retention times of the same peptide between different measurements. A peptide that was not subjected to MS2 measurement in one sample, can still be identified and quantified by alignment of its retention time and the accurate mass to charge ratio to another samples where it was identified.[197] Another option to overcome missing values are label based quantification approach like isobaric labeling of peptides.[200] The most popular isobaric mass tag is tandem mass tag (TMT).[201] The structure of the tag consists of a cleavable mass reporter, a mass normalizer and a peptide reactive group that reacts with lysine residues and the N-terminus of the peptide. The mass reporter and the mass normalizer are labeled with ^{13}C and ^{15}N stable isotopes, so that the overall mass is identical but the position of the isotopes differs between the tags. The isobarically labeled peptides have the same mass, the same retention behavior on the LC column

and physicochemical properties in the mass spectrometer. Upon fragmentation the mass reporter of each tag in cleaved off and generates a specific reporter ion peak that can be used for relative quantification of the samples. TMT quantification enables multiplexing of up to 16 samples and thereby significantly reduces measurement time. A drawback of TMT is ratio compression that occurs by fragmentation of coeluting peptides resulting in an underestimation of the actual peptide abundance differences. Ratio compression can in parts be diminished by selecting fragments of the MS2 scan for a second fragmentation (MS3) step. Hereby the effect of coisolated peptides and therefore the ratio compression is reduced.[186,202]

4 Objectives and Outline

Protein and lipid kinases are involved in almost every cellular signalling pathway, and alterations in their catalytic activity largely affect cellular homeostasis which can lead to the development of human diseases. Thousands of small molecule kinase inhibitors have been developed to target aberrant activated kinases. The majority of such compounds target the ATP binding pocket of the kinase domain which is highly conserved, rendering the development of selective compounds challenging. Although selective small molecules are highly valuable in basic research as chemical probes to study the function of a particular kinase, large parts of the human kinome still miss an appropriate molecule that meet the chemical probe criteria. The full target space and the selectivity of a compound must be known in order to identify a small molecule as potential chemical probe. Chemical proteomics approaches, such as the Kinobeads technology enable the identification of drug-protein interactions on a kinome wide scale in close-to-physiological conditions. The objective of this work was to elucidate the target space of a large library of small molecule kinase inhibitors (clinical drugs and compounds from medicinal chemistry programs in the pharmaceutical industry) using an optimized chemical proteomics (Kinobeads) workflow, in order to find new highly selective chemical probes, novel compounds for the so far undruggable kinome and to better understand their modes of action.

In this work, the Kinobeads matrix was first optimized to extend the kinome coverage to PIKK and PI3K kinases. Additionally, the experimental procedure of a Kinobeads pulldown was changed to reduce the time for sample preparation and data acquisition (Chapter 1). The optimized Kinobeads assay was then used to elucidate the target space of 1,232 small molecule kinase inhibitor (Chapter 2) which led among others to the identification of selective compounds for the kinases CK2 and SYK and compounds targeting the understudied kinase PKN3. In addition to the tool compounds, the Kinobeads assay was used to systematically elucidate the target space of clinical kinase inhibitors with special emphasis on clinical mTOR and BTK inhibitors (Chapter 3). Finally, the influence of different ATP concentrations in the lysates on the targets binding affinities was investigated (Chapter 3).

Experimental Procedures

Table of contents

1 Cell Culture

Cell culture and reagents. Compound profiling was performed using a lysate mixture of five cancer cell lines (OVCAR-8, Colo205, K-562, MV-4-11, and SK-N-BE(2)). To generate the lysate, OVCAR-8 cells were grown in Iscove's Modified Dulbecco's Medium (IMDM, Biochrom GmbH). Colo205, K-562 and MV-4-11 cells were cultured in RPMI medium 1640 (RPMI1640, Biochrom GmbH) and SK-N-BE(2) cells were grown in Dulbecco's modified Eagle medium/Ham's F12 (DMEM:Ham's/F12, Biochrom GmbH). All were supplemented with 10 % (v/v) fetal bovine serum (Biochrom GmbH). RKO cells were cultured in IMDM supplemented with 10 % (v/v) fetal bovine serum. SK-BR-3 cells were grown in DMEM:Ham's/F12 medium supplemented with 10 % (v/v) fetal bovin serum.

Linkable Omipalisib was synthesized as reported previously [203] Published kinase inhibitor set (PKIS) and published kinase inhibitor set 2 (PKIS2) were provided free of charge by the Structure Genomics Consortium (SGC). The kinase chemogenomic set (KCGS) was purchased from the SGC. Roche library was provided free of charge by Roche (Hoffmann-La Roche, Basel, Switzerland). Clinical kinase inhibitors were commercially sourced from Selleckchem, MedChemExpress, Active Biochem and LC Labs.

CK2 inhibitor treatment (performed by Laszlo Gyenis under supervision of David William Litchfield, Western University, London, Canada). U2-OS cells with tetracycline regulated expression of exogenous CSNK2A1 with C-terminal HA tag were cultured in Dulbecco's modified Eagle's medium (DMEM) supplemented with 10 % fetal bovine serum and antibiotic supplements (0.1 mg/mL streptomycin and 100 units/mL penicillin, 15 µg-mL Blasticidine and 150 µg-mL Hygromycin B) at 37 °C with 5% CO_2. The exogenous kinase was either the wild type (WT) or the CX-4945 inhibitor resistant form of the kinase containing a triple mutation of V66A/H160D/I174A. The cell line was developed in the Lichtfield lab following the recommendations of Flp-In™ T-REx cell line development of Thermo Fisher Scientific. Cells were induced by adding tetracycline to the media with a final concentration of 1 µg/mL for 24 h. Subsequently, CK2 inhibitors (final concentration of 10 µM) or DMSO as control were added and cells were incubated for 24 h prior harvesting.

Protein knock down with small interference RNA (siRNA). Knockdown of PKN3 in RKO cells were performed by siRNA (siPOOLs Biotch GmbH, Planegg, Germany) according to the instructions of the manufacture. Briefly, PKN3 siRNA was diluted with Opti-MEM to a concentration of 0.05 µM. siRNA dilution was then mixed in a 1:1 ratio with Lipofectamine RNAiMAX (diluted by a factor 100 in Opti-MEM; Thermo Fisher Scientific) by vortexing and incubated for 5 min at room temperature. The transfection mixture was transferred to the bottom of a fresh 10 cm cell culture plate and RKO cells were added in a density of $1x10^6$ cells/mL. Knockdown was controlled by PRM assay (parallel reaction monitoring mass spectrometry) where specific PKN3 peptides were monitored. A complete knockdown was observed after 48 h and a final siRNA concentration of 1 nM.

NanoBRET target engagement assay (performed by Benedict-Tillman Berger under supervision of Dr. Susanne Mueller-Knapp, Goethe-University in Frankfurt, Germany). The detailed protocol for cell transfection and BRET measurement was published elsewhere.[120,204] In brief, full-length PKN3 ORF (Promega) cloned in frame with a C-terminal NanoLuc-fusion were transfected into HEK293T cells using FuGENE HD (Promega, E2312) and proteins were allowed to express for 20 h. Serially diluted inhibitor and NanoBRET Kinase Tracer K5 (Promega, N2530) at 150 nM were pipetted into a 384-well plates using an Echo acoustic dispenser (Labcyte). The PKN3 transfected cells were added at a density of 2 x 10^5 cells/mL after trypsinization and re-suspending in Opti-MEM without phenol red (Life Technologies). The system was allowed to equilibrate for 2 h at 37°C and 5 % CO_2 prior to BRET measurements. BRET signaling was measured by adding NanoBRET NanoGlo Substrate and Extracellular NanoLuc Inhibitor (Promega) according to the manufacturer's protocol. Filtered luminescence was measured on a PHERAstar plate reader (BMG Labtech) equipped with a luminescence filter pair (450 nm BP filter (donor) and 610 LP filter (acceptor)). Competitive displacement data were then graphed using GraphPad Prism 8 software using a 4-parameter curve fit with the following equation:

$$Y = bottom + \frac{(top - bottom)}{1 + 10^{(LogIC50 - X) * hillslope)}} \quad (7)$$

Cell-based Kinobeads assay. K-562 cells were adjusted to a density of 1.2x10^5, 7.2x10^4, 2.5x10^4, 7.8x10^4 and 2.4x10^5 cells per mL in RPMI1640 medium for Acalabrutinib, Zanubrutinib, Evobrutinib, ONO-4095, and Ibrutinib, respectively. The cell suspension was evenly distributed in 9x 25 mL in 50 mL tubes and compounds were added to a final concentration of 0, 3, 10, 30, 100, 300, 1000, 3000, 10000 nM (final DMSO concentration: 0.1 % (v/v)). The highest compound concentration was substituted by 30 µM for Acalabrutinib, ONO-4095 and Ibrutinib. After incubation of cells for 1 h at 37 °C and 80 rpm shaking, cells were washed twice by re-suspending the cell pellet in 25 mL of fresh medium. In between the washing steps, cells were incubated for 30 min at 37 °C and 80 rpm shaking. Subsequently, cells were washed twice in 10 mL ice cold phosphate-buffered saline (PBS). After each washing step, cells were centrifuged for 5 min at room temperature and 1,000 rpm.

2 Biochemistry

Compound immobilization. Probe 1, 5, 13, 19 and BGT226 were immobilized on NHS-activated sepharose 4 Fast Flow beads (GE Healthcare) by covalent linkage by their primary amine as described previously.[147] Briefly, beads (15 mL) were equilibrated with DMSO and the respective compound was added to the beads. The coupling density was adjusted to 2 µmol/mL beads for probe 5, 13 and 19 and to 1 µmol/mL beads for probe 1 and BGT226. The reaction was initiated by adding triethylamine (225 µL) and took place for 20 h on an end-over-end shaker in the dark. Free remaining NHS-groups on the beads were blocked with aminoethanol (750 µL) and incubated for 20 h on an end-over-end shaker in the dark. To remove o-nitrobenzenesulfonyl (oNBS) protection group of probe 13, beads were equilibrated in dimethylformamide (DMF) and subsequently washed six times using N-methyl-2-pyrrolidon (10 mL), 1,8-diazabicyclo(5.4.0)undec-7-ene (7.5 mL) and β-mercaptoethanol (7.5 mL). Probe 7 and linkable Omipalisib were immobilized on "reverse" NHS-activated sepharose beads through covalent linkage via carboxylic acid functional groups as described previously.[147,203] Briefly, to functionally "reverse" beads, an ethylenediamine spacer was introduced by addition of a mixture of ethylenediamine (40.2 µL), aminoethanol (144.9 µL) and triethylamine (225 µL) to equilibrated beads. After incubation for 20 h on an end-over-end shaker at room temperature in the dark, beads were re-equilibrated in DMF and compound, N,N-diisopropylethylamine (1.5 mL of a 200 mM solution in DMF) and triethylamine (300 µL) was added. The reaction was initiated by addition of the amino coupling reagent PyBrOP (1.5 mL of a 100 mM solution in DMF) and incubated for 20 h at room temperature in the dark on an end-over-end shaker. A coupling densisty of 1 or 2 µmol/ml beads were adjusted for linkable Omipalisib and probe 7, respectively. To block remaining binding sites, NHS-acetate was prepared by mixing equal amounts of 200 mM dicyclohexylcarbodiimide and 200 mM NHS in acetonitrile. The NHS-acetate was added to beads and incubated for 20 h at room temperature in the dark on an end-over-end shaker. Coupling reaction was controlled by LC-MS/MS analysis. Beads were stored in ethanol at 4 °C until further use.

Cell-based competition binding assay. Cell pellets were lyzed in so-called compound pulldown (CP) buffer (50 mM Tris/HCl pH 7.5, 5 % Glycerol, 1.5 mM $MgCl_2$, 150 mM NaCl, 1 mM Na_3VO_4, 25 mM NaF, 1 mM DTT) supplemented with 0.8 % IGEPAL (Sigma Aldrich), protease inhibitor (Sigma Aldrich) and phosphatase inhibitor (prepared in-house according to the formula of Phosphatase inhibitor Cocktail 1, 2, and 3 from Sigma). Subsequent Kinobeads enrichment was performed as describes for lysate-based competition binding assay.

Lysate-based competition binding assay. For inhibitor selectivity profiling cells were lyzed in compound pulldown (CP) buffer supplemented with 0.8 % IGEPAL (Sigma Aldrich), protease inhibitor (Sigma Aldrich) and phosphatase inhibitor (prepared in-house according to the formula of Phosphatase inhibitor Cocktail 1, 2, and 3 from Sigma). Cell lysates of Colo205, SK-N-BE(2), MV-4-11, K-562 and OVCAR-8 were mixed in a ratio of 1:1:1:1:1 regarding to the total protein amount as determined by Bradford assay. If necessary the lysate mixture was further diluted with lysis buffer to reach a final protein concentration of 10 mg/mL. The lysate was cleared by

ultracentrifugation at 52,000 rpm for 20 min at 4°C and further diluted with lysate buffer without IGEPAL to a final protein concentration of 5 mg/mL. A total amount of 2.5 mg of protein was pre-incubated with compound dilutions in DMSO (either 0, 100, 1000 nM final concentrations for two-dose screen or 0, 3, 10, 30, 100, 300, 1000, 3000, 30000 nM final concentrations for full dose screen) for 45 min at 4°C. Subsequently, lysates were incubated with 17.5 µL settled Kinobeads ε for 30 min at 4°C. Flow through of the DMSO control was recovered for pulldown of pulldown experiment where the lysate was incubated a second time to fresh Kinobeads. Beads were washed with 1 mL 1xCP buffer supplemented with 0.4 % IGEPAL, 2 mL 1xCP buffer containing 0.2 % IGEPAL and 3 mL 1xCP buffer.

Kinobeads bound proteins were reduced with 50 mM DTT in 8 M Urea, 40 mM Tric HCl (pH 7.4) for 30 min at room temperature and 700 rpm shaking. Reduced disulfide bridges were alkylated with 55 mM chloroacetamide. The urea concentration was reduce to 1-2 M by adding 6 volumes of 40 mM Tris HCl (pH 7.4). Proteins were digested over night by adding trypsin roughly at a 1:10 enzyme-to-substrate ratio and incubated overnight at 37°C on a shaker at 700 rpm. On the next day, digests were acidified by adding formic acid (FA) to 1 %.

Peptides were desalted on SepPakt tC18 µEluation plates (Waters) using a vacuum chamber. C18 material was conditioned with 500 µL 100 % ACN (acetonitrile), 500 µL desalting solvent B (0.1 % FA in 50 % ACN) and subsequently equilibrated with 500 µL desalting solvent A (0.1 % FA in H_2O). Samples were slowly loaded five times. Subsequently, bound peptides were washed three times with desalting solvent A. Elution of peptides was performed by applying two times 40 µL desalting solvent B. Samples were frozen, dried by vacuum centrifugation, and stored at -20°C.

Kinobeads competition pulldowns with subsequent in-gel digestion of proteins was performed as described previously.[60,147]

Kinase activity assay (performed by ProQinase GmbH, Freiburg, Germany). Dose dependent activity inhibition of CK2alpha1, CK2alpha2 and CDK1/cyclinB were measured for four inhibitors using a FlashPlateTM-based radiometric assay at K_M (ATP) of the corresponding kinase.

Immunodetection of CK2 substrates (performed by Laszlo Gyenis, Western University, London, Canada). Western blotting was performed as reported previously[205,206] using 10 µg of cell lysate and the following antibodies: anti-phospho-EIF2S2 pS2 (1:10.000)[205], EIF2S2 (Novus; 1:500), GAPDH (Millipor; 1:1000), totalCSNK2B[207] (1:10.000), totalCSNK2A1/totalCSNK2A2[208] (1:2000) and phosph-CK2 substrate [(pS/pT)DXE] (Cell Signaling Technology; 1:1000).

Cytokine secretion assay in response to SYK inhibitors (performed by Larsen Vornholz under supervision of Prof. Dr. Jürgen Ruland, Technical University of Munich, Germany). Primary bone marrow-derived dendritic cells (BMDCs) were obtain from 9 weeks old C57BL/6 mice which were maintained under standard specific pathogen-free conditions. BMDCs were differentiated for seven days in RPMI (Gibco) containing 10 % (v/v) fetal calf serum, Penicillin/Streptomycin (Gibco), 0.05 mM 2-Mercaptoethanol (Gibco) and GM-CSF. On day seven, BMDCs were seeded in 96-well plates at 10^5 cells per well in 100 µL culture medium followed by incubation at 37°C for 4 h. Cells were then incubated with SYK inhibitors for 30 min followed by stimulation with Zymosan (final

concentration of 50 ng/mL; Invivogen) and dispersed in culture medium for 24h. Subsequently, cell culture medium was harvested and concentrations of TNF, IL-6 and IL-10 in the supernatant were determined using mouse ELISA kits (IL-6/TNF: eBioscience, IL-10: Invitrogen) according to the manufacturer's protocol.

Drug-perturbed phosphoproteome analysis. For global phosphoproteomic analysis of PKN3 inhibitors, RKO cells were treated with 1 µM GSK949675A, THZ1, GSK902056A, SB-476429A or DMSO as vehicle control for 1 h in four biological replicates. For phosphoproteomics analysis of mTOR inhibitors SK-BR-3 cells were treated with AZD-8055, OSI-027, CC-223, Everolimus or DMSO for 30 min. After the desired treatment duration with indicated compounds, cells were washed twice in PBS (Sigma Aldrich) and lyzed by adding 300 µL lysis buffer (40 mM Tris-HCl pH 7.6, 8 M Urea, EDTA-free protease inhibitor complete mini (Roche) and phosphatase inhibitor cocktail). Lysates were sonicated (10 cycles, 30 sec on, 30 sec pause, at 4°C) and subsequently cleared by centrifugation for 20 min at 21,000xg at 4°C. The protein concentration was determined by Bradford and 300 µg protein per condition was used for digestion. After reduction with 10 mM DTT and alkylation with 50 mM chloroacetamide, the urea concentration was reduced to 1.5 M by adding six volumes of 40 mM Tris-HCl pH 7.6. By adding trypsin in an enzyme-to-substrate ratio of 1:50, proteins were digested over night at 37 °C. On the next day, samples were acidified to a pH of less than 3 with 0.5 % trifluoroacetic acid (TFA) and desalted using 50 mg SepPak columns (Waters; wash solvent: 0.07 % TFA in deionized water; elution solvent: 0.07 % TFA, 50 % ACN). Subsequently, samples were frozen at -80 °C and dried by vaccum centrifucation. Before TMT labelling, peptide concentrations were determined by NanoDrop™ 2000 spectrophotometer (Thermo Fisher Scientific) to adjust the peptide amount. TMT 6-plex labelling were performed as described before.[209] Phosphopeptides were enriched using column based Fe-IMAC as described before.[210] Subsequently, labelled and enriched phosphopeptides were separated into six fraction using high pH reversed-phase stage tips as described previously.[211] After freezing, samples were dried down by vacuum centrifugation and stored at -20°C.

CellTiter-Glo® Luminescent assay. To measure the ATP concentrations in cell lysates the CellTiter-Glo Luminescent assay (Promega) was performed according to the manufacturer's protocol. Briefly, a MgATP standard dilution was prepared (concentrations ranging from 10 nM to 5 mM). Equal volumes of assay reagent and standard dilution or sample were combined in a luminometer compatible tube and mixed briefly. After incubation for 10 min in the dark, the luminescence was recorded.

3 Mass Spectrometry and Data Analysis

LC-MS/MS measurements. NanoLC-ESI-MS measurements of two dose and eight dose Kinobeads pulldown samples were performed using a Dionex Ultimate3000 nano HPLC coupled online to an Orbitrap HF (Thermo Fisher Scientific) mass spectrometer. Peptides were delivered to a trap column (75 µm x 2 cm, packed in-house with 5 µm C18 resin; Reprosil PUR AQ, Dr. Maisch) and washed for 10 min with 0.1 % FA at a flow rate of 5 µL/min. Subsequently, peptides were transferred to an analytical column (75 µm x 45 cm, packed in-house with 3 µm C18 resin; Reprosil Gold, Dr. Maisch) at 300 nL/min and separated within a 52 min gradient ranging from 5 to 33 % solvent B (0.1 % FA, 5 % DMSO in ACN) in solvent A (0.1 % FA in 5 % DMSO). The Orbitrap HF was operated in data dependent acquisition (DDA) and positive ionization mode. MS1 spectra were recorded in the Orbitrap from 360 to 1300 m/z at a resolution of 120K (60K resolution of eight dose Kinobeads pulldown samples), using an automatic gain control (AGC) target value of 3e6 charges and a maximum injection time of 10 ms. Up to 5 (12 for eight dose pulldowns) peptide precursors were selected for fragmentation by higher energy collision-induced dissociation (HCD) using 25 % normalized collision energy (NCE), an isolation width of 1.7 m/z, a maximum injection time of 22 ms (75 ms for eight dose pulldowns), and an AGC value of 1e5 charges (2e5 for full dose pulldowns). Resulted fragment ions were recorded in the Orbitrap. A previous experimentally obtained inclusion list containing approximately 3,700 kinase peptide m/z and their corresponding retention time values, was enabled. Dynamic exclusion was set to 30 sec.

Nano-flow LC-MS/MS measurement of TMT-labeled phosphopeptides was performed using a Dionex Ultimate3000 nano HPLC coupled online to an Orbitrap Fusion Lumos Tribride (Thermo Fisher Scientific) mass spectrometer. Peptides were delivered to a trap column (75 µm x 2 cm, packed in-house with 5 µm C18 resin; Reprosil PUR AQ, Dr. Maisch) and washed for 10 min with 0.1 % FA at a flow rate of 5 µL/min. Subsequently, peptides were transferred to an analytical column (75 µm x 45 cm, packed in-house with 3 µm C18 resin; Reprosil Gold, Dr. Maisch) at 300 nL/min and separated within a 90 min gradient ranging from 4 to 32 % solvent B (0.1 % FA, 5 % DMSO in ACN) in solvent A (0.1 % FA in 5 % DMSO). MS1 spectra were recorded in the Orbitrap from 360 to 1300 m/z at a resolution of 60K, using an AGC target value of 4e5 charges and a maximum injection time of 20 ms. MS2 spectra were recorded in the Orbitrap at 15K resolution after HCD fragmentation using 35 % NCE, an AGC target value of 5e4, maximum injection time of 22 ms, and an isolation width of 0.7 m/z. The first mass was fixed to 100 m/z. The number of MS2 spectra was limited by a Top10 method. For TMT quantification an additional MS3 spectrum was acquired in the Orbitrap over a scan range of 100-1000 m/z at 15K resolution (AGC of 1e5, maximum injection time of 50 ms). For this, fragment ions were selected by multi-notch isolation in the Quadrupole, allowing a maximum of 10 notches, and subsequently fragmentation by HCD at 55 % NCE. Dynamic exclusion was set to 90 sec.

Protein identification and quantification. Peptide and protein identification and quantification were performed using MaxQuant with its built in search engine Andromeda.[190,198] Tandem mass spectra were searched against all canonical protein sequences as annotated in the Uniprot reference database (human proteins only, 20,230 entries, downloaded 06.07.2017). Carbamidomethylated cysteine was set as fixed modification. Variable modifications included

phosphorylation of serine, threonine or tyrosine, oxidation of methionine, and N-terminal protein acetylation. Trypsin/P was specified as proteolytic enzyme with up to two missed cleavage sites. For Kinobeads pulldown samples, label-free quantification[197] and match-between runs option were enabled. For phosphopeptide samples, TMT6plex reporter ions were specified for quantification and isotope impurities of TMT batches were specified in the configuration of modifications to allow automated correction of TMT intensities. Results were filtered for 1 % peptide and protein false discovery rate (FDR) employing a target-decoy approach using reversed protein sequences.

Data analysis of two-dose competition binding assays. Each drug was processed together with all DMSO controls that were performed on the same plate. Additionally, each search was supplemented with high quality DMSO controls. The resultant file (proteinGroups.txt) was used for subsequent filtering, normalization, data visualization and target annotation which was automatically performed by an automatic data processing pipeline written by Mathias Wilhelm (Chair of Proteomics and Bioanalytics, Technical University of Munich, Germany). First, reverse hits, potential contaminants and not quantified proteins in the DMSO control samples were discarded. Protein raw and LFQ intensities were normalized to the median DMSO control intensity to obtain relative residual binding intensities and standard deviations for each protein group at every concentration. IC_{50} values were estimated based on the following equation where [I] is the inhibitor concentration that was used for IC_{50} calculation and "inhibition" the relative residual binding intensity.

$$IC_{50} = [I]\ x\ \frac{100 - inhibiton}{inhibiton} \tag{8}$$

Estimated K_d^{app} values were then calculated by multiplying the estimated IC_{50} values with a protein-dependent correction factor that was limited to a maximum value of one. In this study, the correction factors were set to the median of correction factors across all experiments using the same lysate mixture and the same beads.

Targets of kinase inhibitors were annotated using the random forest classifier developed by Florian Seefried under supervision of Mathias Wilhelm and Tobias Schmidt (Chair of Proteomics and Bioanalytics, Technical University of Munich, Germany). A training dataset was analyzed manually. Hereby, a protein was considered a high-confidence target if the relative residual binding intensity was reduced by at least 30 % at the highest compound concentration and if the standard deviation of the relative residual binding intensity was significantly lower than the overall reduction of the median relative intensity. Additionally, the number of unique peptides and MSMS spectra were also included as target selection criteria. Peptide intensity in DMSO controls and MS/MS data quality were also taken into account.

Targets were considered as direct Kinobeads binders if annotated in Uniprot.org as a protein or lipid kinase, a nucleotide binder, ATPases and GTPases, a FAD cofactor containing protein (e.g. NQO2) and a heme containing protein (e.g. FECH). Most other target proteins were interaction partners/adaptor proteins of kinases and were termed indirect Kinobeads binders.

Binding affinities are reported as pK_d^{app} values which is the negative logarithm of K_d^{app} in mol/L. Figures and tables were produced in GraphPad Prism 5 (version 5.01), Excel and R.

Data analysis of eight-dose competition binding assays. Data processing was performed as described in Klaeger *et al*.[60] Briefly, raw MS files of pulldowns for one drug was processed together with five high-quality DMSO controls. LFQ intensities were normalized to DMSO controls and EC_{50} values were deduced by a four-parameter log-logistic regression using an in-house pipeline based on the drc add-on in R. K_d^{app} values were calculated by multiplying a protein-dependent depletion faction with EC_{50} values.

Targets were annotated manually. A protein was considered as high confidence target if the binding curve showed a sigmoidal shape with a dose-dependent intensity reduction. Proteins that only showed an effect at the highest concentration were not considered as target. The number of unique peptides and MSMS spectra were also taken into account and should ideally show the same behavior as the binding curve with increasing inhibitor concentrations. Peptide intensity in the DMSO control was also included in target selection.

Concentration and target dependent selectivity calculation (CATDS). The CATDS is a measure of the target engagement of a specific protein at a certain drug concentration relative to the target engagement of all targets at that drug concentration. The $CATDS_{target}$ was determined at the respective K_d^{app} concentration of the targeted protein and was calculated as described previously.[60]

Data analysis of phosphoproteomics experiments. All four replicates were searched together. Decoy and potential contaminants were removed. Within one replicate the total sum of each TMT channel was calculated and normalized to the DMSO control (total sum normalization). Additionally, the average intensity for each phosphopeptide per replicate was normalized to the average intensity of the same phosphopeptide across all replicates (row wise normalization).The Perseus software[212] was utilized for Student's t-tests using log-transformed TMT intensities. Statistical tests were corrected for multiple testing by an FDR of 1 %. S0 was computed for each statistical test separately in R (function "samr"). Only phosphopeptides that were detected in at least three of four replicates were considered for analysis. GraphPad and excel were used for data visualization.

Results and Discussion

Table of contents

1 Optimized Kinobeads Assay for Higher Throughput Target Identification of Protein and Lipid Kinase Inhibitors

The Kinobeads technology is a powerful approach for target deconvolution of small molecule ATP-competitive kinase inhibitors under close-to-physiological conditions.[145] It is a quantitative binding assay that relies on an affinity matrix able to compete with a compound of interest for binding to target proteins in cell lysates (Introduction Chapter 3.2). The "target panel" that can be profiled with this chemical proteomics approach is defined by the nature of the immobilized chemical probes and by the input biological material. Even though great efforts have been made to expand assay coverage by combining complementary affinity probes and complementary lysates[147], the previous setup enabled the enrichment of 260 kinases out of a lysate mixture of four cancer cell lines but did not systematically cover the clinically relevant phosphatidylinositol 3-kinase (PI3K) and phosphatidylinositol 3-kinase-related kinase (PIKK) families.[60,145,147,213,214] Hence, this chapter first focuses on the development of a new version of Kinobeads together with an improved cell lysate mixture to increase kinome coverage. Furthermore, chemical proteomic experiments like the Kinobeads technology requires large quantities of cell extract to obtain several milligrams of total protein per experiment. In the previous setup, a competitive Kinobeads pulldown experiment using eight compound concentrations and one vehicle control per compound consumed a total of 45 mg protein. Such large amounts prohibit the profiling of a large number of compounds with the Kinobeads technology. Thus, efforts were also dedicated to reduce the required amount of input material and the number of inhibitor doses without effecting the quality of the data. Additional optimization work were concerned with shortening the time required for samples preparation and data acquisition by reevaluating the digestion and the mass spectrometric measurement time. To envision the profiling of over thousand compounds using the Kinobeads technology, a new data analysis pipeline needed to also be established to leverage all those experimental improvements.

1.1 Increased Kinome Coverage of Kinobeads assay

(In the following subchapter, parts of the publication "Chemoproteomic Selectivity Profiling of PIKK and PI3K Kinase Inhibitors"[203] are included.)

Immobilization of BGT226 and Omipalisib for enrichment of PI3Ks and PIKKs. To develop a novel version of Kinobeads that extends kinome coverage to the PI3K and PIKK families, the first step was to screen the literature for potent ATP-competitive small molecule PIKK and PI3K inhibitors that could be immobilized onto a solid matrix to generate new affinity matrices. The literature search was mainly done by Guillaume Médard and Benjamin Ruprecht from the Chair of Proteomics and Bioanalytics, Technical University of Munich. Among others, the commercially available dual PI3K/mTOR inhibitor BGT226[215,216] with IC_{50} values of 4 nM, 63 nM and 38 nM for PIK3CA, PIK3CB and PIK3CG respectively, could be directly coupled to NHS-activated beads via its

piperazine amine (Figure 11 A). BGT226 shares the tricyclic imidazoquinolinone ring core of NVP-BEZ235 (Figure 11 A) and it has been reported that NVP-BEZ235 potently inhibits PIK3CA, PIK3CB, PIK3CG, mTOR, and ATR.[217,218] Omipalisib has been reported as potent inhibitor for all PI3K isoforms but cannot be directly coupled to beads (Figure 11 B).[219] Yet, a pyridazine-replacing benzoic acid analogue of Omipalisib CAS1313994–59–0 (Patent WO2011082285[220]) can be immobilized via an amide bond. The decision of using this analogue as potential affinity probe was further substantiated by the reported activity of the pyrrolidine ester analogue (CAS1607009–17–5; IC_{50} of 0.70 nM versus 0.77 nM for Omipalisib against PIK3CA in the Kinase-Glo assay (Figure 11 B); Patent WO2014067473[221]) and the X-ray structure of the co-crystal Omipalisib with PIK3CG (PDB: 3L08[219]) indicating that the carboxylic acid should be pointing toward the solvent (Figure 11 C). The immobilizable Omipalisib analogue was synthesized following the route reported for the Omipalisib series.[219]

Next, BGT226 and the linkable analogue of Omipalisib were immobilized on NHS-activated Sepharose beads (referred to as iBGT226 and iOmipalisib from here on) and a pulldown experiment was performed using a cell lysate mixture of four cancer cell lines (MV-4-11, K-562, Colo205 and SK-N-BE(2)) followed by tandem mass spectrometry readout. The affinity matrices efficiently captured PIKKs and PI3Ks and specificity of the enrichment was confirmed by competition experiments using the free respective inhibitors as competitor. In summary, iBGT226 was able to specifically enrich PIK3C2A, PIK3C2B, PIK3CA, PIK3CG, PIK3C3, mTOR, PRKDC, ATM, and ATR and iOmipalisib showed specific enrichment of PIK3C2A, PIK3C2B, PIK3CA, PIK3CB, PIK3C3, PI4KA, PI4KB, PRKDC, and mTOR.

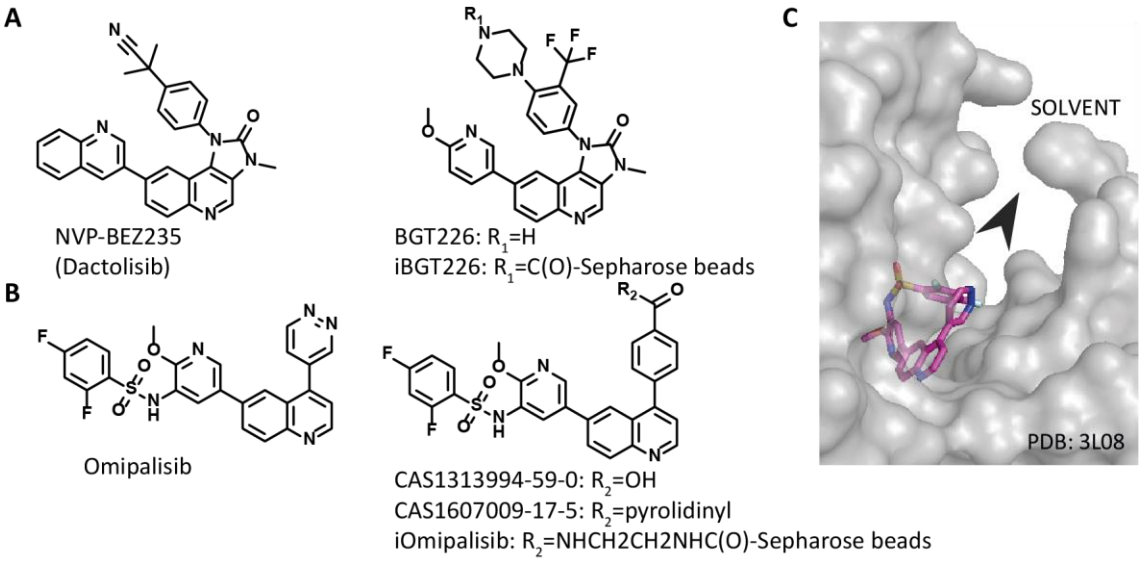

Figure 11 | Chemical structure of novel PIKKs and PI3Ks affinity probes and their parent compounds. (A) Structure of the commercially available pan-PI3K inhibitor BGT226 that shares the tricyclic imidazoquinolinone ring core with the pan mTOR/PI3K and ATR inhibitor NVP-BEZ235. BGT226 can be directly immobilized on beads via its piperazine amine to yield iBGT226. (B) Chemical structure of Omipalisib and its pyridazine-replacing benzoic acid/ester analogues. The benzoic acid can be immobilized on Sepharose beads via its carboxylic acid moiety to yield iOmipalisib. The pyrolidine ester analogue has been reported to exhibit similar activity on PIK3CA as Omipalisib.[221] (C) Co-crystal structure of PIK3CG and Omipalisib, indicating that the carboxylic acid of the analogue points towards the solvent (PDB:3L08).

Extending coverage of Kinobeads to PI3Ks and PIKKs by adding new affinity probes. To extend the kinome coverage of the latest Kinobeads version (Kinobeads γ, KBγ) to PI3Ks and PIKKs, the aim was to combine KBγ with iBGT226 and iOmipalisib. This would enable determination of binding affinities of a compound toward PI3Ks, PIKK and the ePKs captured by KBγ within one experiment. Therefore, iOmipalisib beads were combined with the KBγ matrix in different mixing ratios: iOmipalisib:KBγ in a ratio of 1:1, 1:5, or KBγ alone. A eight dose competitive pulldown experiment (0.3 nM - 1 µM plus vehicle control and pulldown of pulldown for target depletion) was performed using Omipalisib as competitor and a lysate mixture of five cancer cell lines (MV-4-11, K-562, Colo205, SK-N-BE(2) and OVCAR-8). In the resulting dose-response curves, some PIKK family members such as mTOR and PRKDC, could not be completely competed when the proportion of iOmipalisib on the bead mixture was too low (Figure 12 A). One reason for this could be that those proteins are allosterically bound by one of the KBγ affinity probes preventing competition by the ATP-pocket binders. Since the number of captured ePKs did not significantly diminish with a higher ratio of iOmipalisib (1:1) and the number of quantified PIKKs and PIKs remained identical (Figure 12 B), a KBγ:PIK(K)-matrix ratio of 1:1 was chosen to maximize the dynamic range of the observable competition.

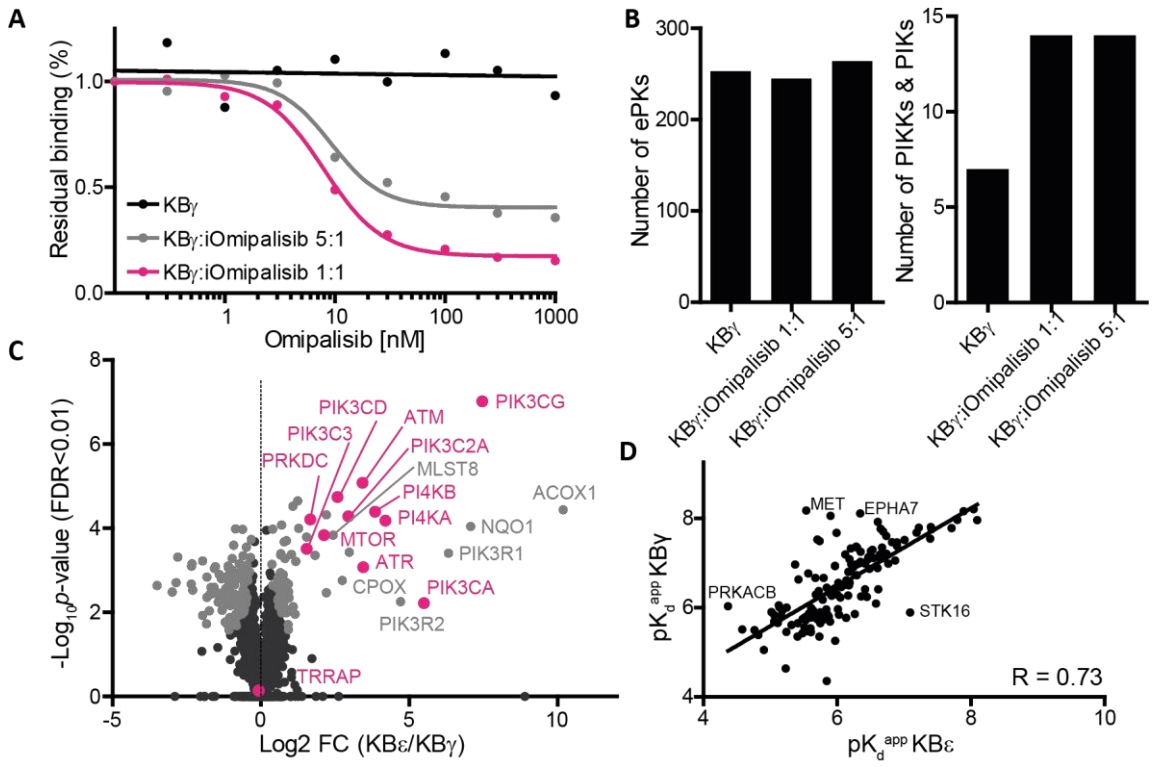

Figure 12 | Addition of iOmipalisib and iBGT226 to KBγ allows for PIKK and PI3K inhibitor profiling. (A) Dose-response curves for mTOR after competitive pulldown experiments with different bead ratios of iOmipalisib and KBγ beads (KBγ:iOmipalisib of 5:1 or 1:1 or KBγ alone) using eight doses of Omipalisib as competitor (0.3 nM–1 µM). (B) Number of competed PI3Ks, PI4Ks, and PIKKs and number of identified ePKs in competitive pulldown experiments. (C) Volcano plot comparing proteins captured by KBγ and KBε in a triplicate experiment. The significance of the differences was tested in a two-sided t test (S_0 = 0.1, 1 % FDR). PIKKs (except for TRRAP), PI3Ks, and PI4Ks (all labeled in pink) were significantly enriched by KBε. Proteins exhibiting significant differences are colored in gray. (D) pK_d^{app} values of targets of the small molecule kinase inhibitor AT-9283 obtained by KBε were correlated to the ones previously published[60] using KBγ.

Next, the identity and intensity of the proteins captured by KBγ in combination with iBGT226 and iOmipalisib were examined more closely. Therefore three bead mixtures (i) KBγ supplemented by iBGT226, (ii) KBγ supplemented by iOmipalisib, and (iii) KBγ supplemented by both iOmipalisib and iBGT226 (termed Kinobeads ε, KBε, later on referred to as Kinobeads) were prepared and compared to KBγ alone. The triplicate pulldown experiments of the different matrices showed that nearly all PIKKs and PI3Ks (except for TRAPP) were statistically significantly enriched (S_0 = 0.1, 1 % FDR) by KBε over KBγ (Figure 12 C). ATM and ATR were mainly enriched by iBGT226, whereas iOmipalisib led to a stronger enrichment of PI3Ks (e.g. PIK3CA and PIK3CB; Appendix Figure S 1 A-C). Of note, interaction partners of several PIKK and PI3K family members were identified, for example MLST8 which is a known interactor of mTOR. In addition, KBε enriched some metabolic enzymes (ACOX1, NQO1, or CPOX; Figure 12 C). If this enrichment was specific, Kinobeads may provide an assay for those non-kinase proteins in the future. Such unexpected off-targets of kinase drugs have already been reported including NQO2 and FECH that are commonly engaged by small molecule kinase inhibitors.[60,148] ACOX1 uses FAD as a cofactor like NQO2, and CPOX, akin to FECH, possess a heme binding site, which renders these proteins highly susceptible to bind specifically to KBε.

Last, the very unselective protein kinase inhibitor AT-9283 was used to compare target K_d^{app} values between KBε and KBγ.[60] Here, AT-9283 was chosen because its more than 100 targets cover a broad spectrum of proteins (different protein kinase families, non-kinase targets) across an affinity range of four orders of magnitude. The target affinities determined by the two affinity matrices were reasonably well conserved (correlation of R = 0.73; Figure 12 D). The discrepancies can be explained by a few outliers caused by technical and/or biological variation. For instance, EPHA7 and MET were represented by few unique peptides in only one of the two data sets. In summary, the newly developed affinity matrix, KBε, was as good for ePKs as KBγ but also allowed studying drug interactions for 14 out of 17 PIK and PIKK kinases (Appendix Figure S 1 D). Thus, the integration of iBGT226 and iOmipalisib to the latest version of Kinobeads enables the profiling of PIKK and PI3K inhibitors.

Five cell line mixture for broad kinome coverage. Since the overall number of kinases amenable to Kinobeads profiling not only depend on the affinity matrix but also on the biological input material, the cell lysate mixture of different cancer cell lines was evaluated to further increase kinome coverage. The previous Kinobeads assay setup used a mixture of four different cancer cell lines (Colo205, K-562, SK-N-BE(2) and MV-4-11) as protein source and was able to enrich around 250 kinases.[60,147] To enhance the kinome coverage it was first tested whether the addition of a fifth cancer cell line would be beneficial. As potential fifth cell line OVCAR-8 was chosen which has been reported as the cell line with the highest diversity of kinase expression within a set of nine cancer cell lines and was easy to cultivate.[147] Therefore, Kinobeads pulldown experiments were performed with lysates from each of the five different cancer cell lines individually (Colo205, K-562, SK-N-BE(2), MV-4-11 and OVCAR-8). A total of 261 different kinases were identified with OVCAR-8 being the cell line expressing the most diverse kinase set (178 kinases in total; Figure 13 A). The number of identified kinases after Kinobeads enrichment ranged from 158 (K-562) to 167 (MV-4-11 and Colo205) for the other four cell lines. An overlap of 96 kinases could be enriched by Kinobeads from all five cell lines (Figure 13 A). Twelve kinases including ERBB3, FGFR4 and PLK2

were exclusively identified in the pulldown experiment using OVCAR-8 lysates (Figure 13 A) indicating that it might be beneficial to add the cell line to the current lysate mixture.

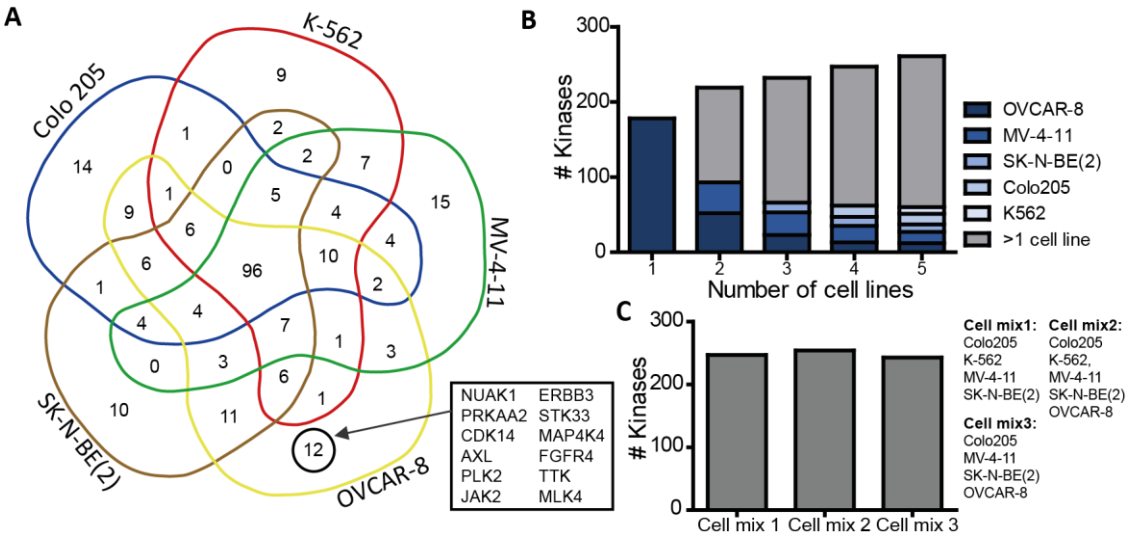

Figure 13 | Optimized cell lysate mixture for broad kinome coverage. (A) The overlap of identified kinases after Kinobeads pulldowns of different cell lines (K-562, MV-4-11, OVCAR-8., SK-N-BE(2), Colo205) is shown. The highest number of kinases are identified in OVCAR-8 lysates. (B) Stacked bar plot that shows the *in silico* prediction of the number of kinases for five different cell mixtures consisting of one to five cell lines, based on experimental single cell line lysate pulldowns. Each cell line is displayed in a different color, whereas the grey color represents kinases that are captured in at least two cell lines of the considered combination of cells. (C) Number of kinases are shown that were identified after Kinobeads enrichment out of three different cell lysate mixtures. Cell mix 2 has the highest number of kinases.

Next, kinaseblender[147] (https://github.com/ThomasKuehne/kinaseblender) was utilized to determine the best cumulative combination of the five different cell lines (Figure 13 B). While OVCAR-8 cells expressed the highest diversity of kinases, MV-4-11 was the most complementary cell line to OVCAR-8 in regard to kinome coverage. Adding a third (SK-N-BE(2)), fourth (Colo205) and fifth (K-562) cell line *in silico* could further increase the number of kinases to a total of 261 kinases. This result suggested that a slight increase in the number of kinases could be gained by adding a fifth cell line to the lysate mixture. To investigate whether this *in silico* calculation would translate in an experiment, three different cell lysate mixtures were prepared and Kinobeads pulldowns were performed. The first cell mix to be tested was a 1:1:1:1 lysate mixture of the four cell lines of the state of the art workflow. The second mix contained again the four cell lines and in addition, lysate of OVCAR-8 cells. Since K-562 showed the lowest number of exclusively expressed kinases (Figure 13 A), a third mixture was prepared with lysates of OVCAR-8, Colo205, SK-N-BE(2) and MV-4-11. Overall, the number of kinases enriched by Kinobeads were relatively similar between the three mixtures and 247, 254 and 243 kinases were identified in cell mixture one (previous setup), cell mixture two and cell mixture three, respectively (Figure 13 C). Although the five cell line mixture obtained slightly better results than the four cell line mixture, the total number of kinases was close but did not match the predicted maximal number from the *in silico* calculation. As expected, mixing different lysates lead to a dilution of low abundant and/or low affine kinases which has already been reported by Médard *et al*.[147] Too many high abundant and

potent binders in the lysate mixture prevent the enrichment of low abundant and/or low affine kinases by Kinobeads. The lysate mixture of five different cancer cell lines was used for further experiments, since it provided the highest kinome coverage.

To summarize, the addition of iOmipalisib and iBGT226 to KBγ has created a novel version of Kinobeads that enables the enrichment of the PIKK and PIK families and hence the profiling of inhibitors thereof. In addition, the coverage of ePKs could be extended by using a protein source consisting of a lysate mixture of five different cancer cell lines. This experimental setup was used for all further experiments, unless otherwise indicated.

1.2 Towards a Higher Throughput Kinobeads Assay

Improved experimental procedure to reduce sample preparation time. To enhance the throughput of Kinobeads drug profiling, the experimental workflow of a competitive Kinobeads assay was re-evaluated. First, in-gel digestion of bead bound proteins was compared to an on-bead digestion protocol. On-bead digestion of proteins does not require an elution step with subsequent SDS polyacrylamide gel electrophoresis and in-gel digestion. As the name suggests, proteins are instead directly digested on the beads potentially resulting in fewer experimental steps and significant time savings. Hence, on-bead digestion was compared to in-gel digestion in terms of number of quantified kinase peptides and reproducibility. Triplicate pulldown experiments with subsequent on-bead or in-gel digestion were performed using Kinobeads γ and lysates of a four cell line mixture (Colo205, K-562, MV-4-11, SK-N-BE(2)). To make on-bead digestion compatible with subsequent measurement, the washing steps after incubation of lysates with Kinobeads had to be changed. The Kinobeads washing buffer (CP Buffer; Experimental Procedure Chapter 2) contains 0.2 % and 0.4 % IGEPAL, a detergent that is not compatible with mass spectrometric measurement because it can block the chromatography column and can result in singly charged ions that overshadow signal of peptide ions. IGEPAL does not pose a problem for in-gel digestion as it is removed during SDS polyacrylamide gel electrophoresis. Thus, after the standard washing procedure, pulldowns subjected to on-bead digestion were washed three times with CP buffer without IGEPAL. After digestion of bead bound proteins, an additional desalting step is also required to clean up peptides and remove salt and other buffer components like urea.

Despite the additional washing steps and desalting of peptides, on-bead digestion outperformed in-gel digestion in terms of numbers of kinases and peptides. The total number of quantified kinases peptides could be increased by more than 15 % resulting in an increased number of identified kinases by 18 (Figure 14 A-B). The two digestion methods exhibit an overlap of 2008 kinase peptides (42 % of 4763 total peptides) indicating that the two methods produced similar peptides (Figure 14 B). The reproducibility was slightly superior for in-gel digestion with an overlap of 68 % of identified kinase peptides between triplicate pulldowns than for on-bead digestion with an overlap of 60 % which could be caused by the desalting step (Figure S2 A). Hence, in view of the higher number of identified kinases and kinase peptides for the more time-efficient unoptimized on-bead digestion protocol, on-bead procedure was deemed advantageous and was further optimized.

The washing procedure and the digestion conditions were evaluated. Various washing buffer volumes were assessed to decrease IGEPAL concentrations without losing low affine binders. In total seven different washing procedures were tested with volumes ranking from 1 mL to 8 mL per washing solvent. Number of identified kinases and peptides as well as unspecific binding were compared (Appendix Figure S2 B). Only minor differences in the number of kinases (231 to 249 kinases) and the total MS1 intensity of kinases relative to the total intensity of all proteins (49 % to 57 % relative intensity) were observed for the different washing procedures (Appendix Figure S2 B). Since the highest number of kinases (249) and the highest relative intensity of kinases were observed for condition 5, Kinobeads were washed with 1 mL CP buffer + 0.4 % IGEPAL, 2 mL CP buffer + 0.2% IGEPAL followed by 3 mL CP buffer for all subsequent pulldown experiments.

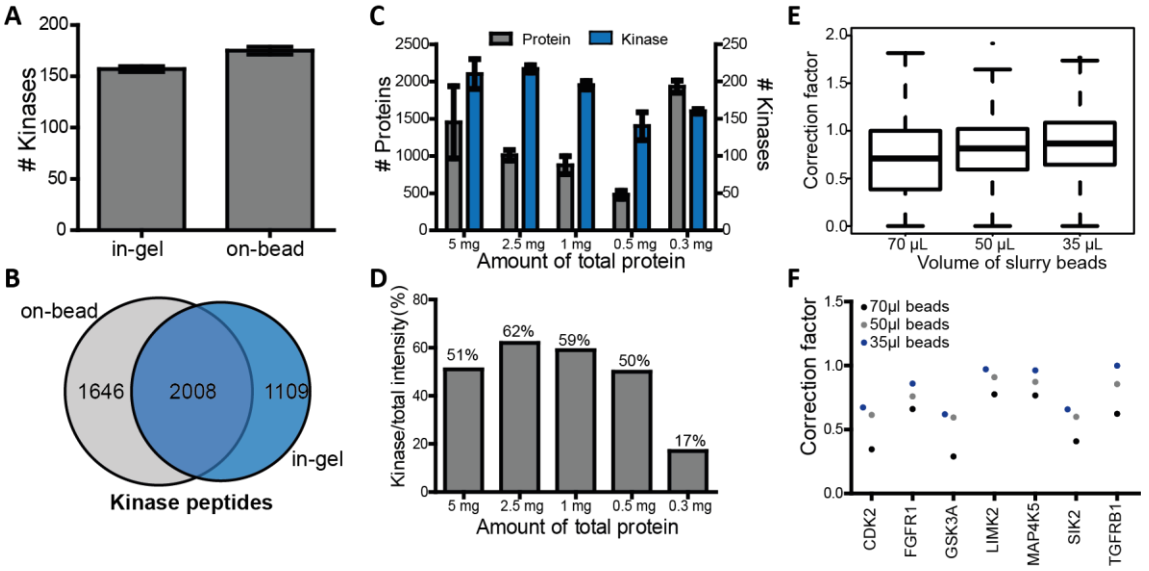

Figure 14 | Optimized experimental procedure of a Kinobeads pulldown to reduce sample preparation time. (A) Comparison of identified kinases between in-gel digestion and on-bead digestion protocol. The number of identified kinases is higher when proteins are digested on-bead. (B) Overlap of identified kinase peptides after Kinobeads pulldowns with different digestion workflows. Number of identified kinases peptides is higher for on-bead digestion. (C) Number of identified proteins and kinases using different amounts of protein while keeping protein concentration at 5 mg/mL. 2.5 mg yield similar numbers as 5 mg of proteins. (D) Relative kinase intensity depending on the amount of total protein. The proportion of kinase intensity compared to the total intensity was highest for 2.5 mg with 62 %. (E) Correction factor distribution using different slurry bead volumes (1:1 slurry in ethanol) and a constant protein amount of 2.5 mg protein. At lower bead volumes with constant protein amount, the correction factor distribution is closer to one. (F) Protein depletion is reduced for certain kinases if lower Kinobeads volumes are used for a pulldown experiment with 2.5 mg of protein.

Having established a new digestion protocol, the amount of cell extract that is needed for a pulldown experiment was re-evaluated. The production of cell extracts is very time consuming and is only feasible for screening a limited number of compounds with the previous set up, where 45 mg of protein were required to perform a selectivity profiling experiment with 8 compound concentrations plus vehicle control. Hence, for a larger profiling campaign the quantities of cell extracts have to be reduced. To miniaturize the Kinobeads workflow, pulldowns were performed using different lysate volumes (corresponding to 5 mg, 2.5 mg, 1 mg, 0.5 mg and 0.3 mg protein)

while keeping protein concentration at 5 mg/mL. Simultaneously, the volume of Kinobeads was decreased in similar ratio (slurry bead volumes of 70 µL, 35 µL, 14 µL, 10 µL, 5 µL) to maintain reasonable protein to bead ratio and void excessive protein depletion. The pulldown with 0.3 mg protein was performed in a 384-well filter plate because the sample volume became too small to be handled reproducibly in a 96-well 2 mL filter plate. Surprisingly, reducing the protein amount by a factor of two did not lead to a decrease in the number of identified kinases. In total, 210 kinases were identified with a protein input of 5 mg and 217 kinases with an input of 2.5 mg (Figure 14 C). Reducing the protein amount further by a factor of five (1 mg) and especially by a factor of ten (0.5 mg) resulted in lower numbers of identified kinases (195 and 140 kinases respectively). Additionally, the relative kinase intensity, which is indicative of the enrichment efficiency, was even higher with lower input material (Figure 14 D). 62 % of the total intensity was assigned to kinases in the 2.5 mg pulldown experiment, whereas only 51 % of the intensity was kinase-related in the 5 mg pulldown. These results led to the conclusion that the quantity of cell extracts could be reduced by a factor of two without losing kinases.

In contrast to this trend, the 384-well format with protein input of 0.3 mg led to a higher number of identified kinases (160 kinases) compared to the pulldown with 0.5 mg of protein in 96-well format (140 kinases). This seems to favor the 384-well format, however, the relative kinase intensity between the pulldowns performed in different filter plates draw another picture. When using the 384-well plate only 17 % of the total intensity was assigned to kinases, compared to over 50 % for the 96-well plate. This was probably caused by adsorption of proteins to the plastic of the plate. Hence, the 384-well plates were considered unfavorable for pulldown experiments where low background target binding is a prerequisite, to avoid dose-response curve compression.

Next, different beads volumes were tested in order to keep protein depletion as low as possible (Introduction Chapter 3.2). Ideally, chemical probes such as Kinobeads should not lead to protein depletion. For Kinobeads, however, a depletion of less than 10 % is estimated. If the bead-to-protein ratio is too high, more proteins get depleted from the lysate which leads to a shift of the compound-target equilibrium towards more dissociated species and results in higher EC_{50} values (since the apparent compound concentration required for 50 % complex concentration becomes higher). The protein depletion is examined experimentally by performing two consecutive pulldowns of the vehicle-treated lysate. The correction factor is calculated by the ratio of the intensity obtained in the second pulldown divided by the intensity measured in the first pulldown. Values close to one mean low depletion and values close to zero refer to high depletion. As expected and shown in Figure 14 D, high volumes of beads resulted in higher protein depletion. The reduction of slurry bead volumes (1:1 slurry in ethanol) from 70 µL to 35 µL led to higher correction factors which were closer to one. This trend was also illustrated for certain kinases (Figure 14 F). For example, the depletion factor of TGFBR1 was 0.62 when 70 µL beads were used and was increased to 1.0 with 35 µL slurry Kinobeads. However, the overall distribution of correction factors was relatively broad with correction factors around 0.2 to 1. As a consequence of these results, the volume of beads was reduced by a factor of two to 35 µL slurry beads, resulting in the same beads-to-protein ratio as in the original protocol.[147]

After reducing the quantity of proteins and beads, it is now possible to perform higher throughput screening using the Kinobeads technology. It might be even possible to further decrease the quantities of biological extracts by using a different 384-well plate which does not bind proteins

unspecifically. This has been reported by Eberl and coworkers[222] who reduced the protein amount to 250 µg while keeping protein concentration and the protein-to-bead ratio constant, or by Golkowski *et al*[223] who used 300 µg of protein and 5 µL beads for a pulldown experiment. Such miniaturized chemoproteomic enrichment protocols enable not only large profiling campaigns of small molecule kinase inhibitors but also the enrichment of kinases from primary material derived from tissues of patients which is often only available in very small quantities.

Optimized mass spectrometry measurement method for fast data acquisition. Within only a few years, technological advances in mass spectrometry instrumentation boosted the number of proteins analyzed per hour extensively. One of the most recent machine generations, the Q Exactive instruments (including Q Exactive HF), feature a quadrupol front for precursor selection, high ion currents provided by the S-lens and a fast fragmentation by parallel filling and detection modes.[224] In combination with almost instantaneous isolation and fragmentation, cycle times of one second for a Top10 method are achieved. Since previous Kinobeads projects[60] were analyzed with a 100 min liquid chromatography gradient on an Orbitrap Elite instrument, the performance of the older generation of mass spectrometer was compared to the performance of a Q Exactive HF instrument. Therefore, Kinobeads pulldown experiments were either measured on the Q Exactive HF with a 50 min gradient or on the Orbitrap Elite with a 100 min gradient. As expected, the number of kinases and proteins identified on the Orbitrap Elite was significantly lower, although the gradient was twice as long (Figure 15 A). The number of identified kinase peptides could be increased by 30 % with the newer generation of mass spectrometers. Hence, a shorter measurement time while increasing identification rates led to the decision to measure Kinobeads pulldown samples on a Q Exactive HF instrument.

A

	Q Exactive HF	Orbitrap Elite
Gradient time	50 min	100 min
Proteins	1998	1521
Kinases	251	215
Peptides	13105	9511
Kinase peptides	4047	3077

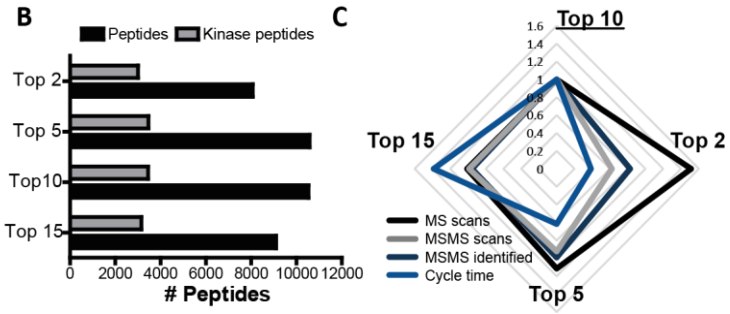

Figure 15 | Comparison of different mass spectrometers and measurement methods. (A) Table of identification features of pulldown samples measured either on a Q Exative HF or an Orbitrap Elite instrument. More proteins and peptides were identified using the Q Exactive HF instrument. (B) Bar plot showing the numbers of identified peptides and kinase peptides using different TopN methods. (C) Radarplot depicting the number of MS scans, MSMS scans, MSMS identified and cycle time of different TopN methods relative to the Top10 method. Different colors represent different parameters.

To further optimize the measurement method on the Q Exactive HF instrument, different parameters were modified to enhance identification rates and quantification. First, different injection times were tested and as expected, longer injection times (75 ms) led to an increased identification rate because more ions, especially low abundant peptides, could be collected

resulting in a better quality of MS2 spectra and higher identification rates (data not shown here). However longer injection times have the disadvantage of longer cycle times which in turn leads to fewer MS1 scans required for MS1-based label-free quantification. Therefore, the injection time was set to 22 ms to reduce the cycle time and enhance peptide quantification. Next, the state of the art Top10 methods was compared to a Top2, Top5 and Top15 methods and the influence on peptide identification as well as number of scans and cycle times were analyzed. The number of identified kinase peptides was similarly high for the Top5 and Top10 method with 3469 and 3451 peptides, respectively (Figure 15 B). The Top2 and Top15 method resulted in a decreased number of peptides (3004 and 3151 kinase peptides respectively; Figure 15 B), indicating that a Top5 or a Top10 method would be the best choice. Using the match-between-runs option in MaxQuant which matches identified features from one sample to another based on retention time and mass-to-charge ratio can further boost the identification rate. In contrary to the identification rate, stable and accurate label-free quantification depends on the number of MS1 scans over an elution peak of a peptide which can be increased by a fast cycle time. As expected the cycle time was shorter with the Top5 method (0.41 sec) than with the Top10 method (0.67 sec). Accordingly, the number of MS1 scans is also higher for the Top5 method (10,967 MS1 scans) than for the Top10 method (9,824 MS1 scans), which is however associated with a reduced number of MS2 scans (35,822 and 38,819 MS2 scans, respectively). Finally, the method of choice was the Top5 method that presented a good balance between identification rate and robust quantification and was used for the measurement of Kinobeads pulldown samples.

Recent advances in mass spectrometry instrumentation (Q Exactive HF-X) in combination with micro-flow liquid chromatography systems facilitate the identification of the same quantity of kinases within a 15 min liquid chromatography gradient, reducing expensive mass spectrometry measurement time by a factor of four.[225] Another option to shorten the measurement time is to multiplex samples by isobaric mass tag labeling like tandem mass tags (TMT).[222] This quantification method allows multiplexing of up to sixteen conditions so that all samples of one experiment (eight compound concentrations, vehicle control and target depletion control) can be combined and measured together.[222] TMT labeling also reduced missing values between samples enabling more robust data analysis. But TMT labeling can lead to ratio compression which results in an underestimation of protein competition off the beads and can hamper proper annotation of target proteins.

In summary, measurement time could be reduced through advances in mass spectrometry instrumentation. In addition, the sample preparation time was reduced by switching from in-gel digestion to the on-bead digestion protocol and by reducing the amount of biological extract required for one experiment. For all further experiments, a protein amount of 2.5 mg per pulldown was used, on-bead digestion was carried out and samples were measured using a Q Exactive HF device with a Top5 method and 50 min gradient time.

1.3 The Challenge of Screening Thousand Inhibitors Using the Kinobeads Technology

Equipped with an optimized Kinobeads profiling assay, the endeavor to profile more than 1,200 tool compounds (see Results and Discussion Chapter 2) was however still out of practical reach. The ten samples per inhibitor to measure would indeed add up to a 1.5 years mass spectrometry measurement time and around three million dose-response curves would need manual inspection. Hence, the reduction of inhibitor concentrations and improvements of the data analysis pipline were investigated. The following section details their implementation as means to face the challenge of profiling libraries of molecules and explicit the selection of quality and reproducibility controls necessary for such screening campaigns.

Reducing the number of compound concentrations for profiling. One major bottleneck of the Kinobeads profiling assay was the number of samples or more precisely the number of evaluated concentrations per inhibitor to establish a dose-response curve. With ten samples to be measured per inhibitor, using this technology as higher throughput method was prohibitive. Hence, it was investigated whether the number of concentrations could be reduced to two (plus vehicle control) and which concentration would yield enough information about compound-protein binding to access the complete target profiles. In this regard, two extreme cases can be considered: very high concentrations of the competing compound can be used to reveal optimally all binding partners, or lower concentrations could be applied to get more fine-tuned information about binding partners and their affinities. The former profits from compound concentrations that are much higher than the inflection point where all the targets are completely competed off the beads. In order to get this picture, one very high concentration like 30 µM and a low concentration like 3 nM where large parts of the interaction partners are not yet competed could be the concentrations of choice to identify all target protein. While this high concentration is suitable to give a good overview over all interactions in general, it is not appropriate to estimate IC_{50} values since most of the intensities will be zero at this concentration. On the contrary, concentrations around the inflection point would be favorable to get a more subtile picture and calculate binding parameters, even though some high affinity targets might be disregarded in such setting. Since kinase inhibitors mainly have binding affinities in the nanomolar range for their primary targets, 100 nM and 1 µM were considered as possible competitor concentrations to distinguish between very affine targets (K_d below 100 nM) and less affine target (K_d up to 1 µM), where respectively two or one datapoint(s) would be nearing zero.

In order to investigate whether this combination is suitable for the calculation of precise binding affinities, Kinobeads pulldowns of 50 clinical kinase inhibitors were performed using the optimized workflow described above and only two inhibitor concentrations. In a previous study by Klaeger *et al,* the target landscape of these 50 clinical kinase inhibitors has already been determined by the previous Kinobeads setup using eight compound concentrations (full dose response), Kinobeads γ and a lysate mixture of four cancer cell lines.[60] This dataset was used as reference to compare Kinobeads assay results of a full dose response with eight concentrations and the novel higher-throughput setup with only two concentrations. EC_{50} values for each interacting protein in

a full dose response Kinobeads pulldown experiment are deduced by a four-parameter log-logistic regression (see Experimental procedure), which is not applicable to two inhibitor concentrations. Another method was imagined, based on the studies of Kuzmic *et al*[226] about determining tight-binding inhibition constants, and the following formula was derived to estimates IC_{50} values based on a single inhibitor concentration:

$$IC_{50} = [I]\ x\ \frac{100 - inhibiton}{inhibiton} \quad (9)$$

[I] is the inhibitor concentration that is used for the IC_{50} calculation (either 100 nM or 1 µM). The 100 reflects the DMSO control intensity which is set to 100 %. 'inhibition' is the relative reduction of the MS signal intensity at the concentration that was used for IC_{50} calculation. The inhibitor concentration closest to 50 % inhibition was used for IC_{50} calculation. Only if the higher concentration led to a residual binding that was closer to 50 % inhibition but was higher than the residual binding of the lower concentration which should per default not happen, then the lower concentration was used. By multiplying with a correction factor (Introduction Chapter 3.2) that accounts for the depletion of the protein out of the lysate, the IC_{50} value was converted into an apparent dissociation constant K_d^{app}. Hence binding affinities of 50 clinical kinase inhibitors were estimated based on this formula.

The calculated apparent dissociation constants were then correlated to the ones obtained by Klaeger *et al*.[60] Overall, the pK_d^{app} values were reasonably well conserved (Pearson correlation of R=0.808) considering that a different Kinobeads version, a different cell lysate mixture and a different sample preparation protocol was used (Figure 16). Dots on the x- or y-axis represent targets that have only been identified in one of the experiments. This was expected because the new Kinobeads matrix enriched kinases that were not assessable before and the new lysate mixture cover a slightly different kinase spectrum. Additionally, the target selection criteria were slightly different between the two approaches. While the targets of the eight dose Kinobeads pulldown experiment were annotated manually as described by Klaeger *et al*[60], target annotation based on the two dose data were performed using an automated classification tool (see next paragraph for detailed description).[227] Manual annotation of targets can lead to more variations, since no strict rules are applied and the annotation depends on the subjective evaluation of an expert. A machine learning model annotates targets of an inhibitor in a more reproducible way because it follows strict rules and evaluates more objectively. In addition, variations in affinities can be caused by targets of low abundance and few unique peptides that are more susceptible to variation in their intensities and thus in their EC_{50} or IC_{50} calculation.

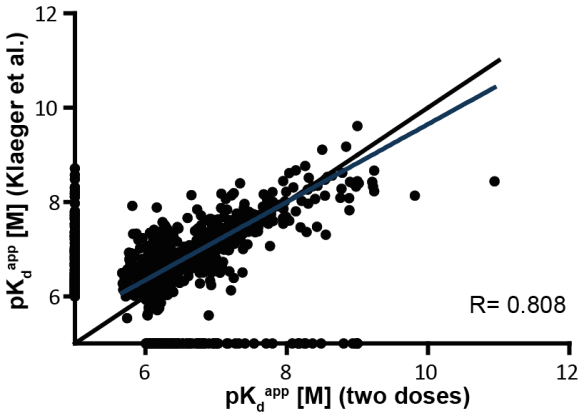

Figure 16 | Number of compound concentrations for Kinobeads pulldown experiments. pK_d^{app} values of targets of 50 clinical kinase inhibitors obtained with two inhibitor concentrations (100 nM and 1 µM) were correlated to the ones previously published[60] using KBγ and a four cell lines lysate mixture. Each dot represents one drug-target combination. Blue line depicts the linear regression whereas the black line represents the diagonal. Affinity values were reasonably well conserved with a Pearson correlation of R=0.808.

Given these influences, the correlation between the two datasets was fairly good. In summary, the two compound concentrations (100 nM and 1 µM) are sufficient to estimate an apparent dissociation constant of small molecule kinase inhibitors, which reduces the time required for experimental data acquisition and sample preparation. The selection of concentrations was further corroborated by another screening campaign of kinase inhibitors that used the same compound concentrations to profile the published kinase inhibitor library.[112]

Automatic data analysis for higher throughput. In order to achieve better reproducibility and consistency and because manual data inspection of over 1,200 compounds (see Results and Discussion Chapter 2) is impossible, targets of two-dose Kinobeads data were annotated using an automated classification tool. A random forest classifier to distinguish targets from non-targets was developed by Florian Seefried under supervision of Mathias Wilhelm and Tobias Schmidt at the Chair of Proteomics and Bioanalytics, TU Munich.[227] Therefor the targets of a limited number of compounds (around 100) were annotated manually. The annotated two-dose Kinobeads dataset was then used to train and optimize the random forest classifier (performed by Florian Seefried). The final classifier assigns a target probability score to each quantified protein in the Kinobeads dataset ranging from 0 to 100 %. Proteins with a target probability higher than 93.5 % were annotated as target of the corresponding compound and proteins below the threshold were annotated as no targets. The target probability threshold of 93.5 % reached a good balance between false positive and false negative rates. Lowering the threshold would lead to more false positive hits and increasing would result in a higher false negative rate.

To achieve an optimal and integrative way of Kinobeads data analysis, several data processing steps are required: protein and peptide identification (MaxQuant), calculation of relative intensity ratios and visualization of data together with annotation of potential targets (see Experimental procedure Chapter 3). Since these steps have to be carried out separately for each compound that has been profiled, Mathias Wilhelm from the Chair of Proteomics and Bioanalytics, Technical

University of Munich, wrote an automatic data processing pipeline containing all data processing steps required for the analysis of a two-dose Kinobeads pulldown experiment (see Experimental procedure). Briefly, the tool was launched by automatically copying raw files generated by mass spectrometry measurement into a designated folder. Proteins and peptides were then identified and quantified by a MaxQuant search with predefined parameters. MS raw files of a specific drug and the corresponding vehicle controls from the same plate were processed together. The resulting output file (proteinGroups.txt) was used for further filtering, normalization and for the generation of relative intensity plots. The final step in the pipeline was the random forest classifier which assigned the target probability. This automatic data analysis pipeline together with the random forest classifier enables consistent and reliable data generation for large Kinobeads screening projects.

Assay stability assessed by quality controls. In order to evaluate the quality and reproducibility of Kinobeads pulldown experiments with two inhibitor concentrations over a longer period of time and to estimate the performance of the random forest classifier for target annotation, suitable quality controls had to be selected. The 96-well assay format enables parallel selectivity profiling of 40 inhibitors leaving 16 wells for vehicle and quality controls (Figure 17 A). DMSO, Lestaurtinib, a compound mixture and blocked beads were used as control.

Six DMSO controls were distributed over the 96-well plate. The median intensity of all DMSO controls per plate was used to calculate relative residual binding intensities for each protein group at every inhibitor concentration. To account for how reproducibly a protein was enriched by Kinobeads, the standard deviation of the six DMSO LFQ intensities for each protein per plate was calculated and visualized in the respective two-dose data plots. In addition, the DMSO controls were used to assess the intra-plate variability of the overall experimental design. Therefore, the protein and kinase $\log_2$ LFQ intensities of the different DMSO controls were correlated. Overall, the Pearson correlations ranged between 0.98 and 0.99 which showed a high reproducibility of the pulldown experiment within one plate (Figure 17 B, kinases are marked in green). DMSO controls with median Person correlation to all other DMSO controls of the plate below 0.96 were excluded from further analysis (see Figure 17 B, Plate MR024 DMSO1 versus DMSO2). In addition, the coefficient of variations for each kinase of the DMSO controls was calculated per assay plate. Around 70 % of the kinases showed coefficient of variation values below 10 % which was also indicative for high reproducibility of the pulldown.

The vehicle pulldowns also served as control to determine which and how many kinases were enriched by the Kinobeads per plate. A compound mixture of seven wide-spectrum kinase inhibitors (OTS-167, AT-9283, Dasatinib, Brigatinib, GSK-690693, PF-3758309 and BGT226), dosed at a concentration of 10 µM were used to compete as many kinases from the beads as possible. Kinobeads pulldowns of the compound mixture were performed in triplicates on each plate (Figure 17 A). In average, statistical testing revealed a significant decrease in LFQ intensities for 212 kinases (Figure 17 C). Apart from the fact that the number and type of kinases competed off the beads were compared between the plates, the compound mix Kinobeads pulldown results were not considered for further analysis.

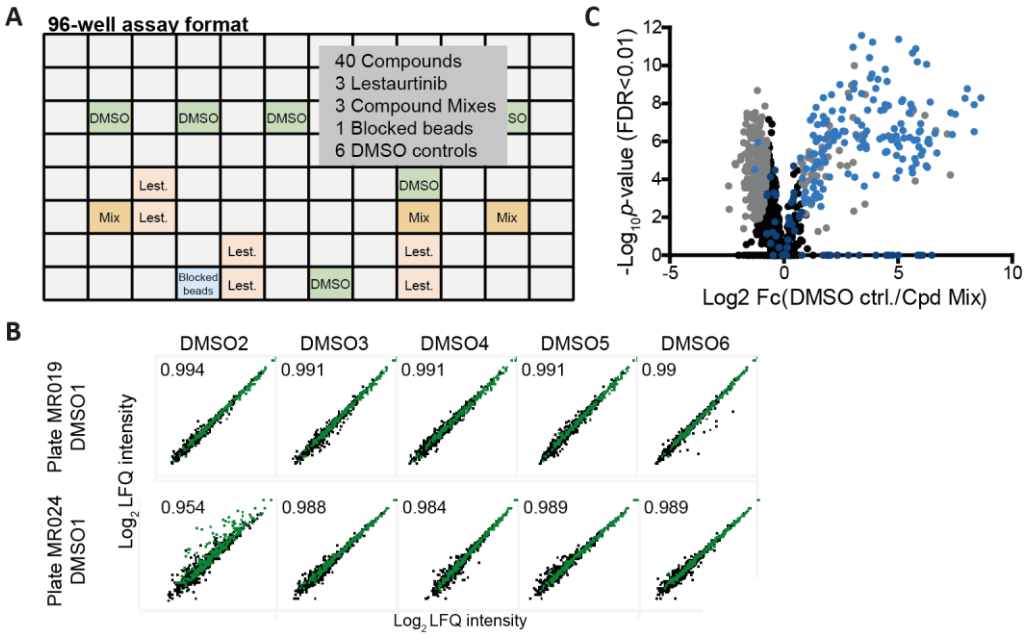

Figure 17 | Quality controls for the large scale Kinobeads profiling study. (A) Layout of a 96-well plate for Kinobeads pulldown experiments. 40 compounds are fitted on one plate (labeled in grey) together with 6 DMSO controls, 3 Lestaurtinib controls (two concentrations), 3 compound mixtures and one well for blocked beads. (B) Log_2 LFQ intensity correlation of DMSO controls of one plate. The Pearson correlation is between 0.98 and 0.99. Kinases are marked in green. (C) Volcano plot showing differently enriched proteins of DMSO control versus broad selective compound mixture pulldowns. Kinases are marked in blue. Differently enriched proteins are marked in grey.

In addition to 40 tool compounds that were profiled together on one 96-well plate, the tyrosine kinase inhibitor Lestaurtinib was analyzed in two concentrations (100 nM and 1 µM) on each plate in triplicates (Figure 17 A). The results of the Lestaurtinib pulldowns were used to check the overall performance of the random forest classifier for target annotation. Lestaurtinib was chosen because its more than 70 targets cover a broad spectrum of proteins (different protein kinase families, non-kinase targets) across a large affinity range. A total of 95 Lestaurtinib pulldowns distributed over 32 plates were conducted during the large scale selectivity profiling study of more than 1,200 tool compounds resulting in a drug target matrix depicting the target space of Lestaurtinib (Figure 18 A). Most targets were identified in all 95 experiments with similar affinities showing again the high intra- and inter-plate reproducibility of the assay. Only one experiment exhibited higher affinities for all targets (Figure 18 A, first line) and another Lestaurtinib pulldown resulted in more identified targets compared to the average (last line in Figure 18 A) both of which indicated to an experimental error in the pulldown experiment. Based on data from Klaeger *et al*[60] and data generated here, 76 proteins were identified as targets of Lestaurtinib with an affinity below 1 µM. Based on the results, the number of false positives and false negatives were calculated (Figure 18 B). In total, the 95 experiments should lead to the identification of 7,220 targets (76 targets per experiment) out of more than 235,000 identified proteins (~2,500 proteins per experiment). The random forest classifier identified 7,079 targets of which 361 proteins were incorrectly annotated as target and represented the false positive hits (0.05 %). In contrast, 483 proteins were falsely classified as non-target while being targets of Lestaurtinib (false negative hits, 0.07 %). As 93 % of the targets were assigned correctly, the overall performance of the

random forest classifier was very satisfying. In order to examine more precisely where the errors derived from, the false negatives and false positives hits were investigated. Especially targets like TGFBR1, with rather low affinities around 1 µM were often falsely classified (Figure 18 C). An affinity of 1 µM was used as cutoff since the Kinobeads assay using two inhibitor concentrations is most reliable the submicromolar range. Therefore, slight variations in residual binding can lead to an affinity below or above 1 µM and thus to an error in target annotation. In addition, low abundant proteins and proteins with low affinity tended to have false annotation. One example was the designated target of Lestaurtinib JAK2, which was annotated as target in only 52 out of 95 experiments (Figure 18 D). The overall intensity of JAK2 was quite low and over 50 % of the quantified proteins had higher intensities. This can be caused by either low expression of JAK2 in the used cell lines or by low affinity of JAK2 to Kinobeads. Low protein intensity also resulted in a high standard deviation of the LFQintensity of the six DMSO controls (Figure 18 E). In addition, only a few unique peptides were identified for JAK2 l (eight unique peptides in the DMSO control; Figure 18 E). Hence, the overall performance of the random forest classifier was excellent and false positive or false negative hits were mainly deriving from experimental errors or detection limits.

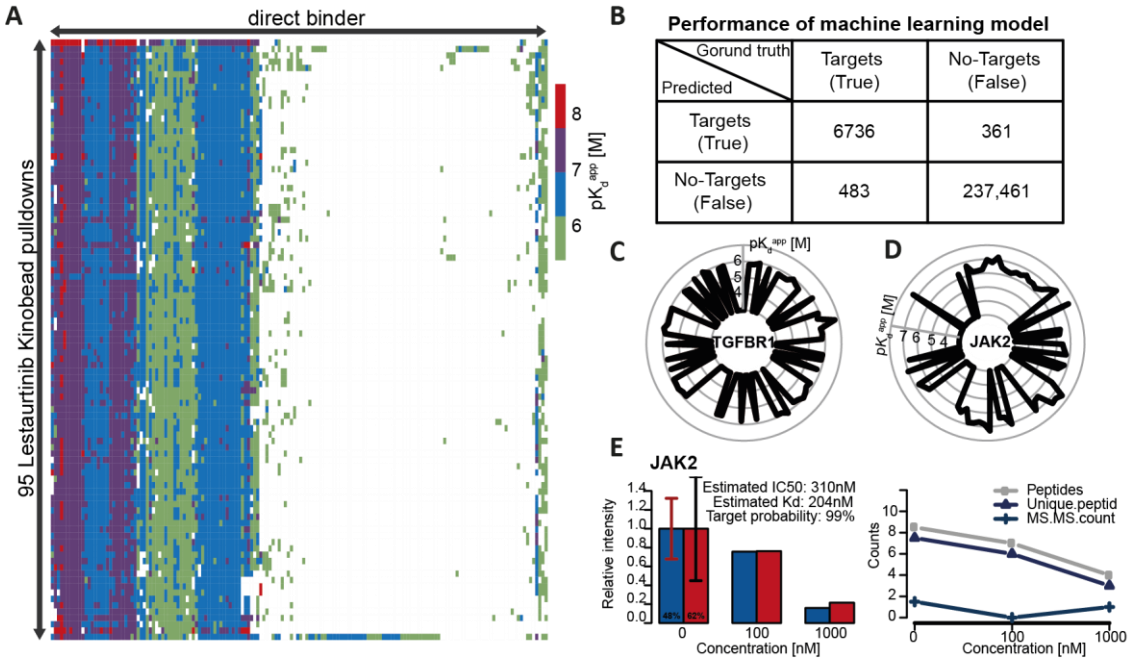

Figure 18 | Evaluation of the random forest classifier using 95 Lestaurtinib pulldowns. (A) Unsupervised clustering of 95 Lestaurtinib pulldowns and their targets (color code reflects the pK_d^{app} of drug-protein interaction). (B) Performance of the random forest classifier determined on the basis of 95 Lestaurtinib Kinobeads pulldown experiments. Lestaurtinib has 76 targets and numbers of false positives and false negatives were calculated. (C, D) Radarplot depicting all Lestaurtinib experiments where binding to TGFBR1 (C) or JAK2 (D) was observed. Each spike represents one Kinobeads experiment were TGFBR1 or JAK2 were identified as target of Lestaurtinib, the length of the spike reflects the binding affinity (pK_d^{app}). (D) Relative intensities, number of peptides, unique peptides and MSMS counts for JAK2 showed a dose dependent (Lestaurtinib) reduction and JAK2 was identified as target.

A total of 95 wells were occupied by tool compounds, DMSO controls, compound mixtures and Lestaurtinib. The last well of the 96-well plate was allocated to blocked beads (Figure 17 A) to assess unspecific binding to plastic ware and the beads. Blocked beads are made by reacting NHS activated sepharose beads with aminoethanol. This reagent is also used for blocking the residual immobilization sites after coupling of amino-probe to Kinobeads and hence coats 80-90 % of the surface of the Kinobeads. In total 84 kinases were identified in pulldowns performed with blocked beads (29 different pulldown experiments) but with more than 90 % lower intensities as compared to kinase intensities in the DMSO control. Hence, unspecific binding to the beads did not substantially affect the calculation of residual binding for kinases.

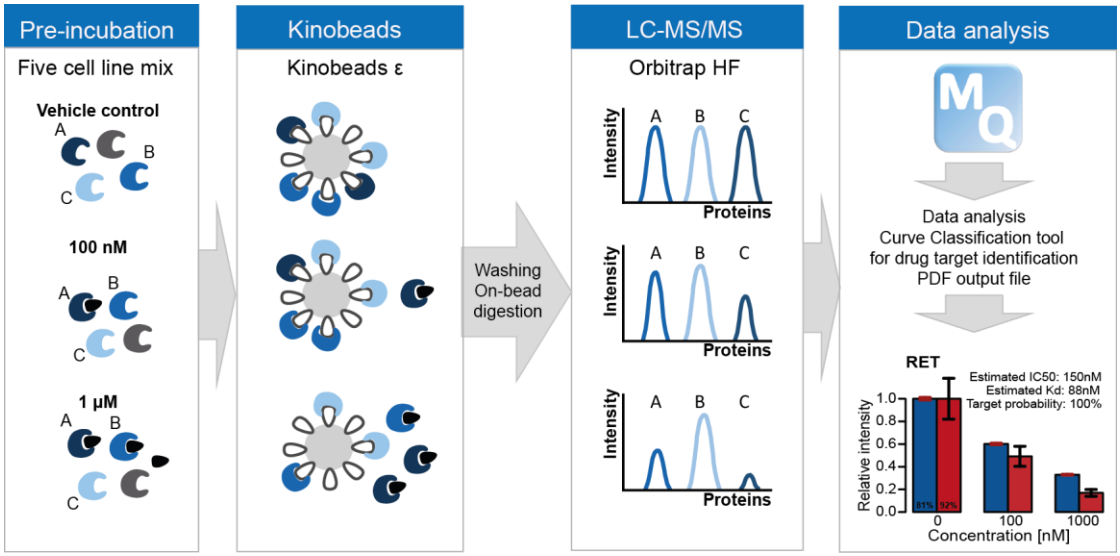

Figure 19 | Schematic representation of Kinobeads workflow designed to profile 1,232 tool compounds. Lysates of five cancer cell lines are separately equilibrated with two inhibitor concentrations or vehicle. Kinobeads ε are used to enrich the fraction of protein targets not engaged by the inhibitor. After washing bead bound proteins are digested on-beads. After LC-MSMS measurement the automatic data analysis pipeline including the random forest classifier is used for peptide and protein identification and quantification, data processing and target annotation.

To summarize, all optimization steps described in this chapter resulted in a more efficient and robust Kinobeads workflow (Figure 19) which enables the selectivity profiling of libraries of kinase inhibitors. Higher kinome coverage was gained by combing lysates of five different cancer cell lines and by using Kinobeads ε. Two compound concentrations, on-bead digestion and an optimized LC-MSMS method resulted into a drastic reduction of the samples preparation and data acquisition time. Together with the automatic data analysis pipeline including the random forest classifier for target annotation, the new Kinobeads workflow constitutes a technological milestone which came to fruition when profiling 1,232 tool compounds as will be discussed in the next chapter.

2 In Search of New Chemical Probes – A Chemoproteomic Selectivity Screen of 1,232 Kinase Inhibitors

Chemical probes are small molecules that have high affinity and selectivity as well as high efficacy for one particular protein (Introduction Chapter 2.3).[73,94] Such selective small molecules enable the mechanistic and phenotypic investigation of its molecular target in biochemical, cell-based and animal experiments. Therefore, they are valuable reagents for basic research, applied biological research and early drug discovery. However, a large part of the human kinome still lacks an adequate chemical probes. Therefore, one major goal of this work was to find new selective kinase inhibitors and inhibitors for the hitherto untargeted kinome. The optimized Kinobeads assay was used in a competitive pulldown setup with two inhibitor concentrations to screen 1,232 compounds and the results of this screening effort are presented in this chapter.

2.1 The Target and Selectivity Landscape of 1,232 Kinase Inhibitors

The profiled compound set. To constitute the library to be profiled, the published kinase inhibitor set (PKIS), PKIS2, and the kinase chemogenomic set (KCGS) introduced in the Introduction Chapter 2.3 were complemented by a compound library provided by Roche (Roche) and a set of cherry picked clinical kinase inhibitors (Clinical KI) (Figure 20 A). A list of all profilied compounds can be found in the Appendix (Supplementary Table 1). The PKIS and PKIS2 count 367 and 645 compounds respectively and have 10 compounds in common.[112,113] Due to solubility problems and missing compounds, only 358 and 521 compounds were screened with the Kinobeads technology. The kinase chemogenomics set (188 molecules) gathers molecules from the PKIS, PKIS2, compounds from the scientific literature, and compounds donated from SGC members.[110] Hence, there is an overlap of 52 compounds between KCGS and PKIS and of 45 compounds between KCGS and PKIS2 (Figure 20 B). Only a subset of the duplicates were profiled twice in order to analyze reproducibility of the compound screen. The library provided by Roche comprises 222 compounds. Additionally, 50 clinically approved or phase III compounds were screened. These clinical kinase inhibitors have already been profiled by Klaeger *et al*[60] in full dose response Kinobeads competition assays and were mainly used as control for the optimized Kinobeads workflow (see Results and Discussion Chapter 1.3). The compound set were structurally diverse. Overall, the 1,232 compounds could be grouped into 58 chemotypes based on the classification of Elkin *et al*[112] and Drewry *et al*.[113] Each chemotype comprised at least 5 compounds (Figure 20 C). Examples of two core structures are given in Figure 20 C showing the structural diversity of the chemotypes.

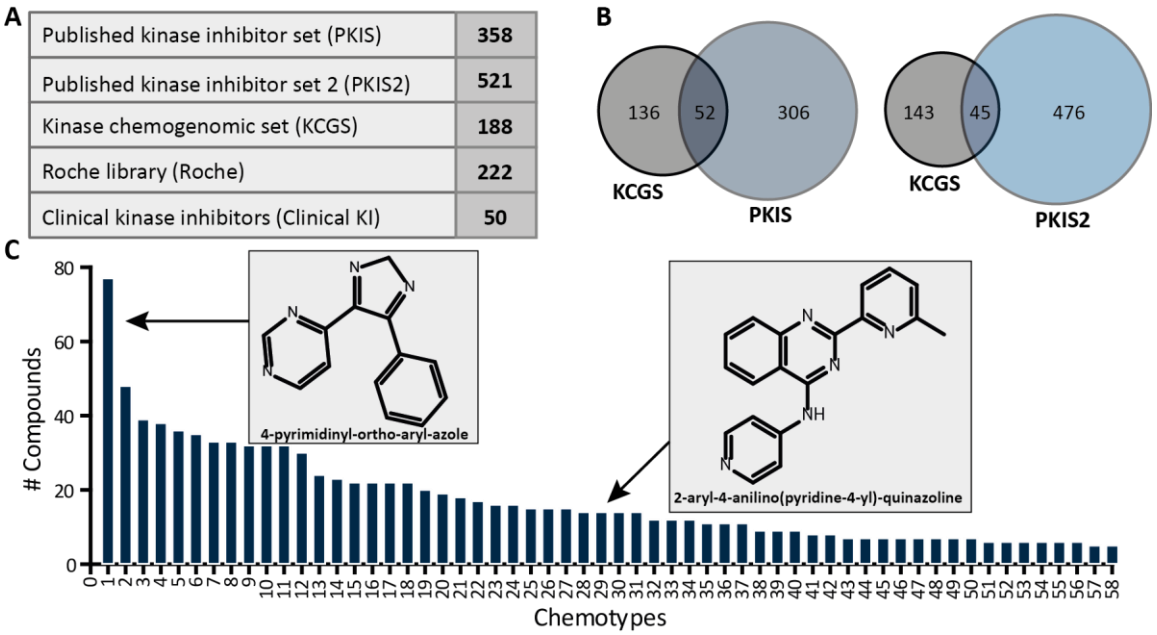

Figure 20 | Composition of the profiled compound set. (A) The compound set is composed of the PKIS and PKIS2 libraries, the KCGS, the Roche library and 50 kinase inhibitors that are in clinical trials or approved. Overall, 1,232 unique compounds were profiled. (B) Overlap of compounds that are included in two libraries. KCGS and PKIS share 52 compounds and KCGS and PKIS2 have 45 compounds in common. (C) Compounds can be grouped into 58 different chemotypes. Minimum number of compounds per chemotype is five. Core chemical structure of two chemotypes are shown as example.

The target landscape of 1,232 kinase inhibitors. The association of Kinobeads ε and mixture of cell line lysates defined a screening "panel" of 308 kinases that can be enriched out of 555 human protein and lipid kinases (Figure 21 A). A total of 239 kinases were targeted by at least one inhibitor (Figure 21 A), including an impressive 228 kinases with submicromolar affinity for at least one compound. Hierarchical clustering of the compounds and their respective kinase targets revealed the druggable kinome, where each colored square represents the strength of one compound-kinase interaction (Figure 21 B). White space indicates no interaction between the compound and the corresponding kinase. Overall, 6,131 compound-kinase interactions with a submicromolar affinity were identified with the Kinobeads technology. The compound set targeted a broad range of kinases from different subfamilies with a slight overrepresentation of the tyrosine kinase (TK) and CMGC families because many inhibitor were originally designed for these two families (Figure 21 C). The most frequently inhibited kinases were GSK3A, PRK3CD, GAK, RIPK2 and RET with more than 100 compounds. GAK and RET in particular appeared to be promiscuous and bound to a larger number of inhibitors in comparison with other kinases, although not a significant number of compounds were specifically designed to target either of these two proteins. Visualization of the data displayed clusters of compounds that selectively inhibited one kinase like the cluster of compounds targeting EGFR. Additionally to some selective inhibitors, several broad spectrum kinase inhibitors were identified in the screen. In contrary, no target was detected for 67 inhibitors and another 194 compounds had no target with submicromolar affinity to any protein. Either the compounds did not bind any kinase and were inactive or the targeted kinase was not presented in the screening panel and represent a blind spot of the assay. In all further analysis of the screen

only compound-target interactions of submicromolar affinity where considered, since the Kinobeads assay using two inhibitor concentrations is most reliable in this affinity range.

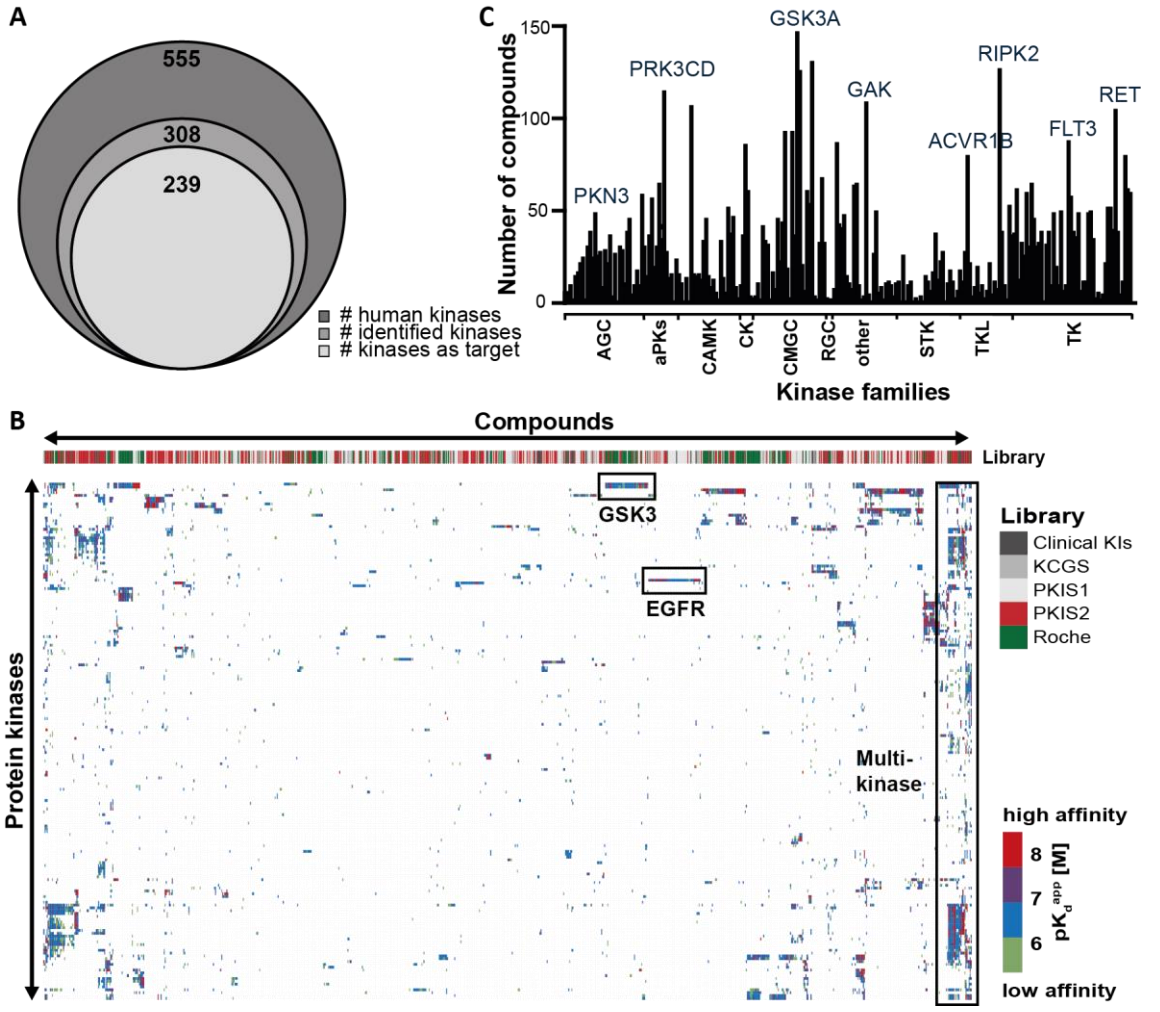

Figure 21 | The target landscape of 1,232 kinase inhibitors. (A) Number of kinases that are enriched by the optimized Kinobeads workflow. 239 kinases show binding to at least one inhibitor. (B) Hierarchical clustering of kinase targets against 1,232 compounds. Each dot represents one compound-kinase interaction and the color indicates the affinity of the interaction. (C) Number of compounds that target one kinase. Kinases are alphabetically ordered by their subfamilies.

Non-kinase targets. In addition to kinase targets, the experimental setup of a Kinobeads assay allows for the identification of non-kinase targets including nucleotide binder, helicases, ATPases, GTPases, FAD (e.g. NQO2) and heme (e.g. FECH) containing proteins. These target classes are typically not included in classic recombinant assays. Non-kinase targets can potentially add to the drug's mode of action or lead to adverse side effects. Examples for this are ferrochelatase (FECH)[148] and ribosyldihydronicotinamide dehydrogenase (NQO2)[145] that have been shown to bind to diverse clinical kinase inhibitors. Within this large scale kinase inhibitor profiling study, 16 nucleotide binding (non-kinase) proteins, five FAD binding proteins, two heme binding proteins and four metabolic kinases were found as targets of various compounds (Figure 22 A). Besides the already known non-kinase off-targets of kinase inhibitors, the FAD binding protein peroxisomal

acyl-coenzyme A oxidase 1 (ACOX1) was discovered as potent target of several compounds (Figure 22 B). The enzyme ACOX1 catalyzes the desaturation of acyl-CoA to 2 trans-enoyl-CoA, the first step of the fatty acid beta-oxidation pathway. Defects in the gene can lead to accumulation of very long chain fatty acids and is associated with a disease called pseudoneonatal-adrenoleukodystrophy.[228,229] One example is the compound GW775608X that induced a dose dependent intensity reduction of ACOX1 and bound this target with an affinity of 808 nM (Figure 22 B). Additionally, NAD(P)H dehydrogenase [quinone]1 (NQO1) was discovered as off-target of various kinase inhibitors. The enzyme serves as quinone reductase and is expressed at higher levels in divers human cancers.[230] Since NQO1 plays a crucial role in chemoresistance and proliferation of some cancer types, inhibition of NQO1 might be beneficial in combination with conventional chemotherapeutics.[231] The metabolic kinase PDXK (pyridoxal kinase) is another example of non-protein kinase target of several tool compounds. PDXK is responsible for phosphorylation of pyridoxal (vitamin B6) to pyridoxal-5-phosphate and has been identified as target of Roscovitine, a clinical CDK inhibitor.[232] The Kinobeads technology allows for the identification of such off-targets but the non-kinase off-targets require further validation in complementary assays.

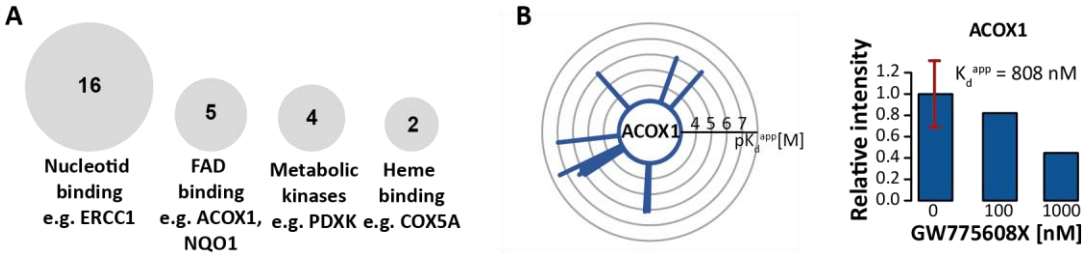

Figure 22 | Non-kinase targets of kinase inhibitors. (A) Nucleotid binding proteins, FAD binding proteins, heme binding proteins as well as metabolic kinases were identified as non protein kinase off-targets of the compounds. (B) Radar plot displays compounds that bind to ACOX1 (each spike is a drug and the length correspond to the affinity of the interaction). Left panel shows dose dependent intensity reduction of ACOX1 with increasing concentrations of GW775608X.

Correlation for affinity results to external data. As already mentioned, PKIS and PKIS2 have been distributed by the SGC to hundreds of research groups and have been extensively studied.[110] Therefore, complementary information on the target profiles of these inhibitors is already available in the scientific literature. In 2016, Elkins *et al*[112] published the results of profiling PKIS compounds against a panel of 224 recombinant kinases including 196 protein kinases, 21 mutated protein kinases and 5 lipid kinases with the Nanosyn enzyme assay using inhibitor concentrations of 100 nM and 1 µM. The Nanosyn assay is an *in vitro* kinase activity assay that utilizes recombinant kinases to screen for targets of inhibitors and reports percentage of inhibition values (Introduction Chapter 3.1).[112] Their screening panel comprised 125 kinases which were also enriched and competed with the Kinobeads. Based on this overlap, the results of the Nanosyn assay were compared to the results of the Kinobeads screen. First, the 125 kinases and their corresponding binding values for 358 compounds were selected. The percentage of inhibition was then plotted against the pK_d^{app} values as determined by the Kinobeads assay (Figure 23 A). Only inhibition values greater than 50 % and affinity values higher than 1 µM (pK_d^{app} of 6) were

considered to exclude potential false positives. Both assays overlapped in the identification of 491 drug-protein interaction (Figure 23 A) and more than 41,000 drug-protein combinations that did not show any binding. A total of 1,800 drug-protein interactions with inhibition of more than 50 % were identified only by the Nanosyn assay (x-axis in Figure 23 A) whereas 189 drug-protein interaction with affinities in the submicromolar range were exclusively discovered by the Kinobeads assay (y-axis Figure 23 A). The overall correlation of the results was rather poor with R=0.26. The differences between the two assays were partly kinase dependent. For example, CDK2 was identified in both assays as target for 13 inhibitors. Results of the Nanosyn assay suggest the binding to CDK2 for additional 23 compounds of the library. In contrast, within the Kinobeads assay 15 compounds bound to PIK3CD whereof only one was confirmed in the recombinant assay. These examples indicated that the correlation between recombinant kinase activity assays and lysate based assay depends to a certain extent on the kinase. These kinase dependent discrepancies might be explained by potential complex partners. For example, CDKs are forming stable complexes with specific cyclins. In recombinant kinase assays like the Nanosyn assay, one CDK/cyclin complex is analyzed at a time whereas several different CDK/cyclin complexes at once are present in the cell lysate mixture used for Kinobeads profiling. PIK3CD also functions in complex with its regulatory subunit which is present in native cell lysate while in recombinant kinase assays only the PI3K kinase without the regulatory subunit is usually analyzed. Hence, the observed differences could be in parts explained by different assay conditions.

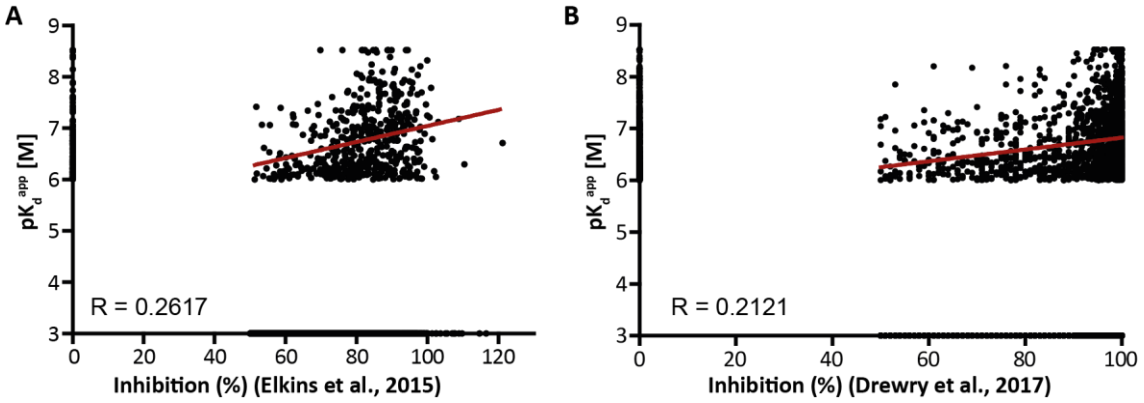

Figure 23 | Comparison to external data. (A) Correlation of inhibition data of PKIS derived from Elkins *et al*[112] against binding data of the Kinobeads screen. Each dot represents one drug-target pair. (B) Correlation of inhibition data of PKIS2 derived from Drewry *et al*[113] to the results of the Kinobeads screen.

The PKIS2 library has been profiled by Drewry *et al.*[113] Here, 645 compounds of PKIS2 were screened in singlicates at a concentration of 1 µM against 392 wild-type human kinases using the commercially available KINOMEscan assay panel.[113] 200 kinases of the screening panel were also enriched and competed by Kinobeads. This overlap was again used to compare the results of the binding assay utilizing recombinant kinases to the results of the lysate based Kinobeads screen. In total, 1,613 drug-protein interactions were identified in both assays with a Pearson correlation of R=0.21 (Figure 23 B). Binding of 828 drug-protein combinations were additionally identified only by Kinobeads while the KINOMEscan assay exclusively elucidated more than 6,000 drug-protein interactions.

Overall, the two recombinant kinase assays identified considerably more targets compared to the lysate based Kinobeads assay. It should be noted that the values that were compared did not have the same dimension and may therefore lead to distorted results. Kinobeads results have been reported with pK_d^{app} values (log scale) while recombinant kinase assay results were reported in percentage of inhibition. But the discrepancy does not change the fact that more targets were identified by Elkins *et al*[112] and Drewry *et al*[113]. The Kinobeads assays accomplish close-to-physiological conditions and features the full length protein with all posttranslational modification and interaction partners which can vary the binding to the inhibitor. It can be just speculated that lysate based assays are closer to physiological conditions in cells and therefore might show higher correlation to in-cell target engagement results in comparison with recombinant assays. A similar observation was made, when the NanoBRET method for in-cell target engagement was compared with classical biochemical approaches like activity assays which revealed that also the NanoBRET identified much less targets.[120] This statement, however, requires further investigation via systematic comparison between NanoBRET, Kinobeads and recombinant kinase assay profiling results for instance.

The selectivity landscape of 1,200 kinase inhibitors. After the target space of the 1,232 kinase inhibitors was elucidated, the selectivity of the compounds based on the CATDS metric was calculated (Introduction Chapter 2.2). CATDS is a concentration and target dependent selectivity score that measures the target engagement of a specific protein at a certain compound concentration relative to the target engagement of all targets at that concentration.[60] Values close to one indicate highly selective compounds with only one target engaged at the given concentration, whereas values close to zero refelects very unselective profiles. Depending on the target(s) and the concentration that are chosen, the same inhibitor will exhibit different selectivities. In order to assess the highest selectivity a compound can achieve, irrespectively of its designated target, the selectivity of each compound was investigated using the CATDS for the most potent target at its respective K_d^{app} concentration.

Calculated $CATDS_{mostpotent}$ scores of the screening panel were ranked and highly selective compounds as well as very unselective inhibitors were identified (Figure 24 A). ERK-IN-1 for instance, appeared to be very selective with only one target (K_d^{app} of 813 nM), whereas GSK1269851A was very unselective with a CATDS close to zero (Figure 24 A). Additionally to the CATDS of the most potent target, the selectivities of a compound to all its targets ($CATDS_{target}$) were calculated (at the respective K_d^{app} concentration), and assembled in a drug-protein interaction matrix using unsupervised clustering (Figure 24 A). Red colored dots illustrate highly selective compounds whereas blue dots reflect unselective inhibitors.

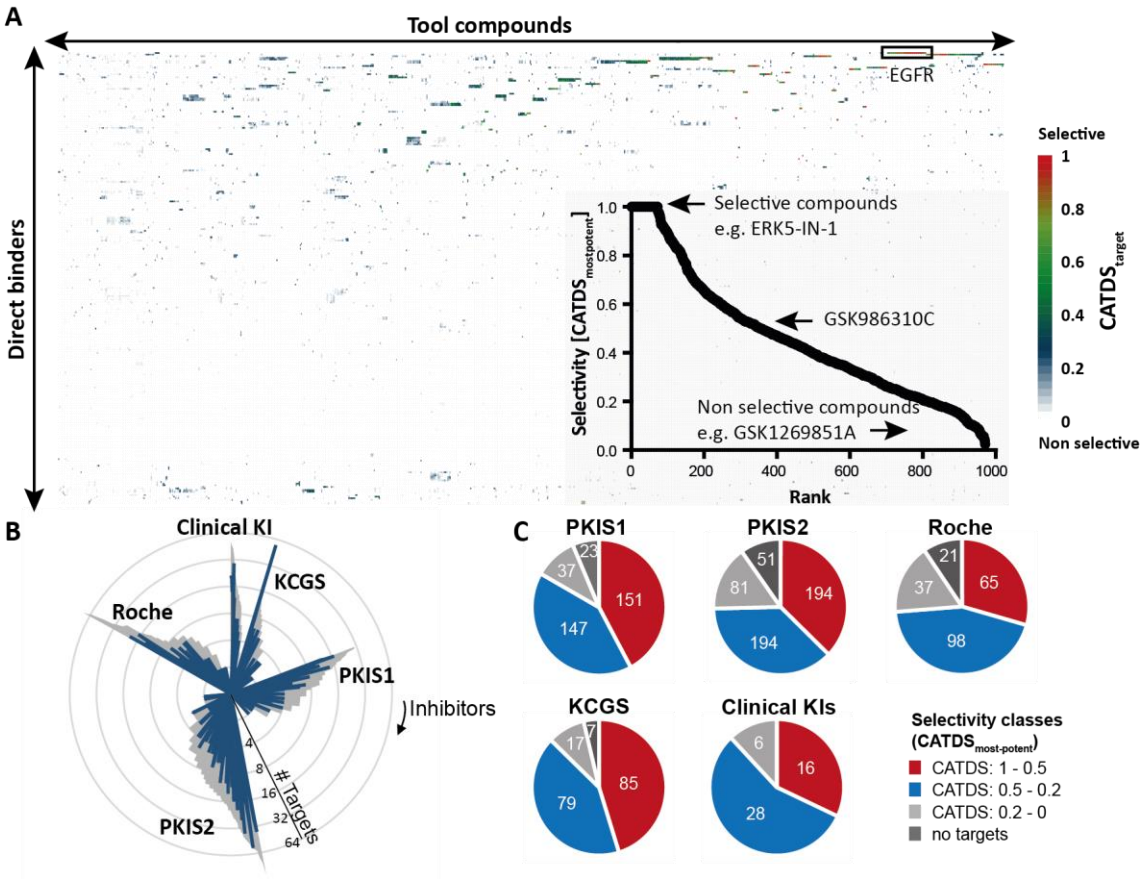

Figure 24 | The selectivity landscape of 1,232 kinase inhibitors. (A) Hierarchical clustering depicting the selectivity of the compound set. Each dot represents one drug-protein interaction and the color indicates the selectivity of the compound towards this target according to its $CATDS_{targets}$. Insert: Ranking of the compounds according to their CATDS of the most potent target. (B) Number of targets per compound sorted by libraries. Blue indicates targets with affinities below 100 nM and grey between 100 nM and 1 µM. (C) Compounds per library are grouped into four selectivity categories. Number of compounds within one category are labeled in white numbers.

The KCGS is composed of the most selective inhibitors of PKIS, PKIS2 and highly selective compounds from the literature leading to the assumption that inhibitors of KCGS are significantly more selective than compounds of the other libraries. Inhibitors were sorted by libraries and the number of targets with an affinity below 100 nM (blue) and between 100 nM and 1 µM were plotted. In each library, compounds with high numbers of targets as well as compounds with only one target were identified (Figure 24 B) and no significant difference between the selectivity of the libraries was observed in this analysis. In addition to counting targets, the CATDS score of the most potent target was used to group compounds into four different selectivity categories (Figure 24 C). Here, the percentage of highly selective compounds with a $CATDS_{mostpotent}$ between 0.5 and 1 was higher for the KCGS library compared to the other libraries. In contrast, the Roche library comprised the smallest fraction of highly selective inhibitors. Even though KCGS was designed to contain only potent and selective kinase inhibitors and showed the best selectivities in this screen, still several broad spectrum compounds have been identified using the Kinobeads technology.

In summary, the target landscape of 1,232 small molecule kinase inhibitors derived from different compound libraries have been elucidated with the Kinobeads technology. The selectivity of the compounds varied strongly between highly selective inhibitors as well as very unselective inhibitors. The CATDS score was used in further analysis to identify potential chemical probes within the compound set.

2.2 Characterization of Potential New Chemical Probes

Selection of new potential chemical probes. With this set of affinity and selectivity data, the search for new chemical probes could commence. Chemical probes must meet certain criteria in terms of selectivity and target engagement as set out in the introduction.[94] For the Kinobeads data, these criteria were translated as following: for a compound to be considered as a potential chemical probe its affinity must be below 1 µM and the $CATDS_{mostpotent}$ must be above 0.5 (Figure 25 A). These thresholds would act as selection criteria. To determine other chemical probe criteria such as cellular potency other tools or assays are required. A few examples are hereafter presented as prototypical cases. Therefore, the identified chemical probes in this data set have to be seen from the perspective of building a profound basis for further validation experiments proving if the compound fulfills also all other chemical probes criteria.

In total, 354 of the 1,232 screened compounds fulfilled the here applied probe selection criteria, targeting 73 different kinases that were scattered across all subfamilies (Figure 25 B). Contrary to what was expected, there was no bias for kinases of the TK and CMGC families, although most of these inhibitors were designed for those two groups. As mentioned above, the chemical probe portal report on probes for 102 human protein kinases. In the data set presented here, candidate probes for an additional 53 kinases were found providing the opportunity to greatly expand the portfolio of chemical probes assuming that the Kinobeads results can be validated. Chemical probes for a further 20 kinases were proposed for which a probe already exist in the chemical probe portal. A total of 20 compounds previously classified as selective probes, were reprofiled using the Kinobeads technology whereof only three (Afatinib, BI2536, GSK583) were identified as chemical probes within this screen and another two compounds (DDR1-IN-1 and CCT24474) barely missed the selection criteria with a $CATDS_{mostpotent}$ of 0.46. For seven compounds, the designated target (e.g. CDK8 or RIPK1) could not be enriched by Kinobeads hampering selectivity determination. The eight remaining compounds showed rather poor selectivity in the Kinobeads assay. Such discrepancies between reported chemical probes and Kinobeads selectivity profiling have already been reported by Klaeger *et al*.[60]

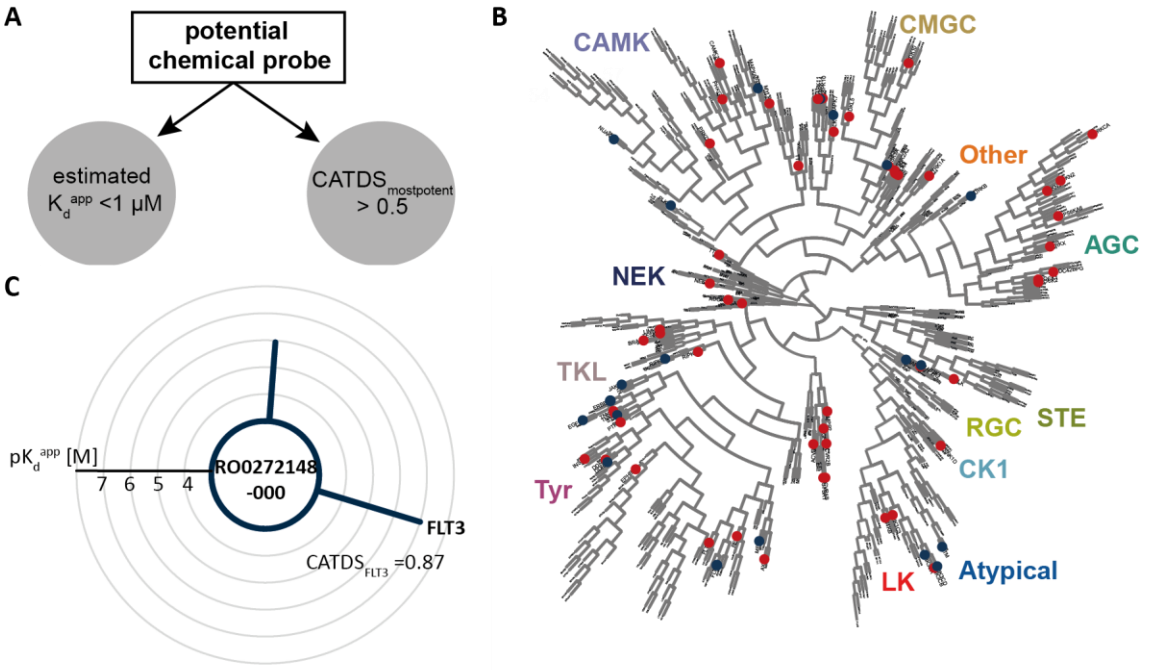

Figure 25 | Identification of potential chemical probes within the dataset. (A) Criteria to search the dataset for potential chemical probes. The affinity of the compound must be below 1 µM and the CATDS of the most potent target should be above 0.5. (B) Kinometree depicting kinases (red and blue circle) that have been targeted by at least one inhibitor that fulfill the criteria of a potential chemical probe. For kinases marked in blue, a chemical probes has been reported on the chemical probe portal. (C) Radarplot depicting targets of the inhibitor RO0272148-000. Each spike represents one target and the length displays the affinity.

Overall, the large data set of over 1,200 compounds revealed potential chemical probes for well-studied kinases as well as understudied kinases (see also Results and Discussion Chapter 2.3). The largest diversity of chemical probes (37 compounds) were detected for the well-studied kinase EGFR. Some of the compounds were derived from EGFR medicinal chemistry programs emphasizing the success of these programs to develop selective EGFR inhibitors. Another example was the receptor tyrosine kinase FLT3 that has been targeted by 88 inhibitors of which several revealed high selectivity. For instance, RO0272148-000 is a potent (K_d^{app} = 99 nM) and highly selective ($CATDS_{FLT3}$ = 0.87) FLT3 inhibitor with ACOX1 as only additional and less affine target (Figure 25 C). Mutations of FLT3 (internal tandem duplication; FLT3-ITD) occur in around 30 % of acute myeloid leukemia (AML), hence, compounds targeting FLT3 are in high demand.[233] In addition, a total of 44 compounds targeted the serine/threonine kinase CDKL5 of which one fulfilled the chemical probes selection criteria. CDKL5 is essential for normal brain development and deficiency is associated with epileptic encephalopathy.[234] Selective and affine compounds might help to better understand the cellular function of this kinase.

Furthermore, several selective ephrin type-B receptor 6 (EPHB6) inhibitors were discovered in the dataset. EPHB6 is a pseudokinase and modulates cell adhesion and migration when stimulated by ephrin-B2.[235] It is unclear how ATP-competitive small molecules could modulate nonenzymatic functions of pseudokinases but with selective inhibitors in hand like GW458344A, this can be further examined. Pseudokinases in general are gaining interest in drug discovery as important new drug targets due to their physiological roles associated with various human diseases.[236]

New selective CK2 inhibitors. Casein kinase 2 (CK2) is a constitutively active serine/threonine kinase and occurs as tetramer that is composed of two catalytic α units and two regulatory β units.[237] The α domain appears as α (CSNK2A1) and α' (CSNK2A2) variant and form either a homotetramer or a heterotetramer. CK2 is involved in regulation of many cellular processes including cell growth and proliferation as well as cell death and is often overexpressed in cancer cells promoting proliferating effects leading to an addiction of the cancer cell to high levels of CK2.[238,239] For this reason, CK2 has emerged as a promising drug target in cancer therapy.[240] Several ATP-competitive CK2 inhibitors have been developed to date and one of these, CX-4945, has progressed to clinical phase II. Although CX-4945 has been reported to be highly selective for CK2 (K_d^{app} of 1 nM as etermined by Kinobeads[60]), several studies showed off-target effects and described several other kinases to be inhibited by the compound.[60,241,242] Kinobeads profiling of CX-4945 also uncovered several off-targets including CLK3 (K_d^{app} of 10 nM), STK10 (K_d^{app} of 96 nM) and SLK (K_d^{app} of 220 nM).[60] Therefore, the data of the Kinobeads screen were searched for potent and selective CK2 inhibitors. In total, 64 compounds were identified as CK2 binders some of which were potent and highly selective for CK2 (Figure 26 A). Due to the two α domains which represent two different proteins to which the compound can bind, a $CATDS_{CSNK2A1}$ of 0.5 indicates already a highly selective inhibitor which only binds to CK2α and CK2α' at the specific K_d^{app} concentration. Compounds, assigned to the quinolinyl-methylene-thiazolinones chemotype, were overrepresented with a total of 25 compounds. This chemotype was originally optimized for selective and potent inhibition of CDK1 and led to the identification of the highly selective CDK1 inhibitor RO-3306.[243,244] 35 compounds of this chemotype were profiled using the Kinobeads technology and especially RO4613269-000, RO4493940-000 and RO4603632-000 appeared to be promising compounds with high selectivity ($CATDS_{CSNK2A1}$ of 0.43, 0.36, 0.3) and relatively high potency for CK2 (pK_d^{app} of 7.2, 6.5, and 6.6, respectively). In addition, GW869516X that belongs to the imidazotriazine chemotype was discovered as potent and selective CK2 binder. Within the Kinobeads screen only CK2 was identified as target of GW869516X whereas RO4613269-000 displayed some off-target effects and bound to three other proteins but with much lower affinity (Figure 26 B).

To validate the results of the Kinobeads assay, the four compounds were tested in a recombinant activity assay that was conducted by Reaction Biology Corporation. The compounds were screened against CSNK2A1 and CSNK2A2 as well as against CDK1/cyclinB as it was the designated target of the quinolinyl-methylene-thiazolinones chemotype. All four tested inhibitors revealed a reduced activity for CK2 with higher inhibitor concentration and IC_{50} values for CSNK2A2 of 34 nM, 65 nM, 372 nM and 51 nM were measured for GW869516X, RO4613269-000, RO4603632-000 and RO4493940-000 (Figure 26 C, D). Activity of CDK1 was only slightly reduced with higher concentrations but no IC_{50} values could be determined. This coincides with published data that reported no activity inhibition of CDK1/cyclinB for the three compounds of the quinolinyl-methylene-thiazolinoes chemotype.[244]

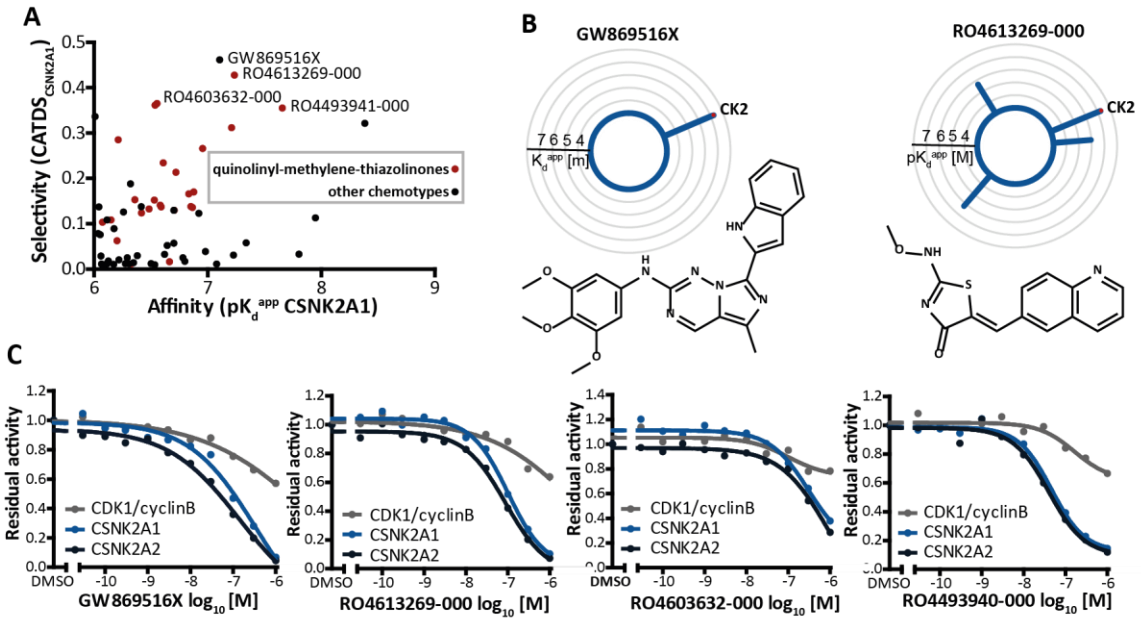

D

	GW869516X		RO4613269-000		RO4603632-000		RO4493940-000	
	CSNK2A1	CSNK2A2	CSNK2A1	CSNK2A2	CSNK2A1	CSNK2A2	CSNK2A1	CSNK2A2
Binding K_d^{app} [nM]	78	56	58	57	279	276	291	203
Activity IC_{50} [nM]	85	34	116	65	579	372	67	51

Figure 26 | Selective CK2 inhibitors. (A) Affinity of CK2 inhibitors is plotted against the selectivity ($CATDS_{CSNK2A1}$) as determined by Kinobeads. Red dots indicate compounds that belong to the quinolinyl-methylene-thiazolinones chemotype. (B) Radar plot depicting the target space of GW869516X (left) and RO4613269-000 (right). Each spike represents one target and the length correspond to the affinity of the interaction. (C) Kinase activity assays of the indicated compounds for CDK1/cyclinB, CSNK2A1 and CSNK2A2 validate the binding results obtained by Kinobeads. (D) K_d^{app} and IC_{50} values for CSNK2A1 and CSNK2A1 in Kinobeads screen (binding) and in recombinant kinase assays (activity, performed by Reaction Biology).

To further explore CK2 target engagement of the four CK2 inhibitors in cells, the phosphorylation state of CK2 downstream targets with and without inhibitor treatment were investigated in collaboration with Laszlo Gyenis and David Litchfield at the Department of Biochemistry at Western University, London. For this purpose, Flp-In T-Rex U-2 OS (human osteosarcoma) cells expressing either CSNK2A1-HA wild type or a triple mutant (TM, V66A/H160D/I174A) form of the kinase, were induced for 48 h with tetracycline and then treated for 24 h with 10 µM of GW869516X, RO4613269-000, RO4603632-000, RO4493940-000, CX-4945 or DMSO as control. The effect of the compounds on the phosphorylation state of CK2 substrate was investigated by Western Blot analysis (Figure 27). It has been reported that CK2 phosphorylates EIF2S2 on serine 2 and serine 67. Hence, the phosphorylation of EIF2S2 S2 was investigated.[205,245] As expected, the phosphorylation of this site was reduced by CX-4945 in the wild type cell line but not in the triple mutant cell line that was engineered to be resistant against CX-4945 inhibition (Figure 27 A). No effect on EIF2S2 pS2 was observed after treatment of GW869516X, RO4613269-000, RO4603632-000 or RO4493940-000 (Figure 27 A). Additionally, only CX-4945 showed a slightly reduced phosphorylation of CSNK2B S2, S3, S4, S8 and slightly reduced levels of total CSNK2A1-HA. Next, a phospho serine/threonine antibody that recognizes proteins containing the CK2 phosphorylation consensus sequence motif pS/pTDXE motif which is also present in EIF2S2, was used to investigate the effect of the compounds on CK2 substrates *in cellulo*. Again CX-4945

treatment led to reduced CK2 substrate phosphorylation (Figure 27 B) which was also observed for the wild type cell line after GW869516X and RO4613269-000 treatment indicating that the compounds were able to enter the cells and potentially bind and inhibit CK2. The effect was smaller compared to CX-4945 speculating that the potency in cells might be lower or that the cells might be less permeable for the compounds. Only GW869516X but not RO4613269-000 had a slight effect on CK2 substrate phosphorylation in the triple mutant cell line indicating that the CX-4945 resistant cell line might still responds to the newly identified CK2 inhibitor RO-4613269-000. Hence, CK2 inhibition in cells could be validated for GW869516X and RO4613269-000 making them interesting CK2 inhibitors with high selectivity but potentially low intracellular activity than CX-4945.

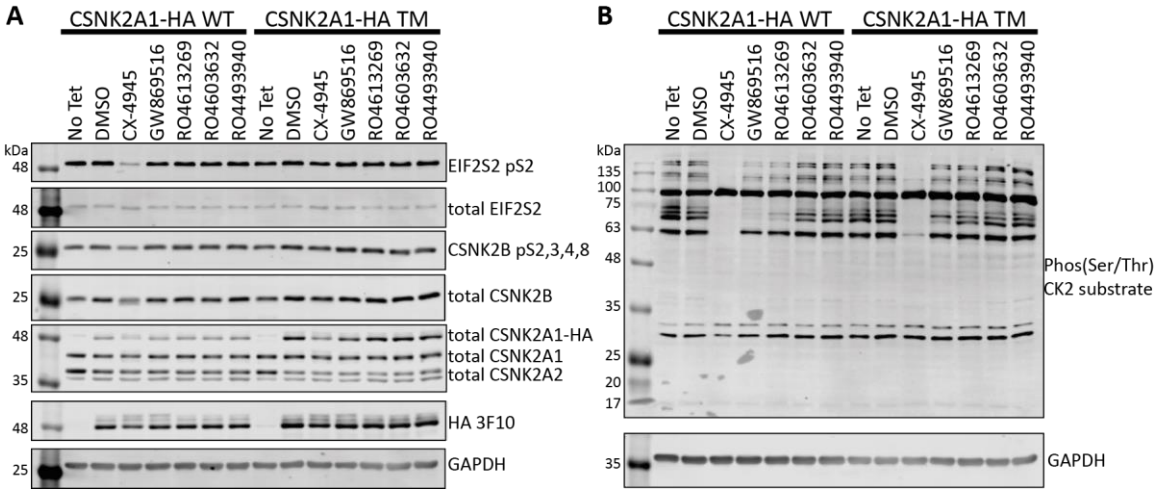

Figure 27 | Cellular CK2 target engagement. (A) Immunoblot analysis of EIF2S2 pS2, a known CK2 substrate, and total CK2 levels as well as (B) of CK2 substrates carrying the CK2 phosphorylation consensus sequence motif (pS/pT)DXE after treating U-2 OS cells with 10 µM of the indicated inhibitors for 24 h. U-2 OS (human osteosarcoma) cells expressing either CSNK2A1-HA wild type (WT) or a triple mutant (TM, V66A/H160D/I174A) form of the kinase were induced by tetracycline. GAPDH was used as loading control. Experiments were performed by Laszlo Gyenis and David Litchfield at Department of Biochemistry of Western University.

A new strategy to develop selective and potent CK2 inhibitors exploits the poorly conserved cryptic pocket close to the ATP binding site of CK2. Hyvoenen and coworkers[62] generated chimeric molecules composed of chemical fragments binding to the cryptic pocket and fragments binding to the ATP-binding pocket to selectively inhibit the activity of CK2. The two highly selective CK2 inhibitors identified in this study might be potential molecules that can be evaluated using this approach in order to generate more affine and selective CK2 binders.

New selective SYK inhibitors. The spleen tyrosine kinase (SYK) is a member of the Src family of non-receptor tyrosine kinases and plays a crucial role in adaptive and innate immune response.[104,246,247] Several studies have validated SYK as potential target for the treatment of various hematological cancers, autoimmune disorders and other inflammatory states.[248-250] To date, several SYK inhibitors including Fostamatinib, TAK659 and Entospletinib are assessed in

clinical phases or are already approved by the FDA.[251-253] These clinical kinase inhibitors are mostly not very selective and lead to several side effects in patients including neutropenia and diarrhea.[60,254] Therefore, there is still a need for highly selective SYK inhibitors that can be used either as chemical probes or as drugs with ideally fewer side effects in patients. To allow a fair comparison between the selectivity of SYK tool compounds and clinical drugs, the target space of two clinical kinase inhibitors (TAK659 and Entospletinib) were determined with the Kinobeads technology (see also Results and Discussion Chapter 3). TAK659 in particular showed binding to many other kinases and appeared to be rather a multikinase inhibitor than a specific SYK inhibitor (Figure 28 A). In contrast, Entospletinib displayed fewer targets but surprisingly, SYK was not the most potent target (Figure 28 A). CK2 and NQO2 were targeted with higher affinities indicating that Entospletinib is also not a highly selective SYK inhibitor. To find new selective SYK inhibitors, the screening results were searched for potential SYK inhibitors with a $CATDS_{SYK}$ above 0.5. The compound GSK986310C displayed a $CATDS_{SYK}$ of 0.51 and an apparent dissociation constant of 80 nM (Figure 28 B). A Kinobeads pulldown experiment using eight inhibitor concentrations (full dose response pulldown) verified the two dose results and a K_d^{app} of 58 nM was determined (Figure 28 B). Even though GSK986310C bound other kinases like PAK4 with an affinity of 322 nM, SYK was the most potently inhibited target and selectivity towards SYK was superior as compared to the clinical kinase inhibitors.

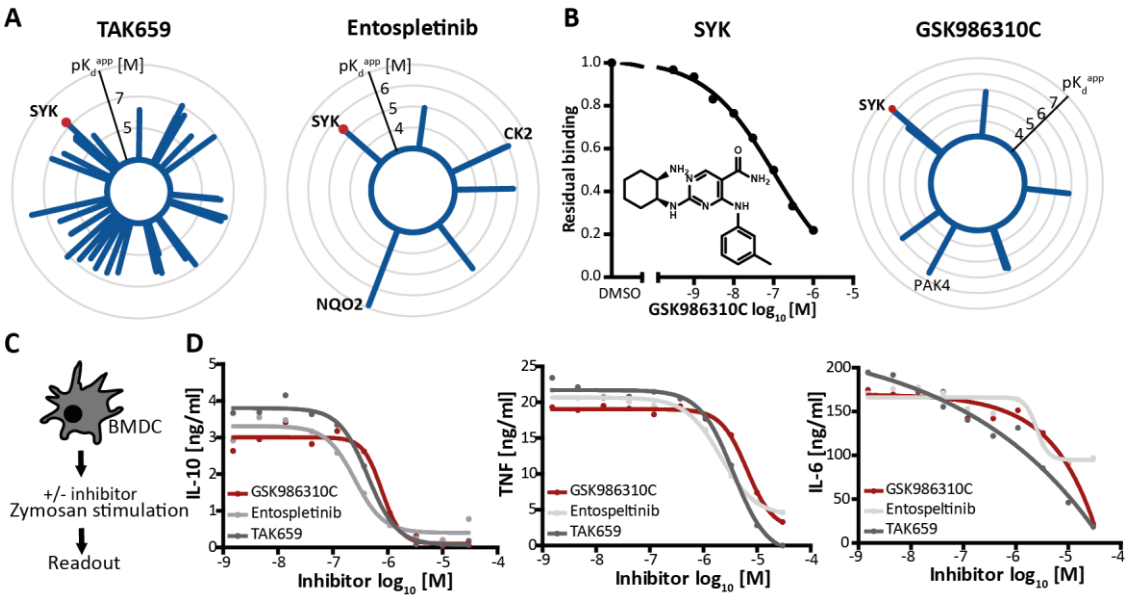

Figure 28 | Compounds targeting the kinase SYK. (A) Target space of the clinical SYK kinase inhibitors TAK659 (left) and Entospletinib (right). Each spike represents one target and the length displays the affinity of the interaction as pK_d^{app}. (B) Dose response curve of the Kinobeads competition experiment with GSK986310C for SYK. Radarplot shows all targets of the tool compound with SYK as the most potent target. (C) Scheme of the cytokine expression assay that was performed by Prof. Dr. Jürgen Ruland and Larsen Vornholtz. (D) IL-10, TNF and IL-6 levels are reduced after treatment of Zymosan stimulated bone marrow-derived dendritic cells with increasing inhibitor concentrations (tool compound GSK986310C in red and two clinical inhibitors Entospletinib and TAK659 in grey).

Cellular target engagement of SYK by GSK986310C was further surveyed in a cytokine secretion assay in collaboration with Prof. Dr. Jürgen Ruland and Larsen Vornholtz from the Institut für Klinische Chemie und Pathobiochemie, Klinikum rechts der Isar, Technical University of Munich. Hereby, bone marrow-derived dendritic cells (BMDC) were stimulated with Zymosan which activates Dectin-1 signaling. This in turn induces downstream SYK signaling and leads to an increased cytokine (IL-10, IL-6 and TNF) production (Figure 28 C).[255,256] Treatment of cells with SYK inhibitors prior to Zymosan stimulation should therefore result in decreased levels of cytokines which has been shown for BAY61-3606, a known SYK inhibitor.[256] In fact, the tool compound as well as the two clinical kinase inhibitors Entospletinib and TAK659 induced a dose dependent reduction of IL-6, IL-10 and TNF levels (Figure 28 D). The tool compound had the same effect on IL-10 and TNF levels as the clinical kinase inhibitor while TAK659 had the strongest effect on IL-6 levels. The cytokine secretion assay confirmed cellular target engagement of SYK by GSK986310C in BMDC. Since GSK986310C had similar cellular effects as the clinical SYK inhibitors but showed less off-targets in the Kinobeads screen, the compound might be a promising highly selective SYK inhibitor for applications as clinical drug as well as chemical probe.

In summary, within the data set several hundred new chemical probes were identified targeting 73 different kinases whereof 53 still lack an appropriate chemical probe. Here, CK2 and SYK were selected as two examples to illustrate the potential of the dataset to find new highly selective inhibitor. The results obtained by the Kinobeads technology for this two kinases were further confirmed by additional activity assays and cellular experiments. Since not only selective inhibitors for well-studied kinase were sought out, but also inhibitors for the hitherto undruggable kinome, the understudied kinase PKN3 was selected as example and will be discussed next.

2.3 Inhibitors for the Understudied Kinase PKN3

The serine/threonine kinase PKN3 is an understudied kinase whose molecular mechanism and downstream targets are largely unknown. In recent studies, PKN3 has been functionally linked to metastasis, invasion and tumor growth making it a promising drug target in pharmaceutical research.[107,257] Kaufmann and coworkers developed a liposomal small interfering RNA (Atu027) against PKN3 which is currently being under investigation in clinical trials for solid tumors and pancreatic cancer.[258,259] In 2019, Browne and coworkers were the first to report on a small molecule inhibitor that covalently target the cysteine at position 840 on PKN3.[260] The compound JZ128 was developed based on the structure of THZ1 which is a CDK9 inhibitor with reported off-target binding to PKN3. A proteome wide assay for inhibitor target-site identification (CITe-Id) revealed covalent binding of JZ128 to PKN3, TNK1, RIOK2, SRC, PIKFYVE and RIPK2 whereas the KiNativ assay only identified binding to PIKFYVE, PIP4K2C and RIPK2 indicating that the compound might not bind to the ATP binding pocket of PKN3. Since, the reported PKN3 inhibitor displayed several off-targets, novel PKN3 targeting compounds are of great interest and could serve as chemical probes or could be used as starting point for medicinal chemistry programs to develop ATP competitive PKN3 inhibitors with higher selectivity and affinity.

Identification of novel PKN3 inhibitors. Kinobeads screening results of 1,232 small molecules were searched for potential PKN3 inhibitors. PKN3 was engaged by 49 different small molecules of the screened compound set with submicromolar affinities (Figure 29 A). Plotting the binding affinities against $CATDS_{PKN3}$ scores (selectivity) of the compounds revealed several highly potent and selective PKN3 inhibitors including GSK902056A and GSK260205A which had a $CATDS_{PKN3}$ of close to one and an affinities of around 1 nM (Figure 29 B, Appendix Figure S 3). PKN3 was so far still unknown as target of PKIS compounds, since PKN3 was not included in any recombinant kinase assay panel in which the PKIS libraries were previously screened with recombinant kinase assay,.[112]

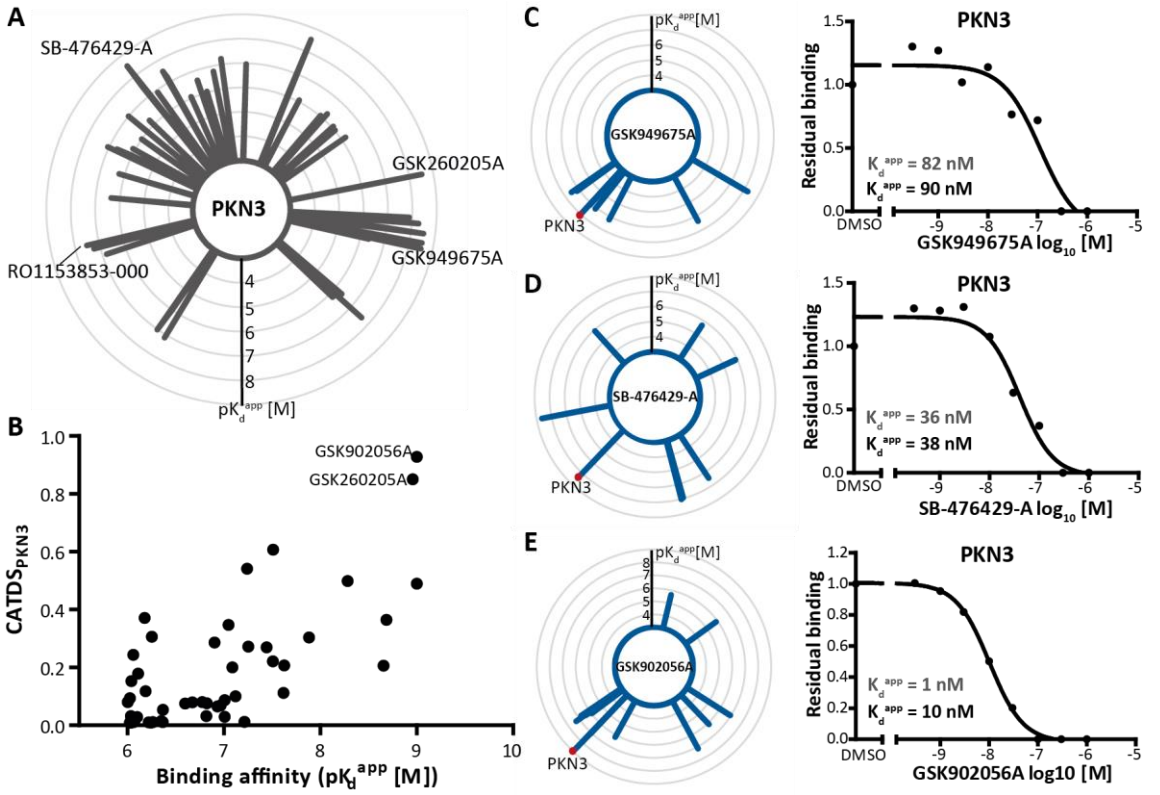

Figure 29 | PKN3 as target of various tool compounds. (A) Radarplot showing compounds that bind to PKN3 (each spike represents one compound and the length corresponds to the affinity). (B) Selectivity for PKN3 as determined by CATDS are plotted against affinities of compounds. Compounds in the top right corner represent high selectivity and affinity. (C-E) Target space (left) of three compounds that led to dose dependent reduction of the intensity of PKN3 (right). K_d^{app} values in grey are derived from two dose data and black K_d^{app} values from full dose response curves.

To confirm affinity values in full dose response manner, several selective and potent PKN3 compounds were profiled using the Kinobeads technology. The compounds were dosed in eight concentrations ranging from 3 nM to 30 µM. As exemplified by GSK949675A (Figure 29 C), SB-476429-A (Figure 29 D) and GSK902056A (Figure 29 E), relative binding of PKN3 to Kinobeads was reduced with increasing compound concentrations. K_d^{app} values of the two dose screen were confirmed and in very good agreement with the full dose response results as exemplified by GSK949675A that showed K_d^{app} values of 82 nM (two dose experiment) and 90 nM (eight dose

experiment). In addition to PKN3, the target space of the three compounds revealed various other targets but with mostly lower affinities (Figure 29 C-E). GSK902056A stood out as the inhibitor with the highest selectivity ($CATDS_{PKN3}$ of 0.93) for PKN3 (10 nM) with PRKCQ (59 nM) being the second most affine target.

***In cell* target engagement of PKN3 inhibitors**. In order to further investigate PKN3 inhibition by the inhibitors, cellular target engagement was measured with a NanoBRET assay in collaboration with Benedict-Tillmann Berger and Dr. Susanne Mueller-Knapp from the Goethe University in Frankfurt, Germany. The NanoBRET assay is a proximity-based assay in live cells that measures the energy transfer of a bioluminescent protein donor to a fluorescent probe (tracer). In the event of competition with an inhibitor of interest, the tracer is displaced and a reduced BRET signal is measured (Introduction Chapter 3.1).[120] In total, sixteen PKN3 inhibitors were selected based on their affinity, selectivity and chemical structure (seven different chemotypes) to be profiled with the NanoBRET assay. Out of the 16 compounds eleven showed a dose dependent reduction of the normalized BRET signal indicating PKN3 target engagement in living cells. Six compounds (structure in Appendix Figure S 3) from four different chemotypes are represented in Figure 30 (remaining compounds are represented in Appendix Figure S 4).

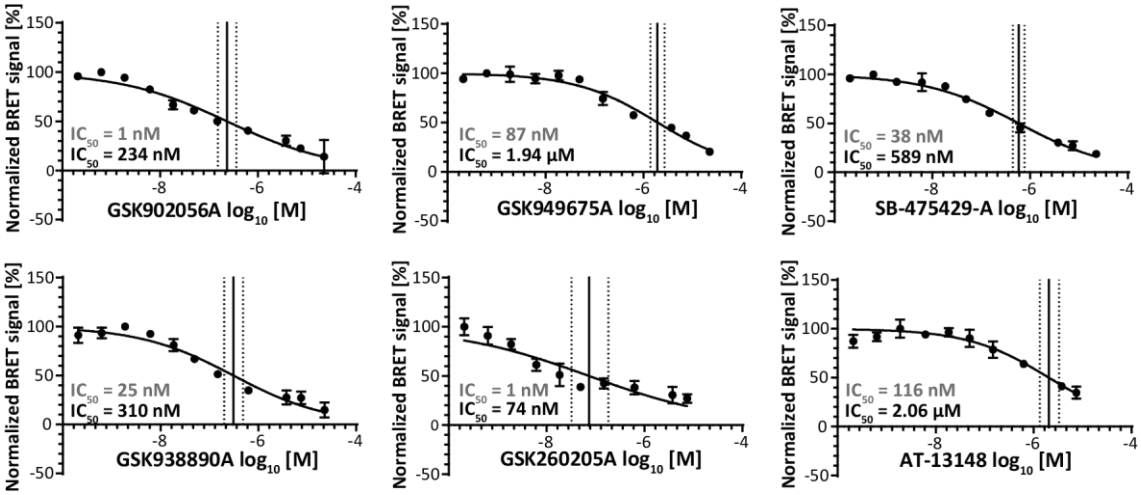

Figure 30 | In-cell target engagement of PKN3 inhibitors. Dose dependent reduction of the BRET signal with increasing inhibitor concentrations were observed indicating PKN3 target engagement in cells. Affinity values (IC_{50}) obtained by Kinobeads experiments are displayed in grey. Experiments were performed by Benedict-Tillmann Berger under supervision of Dr. Susanne Mueller-Knapp at the Goethe University in Frankfurt.

In general, the cellular assay revealed much lower affinities for PKN3 compared to the lysate based assay. For instance, the NanoBret assay unveiled an IC_{50} value of almost 2 µM for GSK949675A while an IC_{50} values of 87 nM was determined using the lysate based Kinobeads technology. Other compounds, like GSK938890A, showed smaller affinity discrepancies between the lysate based assay and the cellular assay with IC_{50} values of 25 nM and 330 nM, respectively. The affinity differences between the two assays are not surprising since the ATP concentration in lysate-based

assays is very low which could lead to an overestimation of the compounds affinity (see Results and Discussion Chapter 3.3). Additionally, it is unknown how well the compounds are transported across the cell membrane which in turn can lead to lower intracellular concentrations of the compounds. A previous study already described affinity and selectivity discrepancies between cellular and recombinant kinase activity assay. Using Dasatinib and Crizotinib as examples, the study revealed improved selectivity in the cellular assay compared to previously published results of biochemical profiling.[59,120] A systematic comparison of affinity and selectivity results obtained by the Kinobeads technology and the NanoBRET assay could help to better estimate cellular target engagement based on Kinobeads screening results.

Identification of potential PKN3 substrates. In the next step, the newly discovered PKN3 inhibitors were utilized to investigate the cellular function and downstream signaling pathways of the understudied kinase in more detail. In order to identify changes in cellular signaling upon PKN3 inhibition, the phosphoproteome of cancer cells in response to PKN3 inhibitor treatment were analyzed. Together with the target space information of the inhibitors, such analysis can help to elucidate potential downstream targets of PKN3. The human colon carcinoma cell line RKO was selected as suitable cell system because of its high expression level of PKN3 according to proteomicsDB.[261] Out of the 49 compounds targeting PKN3, SB-476429-A, GSK902056A and GSK949675A were chosen as they were the most selective and potent compounds with sufficiently material available and most important revealed intra cellular target engagement according to the NanoBRET assay. By overlaying the target space of the three compounds, PKN3 was the only common target (Figure 31 A) which could help to disentangle the drug induced changes of the phosphoproteome of the different inhibitors. In addition, to the three tool compounds identified in this study, phosphoproteomic changes upon THZ1 treatment were investigated. This compound was reported to covalently bind to PKN3 and was commercially available. Phosphoproteomic changes upon THZ1 treatment were already investigated in a previous study in PC3 cells.[260] Moreover, phosphoproteomic changes caused by siRNA knockdown of PKN3 were analyzed. RKO cells were treated with 1 µM of the corresponding inhibitor for 1 h in four biological replicates which led to a total identification of 21,400 phosphosites (Figure 31 B). Significantly regulated phosphosites were identified by statistical testing (t-test, three out of four replicates) and led to a total number of over 8,100 drug-regulated phosphosites (Figure 31 C/D, Appendix Figure S 5). THZ1 and SB-476429-A showed the highest number of significantly regulated phosphosites with 6583 and 3584 respectively whereas GSK949675A, GSK902056A and the siRNA knockdown led to identification of 18, 379 and 801 significantly regulated phosphosites. PKN3 was not completely knocked down by siRNA, since the PKN3 phosphosites T869 and T308 were still identified (Figure 31 C). But as they were detected as significantly down-regulated phosphosites the results were still considered for further analysis.

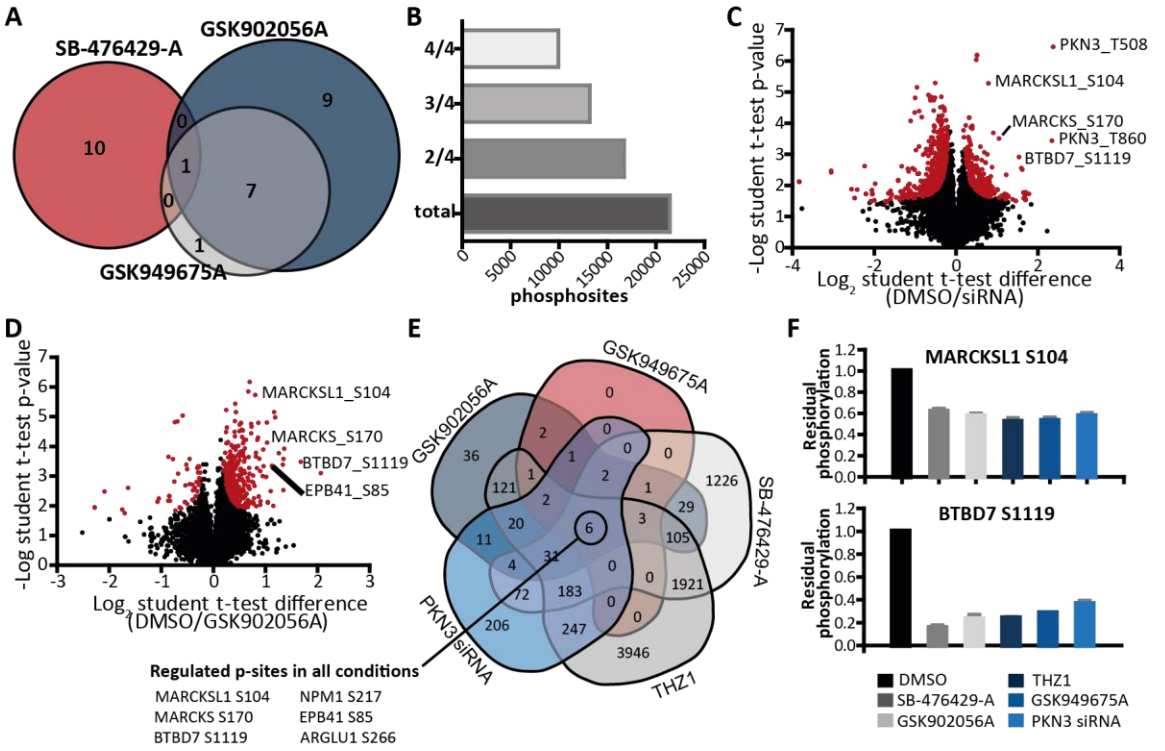

Figure 31 | PKN3 inhibitor perturbed phosphoproteome. (A) The only common target of SB-476429-A, GSK902056A and GSK949675A is PKN3 as determined by the Kinobeads technology. (B) Number of phosphosites identified in the respective numbers of replicates. RKO cells were treated for 1 h with 1 µM of the compounds in quadruplicates. (C, D) Volcano plot showing the regulation of phosphosites after PKN3 knock-down (C) or inhibition by GSK902056A (D). Significantly regulated phosphosites are labeled in red (0.1 % FDR, S0 of 0.05 or 0.04). (E) Overlap of regulated phosphosites after PKN3 inhibition or knockdown. Six phosphosites were down regulated in all conditions. (F) Residual phosphorylation of potential PKN3 downstream targets after inhibition or knock down of PKN3.

Overlaying the regulated phosphosites of all four tested conditions resulted in 6 phosphosites that were down-regulated by all treatment conditions (Figure 31 E). Especially, down-regulation of the phosphosite MARCKSL1 S104 validated the strategy, since it was also identified as potential downstream target of PKN3 in the study of Browne *et al*.[260] The phosphorylation was significantly reduced by almost 50 % after inhibition or knockdown of PKN3 (Figure 31 F). MARCKSL1 is an actin binding protein that controls cell movements. It has been shown that dephosphorylation of MARCKSL1 S120, T148, and T183 which are phosphorylated by JNK, induces cell migration.[262] The function of the phosphosite MARCKSL1 S104 is not yet annotated but since it has been shown that PKN3 and MARCKSL1 are both involved in cell migration one can speculate that MARCKSL1 is a downstream target of PKN3 and that this phosphosite is involved in the migrative phenotype.[106,107,262] Inhibition of PKN3 led to decreased MARCKSL1 S104 phosphorylation which in turn might reduce cell migration. This hypothesis need to be validated by additional experiments which is beyond the scope of this thesis. Like MARCKSK1 S104, the phosphosite MARCKS S170 was also identified as potential downstream target of PKN3 in a previous study.[260] Although this site is reported to be phosphorylated by PKCA, it could theoretically be phosphorylated by both kinases.[263] Furthermore, the phosphosite BTBD7 S1119 was significantly down-regulated upon PKN3 inhibition or knockdown and might thus also be a potential downstream target of PKN3 (Figure 31 F). The protein promotes epithelial-mesenchymal

transition in cancer cells and is associated with metastasis in non-small-cell-lung cancer patient and thus has similar functions to PKN3.[264,265] Here again, further experiments must validate BTBD7 as downstream target of PKN3. In addition, the phosphosites NPM1 S217, EPB41 S85 and ARGLU1 S266 whose function are all unknown, were significantly down-regulated in all treatment conditions.

Overall, Kinobeads profiling of 1,232 small molecule kinase inhibitors revealed more than 6,000 compound-protein interactions and a total of 354 potential chemical probes were identified that target 73 different kinases. Examples of highly selective inhibitors for the kinases CK2 and SYK were validated with functional assays resulting in the identification of novel valuable chemical probes. Also, inhibitors for the understudied kinase PKN3 have been found and utilized for a functional phosphoproteomic study elucidating six potential substrate phosphosites of PKN3. The screening results are publicly available on proteomicsDB[261] so that other scientist can view the data and use them for their specific research question.

3 The Target Landscape of Clinical Kinase Inhibitors

Within the past ten years, 55 small molecule kinase inhibitors have been approved by the FDA and hundreds more entered clinical trials, making small molecule kinase inhibitors one of the fastest growing therapeutical area.[7] In comparison to the tool compounds, knowning the target space of clinical kinase inhibitors is even more important as they are administered to patients. In 2017, Klaeger *et al* published the results of a large scale selectivity profiling study, where the Kinobeads technology was used in a competitive set up to elucidate the target space of 243 clinical kinase inhibitors.[60] Since the publication by Klaeger *et al* does not cover all kinase inhibitors currently in clinical trials, the aim was to continue the Kinobeads profiling of clinical kinase inhibitors. Special emphasize was put on profiling clinical mTOR and PI3K inhibitors, since only due to the new Kinobeads matrix, profiling of such inhibitors was possible. Additionally, an adapted cell-based Kinobeads approach developed by Dittus *et al*[266] was utilized to distinguish between reversible and irreversible targets of clinical covalent BTK inhibitors. Last, the influence of ATP supplementation of cell lysates on the target space of Brigatinib was investigated.

3.1 Compound and Protein Centric Evaluation

The Kinobeads technology was utilized to elucidate the target landscape of 55 clinical small molecule kinase inhibitors. Hereby, compounds were dosed in eight concentrations ranging from 3 nM to 30 µM plus vehicle and target depletion control in a combined lysate of five cancer cell lines (SK-N-BE(2), MV-4-11, K-562, OVCAR8, Colo205) and Kinobeads ε, as an optimal combination (Results and Discussion Chapter 1).

The inhibitor set contained 10 approved drugs, 12 drugs in clinical phase III, 3 in phase II/III, 14 drugs in phase II, 3 in phase I/II and 13 drug in clinical phase I (as of March 2020; a complete list of inhibitors can be found in Supplementary Table 2). The pK_d^{app} values of 55 clinical kinase inhibitors and their corresponding targets were assembled in a drug-target interaction matrix using unsupervised clustering (Figure 32). In total, the 55 drugs targeted 218 direct binders, of which 210 were protein kinases, three were FAD binding proteins, one was a heme binding protein, one metabolic kinase and three were nucleotide binders. The dataset can be analyzed either from a drug centered perspective which provided insights into the target space of a particular drug to uncover off-targets important for toxicity or polypharmacology, or from a protein centered perspective which allowed identification of inhibitors binding to a particular protein, useful, for example, for probe discovery.

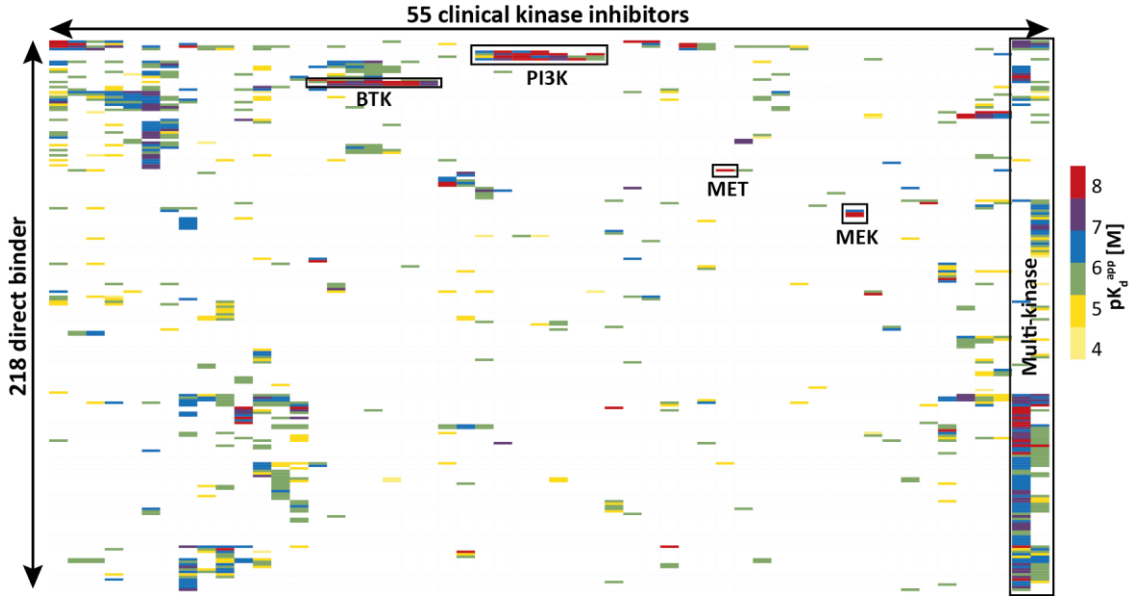

Figure 32 | Target landscape of clinical kinase inhibitors. Unsupervised clustering of 55 clinical kinase inhibitors and their corresponding targets (color code reflects the K_d^{app} of drug-protein interaction). Groups of highly selective (for example MET and MEK inhibitors) and relatively unselective inhibitors (for example multi-kinase inhibitors such as Brigatinib) were identified.

Drug centered perspective. From a drug centered perspective, the data set included several highly selective inhibitors as well as broad spectrum kinase inhibitors. Brigatinib, a designated ALK and ROS1 inhibitor (approved for NSCLC[267]) and Peficitinib, a designated JAK and TYK2 inhibitor (approved for rheumatoid arthritis in Japan[268]) were identified as broad selective inhibitors with 107 and 90 targets, respectively (Figure 32). Contrary, the dataset comprised several highly selective inhibitors such as AMG-337 which showed binding only towards the designated target MET with submicromolar affinity.

Among the 55 clinical kinase inhibitors, 17 were highly selective compounds. As all these molecules have passed stringent criteria of cellular activity to enter clinical trials, they can be considered as chemical probes which target 16 different kinases (Figure 33A). These selective compounds bound to an additional seven kinases (MAP2K4, PKN1, PIK3CG, FGFR1, PLK4, NTRK1 and CDK9) that have not been covered by any selective tool compound (see Results and Discussion Chapter 2.2). The other nine kinases were also targeted by at least one highly selective tool compound.

One example is BAY1251152 (Figure 33 B) which is a selective CDK9 inhibitor with a K_d^{app} of 4 nM and almost 40 times higher affinity to CDK9 over its second most potent target GSK3A (154 nM). Furthermore, Larotectinib is a designated NTRK1 inhibitor. Kinobeads screening results confirmed selective inhibition of NTRK1 with an affinity of 13 nM (Figure 33 B). However, with the used Kinobeads assay setup, enrichement and profiling of the closely related kinases NTRK2 and NTRK3 was not possible, so that it is not known whether the two kinases were also inhibited.

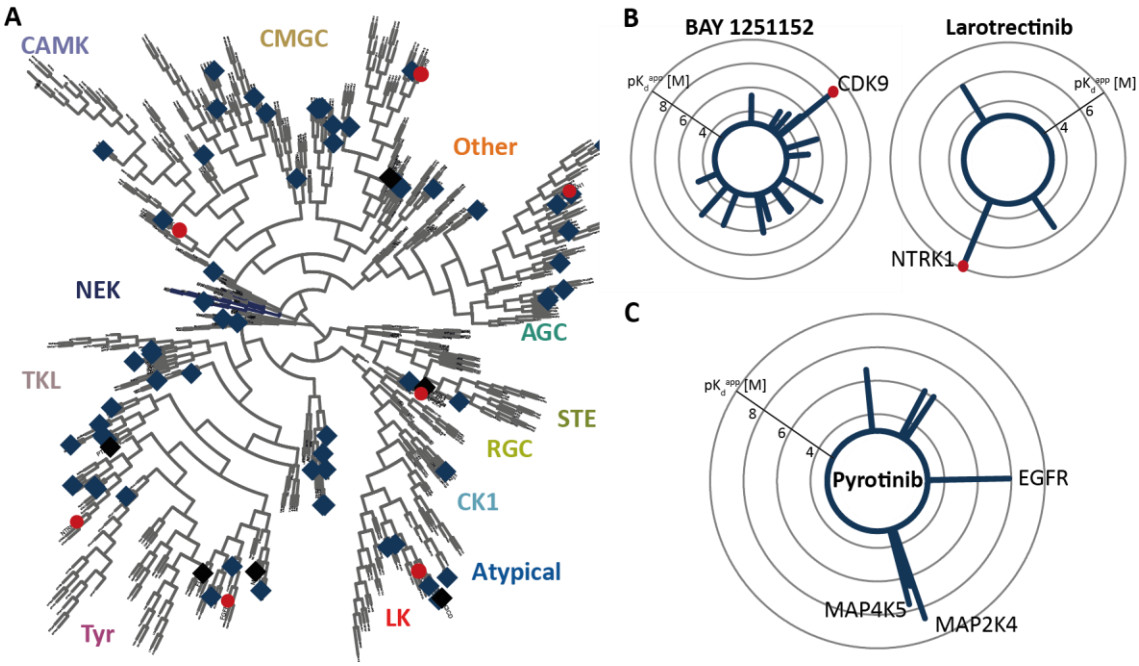

Figure 33 | Identification of potential chemical probes. (A) Kinometree depicting kinases that have been targeted by a selective chemical probe. Kinases marked in red were only selectively targeted by clinical kinase inhibitors, kinases in black were selectively targeted by both tool compounds (Results and Discussion Chapter 2) and clinical kinase inhibitor and kinases in blue were targeted only by selective tool compounds. (B,C) Radarplots showing targets of BAY 1251152, Larotrectinib (B) and Pyrotinib (C). Each spike represents one target and the length displays the affinity.

In contrast to these inhibitors that both targeted their designated target with highest affinity, Pyrotinib, a designated EGFR and HER2 inhibitor, bound to MAP2K4 most potently (K_d^{app} of 2 nM, Figure 33 C). The designated target EGFR was targeted with the second highest affinity (K_d^{app} of 13 nM). MAP2K4 as well as MAP4K5 (K_d^{app} of 24 nM) have not been reported as targets of the approved EGFR/HER2 inhibitor Pyrotinib. Since the affinities were in the same range as for the designated target, MAP2K4 and MAP4K5 probably contribute to the drug's mode of action in patients. MAP2K4 is a dual specific kinase that is involved in the MAP kinase signaling pathway and the SAP/JNK signaling pathway.[269] Large scale genomic studies identified loss-of-function mutations in the MAP2K4 gene in divers cancers.[270] Additionally, other studies categorized MAP2K4 as tumor suppressor and that inhibition promote proliferation of cancer cells.[271,272] Hence, inhibition of MAP2K4 might not be beneficial in cancer patients and it needs to be confirmed, whether Pyrotinib is indeed a MAP2K4 inhibitor.

Next, the selectivity of the profiled clinical kinase inhibitors were analyzed depending on the clinical phase they reached (as of March 2020). Therefore, compounds were sorted according to their clinical status and the number of targets (total, < 1 µM and < 100 nM) were plotted (Figure 34 A). In each clinical phase the number of targets for each inhibitor ranked from only very few to almost 100 targets. As already shown by Klaeger *et al*[60] for 243 clinical kinase inhibitors, the progress of compounds in the clinic is not dependent on the selectivity of the compound and compounds that recently entered clinical trials are not more selective than compounds that have been in clinical trials for some time.

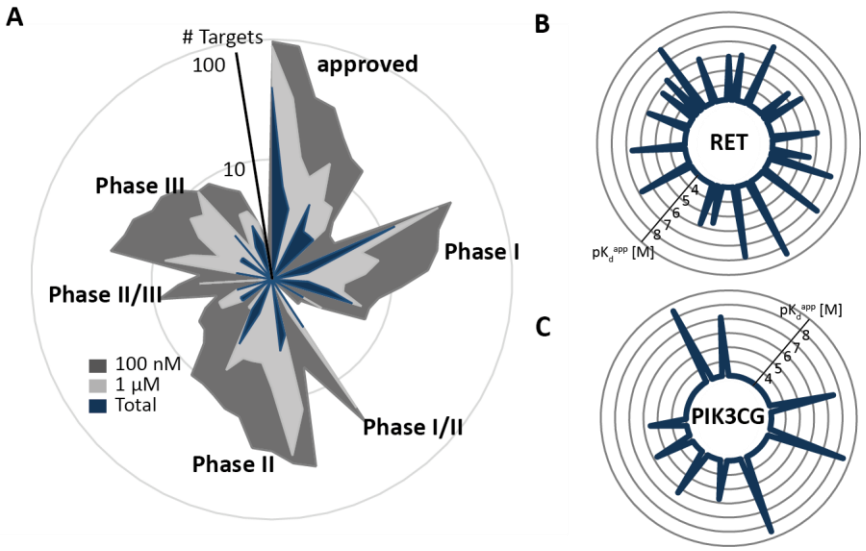

Figure 34 | Selectivity of clinical kinase inhibitors & protein centric view. (A) Compounds are sorted according to their clinical status and the number of targets are plotted (blue < 100 nM; light grey < 1 µM, dark grey total targets). The clinical phase the compound reached so far, is not dependent on their selectivity. (B, C) Radarplots depicting compounds that bind to the kinases RET (B) or PIK3CG (C). Each spike represents one drug and the length of the spike displays the affinity.

Protein centered perspective. The results of Kinobeads screening can be used not only to study the selectivity of a particular drug, but also to investigate the number of drugs against a certain kinase of interest. The most often hit protein was the kinase RET which was targeted by 20 compounds followed by FLT3 with 14 compounds. None of the two kinases were a designated target of any screened compound, indicating that they are very promiscuous kinases.[273] The clinical kinase inhibitor screen revealed that nine clinically relevant inhibitors bind to PIK3CG, three of which were not designated PIK3CG inhibitors (PI3K inhibitors will be further discussed in Results and Discussion Chapter 3.2).

As expected, the majority of targets are protein or lipid kinases but several non-kinase targets were identified. For example, the quinone reductase NQO2 was targeted by three compounds. BGJ398 was the compound with the highest affinity for NQO2 and represented the second most potently inhibited protein of the compound. Previous studies already reported NQO2 as off-target of various kinase inhibitors but the physiological relevance of this off-target still remains unclear.[60,145]

Here, only a brief overview of the Kinobeads drugs screen of 55 kinase inhibitors were given. This project is still ongoing and further clinical kinase inhibitors will be profiled.

3.2 Mode of Action Analysis of Clinical mTOR and PI3K Inhibitors

(The following subchapter is based on data generated by Stephan Eckert during his Master Thesis "Mode of action analysis of clinical mTOR and PI3K inhibitors using chemical proteomics and phosphoproteomics" conducted under the author's continuous supervision at the Chair of Proteomics and Bioanalytics, Technical University of Munich.)

The target landscape of clinical mTOR and PI3K inhibitors. The PI3K/AKT/mTOR signaling pathway is one of most frequently dysregulated signaling pathways in cancer and can be inhibited by various compounds addressing different members of the pathway including mTOR and class I PI3K (referred to as PI3K hereafter). Klaeger *et al*[60] have already analyzed the selectivity of several clinical PI3K and mTOR inhibitors but the used Kinobeads version (Kinobeads γ) was not capable of enriching and competing mTOR and PI3K kinases. By adding iOmipalisib and iBGT226 to Kinobeads γ, profiling of PIK (including PI3K) and PIKK (including mTOR) inhibitors became possible (see Results and Discussion Chapter 1.1). Therefore, 16 PI3K, 11 mTOR and 9 dual PI3K/mTOR inhibitors were (re-)profiled using Kinobeads ε in a competitive pulldown setup. Compounds were dosed at eight inhibitor concentrations ranging from 3 nM to 30 µM and lysates of five cancer cell lines were used. The inhibitor set contained six approved drugs, three drugs in clinical phase III, 13 inhibitors in phase II, two in phase I/II and 12 drugs in clinical phase I. Unsupervised clustering of 36 PI3K and mTOR inhibitors and their respective targets was visualized in a drug-target interaction matrix (Figure 35).

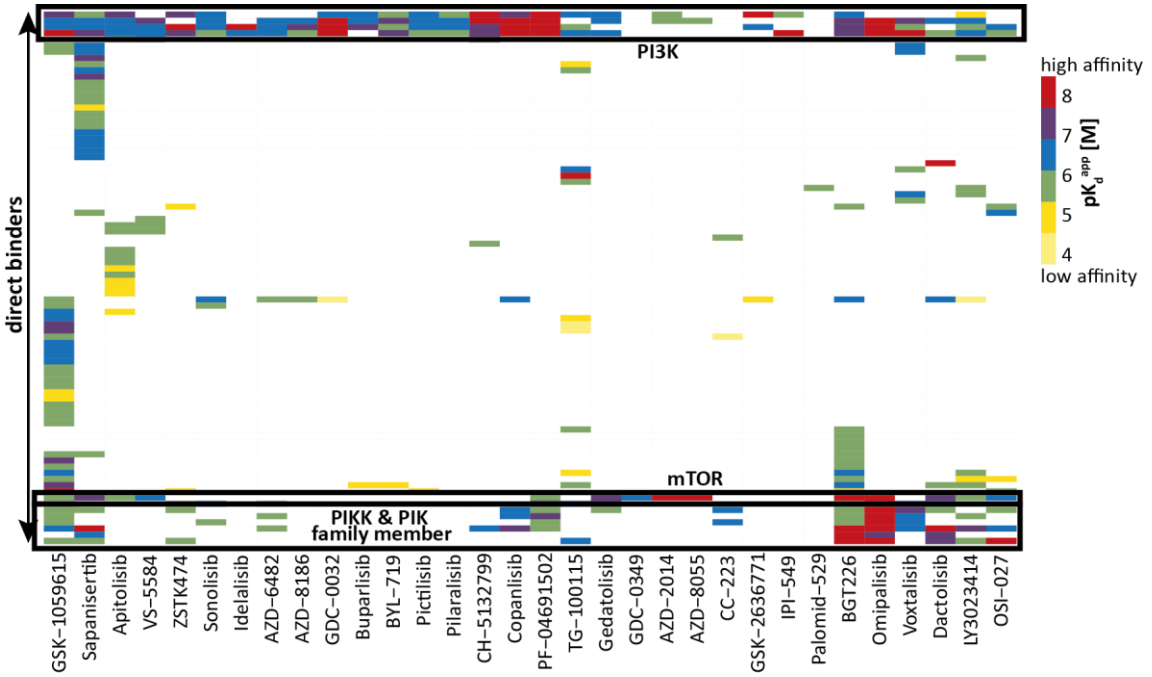

Figure 35 | Drug Matrix of PIKK and PIK inhibitors. Unsupervised clustering of 36 clinical mTOR and PI3K inhibitors and their corresponding targets (color code reflects the pK_d^{app} of drug-protein interactions). Mainly kinases of the PIKK and PI3K family were targeted by the inhibitors.

A total of 86 proteins were targeted by the 36 mTOR and PI3K inhibitors including 79 protein kinases, whereof 13 belong to the PIK and PIKK families, four non-kinase targets and three metabolic kinases. As expected, PI3K and mTOR were predominantly targeted by the inhibitors with high affinities and formed distinct clusters (pK_d^{app} greater than 6). Other family members of the PIK and PIKK were also frequently addressed by the compounds.

Rapamycin, Deforolimus, Temsirolimus and Everolimus (known as Rapalogues) were not listed in the drug matrix because no targets have been annotated. Rapamycin and its analogues exert their inhibitory function in an allosteric way. They form a ternary complex together with FKBP12 and mTOR in mTORC1 preventing the kinase from binding its substrate.[274] Since the Kinobeads technology can only be used to profile ATP competitive compounds unless allosteric inhibitors cause a conformational change in the ATP binding pocket of their targets, the Rapalogues did not score in this assay. Palomid-529 is another known clinical mTOR inhibitor that inhibits both mTORC1 and mTORC2 in an allosteric manner by disrupting the kinase complexes. As expected, binding to mTOR was not observed for Palomid-529 and only NQO1 was identified as off-target of Palomid-529 (Figure 35). CC-223 is a designated ATP competitive mTOR inhibitor but mTOR was not identified as a target, which will be discussed in detail below. Furthermore, co-competition of interaction partners of several PIKK and PI3K family members was detected. For example MLST8 is a known complex partner of mTOR and showed the same dose response behavior as mTOR.[18] Additionally, TTC7B was always co-competed from the beads together with the complex component PI4K that was enriched by the Kinobeads matrix.

Selectivity of mTOR and PI3K inhibitors. To investigate the selectivity more closely in regard to clinical progress and kinase families, the compounds were grouped according to their clinical phases and the number of targets were plotted (Figure 36 A). Additionally, the number of targets within and outside the PIKK and PI3K family were separated by different colors. Rapamycin and its analogs were not included in the analysis, since no statement on the selectivity could be made based on the Kinobeads screening results. The global number of targets of the inhibitors ranked from one target (e.g. GDC-0349) to more than forty (GSK-1059615). Despite off-target binding of some inhibitors (especially GSK-1059615 and Sapanisertib) to several kinases outside the PIKK and PI3K families, most inhibitors were fairly selective for the PIKK and PI3K families. As the PIKK and PI3K families belong to aPKs one can speculate that despite the high structural similarity of the catalytic domain of aPKs to ePKs, the improved selectivity to PIKKs and PI3Ks over ePKs is caused by low sequence similarity of aPks and ePKs. In terms of clinical phases, advanced clinical compounds (phase III and approved) appeared to have fewer targets than compounds currently in clinical phase I or II (Figure 36 A). But only five compounds are currently approved or in clinical phase III making it difficult to draw a conclusion, especially since such a trend was not observed for other clinical compounds targeting ePKs (see Results and Discussion Chaper 3.1). Therefore, the future will show whether the unselective inhibitors currently in phase I or II will also reach clinical approval.

Idelalisib was the first approved aPK inhibitor and was designed as selective PIK3CD inhibitor. The Kinobeads screen confirmed PIK3CD (K_d^{app} of 2 nM) as the most potent target of Idelalisib. Only PIK3CG was identified as additional target but with 150 times lower affinity (K_d^{app} of 300 nM) (Figure 36 B). In addition, selective compounds for other PI3K isoforms and mTOR were found

(Appendix Figure S 6). For example IPI-549 was identified as highly selective PIK3CG inhibitor with over 300 times higher affinity for the main target compared to the other targets. mTOR was selectively inhibited by GDC-0349 and AZD-8055 with K_d^{app} values of 438 nM and 1 nM, respectively.

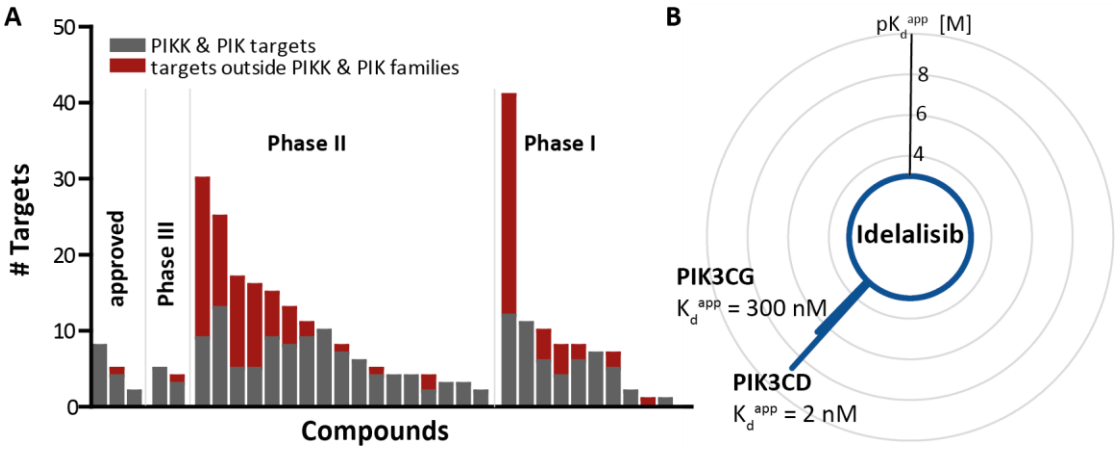

Figure 36 | Selectivity of mTOR and PI3K inhibitors. (A) Number of targets of 32 clinical mTOR and PI3K inhibitors sorted according to their clinical phase. Color reflects off-targets outside the PIKK and PIK families (red) and targets within the PIKK and PIK families (grey). (B) Radar plots representing the targets and the corresponding affinities for Idelalisib. Idelalisib was identified as selective PIK3CD inhibitor.

Novel targets of PI3K and mTOR inhibitors. OSI-027 is a designated mTOR inhibitor and a more than 100-fold higher affinity for mTOR relative to PIK3CA, PIK3CB, PIK3CG and DNA-PK has been reported.[275] The Kinobeads assay revealed nine additional targets to mTOR (K_d^{app} of 118 nM) of OSI-027 with ATR (K_d^{app} of 14 nM) as the most potently bound kinase (Figure 37 A). Up to now, ATR has not been reported as target of OSI-027 which is currently investigated in clinical phase I. To confirm ATR inhibition by OSI-027, a quantitative phosphoproteomic experiment was performed to measure cellular target engagement. SK-BR-3 cells that are characterized by overexpression of HER2 which leads to dysregulated PI3K/AKT/mTOR signalling pathway were treated with 1 µM OSI-027 for 30 min in four biological replicates. After stringent filtering and statistical analysis (FDR of 1 % and S_0=0.24), 51 phosphosites were found to be significantly downregulated after OSI-027 treatment (Figure 37 B). Of these, 32 phosphosites were associated with known substrates of mTOR (marked in blue) like EIF4E-BP1 (S65, T68 and T70) and AKT1S1 (S246) confirming mTOR as target of OSI-027. Additionally, 5 of the downregulated phosphosites could be associated with ATR signalling. For example the nuclear casein kinase and cyclin-dependent kinase substrate 1 (NUCKS1)[276] and mini-chromosome maintenance 3 (MCM3)[277] are known substrates of ATR and both showed reduced phosphorylation (NUCKS1 S75/79 and MCM3 T722) upon OSI-027 treatment. Taken together, the global phosphoproteomic analysis confirmed inhibition of the designated target mTOR and ATR was validated as target of OSI-027 which opens up the opportunity to repurpose the compound as ATR inhibitor.

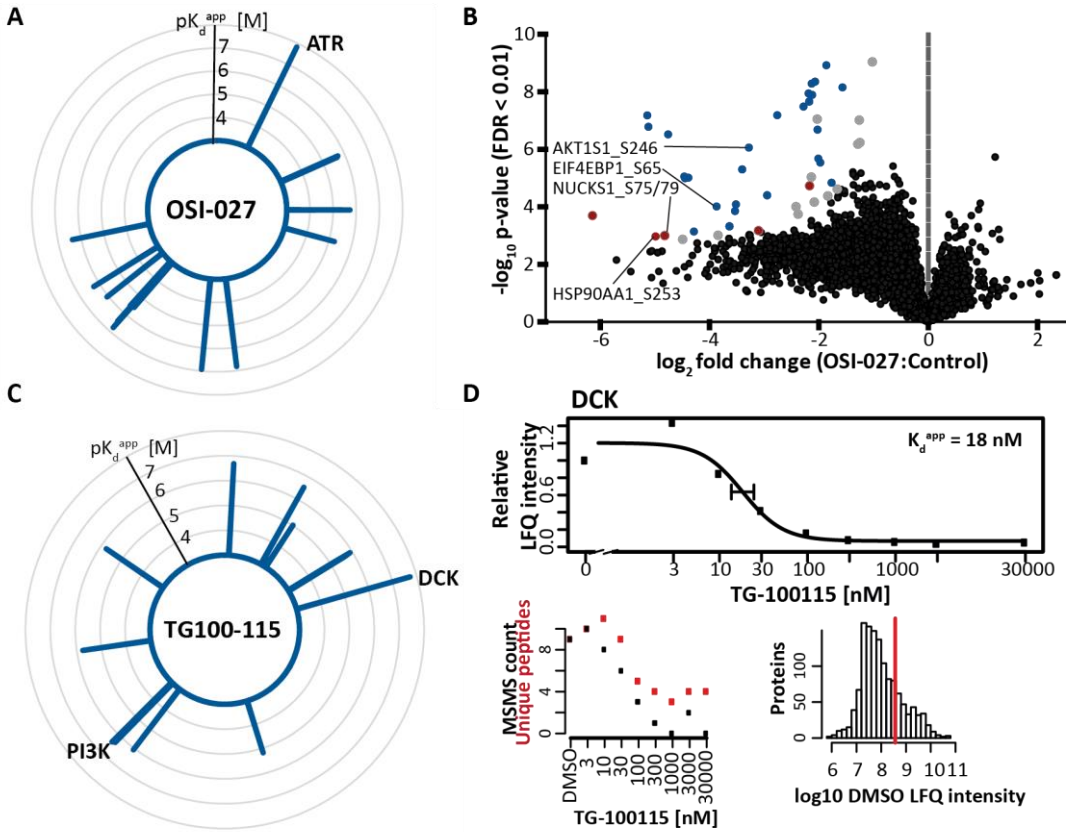

Figure 37 | Unknown off-targets of mTOR and PI3K inhibitors. (A) Radarplot depicting the targets and corresponding affinities of OSI-027. (B) Volcano plot showing log_2 fold changes of quantified phosphorylation sites after treating SK-BR-3 cells with 1 µM OSI-027 for 30 min. Phosphorylation of AKT1S1 S246 and NUCKS1 S75/79 were reduced after OSI-027 treatment. Significantly regulated phosphosites are marked in grey, mTOR associated phosphosites in blue and ATR associated phosphosites in red. (C) Radar plot showing the targets and corresponding affinities of TG100-115. (D) Dose response curve of DCK, peptide and MS/MS counts per TG100-115 dose as well as overall intensity abundance of DCK across all identified proteins within the Kinobeads pulldown experiment are shown.

TG100-115 is a dual PIK3CG and PIK3CD inhibitor that is investigated in clinical phase I/II for myocardial infarction. Selectivity profiling using Kinobeads revealed 20 proteins that were targeted by TG100-115 (Figure 37 C). Affinities of 404 nM and 2 µM were measured for the designated targets PIK3CG and PIK3CD. In comparison, IC_{50} values of 83 nM and 235 nM for PIK3CG and PIK3CD have been reported from a recombinant kinase assay showing discrepancies in the affinity of the compound between Kinobeads and recombinant kinase assay.[278] Deoxycytidine kinase (DCK) was the most potent target of TG100-115 with a K_d^{app} of 18 nM. Dose response curve for DCK derived from Kinobeads pulldowns showed a good sigmoidal shape. This in combination with the overall intensity of DCK in the pulldown and the dose-response behaviour of unique peptides and MS/MS counts indicates DCK as very likely target of TG100-115 (Figure 37 D). DCK phosphorylates deoxycytidine (dC), deoxyguanosine (dG) and deoxyadenosine (dA) and is one of the initial steps in the nucleoside salvage pathway (NSP). Additionally, DCK is responsible for the activation of pro-drugs such as AraC and Cladribine as well as of chemotherapeutic agents like Gemcitabine and Troxacabine.[279] Hence, inhibition of DCK is unfavourable in combination with chemotherapeutics or nucleoside analog pro-drugs due to the reduced conversion rates of the

prodrug into its active phosphorylated form.[280] On the other hand, a previous study showed that inhibition of DCK in combination with thymidine leads to CEM tumor growth inhibition in mice which might open up the opportunity to repurpose TG100-115 as DCK inhibitor for treating some forms of cancers.[281] But DCK first needs to be validated as target of TG100-115 by further experiments.

Characterization of CC-223. The clinical phase II compound CC-223 has been reported to be a selective mTOR inhibitor with an IC_{50} value of 16 nM and FLT4, CSF1R and EPHB3 as off-targets with much lower affinities.[282] While EPHB3 was confirmed as off-target of CC-223 in the Kinobeads assay, no binding to mTOR was detected (Figure 38 A,B). This was quite surprising, since CC-223 is a designated ATP-competitive mTOR inhibitor and profiling using the KiNativ technology has already shown mTOR inhibition by CC-223. The reported results ruled out that CC-223 could be an allosteric inhibitor not accessible to Kinobeads profiling. Additionally, the structure of CC-223 comprises features that are typical for an ATP competitive inhibitor such as the hinge binding region (Figure 38 C). A hypothesis why mTOR was not identified as target in the Kinobeads assay was that the supplier provided a wrong isomer of the compound. Looking at the chemical structure, the substituent of the heterocyclic core structure exhibits stereochemistry. The trans conformation in which the methoxy group and the heterocyclic core show the opposite orientation to the cyclohexane ring was identified as the best mTOR inhibitor in the original SAR study.[283] In order to evaluate the hypothesis that the wrong isomer was provided, CC-223 was purchased from Cazman, Adooq and again from Selleckchem (same batch, new aliquot) and Kinobeads pulldowns of the compounds were performed using lysates of a five cancer cell line mixture. The drug-target matrix revealed submicromolar mTOR inhibition by all newly purchased inhibitors (Figure 38 B). ATM, ATR, PIK3C2A, PI4KB and MAP3K1 were identified as novel off-targets of CC-223 in addition to the already known off-targets FLT4 and EPHB3. This outcome overlaps with reported results by Mortensen *et al.*[282,283]

In conclusion, the first aliquot obtained from Selleckchem did not contain the correct compound but since the total mass of the molecule as analyzed by an amazon speed ETD ion trap mass spectrometer was 397 Da as expected, the compound is most likely an isomer of the original compound. A previous study for instance also revealed that a incorrectly synthesized regioisomer of NVP-BHG712, which led to strong effects on the binding mode of the compound, are provided by several chemical vendors.[284] It was still surprising that the new Selleckchem aliquot showed mTOR inhibition while the first aliquot did not, although both were from the same batch. A Kinobeads pulldown experiment from the first Selleckchem aliquot was even repeated by two independent people with newly generated compound dilution stocks so that an experimental error could be excluded. One explanation could be that the compound is not stable in DMSO but this needs to be tested with further experiments. Nevertheless, Kinobeads profiling of CC-223 revealed PIK3C2A as most potent target of the inhibitor which makes the molecule interesting for the development of PIK3C2A inhibitors. The class II PI3K isoform currently lacks a selective inhibitor and CC-223 could be a starting point for medicinal chemistry to develop a chemical probe for PIK3C2A.

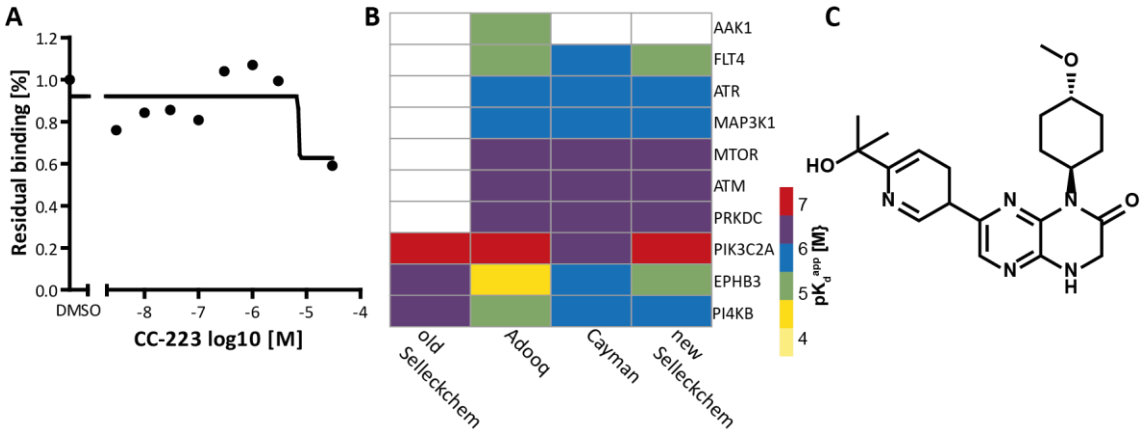

Figure 38 | Characterization of CC-223. (A) Residual binding of mTOR to Kinobeads was not reduced with increasing concentrations of CC-223 (first aliquot provided by Selleckchem). (B) Drug-target matrix depicting pK_d^{app} values of CC-223 obtained from different suppliers and its corresponding targets. (C) Chemical structure of CC-223.

3.3 Kinobeads for Target Identification of Irreversible BTK Inhibitors

(The following subchapter is based on data generated by Doil Yun during his Bachelor Thesis "Establishing a chemical proteomics assay for target identification of irreversible BTK inhibitors" conducted under the author's continuous supervision at the Chair of Proteomics and Bioanalytics, Technical University of Munich.)

The Kinobeads technology was originally developed to profile reversible ATP competitive kinase inhibitors. Dittus and colleagues[266] have adapted the Kinobeads technology to enable the differentiation between irreversible and reversible binding of type VI inhibitors to kinase targets (Figure 39). Hereby, a lysate-based and a cell-based Kinobeads assay are performed in parallel. In the lysate-based Kinobeads assay, the drug is added to lysates and Kinobeads pulldowns are performed as usual. In contrast, in a cell-based Kinobeads assay, the drug is incubated with live cells and after incubation, washing, and lysis, a Kinobeads pulldown is performed. Drug dilution after washing and lysis leads to re-equilibration of the binding equilibrium of reversible drug-target interactions and results in an IC_{50} shift to lower affinities in the cell-based compared to the lysate-based Kinobeads assay. In contrast, irreversible covalent drug-target interactions were not affected and appear equipotent or even more potent in cell-based assays. Higher target engagement in cells can be explained by higher incubation temperatures and longer incubation times in the cell-based Kinobeads assay. Additionally, the lysis of cells causes disruption of the native cellular redox environment and local pH which influences cysteine reactivity.[266,285]

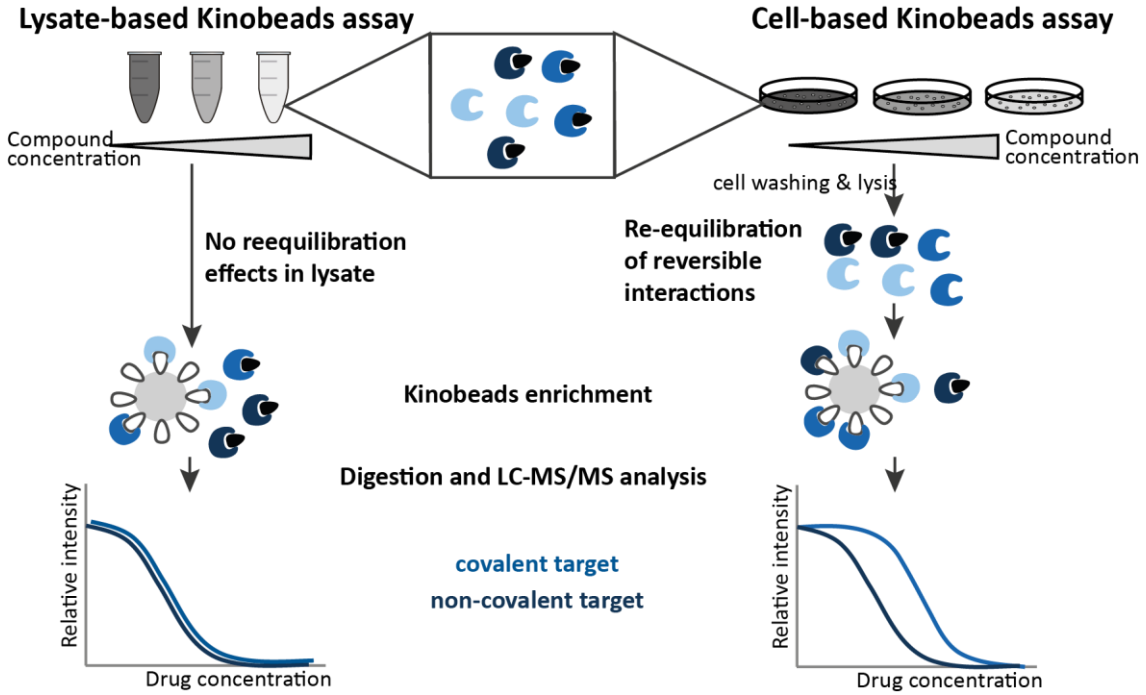

Figure 39 | Concept of Kinobeads selectivity profiling of irreversible kinase inhibitors. Lysate-based and cell-based Kinobeads assays are performed in order to distinguish between reversible and irreversible binding of kinase inhibitors. While irreversible targets display similar potencies in both assays, reversible targets display an IC_{50} shift towards lower affinities in a cell-based Kinobeads assay. Modified from Dittus *et al.*[266]

BTK is a kinase that plays an essential role in activation of B-cell receptor signaling which stimulates cellular processes such as B-lymphocyte proliferation and survival.[286] Constitutively active BTK leads to pathogensis of B-cells making it an important therapeutic target for treatment of blood-related cancer types such as leukemia and lymphoma.[287] Several irreversible covalent BTK inhibitors have been profiled in the clinical kinase inhibitor screen (Figure 32). The first approved covalent BTK inhibitor was Ibrutinib which targets the cysteine at position 481 within the ATP binding site.[288] A wide range of side effects and resistance to Ibrutinib has led to the development of second-generation BTK inhibitors (for example Acalabrutinib, ONO-4059, Evobrutinib and Zanubrutinib).[289] To better understand the drug mode of action and to distinguish between reversible and irreversible target inhibition, the adapted Kinobeads assay by Dittus *et al*[266] for covalent inhibitors was performed. The myelogenous leukemia cell line K-562 or lysates thereof were incubated with Ibrutinib, Acalabrutinib, ONO-4059, Evobrutinib and Zanubrutinib over a range of concentrations (3 nM to 30 µM plus vehicle) and subsequent Kinobeads pulldowns were performed. Obtained pK_d^{app} values of the two experiments were compared for each inhibitor (Figure 40). Irreversible targets were located on the left side of the diagonal and could be differentiated from reversible targets that were located on the right side.

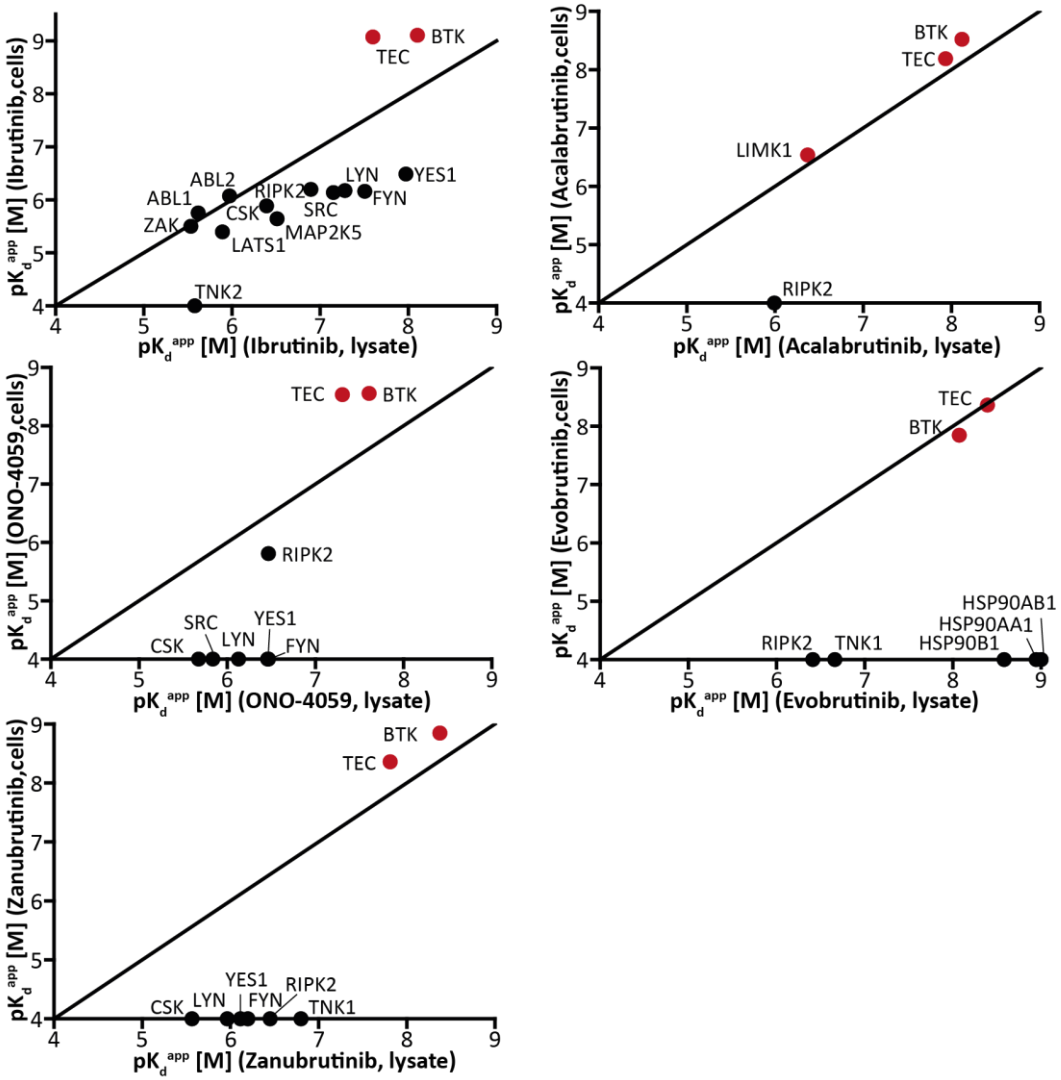

Figure 40 | Reversible and irreversible target space of covalent BTK kinase inhibitors. pK_d^{app} values obtained by K-562 lysate-based and cell-based Kinobeads assays are compared. Data points left of the line represent irreversible targets (marked in red) and points on the right reversible targets (marked in black). Data points on the axes are imputed targets that were exclusively identified in the lysate based assay.

BTK was identified as covalent target of all five BTK inhibitors with IC_{50} values of 1 to 14 nM in cells and 4 to 24 nM in lysates (Figure 40) indicating that the cell based Kinobeads assay resulted in equipotent or even slightly higher affinities compared to the lysate-based assay. Additionally, TEC was a common off-target for all inhibitors showing IC_{50} values between 1 to 6 nM in cells and 4 to 49 nM in lysates (Figure 40). Beside these two kinases another eight kinases including the whole TEC kinase family (BTK, TEC, ITK, BMX and TXK), have been reported to contain a cysteine in the front pocket that can theoretically covalently attacked the BTK inhibitors.[290] In fact, some adverse side effects of Ibrutinib has been reported to be caused by covalent EGFR[291], TEC and ITK[292] inhibition.[293] While TEC was identified as irreversible target of Ibrutinib in the Kinobeads assay, EGFR and ITK were not detected as targets. EGFR and ITK are not expressed in K-562 cells according to full proteome analysis of the cell line, which prohibit Kinobeads profiling of these kinases in the experiment.[60] BMX[294], ERBB4[295] and MAP2K7[296], all carrying a reactive cysteine in the front pocket of the kinase domain, were also reported as covalent targets of Ibrutinib but

could not be identified as targets with the Kinobeads assay. BMX and ERBB4 were both not expressed in K-562 cells, whereas MAP2K7 was highly expressed but could not be enriched by Kinobeads ε. Kinases that are not expressed in the used cell line or cannot be enriched by the affinity matrix are not amenable to Kinobeads profiling. This feature of the Kinobeads assay prevent comprehensive target deconvolution of BTK inhibitors, so that potential covalent off-targets such as BMX and ERBB2 also remain undetected for the other four compounds. An optimized affinity matrix that can enrich the whole TEC family and another cell system that highly express proteins of the TEC family might therefor be beneficial for BTK inhibitor profiling.

The Kinobeads assay also displayed LIMK1 as irreversible covalent target of Acalabrutinib (Figure 40) whereas Dittus *et al*[266] reported the kinase as reversible target. LIMK1 was identified only with a few peptides and showed a low intensity. In addition, LIMK1 lack a reactive cysteine in the front pocket of the kinase domain suggesting that LIMK1 is rather a reversible than an irreversible target of Accalabrutinib.

Overall, Ibrutinib, a first-generation BTK inhibitor displayed the highest number (12) of reversible off-targets whereas second-generation BTK inhibitors were more selective towards BTK with a significantly lower number of off-targets. The adapted Kinobeads assay detected 13 kinase and three other proteins (HSP90) as reversible targets of the screened BTK inhibitors. All five compounds showed reversible binding to RIPK2. Additionally, members of the SRC kinase family, including SRC, LYN, FYN, YES1, and CSK were also targeted by three compounds (Ibrutinib, ONO-4059 and Zanubrutinib). These kinases appeared to be common off-targets of BTK inhibitors and binding to such kinases should be considered in the development of new covalent BTK inhibitors. In contrary, several kinases were only inhibited by one of the screened compounds like LIMK1 (Acalabrutinib) or ABL1, ABL2, LATS1 (Ibrutinib). Evobrutinib revealed binding to multiple heat shock protein 90 isoforms (HSP90B1, HSP90AA1, HSP90AB1). These were however targets of low confidence with very low affinity values (0.01-3 nM) which were difficult to detect with the used assay set up (lowest inhibitor concentration of 3 nM). Nevertheless, since three isoforms of HSP90 showed the same binding behavior and the HSP90 has ATPase activity so that it can theoretically be enriched by Kinobeads, HSP90B1, HSP90AA1, HSP90AB1 were still considered as potential target. Further experiments are required to validate HSP90 inhibition of Evobrutinib.

In general, reversible targets were mostly identified only in the lysate based assay due to drug washout and dilution in the cell based assay that led to re-equilibration of the drug-target binding equilibrium and a shift of IC_{50} values outside the examined concentration range. However, some exceptions occurred such as RIPK2 in ONO-4059 treatment which can be caused by long residence times of the compound to this target, or in the case of Ibrutinib due to insufficient re-suspension of cells during the washing steps.

In summary, the methodology of Dittus *et al*[266] could successfully be reproduced and was used to distinguish between irreversible and reversible target inhibition of five BTK inhibitors. Differentiation between reversible and irreversible targets is of great importance for clinical application of the drugs. The turnover of BTK has been estimated to be between 18 and 24 h.[297] This rather slow turnover rate causes high level of target engagement and inhibition of BTK long after clearance of the irreversible inhibitor from the body. Hence, less dosing of the drug is required to block the activity of the designated target. This in turn mitigate off-target effects of reversible targets *in vivo*, since the concentration of the drug is only transiently above a level

where off-target binding matters. In contrast, covalent off-target are still highly relevant for *in vivo* administration of the drug where the duration of the effect is only dependent on the turnover rate of the protein.

3.4 Influence of ATP Concentrations on the Target Landscape of Brigatinib

(The following subchapter is based on data generated by Felix Klingelhuber during his Master Thesis "Influence of the ATP concentration on the affinity between Brigatinib and its targets in kinome-wide binding assays" conducted under the author's continuous supervision at the Chair of Proteomics and Bioanalytics, Technical University of Munich.)

Most small molecule kinase inhibitors bind to the ATP binding pocket of the kinase and thus compete with ATP for binding to that pocket (Introduction Chapter 2.1). The concentration of ATP in human cells has been reported to be between 1 mM and 5 mM and can vary between cell type, cell state and on sub-cellular levels between different organelles and compartments.[298-300] Depending on the Michaelis-Menten constant K_M of ATP towards protein kinases in cells, the high ATP concentrations can prevent target engagement of kinase inhibitors in cells. Cell lysis leads to a drastic dilution of the ATP concentration to less than 1 µM which was determined by a luminescent CellTiter-Glo assay (data not shown here). The Kinobeads assay that was used in this study, is a lysate based method and previous results have shown that values derived from lysate based assays do not always correlate well with *in vivo* target engagement (see Results and Discussion Chapter 2.3). Such discrepancies can not only be caused by cell permeability which can lead to lower intracellular drug concentrations but also for example by different ATP concentration in cells and in lysates.

The target landscape of Brigatinib. To investigate the influence of increasing ATP concentrations on the binding affinities as determined by Kinobeads, a series of competitive Kinobeads pulldowns of Brigatinib with addition of different ATP concentrations in the lysates were performed. Brigatinib, a type I inhibitor, was chosen here because the clinical kinase inhibitor screen revealed Brigatinib as multi-kinase inhibitors with a total of 107 targets covering a broad spectrum of different kinases and other proteins across an affinity range of four orders of magnitude. MgATP were dosed in eight concentrations ranging from 0.32 µM to 5 mM and was added together with the inhibitor to the lysate. Unbound proteins were subsequently enriched by Kinobeads.

As stated above (Results and Discussion Chapter 3.1), the Kinobeads pulldown without ATP supplementation revealed 107 targets of Brigatinib with TNK1 being the most potent target with an affinity of 0.6 nM (Figure 41 A, B). Seven Brigatinib targets had affinities below 10 nM and another 17 proteins an affinity lower than 100 nM. With increasing ATP concentrations the number of Brigatinib targets decreased. In particular at an ATP concentration of 5 mM, significantly fewer targets (65 targets) were identified including only 14 targets with affinities below 100 nM (Figure 41 B). Targets with high affinities in pulldowns without the addition of MgATP generally drifted to higher K_d^{app} values, while proteins with already low affinities tended

not to be identified as targets any more. This global trend did not apply to every single kinase, therefore, the differences in affinities of individual kinases were investigated in the following.

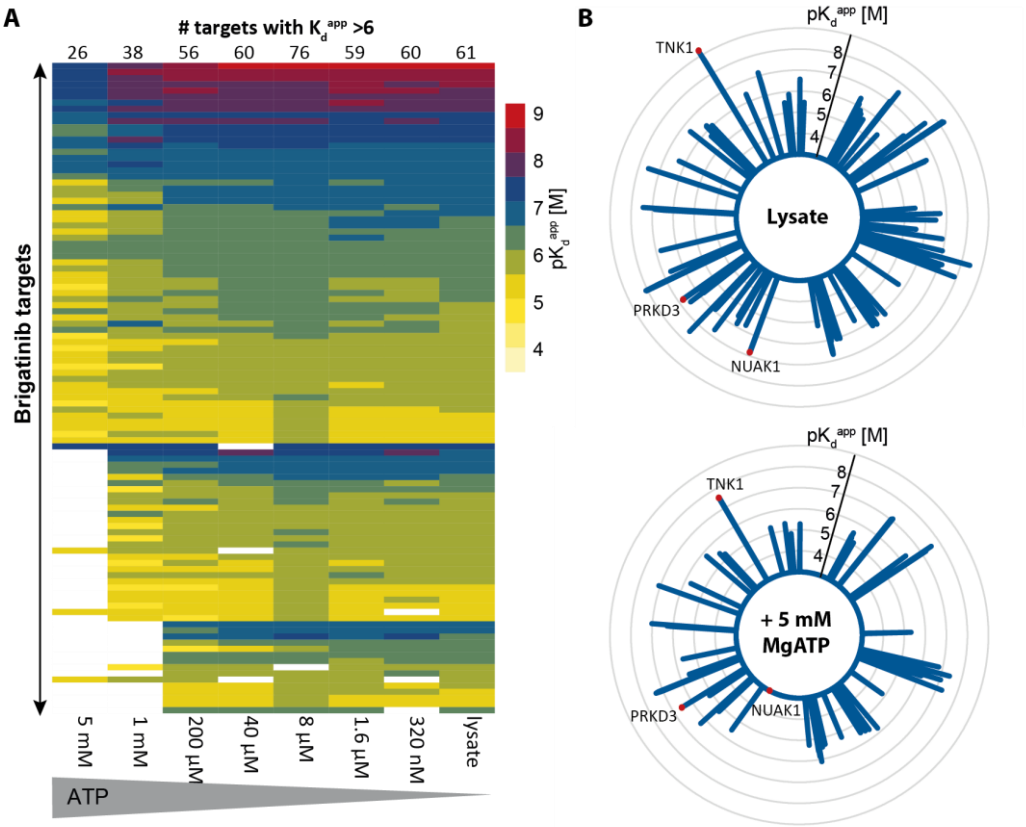

Figure 41 | Target space of Brigatinib dependent on ATP concentrations in lysates. (A) Matrix of all Brigatinib targets that were determined in a Kinobeads pulldowns supplemented with increasing ATP concentration as indicated. Number of targets with an affinity below 1 µM are displayed above the heatmap. (B,C) Radarplots depicting the targets of Brigatinib with and without addition of 5 mM MgATP to the lysates. Increasing ATP concentrations led to fewer Brigatinib targets.

Addition of 5 mM MgATP to lysates resulted in a 50-fold shift of the affinity of the most potent Brigatinib target TNK1 from 0.6 nM to 28 nM (Figure 41 B; Figure 42 A). For another 47 Brigatinib targets, the affinity was also reduced at least by a factor of two. The kinases NUAK1 and CSNK2B were detected as submicromolar targets of Brigatinib with affinities of 157 nM and 310 nM. The two kinases could not be identified as targets anymore, when lysates were supplemented with 5 mM of MgATP. The affinities of an additional 42 targets were shifted outside of the examined drug concentration range and no dose response curves were detected when the lysate was supplemented with 5 mM MgATP. In contrast, increasing MgATP concentrations in the cell lysates had no effect on the affinities of 19 targets including PRKD3 with affinities of 209 nM and 276 nM. Hence, supplementation of lysates with MgATP led to different affinity shifts of Brigatinib targets.

The different affinity offsets additionally resulted in a new order of ranked affinities. For example, while PTK6 was classified as the 14th most potent target in the pulldown experiment without

MgATP addition, it became the 7th most potent target when lysates were supplemented with 5 mM MgATP. The affinity of PTK6 (42 nM) in the experiment without MgATP supplementation, was about 40 times higher than the affinity of TNK1 (0.6 nM). This affinity difference was drastically minimized to a factor of two, when 5 mM MgATP was added to the lysate. In this case affinities of 59 nM and 28 nM were determined for PTK6 and TNK1. Overall, the results suggest that the selectivity of a compound as determined by a Kinobeads pulldown experiment, might change in cells due to the presence of high ATP concentrations. Some targets might not be targeted in cells anymore while other targets might gain importance in cells and become one of the most potently inhibited protein (like PTK6).

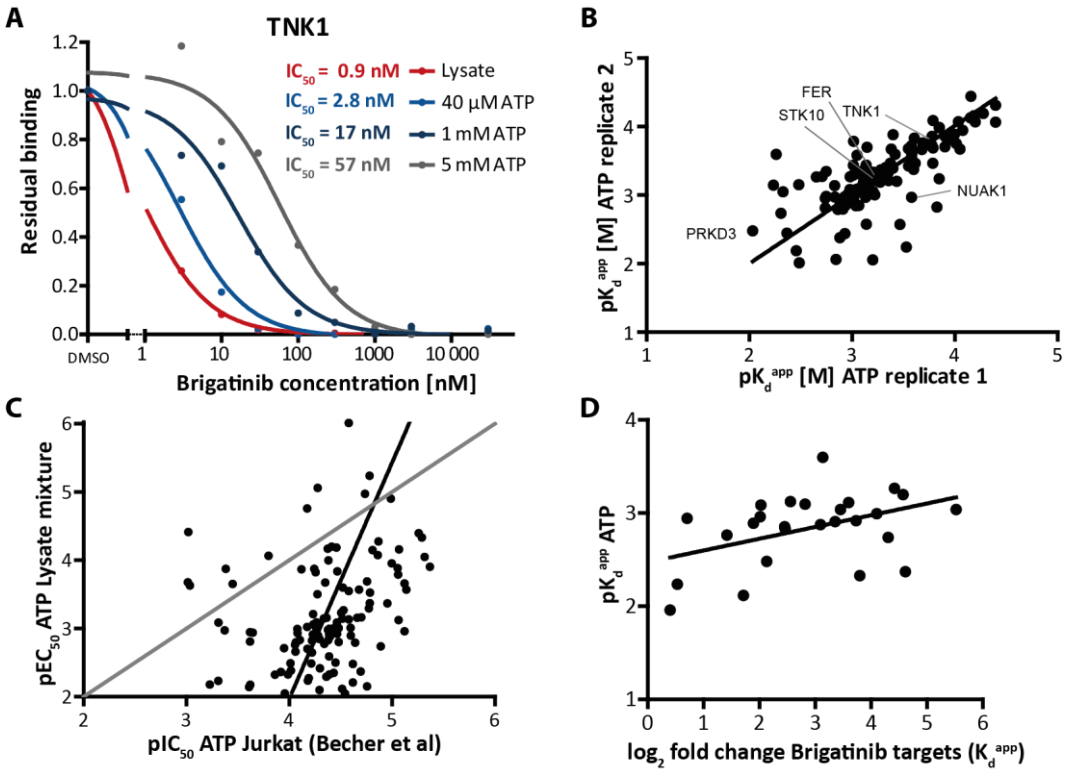

Figure 42 | Affinity shift of Brigatinib targets with higher ATP concentrations. (A) Dose response curves of Kinobeads competition assays with Brigatinib and different MgATP concentrations for TNK1. With higher MgATP concentrations, IC_{50} values are shifted towards lower affinities. (B) Correlation of MgATP pK_d^{app} values as determined by competition Kinobeads assay in two individual replicates. (C) Correlation of MgATP pEC_{50} values as determined by competition Kinobeads assay to reported pIC_{50} values by Becher et al.[301] (D) Correlation of the log_2 fold change in the affinities of Brigatinib targets measured with or without 5 mM ATP supplementation of cell lysates to the measured ATP affinities. Higher ATP affinities seems to result in a larger target affinity shifts.

ATP affinities of kinases. Similar to Brigatinib competition curves which were derived from different inhibitor concentrations, the DMSO controls of these pulldown experiments with increasing ATP concentrations were used to generate target competition curves for MgATP. A prerequisite for this ATP affinity calculation is the assumption that ATP only binds to the kinase but is not converted to ADP. To test this, a luminescent CellTiter-Glo assay was performed and the concentration of ATP in the lysate after addition of 1 mM MgATP were measured. Over a time

course of 1.5 h incubated at 4°C, no decrease in the ATP concentration was measured (data not shown here).

ATP binding affinities were determined for 165 proteins, including 123 kinases. K_d^{app} values for ATP were in a range between 40 µM and 5 mM. ATP affinity values of two individually performed Kinobeads pulldowns experiments correlated well (Figure 42 B). ATP binding properties of kinases in Jurkat and SK-MEL-28 has been reported previously by Becher *et al*.[301] They utilized a different version of Kinobeads for affinity enrichment of kinases out of lysates supplemented with increasing MgATP concentrations. Although the experimental setup was similar to the one presented here, the correlation of pIC_{50} values for ATP was poor (Figure 42 C). Becher *et al* reported in general 10 to 100 fold higher affinities for ATP. The major differences between the two experiments was that i) Becher *et al* used lysates of one cell line compared to a lysate mixture of five cell lines as used here in this study and ii) they gel-filtered their lysates to remove endogenous nucleotides and other low molecular weight compounds. It can be speculated that the depletion of ATP and other nucleotides largely impact the experimental outcome and led to the differences in observed ATP affinities.

In the next step, it was evaluated whether changes in the affinities of different Brigatinib targets was dependent on the ATP affinities. Therefore, the K_d^{app} shift (log_2 fold changes) of Brigatinib targets determined in pulldowns with or without 5 mM MgATP supplementation were correlated to their determined ATP affinities (pK_d^{app} values). Only 26 proteins were considered for which a K_d^{app} shift and an affinity to ATP could be calculated. Kinases, which were not identified as targets in the Kinobeads experiment with 5 mM ATP, were excluded from this analysis. Here, a general trend was observed where slightly higher ATP affinities led to a higher affinity shift of the protein to Brigatinib. Hence, the different affinity shifts of Brigatinib targets could be explained at least in parts by the ATP affinities of the kinases.

Prediction of ATP related inhibitor affinities. In the next step, it was investigated whether the ATP affinities could be utilized to predict affinity values of Brigatinib targets in the presence of excess ATP without performing an extra experiment where lysates are supplemented with the corresponding ATP concentration. According to Cheng and Prusoff[153,301], the IC_{50} value of a cell permeable compound to its targets in the presence of competing cellular ATP can be approximated by the following equation:

$$IC_{50} = K_d^{app} * (1 + \frac{[ATP]}{K_d^{app}(ATP)}) \quad (10)$$

With K_d^{app} as the target affinity determined by Kinobeads pulldowns, the concentration of ATP and the affinity of the kinase to ATP, IC_{50} values of Brigatinib targets at different ATP concentrations were calculated. Such calculated pIC_{50} values were then correlated to the experimental obtained pK_d^{app} values (Figure 43). Here again, kinases which were not identified as targets in the Kinobeads experiment where lysates were supplemented with 5 mM or 1 mM ATP, are not displayed in the correlation. Hence, the number of data points for 5 mM ATP supplementation was much lower than the number of data points for 1 mM ATP. In addition, only proteins were correlated for which

an ATP affinity could be determined. Overall, the predicted pIC_{50} values correlated very well to experimental obtained pK_d^{app} (Figure 43). Moreover, targets that were not detected in the ATP supplemented pulldowns, had predicted affinities mainly below 10 µM. Overall, the very good agreement of calculated and measured target pIC_{50} and pK_d^{app} values dependent on the ATP concentration, enables the opportunity to calculate compound affinity values dependent on different ATP concentrations without the need for additional experiments as long as the ATP affinity of a kinase is known. The next step would be to investigate whether accounting for higher ATP concentrations would lead to more comparable reults between the Kinobeads technology and *in cell* compound profiling assays which is beyond the scope of this thesis.

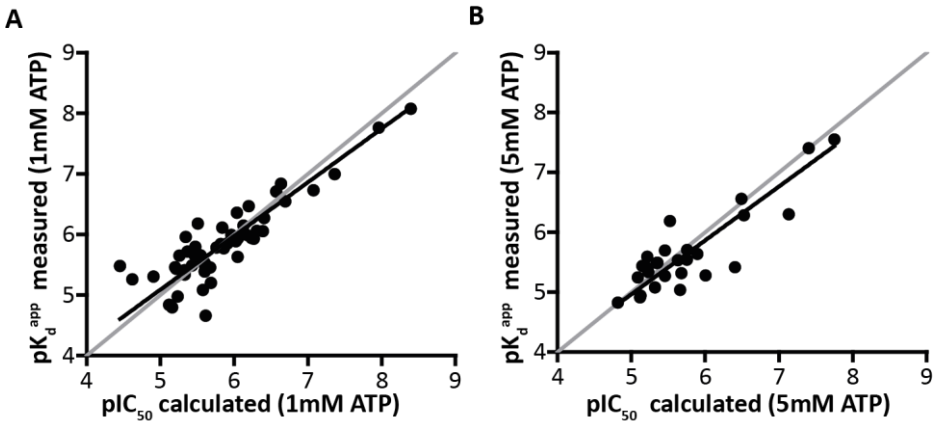

Figure 43 | Prediction of affinity values dependent on ATP concentrations. (A,B) Correlation of calculated pIC_{50} values according to the Cheng and Prusoff equation to measured pK_d^{app} values when lysates were supplemented with 1 mM (B) or 5 mM (C) MgATP. Calculated and measured affinities correlated very well.

In summary, target deconvolution of 55 clinical kinase inhibitors were performed which led to the discovery of highly selective inhibitors as well as highly unselective inhibitors. Special emphasis was put on the profiling of mTOR and PI3K inhibitors which was made possible by the new Kinobeads matrix. Kinobeads profiling revealed an interesting off-target (DCK) of the designated mTOR inhibitor TG100-115. In addition, an adaptive Kinobeads workflow enabled distinguishing between reversible and irreversible off-target of five covalent BTK inhibitors. Furthermore, it was shown that ATP supplementation of the lysate prior to Kinobeads enrichment resulted in a shift of affinities for some kinases which can be predicted by the Cheng and Prusoff equation.

General Discussion and Outlook

Table of contents

1 Future Prospects of Kinobeads

Kinobeads - an outdated technology. The Kinobeads technology was first described in 2007 by Bantscheff *et al* and is a powerful technique to elucidate the target space of small molecule kinase inhibitors. In comparison to recombinant kinase assays, Kinobeads enable inhibitor profiling under close-to physiological conditions by using complex cell lysates that contain endogenously expressed full-length proteins that have been functionalized in a cellular context and carry all required post translational modifications, cofactors and binding partners. However, using purified isolated catalytic domains, like done in recombinant kinase assays, facilitate higher throughput than the lysate-based Kinobeads assay and enable profiling of thousands of compounds against many kinases in a short period of time. Although the Kinobeads workflow was optimized towards higher throughput in this thesis (mainly by reducing input material, inhibitor concentrations and data acquisition time), profiling of over 1,200 kinase inhibitors still required 8 g of protein from cell extracts and resulted in a total mass spectrometric measurement time of more than 180 days prohibiting large scale screening campaigns of thousands of small molecule kinase inhibitors. Further workflow optimization may increase throughput but recombinant assays still remain the better high throughput screening method for small molecule kinase inhibitors.

Although the Kinobeads technology accomplishes close-to nature conditions, detection of drug-kinase interactions with the lysate based method does not necessarily translate into binding of the drug to the kinase in living cells. Recent studies have shown that lysate-based and intracellular assays largely differ in their affinity and selectivity results.[120,140] Target localization, cellular compartments, intracellular ATP concentrations and naturally occurring metabolite concentrations are not considered in lysate based methods and influence intracellular target engagement of kinase inhibitors. Over the past few years new technologies have been developed that enable intracellular profiling of kinase inhibitors. NanoBRET[120] is one such technology which was also used in this thesis to confirm PKN3 target engagement in cells. Additionally, mass spectrometry based approaches like activity based proteome profiling (ABPP) and photo affinity labelling (PAL)[142] enable intracellular target identification.[302] These two approaches rely on compounds bearing reactive capturing groups and an affinity tag (e.g. XO44[140]). In a competitive setup these approaches are used for compound profiling in cells. In addition, the cellular thermal shift assay (CETSA) has emerged as target identification and target engagement assay.[131] All these technologies can help to better understand and to explain the gap between *in vitro* assay results and *in vivo* observations of a given drug. Compared to the Kinobeads technology which is now over 13 years old, cellular assays for target identification have been developed and matured only over the past few years. At the time the Kinobeads assay was first described, the technology was highly valuable for identification of drug-kinase interaction on a kinome wide level under close-to physiological condition. But since intracellular target engagement methods are becoming increasingly matured and more miniature, they are a good or even better alternatives to the well-established Kinobeads assay.

The Kinobeads technology is well suited for selectivity profiling of small molecule kinase inhibitors which has been extensively executed in this study, where a total of 1,287 kinase inhibitors were profiled and by Klaeger *et al*[60] who screened 243 clinical kinase inhibitors. Therefore, most of the frequently used kinase inhibitors in the scientific community (clinical kinase inhibitor, prominent tool compound libraries) have already been profiled by the Kinobeads technology and there is currently no urgent need to profile additional kinase inhibitors.

Future applications of the Kinobeads technology. Even if there are some arguments against the future application of the Kinobeads technology, it is still a valuable approach to address certain research questions. As described above, the technology is not the first choice for large scale profiling campaigns due to its lower throughput compared to recombinant kinase assays, but it is still highly suitable for target deconvolution of a limited number of kinase inhibitors. Hence, the technology is still valuable to continually screen new clinical kinase inhibitors or tool compounds that are frequently used by the scientific community. To minimize the reported affinity and selectivity differences between lysate and cell-based assays, supplementation of lysates with ATP can be considered for further Kinobeads experiments. But this requires a thorough comparison of affinity and selectivity results obtained by Kinobeads with or without ATP supplementation and an *in cell* profiling assay. In addition, Kinobeads selectivity profiling of newly synthesized inhibitor candidates can be used to guide academic medicinal chemistry and inhibitor design. This allows early determination not only of the affinity to a specific kinase of interest, but also selectivity profiling against the whole kinome.[85,303]

Profiling of kinase inhibitors is usually performed in a cell lysate mixture of different cancer cell lines with varying overexpressed signalling pathways to cover a broad range of protein kinases. This leads to the fact that one kinase cannot only be present in different proteoforms, splice variants and protein complexes, but can also carry different mutations. The Kinobeads results or more precisely the determined binding curve for a kinase is the sum of all these different forms of the kinase binding to the compound of interest. Hence, in this setup, the Kinobeads technology is not able to distinguish between interactions of an inhibitor to different mutated forms of the kinase. This is a major drawback of the method, since many kinases are mutated in human diseases and several kinase inhibitors have been developed to specifically target only the mutated version of the kinase.[304] However, in the future, only one cell line or tissue of a cancer patient carrying a specific kinase mutation of interest could be used for Kinobeads selectivity profiling in order to determine whether this specific mutated kinase still binds to an inhibitor of interest. A mutation in the ATP binding pocket of the kinase that is usually accessible for Kinobeads enrichment, can also prevent binding of the kinase to the affinity matrix. To circumvent this problem, the Kinobeads assay could be combined with the KiNativ approach[149] which utilizes desthiobiotinylated ATP to enrich ATP-binding proteins and is therefore more likely to bind kinases containing a mutation in the ATP binding pocket as long as the mutation does not lead to reduced ATP binding.

Since lysates can be produced from all types of biological input material including cell lines, primary cells or even tissues from all kinds of organisms, the Kinobeads technology also facilitate profiling of kinase inhibitors in other species than human. As example, Kinobeads have enabled the discovery of kinase inhibitors targeting pathogens such as *Plasmodium falciparum*[305] or

Trypanosome brucei[303] and were used to enrich kinases out of a zebrafish cell line or even of Arabidopsis thaliana.[79] Other organisms than human are usually not covered by classic *in vitro* screens and so far intracellular assays have only been performed in human cells. The applicability of *in cell* assays in other organisms could be restrained, for example, by cell permeability issues. Additionally, special knowledge is often required for culturing and handling other organisms which is often not available in laboratories performing such intracellular inhibitor screens. Hence, lysate-based chemoproteomic technologies, where lysates can be produced everywhere, are more applicable for profiling compounds in other species than human.

In addition to compound profiling, the Kinobeads technology is used for quantification of kinase expression in cell lines or tissues.[306] Since kinases are often overexpressed and dysregulated in human diseases it might be advantageous to analyze the kinome expression in such disease tissues to better understand the molecular mechanisms and to enhance treatment recommendation for patients. But due to technological advances in mass spectrometry with faster and more sensitive instruments, enrichment of kinases with Kinobeads might not be necessary and full proteome or even phosphoproteome analysis might be even more beneficial.

In conclusion, the Kinobeads technology should be further used but for other applications than it was used so far. The Kinobeads technology is not the first choice anymore for larger scale selectivity profiling studies like presented here in this thesis, since the approach is very time consuming and requires lots of resources (cell culture and mass spectrometric measurement time). In addition, *in cell* profiling techniques are gaining in importance and might replace the Kinobeads technology for compound profiling in human cells. While the Kinobeads technology can only identify potential binding partners of a certain drug, *in cell* assays can measure target engagement in living cells and better reflect the drugs mode of action. But the technology is still highly valuable to screen compounds in other organisms or to answer specific questions like does a mutated kinase still bind to a specific inhibitor.

2 Advantages and Risks of Chemical Probes

Advantages of chemical probes. Chemical probes are properly characterized small molecules with defined cellular potency, selectivity and cell permeability (Introduction Chapter 2.3). In the best case, a certain protein has two structurally diverse chemical probes with high intracellular affinity, excellent selectivity and two inactive derivatives. All parameters that a small molecule has to fulfil to be classified as chemical probe are reviewed by the expert community.[73,94,307] High quality chemical probes can help to elucidate the mechanistic and phenotypic function of the targeted protein in healthy and diseased tissue. For example, JQ1 and its inactive partner contributed to the current understanding of bromodomain biology and pharmacology.[308] In addition, from a drug discovery perspective, chemical probes can be used to validate potential drug targets and to minimize the biological risk of targeting a specific protein.[96] Although clinical kinase inhibitors are often very promiscuous compounds, the field of precision medicine (see General Discussion and Outlook Chapter 3) in particular would benefit from highly selective small molecule kinase inhibitors. A combination of highly selective kinase inhibitors that specifically target aberrantly activated kinases, may lead to less side effects in patients than broad spectrum kinase inhibitors.

Chemical probes are complementary to genetic tools like RNAi or CRISPR and have the advantage that they can rapidly and reversibly inhibit a certain protein in nearly all cell types and animals. In combination with RNAi, they can distinguish between scaffolding effects of the proteins and effects due to inhibition of the catalytic activity.[73]

Discovery of new chemical probes. Despite the high value of chemical probes in basic research and drug discovery, many kinases, especially understudied kinases, still lack a suitable chemical probe. Currently only 77 probes targeting 102 protein kinases are listed in the chemical probe portal (www.chemicalprobes.org as of March 2020). The development of high quality chemical probes is difficult and requires substantial resources, skills and commitment. In the presented study, over 1,200 small molecule kinase inhibitors were profiled using the Kinobeads technology, in order to identify potential new chemical probes. A total of 354 compound were identified as potential chemical probes targeting 73 different kinases illustrating the high value of the dataset for the discovery of new chemical probes. In addition, 239 kinases were in total targeted by the compounds so that theoretically many new lead structures can be found for kinases lacking a chemical probe like PKN3. Since the data set can be grouped into 58 different chemotypes of with each containing between 5 and 78 compounds, it can be used to analyse structure selectivity relationships and structure affinity relationships which might help for the development of new chemical probes.

Furthermore, the comprehensive data set containing selectivity profiles of over 1,200 compounds can be used to train machine learning models that try to predict targets of compounds. Advances in machine learning give hope that it might be possible to predict potential targets of an inhibitor only based on its chemical structure.[309,310] This could extremely simplify the identification of chemical probes because only those compounds that reached high selectivity and affinity with the prediction tool need to be synthesized. Such machine learning models rely on a high quality training dataset that covers as many diverse compounds and proteins as possible. Whether the

prediction of targets with a machine learning model will ever be possible remains questionable but the here presented data might be a well suitable training dataset.

Chemical probes as risk factor. Despite the high value of chemical probes, they are bearing several risk factors. The development of small molecules that fulfil all chemical probe criteria is often not possible for most proteins and especially kinases. Hence, it is important to make all profiling and validation data of a compound publicly available and easily accessible, so that potential off-targets can be considered for subsequent analysis of biological experiments where the probe was utilized. Usage of inadequate characterized chemical probes or not considering off-targets for data interpretation are major problems and often lead to the generation of research results of suspicious conclusions.[73] Many compounds have proven to be unselective and do not fulfil the strict chemical probe criteria, however, they are still used for mechanistic studies. One example is the PI3K inhibitor LY294002, a popular but unsuited chemical probe since it exerts at least part of its function through inhibition of the BET bromodomain.[311] The first publication of a compound often contains affinity profiling results for a very limited number of proteins. Broad selectivity profiles of the compound mainly accumulate in the literature over time, when the compound was included in large screening projects. Such data can be viewed in public databases like the chemical probe portal that report on the probe quality and can be used by the scientific community to select an appropriate chemical probe.[73] These platforms are highly valuable as vendors usually only specify the designated target of the compound and not all known targets from the literature. Hence, researchers have to be aware of the fact that many inhibitors are not as selective as described on a vendor webpage.

This is especially the case for clinical kinase inhibitors. The above mentioned criteria for compounds to be classified as chemical probes are not mandatory for a compound to be used as drug. Chemical probes and drugs can vary greatly in their characteristics and purpose.[73] While it is inevitable for a chemical probe to be highly selective, a drug does not have to be selective. Even the opposite is usually the case and many drugs achieve their clinical effects through polypharmacology.[60] Hence, researchers must be aware of the fact that most clinical drugs that are claim to be highly selective for the designated target are not as selective as anticipated and can often not be used as chemical probes.

One can also ask the question, whether selective chemical probes are really necessary. As shown for PKN3 in this study, a combination of rather unselective inhibitors that only have one target in common could be used to study kinase-substrate relationships or to elucidate signalling pathways of kinases. Hence, several research questions could be addressed by such an exclusion procedure. However, complex phenotypic readouts would still require very selective inhibitors, as the analysis would be too complex and the effect of different targets difficult to disentangle.

Protein kinases have been extensively studied in regard to their catalytic activities but over the past decade more evidence has accumulated that kinases also have important non-catalytic functions like scaffolding of protein complexes, allosteric effects on other enzymes and DNA-binding.[312,313] ATP-competitive kinase inhibitors that are often used as chemical probes, tend to stabilize the kinase in a specific conformational state and it is often unknown how this affects the non-catalytic function of a protein kinase. Hence, chemical probes are only suitable for investigating the catalytic function, but not the non-catalytic function of a protein kinase. As

described above, a combination of chemical probes and genetic tools or even PROTACs (proteolysis-targeting chimeras)[314] might be favourable to investigate the non-catalytic function of a protein kinase. Hence, chemical probes alone might not be sufficient to study the function of a kinase, rather a combination of different strategies would be advantageous in order to fully explore the catalytic and non-catalytic function of a kinase.

In summary, correctly applied chemical probes in combination with genetic tools or PROTACs are valuable tools for basic research and drug discovery to better understand the cellular function of a protein and to identify potential new drug targets. There is still a high need for chemical probes for understudied kinases in order to better understand their function and their potential as drug target. But choosing the right chemical probe is not a trivial task and requires thorough literature search in order to correctly interpret the results of an experiment.

3 Role of Chemical Proteomics in Changing Precision medicine

Precision oncology. The concept of precision medicine aims to classify patients based on individual molecular characteristics into different treatment groups, in order to optimize the benefit and to reduce side effects of the treatment.[315-317] In oncology, the branch of precision medicine is known as "precision oncology". Molecular stratification of cancer patients by next-generation sequencing of tumor DNA and RNA can reveal genomic alterations. Such genetic alterations are not restricted to one histologic entity but are shared across multiple entities so that treatment recommendation should be given based on the molecular characteristics of the tumor and not only by the origin of the tumor. Suitable molecular targeting agents (MTA) like small molecule kinase inhibitors or antibodies can then specifically address the genetic alteration of the individual patient and provide the basis for precision medicine. In interdisciplinary molecular tumor boards, patients are categorized into intervention baskets based on their molecular characteristics (genetic alterations) and treatment recommendations are given.[318] In reality, the molecular data of a patient often provide the rational for more than one drug. The different treatment recommendations are categorized into different evidence level depending on the data basis that led to the recommendation (clinical data (level I and II) or preclinical data (level III and IV)) which facilitates prioritization of treatment strategies.[318] Based on the acquired data in molecule tumor boards on large patient cohorts, new treatment strategies can be developed as well as new clinical trials can be initiated.

Selectivity profiling of drugs to improve treatment recommendation. As already described in detail, kinases play an important role in onset and progression of cancer. Hence, kinase inhibitors are among the most important drugs in precision medicine and are used for various tumor entities.[319] Precision medicine would highly profit from very selective kinase inhibitors that specifically inhibit the pathogenic alterations of a patient. Combinations of highly selective kinase inhibitors could be optimized for each patient to gain the best treatment option with less side effects. But as profiling of more than 50 clinical kinase inhibitors and the study of Klaeger *et al*[60] have shown, many kinase drugs are not selective for one particular kinase. Off-target inhibition can lead for example to toxic or adverse side effects in patients which could result in failure of clinical trials. On the other hand, unselective kinase inhibitors create the opportunity to reposition an already approved drug for another indication based on off-target inhibition (Introduction Chapter 2.3). Imatinib, for example, was repurposed for gastro intestinal stromal tumors due to its additional KIT-inhibition.[320] To take advantage of the opportunity of repositioning a drug, the target profile of a drug must be known. If patient stratification then reveals new genetic alterations, already approved drugs can be screened for targeting this genetic alterations. But patients that need a treatment recommendation rather sooner than later do not directly profit from this approach. Although treatment recommendation can be given based on preclinical data that indicate inhibition of the genetic alteration by a given drug, the level of evidence is low and the patient will probably not be treated with the drug. Further pre-clinical tests are required before clinical trials can investigate the efficacy of the repurposed drug. But in the long run, drug repositioning is a successful approach that reduces research and economic efforts.

Selectivity profiling of clinical drugs can still help to choose the potentially "best" drug for a patient. Here a brief gedanken experiment: several EGFR inhibitors with various target profiles are currently in the clinics. If a patient suffers from two genetic alterations like EGFR and ALK, an EGFR inhibitor that also targets ALK can be chosen as best treatment option. For such an approach the Kinobeads results are advantageous since they provide a kinome wide view on the compounds target space and can help clinicians to choose the best drug for the patient. But the technology also has one major drawback. Several clinically highly relevant kinases are not covered by the lysate mixture and/or the affinity matrix. For example, the PIKK and PI3K families were not accessible to Kinobeads profiling with the previous setup. The new Kinobeads matrix enables now profiling of mTOR and PI3K inhibitors. Therefore, all PI3K and mTOR inhibitors currently in clinical trials were re-profiled utilizing the new Kinobeads matrix to get a broader view on the selectivity within the PI3K and PIKK families However, other families are still missing. For instance the FGFR family is often dysregulated in many cancer types[321], but these kinases (except for FGFR1) are not expressed in the used cell lysate mixture.

Future perspectives of chemical proteomics in precision medicine. For patients carrying a well-known and well-studied genetic mutation, treatment recommendation is a simple task and kinase inhibitors or other MTAs can be suggested that have been extensively investigated in clinical trials for this specific genetic alteration. But for patients carrying rare mutations, treatment recommendation is not as simple. First, it is often unknown whether the mutation is activating or inactivating, which makes the choice of the best treatment difficult, since it is unclear whether inhibitors would be useful at all. In addition, if the mutations occur in the active site of the kinase where most of the small molecules bind, it is often not known if a kinase inhibitor that theoretically targets the kinase would still bind to the mutated version of the kinase. The latter problem could in principle be addressed by a chemical proteomic approach like the Kinobeads technology as already discussed (see Discussion and Outlook Chapter 1). The knowledge if an inhibitor can bind to a specific mutated kinase would help the patient, as it would prevent unnecessary treatments of a patient without any outcome. Additionally, if a larger cohort of patients carry the same mutation, medicinal chemistry programs could develop novel inhibitors that specifically target the mutated kinase.

Currently, treatment recommendation for cancer patients only consider sequencing results of tumor DNA and RNA.[318] As most MTAs act on protein level, analysis of the tumor proteome or even phosphoproteome could guide treatment recommendation. Especially since RNA and protein levels do not always correlate well[322], measuring protein expression rather than RNA levels might be more beneficial. Hereby, proteins with abnormal expression level or over activated pathways as identified by phosphoproteomic measurement, can specifically be inhibited by an appropriate MTA.

In addition, the overall expression level of kinases varies strongly between different cell lines, tissues or organs in healthy and disease state.[323,324] Hence, depending on the tissue the tumor derived from, the selectivity of a kinase inhibitor might vary greatly. While a drug might be a potent and selective drug for one tumor entity, the inhibitor can have several targets or even toxic targets in another entity. Chemical proteomic strategies are suitable for tissue specific selectivity profiling. Here, activity based probes, like XO44, could be used in patient-derived xenografts or

patient-derived organoids to investigate intracellular target engagement of kinase inhibitors. Using this approach could help to identify tissue specific drug-protein interaction and could help to minimize off-target effects.

In summary, chemical proteomic has the potential to change precision medicine. The research area with its new and ever improving technologies can be beneficial in finding new drugs, in better understanding the drugs mode of action and in assigning the drugs to the appropriate indication. Especially since most drugs act on proteins, studying the effect of a drug on a proteome wide scale is essential.

References

1 Cohen, P. The role of protein phosphorylation in human health and disease. *European Journal of Biochemistry* **268**, 5001-5010, doi:10.1046/j.0014-2956.2001.02473.x (2001).

2 Cohen, P. The origins of protein phosphorylation. *Nature Cell Biology* **4**, E127-E130, doi:10.1038/ncb0502-e127 (2002).

3 Hunter, T. Why nature chose phosphate to modify proteins. *Philos Trans R Soc Lond B Biol Sci* **367**, 2513-2516, doi:10.1098/rstb.2012.0013 (2012).

4 Ardito, F., Giuliani, M., Perrone, D., Troiano, G. & Lo Muzio, L. The crucial role of protein phosphorylation in cell signaling and its use as targeted therapy (Review). *Int J Mol Med* **40**, 271-280, doi:10.3892/ijmm.2017.3036 (2017).

5 Manning, G., Whyte, D. B., Martinez, R., Hunter, T. & Sudarsanam, S. The Protein Kinase Complement of the Human Genome. *Science* **298**, 1912-1934, doi:10.1126/science.1075762 (2002).

6 Burke, J. E. Structural Basis for Regulation of Phosphoinositide Kinases and Their Involvement in Human Disease. *Molecular Cell* **71**, 653-673, doi:10.1016/j.molcel.2018.08.005 (2018).

7 Kanev, G. K. *et al.* The Landscape of Atypical and Eukaryotic Protein Kinases. *Trends in Pharmacological Sciences* **40**, 818-832, doi:10.1016/j.tips.2019.09.002 (2019).

8 Scheeff, E. D. & Bourne, P. E. Structural Evolution of the Protein Kinase–Like Superfamily. *PLOS Computational Biology* **1**, e49, doi:10.1371/journal.pcbi.0010049 (2005).

9 Roskoski, R. A historical overview of protein kinases and their targeted small molecule inhibitors. *Pharmacological Research* **100**, 1-23, doi:10.1016/j.phrs.2015.07.010 (2015).

10 Jacobsen, A. V. & Murphy, J. M. The secret life of kinases: insights into non-catalytic signalling functions from pseudokinases. *Biochemical Society Transactions* **45**, 665-681, doi:10.1042/bst20160331 (2017).

11 Yu, J. S. L. & Cui, W. Proliferation, survival and metabolism: the role of PI3K/AKT/mTOR signalling in pluripotency and cell fate determination. *Development* **143**, 3050-3060, doi:10.1242/dev.137075 (2016).

12 Vanhaesebroeck, B., Guillermet-Guibert, J., Graupera, M. & Bilanges, B. The emerging mechanisms of isoform-specific PI3K signalling. *Nature Reviews Molecular Cell Biology* **11**, 329-341, doi:10.1038/nrm2882 (2010).

13 Lien, E. C., Dibble, C. C. & Toker, A. PI3K signaling in cancer: beyond AKT. *Curr Opin Cell Biol* **45**, 62-71, doi:10.1016/j.ceb.2017.02.007 (2017).

14 Díaz, M. E. *et al.* Growth hormone modulation of EGF-induced PI3K-Akt pathway in mice liver. *Cell Signal* **24**, 514-523, doi:10.1016/j.cellsig.2011.10.001 (2012).

15 Andrs, M. *et al.* Phosphatidylinositol 3-Kinase (PI3K) and Phosphatidylinositol 3-Kinase-Related Kinase (PIKK) Inhibitors: Importance of the Morpholine Ring. *Journal of Medicinal Chemistry* **58**, 41-71, doi:10.1021/jm501026z (2015).

16 Efeyan, A. & Sabatini, D. M. mTOR and cancer: many loops in one pathway. *Curr Opin Cell Biol* **22**, 169-176, doi:10.1016/j.ceb.2009.10.007 (2010).

17 Peterson, T. R. *et al.* DEPTOR Is an mTOR Inhibitor Frequently Overexpressed in Multiple Myeloma Cells and Required for Their Survival. *Cell* **137**, 873-886, doi:10.1016/j.cell.2009.03.046 (2009).

18 Kim, D.-H. *et al.* GβL, a Positive Regulator of the Rapamycin-Sensitive Pathway Required for the Nutrient-Sensitive Interaction between Raptor and mTOR. *Molecular Cell* **11**, 895-904, doi:10.1016/S1097-2765(03)00114-X (2003).

19 Frias, M. A. *et al.* mSin1 Is Necessary for Akt/PKB Phosphorylation, and Its Isoforms Define Three Distinct mTORC2s. *Current Biology* **16**, 1865-1870, doi:10.1016/j.cub.2006.08.001 (2006).

20 Pearce, L. R. *et al.* Identification of Protor as a novel Rictor-binding component of mTOR complex-2. *Biochem J* **405**, 513-522, doi:10.1042/bj20070540 (2007).

21 Garcia-Martinez, J. M. & Alessi, D. R. mTOR complex 2 (mTORC2) controls hydrophobic motif phosphorylation and activation of serum- and glucocorticoid-induced protein kinase 1 (SGK1). *Biochem J* **416**, 375-385, doi:10.1042/bj20081668 (2008).

22 Manning, B. D. & Cantley, L. C. AKT/PKB Signaling: Navigating Downstream. *Cell* **129**, 1261-1274, doi:10.1016/j.cell.2007.06.009 (2007).

23 Sancak, Y. *et al.* PRAS40 Is an Insulin-Regulated Inhibitor of the mTORC1 Protein Kinase. *Molecular Cell* **25**, 903-915, doi:10.1016/j.molcel.2007.03.003 (2007).

24 Hara, K. *et al.* Raptor, a Binding Partner of Target of Rapamycin (TOR), Mediates TOR Action. *Cell* **110**, 177-189, doi:10.1016/S0092-8674(02)00833-4 (2002).

25 D'Agati, V. D. *et al.* Obesity-related glomerulopathy: clinical and pathologic characteristics and pathogenesis. *Nature Reviews Nephrology* **12**, 453-471, doi:10.1038/nrneph.2016.75 (2016).

26 Yamaguchi, H., Matsushita, M., Nairn, A. C. & Kuriyan, J. Crystal Structure of the Atypical Protein Kinase Domain of a TRP Channel with Phosphotransferase Activity. *Molecular Cell* **7**, 1047-1057, doi:10.1016/S1097-2765(01)00256-8 (2001).

27 Walker, E. H., Perisic, O., Ried, C., Stephens, L. & Williams, R. L. Structural insights into phosphoinositide 3-kinase catalysis and signalling. *Nature* **402**, 313-320, doi:10.1038/46319 (1999).

28 McClendon, C. L., Kornev, A. P., Gilson, M. K. & Taylor, S. S. Dynamic architecture of a protein kinase. *Proceedings of the National Academy of Sciences* **111**, E4623-E4631, doi:10.1073/pnas.1418402111 (2014).

29 Huse, M. & Kuriyan, J. The Conformational Plasticity of Protein Kinases. *Cell* **109**, 275-282, doi:10.1016/S0092-8674(02)00741-9 (2002).

30 Kornev, A. P., Haste, N. M., Taylor, S. S. & Ten Eyck, L. F. Surface comparison of active and inactive protein kinases identifies a conserved activation mechanism. *Proceedings of the National Academy of Sciences* **103**, 17783-17788, doi:10.1073/pnas.0607656103 (2006).

31 Hu, J. *et al.* Kinase regulation by hydrophobic spine assembly in cancer. *Mol Cell Biol* **35**, 264-276, doi:10.1128/MCB.00943-14 (2015).

32 Kornev, A. P., Taylor, S. S. & Ten Eyck, L. F. A helix scaffold for the assembly of active protein kinases. *Proc Natl Acad Sci U S A* **105**, 14377-14382, doi:10.1073/pnas.0807988105 (2008).

33 Johnson, L. N. & Lewis, R. J. Structural Basis for Control by Phosphorylation. *Chemical Reviews* **101**, 2209-2242, doi:10.1021/cr000225s (2001).

34 Vadas, O., Burke, J. E., Zhang, X., Berndt, A. & Williams, R. L. Structural Basis for Activation and Inhibition of Class I Phosphoinositide 3-Kinases. *Science Signaling* **4**, re2-re2, doi:10.1126/scisignal.2002165 (2011).

35 Jeffrey, P. D. *et al.* Mechanism of CDK activation revealed by the structure of a cyclinA-CDK2 complex. *Nature* **376**, 313-320, doi:10.1038/376313a0 (1995).

36 Hubbard, M. J. & Cohen, P. On target with a new mechanism for the regulation of protein phosphorylation. *Trends in Biochemical Sciences* **18**, 172-177, doi:10.1016/0968-0004(93)90109-Z (1993).

37 Blume-Jensen, P. & Hunter, T. Oncogenic kinase signalling. *Nature* **411**, 355-365, doi:10.1038/35077225 (2001).

38 Cohen, P. Protein kinases — the major drug targets of the twenty-first century? *Nature Reviews Drug Discovery* **1**, 309-315, doi:10.1038/nrd773 (2002).

39 Patterson, H., Nibbs, R., McInnes, I. & Siebert, S. Protein kinase inhibitors in the treatment of inflammatory and autoimmune diseases. *Clin Exp Immunol* **176**, 1-10, doi:10.1111/cei.12248 (2014).

40 Chico, L. K., Van Eldik, L. J. & Watterson, D. M. Targeting protein kinases in central nervous system disorders. *Nat Rev Drug Discov* **8**, 892-909, doi:10.1038/nrd2999 (2009).

41 Ferguson, F. M. & Gray, N. S. Kinase inhibitors: the road ahead. *Nature Reviews Drug Discovery* **17**, 353-377, doi:10.1038/nrd.2018.21 (2018).

42 Weinstein, I. B. & Joe, A. Oncogene Addiction. *Cancer Research* **68**, 3077-3080, doi:10.1158/0008-5472.Can-07-3293 (2008).

43 Weinstein, I. B. Addiction to Oncogenes--the Achilles Heal of Cancer. *Science* **297**, 63-64, doi:10.1126/science.1073096 (2002).

44 Weinstein, I. B. & Joe, A. K. Mechanisms of Disease: oncogene addiction—a rationale for molecular targeting in cancer therapy. *Nature Clinical Practice Oncology* **3**, 448-457, doi:10.1038/ncponc0558 (2006).

45 Collett, M. S. & Erikson, R. L. Protein kinase activity associated with the avian sarcoma virus src gene product. *Proc Natl Acad Sci U S A* **75**, 2021-2024, doi:10.1073/pnas.75.4.2021 (1978).

46 Davies, H. *et al.* Mutations of the BRAF gene in human cancer. *Nature* **417**, 949-954, doi:10.1038/nature00766 (2002).

47 Buchdunger, E., Matter, A. & Druker, B. J. Bcr-Abl inhibition as a modality of CML therapeutics. *Biochimica et Biophysica Acta (BBA) - Reviews on Cancer* **1551**, M11-M18, doi:10.1016/S0304-419X(01)00022-1 (2001).

48 Campbell, I. G. *et al.* Mutation of the PIK3CA Gene in Ovarian and Breast Cancer. *Cancer Research* **64**, 7678-7681, doi:10.1158/0008-5472.Can-04-2933 (2004).

49 Mundi, P. S., Sachdev, J., McCourt, C. & Kalinsky, K. AKT in cancer: new molecular insights and advances in drug development. *Br J Clin Pharmacol* **82**, 943-956, doi:10.1111/bcp.13021 (2016).

50 Hoxhaj, G. & Manning, B. D. The PI3K–AKT network at the interface of oncogenic signalling and cancer metabolism. *Nature Reviews Cancer*, doi:10.1038/s41568-019-0216-7 (2019).

51 Hanahan, D. & Weinberg, R. A. The Hallmarks of Cancer. *Cell* **100**, 57-70, doi:10.1016/S0092-8674(00)81683-9 (2000).

52 Faivre, S., Djelloul, S. & Raymond, E. New Paradigms in Anticancer Therapy: Targeting Multiple Signaling Pathways With Kinase Inhibitors. *Seminars in Oncology* **33**, 407-420, doi:10.1053/j.seminoncol.2006.04.005 (2006).

53 Imai, K. & Takaoka, A. Comparing antibody and small-molecule therapies for cancer. *Nat Rev Cancer* **6**, 714-727, doi:10.1038/nrc1913 (2006).

54 Dar, A. C. & Shokat, K. M. The Evolution of Protein Kinase Inhibitors from Antagonists to Agonists of Cellular Signaling. *Annual Review of Biochemistry* **80**, 769-795, doi:10.1146/annurev-biochem-090308-173656 (2011).

55 Zuccotto, F., Ardini, E., Casale, E. & Angiolini, M. Through the "Gatekeeper Door": Exploiting the Active Kinase Conformation. *Journal of Medicinal Chemistry* **53**, 2681-2694, doi:10.1021/jm901443h (2010).

56 Roskoski, R. Classification of small molecule protein kinase inhibitors based upon the structures of their drug-enzyme complexes. *Pharmacological Research* **103**, 26-48, doi:10.1016/j.phrs.2015.10.021 (2016).

57 Liao, J. J.-L. Molecular Recognition of Protein Kinase Binding Pockets for Design of Potent and Selective Kinase Inhibitors. *Journal of Medicinal Chemistry* **50**, 409-424, doi:10.1021/jm0608107 (2007).

58 van Linden, O. P. J., Kooistra, A. J., Leurs, R., de Esch, I. J. P. & de Graaf, C. KLIFS: A Knowledge-Based Structural Database To Navigate Kinase–Ligand Interaction Space. *Journal of Medicinal Chemistry* **57**, 249-277, doi:10.1021/jm400378w (2014).

59 Davis, M. I. *et al.* Comprehensive analysis of kinase inhibitor selectivity. *Nature Biotechnology* **29**, 1046-1051, doi:10.1038/nbt.1990 (2011).

60 Klaeger, S. *et al.* The target landscape of clinical kinase drugs. *Science* **358**, eaan4368, doi:10.1126/science.aan4368 (2017).

61 Zhao, Z., Xie, L. & Bourne, P. E. Insights into the binding mode of MEK type-III inhibitors. A step towards discovering and designing allosteric kinase inhibitors across the human kinome. *PLoS One* **12**, e0179936-e0179936, doi:10.1371/journal.pone.0179936 (2017).

62 Brear, P. *et al.* Specific inhibition of CK2α from an anchor outside the active site. *Chemical Science* **7**, 6839-6845, doi:10.1039/C6SC02335E (2016).

63 Chaikuad, A., Koch, P., Laufer, S. A. & Knapp, S. The Cysteinome of Protein Kinases as a Target in Drug Development. *Angewandte Chemie International Edition* **57**, 4372-4385, doi:10.1002/anie.201707875 (2018).

64 Singh, J., Petter, R. C., Baillie, T. A. & Whitty, A. The resurgence of covalent drugs. *Nat Rev Drug Discov* **10**, 307-317, doi:10.1038/nrd3410 (2011).

65 Bandyopadhyay, A. & Gao, J. Targeting biomolecules with reversible covalent chemistry. *Current opinion in chemical biology* **34**, 110-116, doi:10.1016/j.cbpa.2016.08.011 (2016).

66 Wu, J., Zhang, M. & Liu, D. Acalabrutinib (ACP-196): a selective second-generation BTK inhibitor. *J Hematol Oncol* **9**, 21, doi:10.1186/s13045-016-0250-9 (2016).

67 Honigberg, L. A. *et al.* The Bruton tyrosine kinase inhibitor PCI-32765 blocks B-cell activation and is efficacious in models of autoimmune disease and B-cell malignancy. *Proc Natl Acad Sci U S A* **107**, 13075-13080, doi:10.1073/pnas.1004594107 (2010).

68 Wu, S.-G. *et al.* The mechanism of acquired resistance to irreversible EGFR tyrosine kinase inhibitor-afatinib in lung adenocarcinoma patients. *Oncotarget* **7**, 12404-12413, doi:10.18632/oncotarget.7189 (2016).

69 Tiwari, S. R., Mishra, P. & Abraham, J. Neratinib, A Novel HER2-Targeted Tyrosine Kinase Inhibitor. *Clin Breast Cancer* **16**, 344-348, doi:10.1016/j.clbc.2016.05.016 (2016).

70 Mah, R., Thomas, J. R. & Shafer, C. M. Drug discovery considerations in the development of covalent inhibitors. *Bioorganic & Medicinal Chemistry Letters* **24**, 33-39, doi:10.1016/j.bmcl.2013.10.003 (2014).

71 Müller, S., Chaikuad, A., Gray, N. S. & Knapp, S. The ins and outs of selective kinase inhibitor development. *Nature Chemical Biology* **11**, 818-821, doi:10.1038/nchembio.1938 (2015).

72 Miljković, F. & Bajorath, J. Exploring Selectivity of Multikinase Inhibitors across the Human Kinome. *ACS Omega* **3**, 1147-1153, doi:10.1021/acsomega.7b01960 (2018).

73 Arrowsmith, C. H. *et al.* The promise and peril of chemical probes. *Nature Chemical Biology* **11**, 536-541, doi:10.1038/nchembio.1867 (2015).

74 Shapiro, P. A promiscuous kinase inhibitor reveals secrets to cancer cell survival. *J Biol Chem* **294**, 8674-8675, doi:10.1074/jbc.H119.009103 (2019).

75 Amato, K. R. *et al.* EPHA2 Blockade Overcomes Acquired Resistance to EGFR Kinase Inhibitors in Lung Cancer. *Cancer Research* **76**, 305-318, doi:10.1158/0008-5472.Can-15-0717 (2016).

76 Koch, H., Busto, M. E., Kramer, K., Médard, G. & Kuster, B. Chemical Proteomics Uncovers EPHA2 as a Mechanism of Acquired Resistance to Small Molecule EGFR Kinase Inhibition. *Journal of Proteome Research* **14**, 2617-2625, doi:10.1021/acs.jproteome.5b00161 (2015).

77 Pushpakom, S. *et al.* Drug repurposing: progress, challenges and recommendations. *Nature Reviews Drug Discovery* **18**, 41-58, doi:10.1038/nrd.2018.168 (2019).

78 Reddy, A. S. & Zhang, S. Polypharmacology: drug discovery for the future. *Expert Rev Clin Pharmacol* **6**, 41-47, doi:10.1586/ecp.12.74 (2013).

79 Reinecke, M. *et al.* in *Target Discovery and Validation, A.T. Plowright (Ed.)* 97-130 (2020).

80 Uitdehaag, J. C. M. & Zaman, G. J. R. A theoretical entropy score as a single value to express inhibitor selectivity. *BMC Bioinformatics* **12**, 94, doi:10.1186/1471-2105-12-94 (2011).

81 Uitdehaag, J. C. *et al.* A guide to picking the most selective kinase inhibitor tool compounds for pharmacological validation of drug targets. *British Journal of Pharmacology* **166**, 858-876, doi:10.1111/j.1476-5381.2012.01859.x (2012).

82 Karaman, M. W. *et al.* A quantitative analysis of kinase inhibitor selectivity. *Nature Biotechnology* **26**, 127-132, doi:10.1038/nbt1358 (2008).

83 Graczyk, P. P. Gini Coefficient: A New Way To Express Selectivity of Kinase Inhibitors against a Family of Kinases. *Journal of Medicinal Chemistry* **50**, 5773-5779, doi:10.1021/jm070562u (2007).

84 Cheng, A. C., Eksterowicz, J., Geuns-Meyer, S. & Sun, Y. Analysis of Kinase Inhibitor Selectivity using a Thermodynamics-Based Partition Index. *Journal of Medicinal Chemistry* **53**, 4502-4510, doi:10.1021/jm100301x (2010).

85 Heinzlmeir, S. *et al.* Chemoproteomics-Aided Medicinal Chemistry for the Discovery of EPHA2 Inhibitors. *ChemMedChem* **12**, 999-1011, doi:10.1002/cmdc.201700217 (2017).

86 Carles, F., Bourg, S., Meyer, C. & Bonnet, P. PKIDB: A Curated, Annotated and Updated Database of Protein Kinase Inhibitors in Clinical Trials. *Molecules* **23**, 908, doi:10.3390/molecules23040908 (2018).

87 Roskoski, R. Properties of FDA-approved small molecule protein kinase inhibitors. *Pharmacological Research* **144**, 19-50, doi:10.1016/j.phrs.2019.03.006 (2019).

88 Cohen, M. H. *et al.* Approval Summary for Imatinib Mesylate Capsules in the Treatment of Chronic Myelogenous Leukemia. *Clinical Cancer Research* **8**, 935-942 (2002).

89 Kane, R. C. *et al.* Sorafenib for the Treatment of Unresectable Hepatocellular Carcinoma. *The Oncologist* **14**, 95-100, doi:10.1634/theoncologist.2008-0185 (2009).

90 Kane, R. C. *et al.* Sorafenib for the Treatment of Advanced Renal Cell Carcinoma. *Clinical Cancer Research* **12**, 7271-7278, doi:10.1158/1078-0432.Ccr-06-1249 (2006).

91 Yang, Q., Modi, P., Newcomb, T., Quéva, C. & Gandhi, V. Idelalisib: First-in-Class PI3K Delta Inhibitor for the Treatment of Chronic Lymphocytic Leukemia, Small Lymphocytic Leukemia, and Follicular Lymphoma. *Clinical Cancer Research* **21**, 1537-1542, doi:10.1158/1078-0432.Ccr-14-2034 (2015).

92 Sehgal, S. N. Sirolimus: its discovery, biological properties, and mechanism of action. *Transplantation Proceedings* **35**, S7-S14, doi:10.1016/S0041-1345(03)00211-2 (2003).

93 Li, J., Kim, S. G. & Blenis, J. Rapamycin: one drug, many effects. *Cell Metab* **19**, 373-379, doi:10.1016/j.cmet.2014.01.001 (2014).

94 Müller, S. *et al.* Donated chemical probes for open science. *Elife* **7**, e34311, doi:10.7554/eLife.34311 (2018).

95 Blagg, J. & Workman, P. Choose and Use Your Chemical Probe Wisely to Explore Cancer Biology. *Cancer Cell* **32**, 9-25, doi:10.1016/j.ccell.2017.06.005 (2017).

96 Workman, P. & Collins, I. Probing the Probes: Fitness Factors For Small Molecule Tools. *Chemistry & Biology* **17**, 561-577, doi:10.1016/j.chembiol.2010.05.013 (2010).

97 Antolin, A. A., Workman, P. & Al-Lazikani, B. Public resources for chemical probes: the journey so far and the road ahead. *Future Medicinal Chemistry* **0**, null, doi:10.4155/fmc-2019-0231.

98 Pouliot, M. & Jeanmart, S. Pan Assay Interference Compounds (PAINS) and Other Promiscuous Compounds in Antifungal Research. *J Med Chem* **59**, 497-503, doi:10.1021/acs.jmedchem.5b00361 (2016).

99 Grueneberg, D. A. *et al.* Kinase requirements in human cells: I. Comparing kinase requirements across various cell types. *Proceedings of the National Academy of Sciences* **105**, 16472-16477, doi:10.1073/pnas.0808019105 (2008).

100 Fedorov, O., Müller, S. & Knapp, S. The (un)targeted cancer kinome. *Nature Chemical Biology* **6**, 166-169, doi:10.1038/nchembio.297 (2010).

101 Isserlin, R. *et al.* The human genome and drug discovery after a decade. Roads (still) not taken. doi:arXiv:1102.0448 (2011).

102 Wilson, L. J. *et al.* New Perspectives, Opportunities, and Challenges in Exploring the Human Protein Kinome. *Cancer Research* **78**, 15-29, doi:10.1158/0008-5472.Can-17-2291 (2018).

103 Oprea, T. I. *et al.* Unexplored therapeutic opportunities in the human genome. *Nature Reviews Drug Discovery* **17**, 317-332, doi:10.1038/nrd.2018.14 (2018).

104 Mócsai, A., Ruland, J. & Tybulewicz, V. L. J. The SYK tyrosine kinase: a crucial player in diverse biological functions. *Nature Reviews Immunology* **10**, 387-402, doi:10.1038/nri2765 (2010).

105 Krisenko, M. O. & Geahlen, R. L. Calling in SYK: SYK's dual role as a tumor promoter and tumor suppressor in cancer. *Biochimica et Biophysica Acta (BBA) - Molecular Cell Research* **1853**, 254-263, doi:10.1016/j.bbamcr.2014.10.022 (2015).

106 Leenders, F. *et al.* PKN3 is required for malignant prostate cell growth downstream of activated PI 3-kinase. *The EMBO Journal* **23**, 3303-3313, doi:10.1038/sj.emboj.7600345 (2004).

107 Unsal-Kacmaz, K. *et al.* The interaction of PKN3 with RhoC promotes malignant growth. *Molecular Oncology* **6**, 284-298, doi:10.1016/j.molonc.2011.12.001 (2012).

108 Kung, J. E. & Jura, N. Prospects for pharmacological targeting of pseudokinases. *Nature Reviews Drug Discovery* **18**, 501-526, doi:10.1038/s41573-019-0018-3 (2019).

109 Jones, M. M. *et al.* The Structural Genomics Consortium: A Knowledge Platform for Drug Discovery: A Summary. *Rand Health Q* **4**, 19-19 (2014).

110 Drewry, D. H., Wells, C. I., Zuercher, W. J. & Willson, T. M. A Perspective on Extreme Open Science: Companies Sharing Compounds without Restriction. *SLAS DISCOVERY: Advancing the Science of Drug Discovery* **24**, 505-514, doi:10.1177/2472555219838210 (2019).

111 Drewry, D. H., Willson, T. M. & Zuercher, W. J. Seeding collaborations to advance kinase science with the GSK Published Kinase Inhibitor Set (PKIS). *Curr Top Med Chem* **14**, 340-342, doi:10.2174/1568026613666131127160819 (2014).

112 Elkins, J. M. *et al.* Comprehensive characterization of the Published Kinase Inhibitor Set. *Nature Biotechnology* **34**, 95-103, doi:10.1038/nbt.3374 (2016).

113 Drewry, D. H. *et al.* Progress towards a public chemogenomic set for protein kinases and a call for contributions. *PLoS One* **12**, e0181585-e0181585, doi:10.1371/journal.pone.0181585 (2017).

114 Jones, L. H. & Bunnage, M. E. Applications of chemogenomic library screening in drug discovery. *Nature Reviews Drug Discovery* **16**, 285-296, doi:10.1038/nrd.2016.244 (2017).

115 Wells, C. I. *et al.* The Kinase Chemogenomic Set (KCGS): An open science resource for kinase vulnerability identification. *bioRxiv*, 2019.2012.2022.886523, doi:10.1101/2019.12.22.886523 (2019).

116 Lee, J. & Bogyo, M. Target deconvolution techniques in modern phenotypic profiling. *Curr Opin Chem Biol* **17**, 118-126, doi:10.1016/j.cbpa.2012.12.022 (2013).

117 Goldstein, D. M., Gray, N. S. & Zarrinkar, P. P. High-throughput kinase profiling as a platform for drug discovery. *Nature Reviews Drug Discovery* **7**, 391-397, doi:10.1038/nrd2541 (2008).

118 Rudolf, A. F., Skovgaard, T., Knapp, S., Jensen, L. J. & Berthelsen, J. A Comparison of Protein Kinases Inhibitor Screening Methods Using Both Enzymatic Activity and Binding Affinity Determination. *PLoS One* **9**, e98800, doi:10.1371/journal.pone.0098800 (2014).

119 Wang, Y. & Ma, H. Protein kinase profiling assays: a technology review. *Drug Discov Today Technol* **18**, 1-8, doi:10.1016/j.ddtec.2015.10.007 (2015).

120 Vasta, J. D. *et al.* Quantitative, Wide-Spectrum Kinase Profiling in Live Cells for Assessing the Effect of Cellular ATP on Target Engagement. *Cell Chemical Biology* **25**, 206-214.e211, doi:10.1016/j.chembiol.2017.10.010 (2018).

121 Hall, M. P. *et al.* Engineered Luciferase Reporter from a Deep Sea Shrimp Utilizing a Novel Imidazopyrazinone Substrate. *ACS Chemical Biology* **7**, 1848-1857, doi:10.1021/cb3002478 (2012).

122 Daub, H. Quantitative Proteomics of Kinase Inhibitor Targets and Mechanisms. *ACS Chemical Biology* **10**, 201-212, doi:10.1021/cb5008794 (2015).

123 Schirle, M., Bantscheff, M. & Kuster, B. Mass Spectrometry-Based Proteomics in Preclinical Drug Discovery. *Chemistry & Biology* **19**, 72-84, doi:10.1016/j.chembiol.2012.01.002 (2012).

124 Cravatt, B. F., Simon, G. M. & Yates Iii, J. R. The biological impact of mass-spectrometry-based proteomics. *Nature* **450**, 991-1000, doi:10.1038/nature06525 (2007).

125 Limbutara, K., Kelleher, A., Yang, C.-R., Raghuram, V. & Knepper, M. A. Phosphorylation Changes in Response to Kinase Inhibitor H89 in PKA-Null Cells. *Scientific Reports* **9**, 2814, doi:10.1038/s41598-019-39116-2 (2019).

126 Casado, P., Hijazi, M., Britton, D. & Cutillas, P. R. Impact of phosphoproteomics in the translation of kinase-targeted therapies. *PROTEOMICS* **17**, 1600235, doi:10.1002/pmic.201600235 (2017).

127 Olsen, J. V. & Mann, M. Status of large-scale analysis of post-translational modifications by mass spectrometry. *Mol Cell Proteomics* **12**, 3444-3452, doi:10.1074/mcp.O113.034181 (2013).

128 Ruprecht, B. *et al.* Comprehensive and reproducible phosphopeptide enrichment using iron immobilized metal ion affinity chromatography (Fe-IMAC) columns. *Mol Cell Proteomics* **14**, 205-215, doi:10.1074/mcp.M114.043109 (2015).

129 Ochoa, D. *et al.* The functional landscape of the human phosphoproteome. *Nature Biotechnology*, doi:10.1038/s41587-019-0344-3 (2019).

130 Franken, H. *et al.* Thermal proteome profiling for unbiased identification of direct and indirect drug targets using multiplexed quantitative mass spectrometry. *Nature Protocols* **10**, 1567-1593, doi:10.1038/nprot.2015.101 (2015).

131 Savitski, M. M. *et al.* Tracking cancer drugs in living cells by thermal profiling of the proteome. *Science* **346**, 1255784, doi:10.1126/science.1255784 (2014).

132 Molina, D. M. *et al.* Monitoring Drug Target Engagement in Cells and Tissues Using the Cellular Thermal Shift Assay. *Science* **341**, 84-87, doi:10.1126/science.1233606 (2013).

133 Dart, M. L. *et al.* Homogeneous Assay for Target Engagement Utilizing Bioluminescent Thermal Shift. *ACS medicinal chemistry letters* **9**, 546-551, doi:10.1021/acsmedchemlett.8b00081 (2018).

134 Heinzlmeir, S. When chemical proteomics meets medicinal chemistry: Guided drug discovery towards EPHA2 inhibitors. *PhD thesis Retrieved from media TUM Universitätsbibliothek Technische Universität München* **(urn:nbn:de:bvb:91-diss-20171215-1380642-1-5)** (2017).

135 Jones, L. H. & Neubert, H. Clinical chemoproteomics—Opportunities and obstacles. *Science Translational Medicine* **9**, eaaf7951, doi:10.1126/scitranslmed.aaf7951 (2017).

136 Bantscheff, M. & Drewes, G. Chemoproteomic approaches to drug target identification and drug profiling. *Bioorganic & Medicinal Chemistry* **20**, 1973-1978, doi:10.1016/j.bmc.2011.11.003 (2012).

137 Liu, Y., Patricelli, M. P. & Cravatt, B. F. Activity-based protein profiling: The serine hydrolases. *Proceedings of the National Academy of Sciences* **96**, 14694-14699, doi:10.1073/pnas.96.26.14694 (1999).

138 Cravatt, B. F., Wright, A. T. & Kozarich, J. W. Activity-Based Protein Profiling: From Enzyme Chemistry to Proteomic Chemistry. *Annual Review of Biochemistry* **77**, 383-414, doi:10.1146/annurev.biochem.75.101304.124125 (2008).

139 Nomura, D. K., Dix, M. M. & Cravatt, B. F. Activity-based protein profiling for biochemical pathway discovery in cancer. *Nature Reviews Cancer* **10**, 630-638, doi:10.1038/nrc2901 (2010).

140 Zhao, Q. *et al.* Broad-Spectrum Kinase Profiling in Live Cells with Lysine-Targeted Sulfonyl Fluoride Probes. *Journal of the American Chemical Society* **139**, 680-685, doi:10.1021/jacs.6b08536 (2017).

141 Singh, A., Thornton, E. R. & Westheimer, F. H. The photolysis of diazoacetylchymotrypsin. *J Biol Chem* **237**, 3006-3008 (1962).

142 Smith, E. & Collins, I. Photoaffinity labeling in target- and binding-site identification. *Future Med Chem* **7**, 159-183, doi:10.4155/fmc.14.152 (2015).

143 Flaxman, H. A., Miyamoto, D. K. & Woo, C. M. Small Molecule Interactome Mapping by Photo-Affinity Labeling (SIM-PAL) to Identify Binding Sites of Small Molecules on a Proteome-Wide Scale. *Curr Protoc Chem Biol* **11**, e75, doi:10.1002/cpch.75 (2019).

144 Rix, U. & Superti-Furga, G. Target profiling of small molecules by chemical proteomics. *Nature Chemical Biology* **5**, 616-624, doi:10.1038/nchembio.216 (2009).

145 Bantscheff, M. *et al.* Quantitative chemical proteomics reveals mechanisms of action of clinical ABL kinase inhibitors. *Nature Biotechnology* **25**, 1035-1044, doi:10.1038/nbt1328 (2007).

146 Bantscheff, M. *et al.* Chemoproteomics profiling of HDAC inhibitors reveals selective targeting of HDAC complexes. *Nature Biotechnology* **29**, 255-265, doi:10.1038/nbt.1759 (2011).

147 Médard, G. *et al.* Optimized Chemical Proteomics Assay for Kinase Inhibitor Profiling. *Journal of Proteome Research* **14**, 1574-1586, doi:10.1021/pr5012608 (2015).

148 Klaeger, S. *et al.* Chemical Proteomics Reveals Ferrochelatase as a Common Off-target of Kinase Inhibitors. *ACS Chemical Biology* **11**, 1245-1254, doi:10.1021/acschembio.5b01063 (2016).

149 Patricelli, Matthew P. *et al.* In Situ Kinase Profiling Reveals Functionally Relevant Properties of Native Kinases. *Chemistry & Biology* **18**, 699-710, doi:10.1016/j.chembiol.2011.04.011 (2011).

150 Patricelli, M. P. *et al.* Functional Interrogation of the Kinome Using Nucleotide Acyl Phosphates. *Biochemistry* **46**, 350-358, doi:10.1021/bi062142x (2007).

151 Lemeer, S., Zörgiebel, C., Ruprecht, B., Kohl, K. & Kuster, B. Comparing Immobilized Kinase Inhibitors and Covalent ATP Probes for Proteomic Profiling of Kinase Expression and Drug Selectivity. *Journal of Proteome Research* **12**, 1723-1731, doi:10.1021/pr301073j (2013).

152 Sharma, K. *et al.* Proteomics strategy for quantitative protein interaction profiling in cell extracts. *Nature Methods* **6**, 741-744, doi:10.1038/nmeth.1373 (2009).

153 Yung-Chi, C. & Prusoff, W. H. Relationship between the inhibition constant (KI) and the concentration of inhibitor which causes 50 per cent inhibition (I50) of an enzymatic reaction. *Biochemical Pharmacology* **22**, 3099-3108, doi:10.1016/0006-2952(73)90196-2 (1973).

154 Copeland, R. A., Pompliano, D. L. & Meek, T. D. Drug–target residence time and its implications for lead optimization. *Nature Reviews Drug Discovery* **5**, 730-739, doi:10.1038/nrd2082 (2006).

155 Ge, Y. *et al.* Top Down Characterization of Larger Proteins (45 kDa) by Electron Capture Dissociation Mass Spectrometry. *Journal of the American Chemical Society* **124**, 672-678, doi:10.1021/ja011335z (2002).

156 Donnelly, D. P. *et al.* Best practices and benchmarks for intact protein analysis for top-down mass spectrometry. *Nature Methods* **16**, 587-594, doi:10.1038/s41592-019-0457-0 (2019).

157 Aebersold, R. & Mann, M. Mass-spectrometric exploration of proteome structure and function. *Nature* **537**, 347-355, doi:10.1038/nature19949 (2016).

158 Zhang, Y., Fonslow, B. R., Shan, B., Baek, M.-C. & Yates, J. R., 3rd. Protein analysis by shotgun/bottom-up proteomics. *Chemical reviews* **113**, 2343-2394, doi:10.1021/cr3003533 (2013).

159 Alpert, A. J. in *Modern Proteomics – Sample Preparation, Analysis and Practical Applications* (eds Hamid Mirzaei & Martin Carrasco) 23-41 (Springer International Publishing, 2016).

160 Tsiatsiani, L. & Heck, A. J. R. Proteomics beyond trypsin. *The FEBS Journal* **282**, 2612-2626, doi:10.1111/febs.13287 (2015).

161 Giansanti, P., Tsiatsiani, L., Low, T. Y. & Heck, A. J. R. Six alternative proteases for mass spectrometry–based proteomics beyond trypsin. *Nature Protocols* **11**, 993-1006, doi:10.1038/nprot.2016.057 (2016).

162 Larsen, M. R., Trelle, M. B., Thingholm, T. E. & Jensen, O. N. Analysis of posttranslational modifications of proteins by tandem mass spectrometry. *BioTechniques* **40**, 790-798, doi:10.2144/000112201 (2006).

163 Manadas, B., Mendes, V. M., English, J. & Dunn, M. J. Peptide fractionation in proteomics approaches. *Expert Review of Proteomics* **7**, 655-663, doi:10.1586/epr.10.46 (2010).

164 Zhou, F., Sikorski, T. W., Ficarro, S. B., Webber, J. T. & Marto, J. A. Online nanoflow reversed phase-strong anion exchange-reversed phase liquid chromatography-tandem mass spectrometry platform for efficient and in-depth proteome sequence analysis of complex organisms. *Anal Chem* **83**, 6996-7005, doi:10.1021/ac200639v (2011).

165 Steen, H. & Mann, M. The abc's (and xyz's) of peptide sequencing. *Nature Reviews Molecular Cell Biology* **5**, 699-711, doi:10.1038/nrm1468 (2004).

166 Savaryn, J. P., Toby, T. K. & Kelleher, N. L. A researcher's guide to mass spectrometry-based proteomics. *PROTEOMICS* **16**, 2435-2443, doi:10.1002/pmic.201600113 (2016).

167 Fenn, J., Mann, M., Meng, C., Wong, S. & Whitehouse, C. Electrospray ionization for mass spectrometry of large biomolecules. *Science* **246**, 64-71, doi:10.1126/science.2675315 (1989).

168 Konermann, L., Ahadi, E., Rodriguez, A. D. & Vahidi, S. Unraveling the Mechanism of Electrospray Ionization. *Analytical Chemistry* **85**, 2-9, doi:10.1021/ac302789c (2013).

169 Kebarle, P. & Tang, L. From ions in solution to ions in the gas phase - the mechanism of electrospray mass spectrometry. *Analytical Chemistry* **65**, 972A-986A, doi:10.1021/ac00070a001 (1993).

170 Mann, M. & Kelleher, N. L. Precision proteomics: the case for high resolution and high mass accuracy. *Proc Natl Acad Sci U S A* **105**, 18132-18138, doi:10.1073/pnas.0800788105 (2008).

171 Miller, P. E. & Denton, M. B. The quadrupole mass filter: Basic operating concepts. *Journal of Chemical Education* **63**, 617, doi:10.1021/ed063p617 (1986).

172 Douglas, D. J., Frank, A. J. & Mao, D. Linear ion traps in mass spectrometry. *Mass Spectrometry Reviews* **24**, 1-29, doi:10.1002/mas.20004 (2005).

173 Hu, Q. *et al.* The Orbitrap: a new mass spectrometer. *Journal of Mass Spectrometry* **40**, 430-443, doi:10.1002/jms.856 (2005).

174 Zubarev, R. A. & Makarov, A. Orbitrap Mass Spectrometry. *Analytical Chemistry* **85**, 5288-5296, doi:10.1021/ac4001223 (2013).

175 Scigelova, M., Hornshaw, M., Giannakopulos, A. & Makarov, A. Fourier transform mass spectrometry. *Mol Cell Proteomics* **10**, M111.009431-M009111.009431, doi:10.1074/mcp.M111.009431 (2011).

176 Scheltema, R. A. *et al.* The Q Exactive HF, a Benchtop Mass Spectrometer with a Pre-filter, High-performance Quadrupole and an Ultra-high-field Orbitrap Analyzer. *Molecular & Cellular Proteomics* **13**, 3698-3708, doi:10.1074/mcp.M114.043489 (2014).

177 Michalski, A. *et al.* Ultra High Resolution Linear Ion Trap Orbitrap Mass Spectrometer (Orbitrap Elite) Facilitates Top Down LC MS/MS and Versatile Peptide Fragmentation Modes. *Molecular & Cellular Proteomics* **11**, O111.013698, doi:10.1074/mcp.O111.013698 (2012).

178 Pachl, F., Ruprecht, B., Lemeer, S. & Kuster, B. Characterization of a high field Orbitrap mass spectrometer for proteome analysis. *PROTEOMICS* **13**, 2552-2562, doi:10.1002/pmic.201300076 (2013).

179 Clauser, K. R., Baker, P. & Burlingame, A. L. Role of Accurate Mass Measurement (±10 ppm) in Protein Identification Strategies Employing MS or MS/MS and Database Searching. *Analytical Chemistry* **71**, 2871-2882, doi:10.1021/ac9810516 (1999).

180 McLafferty, F. W. Tandem mass spectrometry. *Science* **214**, 280-287, doi:10.1126/science.7280693 (1981).

181 Olsen, J. V. *et al.* Higher-energy C-trap dissociation for peptide modification analysis. *Nature Methods* **4**, 709-712, doi:10.1038/nmeth1060 (2007).

182 Roepstorff, P. & Fohlman, J. Proposal for a common nomenclature for sequence ions in mass spectra of peptides. *Biomed Mass Spectrom* **11**, 601, doi:10.1002/bms.1200111109 (1984).

183 Nesvizhskii, A. I., Vitek, O. & Aebersold, R. Analysis and validation of proteomic data generated by tandem mass spectrometry. *Nature Methods* **4**, 787-797, doi:10.1038/nmeth1088 (2007).

184 Michalski, A., Cox, J. & Mann, M. More than 100,000 Detectable Peptide Species Elute in Single Shotgun Proteomics Runs but the Majority is Inaccessible to Data-Dependent LC−MS/MS. *Journal of Proteome Research* **10**, 1785-1793, doi:10.1021/pr101060v (2011).

185 Gillet, L. C., Leitner, A. & Aebersold, R. Mass Spectrometry Applied to Bottom-Up Proteomics: Entering the High-Throughput Era for Hypothesis Testing. *Annual Review of Analytical Chemistry* **9**, 449-472, doi:10.1146/annurev-anchem-071015-041535 (2016).

186 Ting, L., Rad, R., Gygi, S. P. & Haas, W. MS3 eliminates ratio distortion in isobaric multiplexed quantitative proteomics. *Nature methods* **8**, 937-940, doi:10.1038/nmeth.1714 (2011).

187 Wang, P. & Wilson, S. R. Mass spectrometry-based protein identification by integrating de novo sequencing with database searching. *BMC bioinformatics* **14 Suppl 2**, S24-S24, doi:10.1186/1471-2105-14-S2-S24 (2013).

188 Seidler, J., Zinn, N., Boehm, M. E. & Lehmann, W. D. De novo sequencing of peptides by MS/MS. *PROTEOMICS* **10**, 634-649, doi:10.1002/pmic.200900459 (2010).

189 Perkins, D. N., Pappin, D. J. C., Creasy, D. M. & Cottrell, J. S. Probability-based protein identification by searching sequence databases using mass spectrometry data. *ELECTROPHORESIS* **20**, 3551-3567, doi:10.1002/(sici)1522-2683(19991201)20:18<3551::Aid-elps3551>3.0.Co;2-2 (1999).

190 Cox, J. *et al.* Andromeda: A Peptide Search Engine Integrated into the MaxQuant Environment. *Journal of Proteome Research* **10**, 1794-1805, doi:10.1021/pr101065j (2011).

191 Eng, J. K., McCormack, A. L. & Yates, J. R. An approach to correlate tandem mass spectral data of peptides with amino acid sequences in a protein database. *Journal of the American Society for Mass Spectrometry* **5**, 976-989, doi:10.1016/1044-0305(94)80016-2 (1994).

192 Elias, J. E. & Gygi, S. P. Target-decoy search strategy for increased confidence in large-scale protein identifications by mass spectrometry. *Nat Methods* **4**, 207-214, doi:10.1038/nmeth1019 (2007).

193 Nesvizhskii, A. I. A survey of computational methods and error rate estimation procedures for peptide and protein identification in shotgun proteomics. *J Proteomics* **73**, 2092-2123, doi:10.1016/j.jprot.2010.08.009 (2010).
194 Bantscheff, M., Schirle, M., Sweetman, G., Rick, J. & Kuster, B. Quantitative mass spectrometry in proteomics: a critical review. *Anal Bioanal Chem* **389**, 1017-1031, doi:10.1007/s00216-007-1486-6 (2007).
195 Bantscheff, M., Lemeer, S., Savitski, M. M. & Kuster, B. Quantitative mass spectrometry in proteomics: critical review update from 2007 to the present. *Anal Bioanal Chem* **404**, 939-965, doi:10.1007/s00216-012-6203-4 (2012).
196 Tang, K., Page, J. S. & Smith, R. D. Charge competition and the linear dynamic range of detection in electrospray ionization mass spectrometry. *J Am Soc Mass Spectrom* **15**, 1416-1423, doi:10.1016/j.jasms.2004.04.034 (2004).
197 Cox, J. *et al.* Accurate proteome-wide label-free quantification by delayed normalization and maximal peptide ratio extraction, termed MaxLFQ. *Mol Cell Proteomics* **13**, 2513-2526, doi:10.1074/mcp.M113.031591 (2014).
198 Tyanova, S., Temu, T. & Cox, J. The MaxQuant computational platform for mass spectrometry-based shotgun proteomics. *Nat Protoc* **11**, 2301-2319, doi:10.1038/nprot.2016.136 (2016).
199 Lazar, C., Gatto, L., Ferro, M., Bruley, C. & Burger, T. Accounting for the Multiple Natures of Missing Values in Label-Free Quantitative Proteomics Data Sets to Compare Imputation Strategies. *Journal of Proteome Research* **15**, 1116-1125, doi:10.1021/acs.jproteome.5b00981 (2016).
200 Rauniyar, N. & Yates, J. R., 3rd. Isobaric labeling-based relative quantification in shotgun proteomics. *J Proteome Res* **13**, 5293-5309, doi:10.1021/pr500880b (2014).
201 Thompson, A. *et al.* Tandem Mass Tags: A Novel Quantification Strategy for Comparative Analysis of Complex Protein Mixtures by MS/MS. *Analytical Chemistry* **75**, 1895-1904, doi:10.1021/ac0262560 (2003).
202 McAlister, G. C. *et al.* MultiNotch MS3 enables accurate, sensitive, and multiplexed detection of differential expression across cancer cell line proteomes. *Anal Chem* **86**, 7150-7158, doi:10.1021/ac502040v (2014).
203 Reinecke, M. *et al.* Chemoproteomic Selectivity Profiling of PIKK and PI3K Kinase Inhibitors. *ACS Chemical Biology* **14**, 655-664, doi:10.1021/acschembio.8b01020 (2019).
204 Rohm, S. *et al.* Fast Iterative Synthetic Approach toward Identification of Novel Highly Selective p38 MAP Kinase Inhibitors. *J Med Chem* **62**, 10757-10782, doi:10.1021/acs.jmedchem.9b01227 (2019).
205 Gandin, V. *et al.* mTORC1 and CK2 coordinate ternary and eIF4F complex assembly. *Nat Commun* **7**, 11127-11127, doi:10.1038/ncomms11127 (2016).
206 Gyenis, L., Duncan, J. S., Turowec, J. P., Bretner, M. & Litchfield, D. W. Unbiased functional proteomics strategy for protein kinase inhibitor validation and identification of bona fide protein kinase substrates: application to identification of EEF1D as a substrate for CK2. *Journal of proteome research* **10**, 4887-4901, doi:10.1021/pr2008994 (2011).
207 Litchfield, D. W., Lüscher, B., Lozeman, F. J., Eisenman, R. N. & Krebs, E. G. Phosphorylation of casein kinase II by p34cdc2 in vitro and at mitosis. *J Biol Chem* **267**, 13943-13951 (1992).
208 Bosc, D. G., Slominski, E., Sichler, C. & Litchfield, D. W. Phosphorylation of casein kinase II by p34cdc2. Identification of phosphorylation sites using phosphorylation site mutants in vitro. *J Biol Chem* **270**, 25872-25878, doi:10.1074/jbc.270.43.25872 (1995).
209 Zecha, J. *et al.* TMT Labeling for the Masses: A Robust and Cost-efficient, In-solution Labeling Approach. *Mol Cell Proteomics* **18**, 1468-1478, doi:10.1074/mcp.TIR119.001385 (2019).

210 Ruprecht, B. *et al.* Optimized Enrichment of Phosphoproteomes by Fe-IMAC Column Chromatography. *Methods Mol Biol* **1550**, 47-60, doi:10.1007/978-1-4939-6747-6_5 (2017).

211 Ruprecht, B., Zecha, J., Zolg, D. P. & Kuster, B. High pH Reversed-Phase Micro-Columns for Simple, Sensitive, and Efficient Fractionation of Proteome and (TMT labeled) Phosphoproteome Digests. *Methods Mol Biol* **1550**, 83-98, doi:10.1007/978-1-4939-6747-6_8 (2017).

212 Tyanova, S. & Cox, J. Perseus: A Bioinformatics Platform for Integrative Analysis of Proteomics Data in Cancer Research. *Methods Mol Biol* **1711**, 133-148, doi:10.1007/978-1-4939-7493-1_7 (2018).

213 Pachl, F. *et al.* Characterization of a chemical affinity probe targeting Akt kinases. *J Proteome Res* **12**, 3792-3800, doi:10.1021/pr400455j (2013).

214 Ku, X., Heinzlmeir, S., Liu, X., Medard, G. & Kuster, B. A new chemical probe for quantitative proteomic profiling of fibroblast growth factor receptor and its inhibitors. *J Proteomics* **96**, 44-55, doi:10.1016/j.jprot.2013.10.031 (2014).

215 Chang, K.-Y. *et al.* Novel Phosphoinositide 3-Kinase/mTOR Dual Inhibitor, NVP-BGT226, Displays Potent Growth-Inhibitory Activity against Human Head and Neck Cancer Cells In Vitro and In Vivo. *Clinical Cancer Research* **17**, 7116-7126, doi:10.1158/1078-0432.Ccr-11-0796 (2011).

216 Markman, B. *et al.* Phase I safety, pharmacokinetic, and pharmacodynamic study of the oral phosphatidylinositol-3-kinase and mTOR inhibitor BGT226 in patients with advanced solid tumors. *Annals of Oncology* **23**, 2399-2408, doi:10.1093/annonc/mds011 (2012).

217 Maira, S.-M. *et al.* Identification and characterization of NVP-BEZ235, a new orally available dual phosphatidylinositol 3-kinase/mammalian target of rapamycin inhibitor with potent in vivo antitumor activity. *Molecular Cancer Therapeutics* **7**, 1851-1863, doi:10.1158/1535-7163.Mct-08-0017 (2008).

218 Toledo, L. I. *et al.* A cell-based screen identifies ATR inhibitors with synthetic lethal properties for cancer-associated mutations. *Nature Structural & Molecular Biology* **18**, 721-727, doi:10.1038/nsmb.2076 (2011).

219 Knight, S. D. *et al.* Discovery of GSK2126458, a Highly Potent Inhibitor of PI3K and the Mammalian Target of Rapamycin. *ACS Medicinal Chemistry Letters* **1**, 39-43, doi:10.1021/ml900028r (2010).

220 Petter, R. C. *et al.* Ligand-directed covalent modification of lysine-containing proteins, enzyme inhibitors and treatment of diseases. WO2011082285A1 (2011).

221 Zhu, J. *et al.* Preparation of N-(5-(quinolin-6-yl)pyridin-3-yl) benzenesulfamide derivatives for treating tumor and immune disease. (2014).

222 Eberl, H. C. *et al.* Chemical proteomics reveals target selectivity of clinical Jak inhibitors in human primary cells. *Scientific Reports* **9**, 14159, doi:10.1038/s41598-019-50335-5 (2019).

223 Golkowski, M. *et al.* Kinobead and Single-Shot LC-MS Profiling Identifies Selective PKD Inhibitors. *J Proteome Res* **16**, 1216-1227, doi:10.1021/acs.jproteome.6b00817 (2017).

224 Michalski, A. *et al.* Mass Spectrometry-based Proteomics Using Q Exactive, a High-performance Benchtop Quadrupole Orbitrap Mass Spectrometer. *Molecular & Cellular Proteomics* **10**, M111.011015, doi:10.1074/mcp.M111.011015 (2011).

225 Bian, Y. *et al.* Robust, reproducible and quantitative analysis of thousands of proteomes by micro-flow LC-MS/MS. *Nat Commun* **11**, 157, doi:10.1038/s41467-019-13973-x (2020).

226 Kuzmič, P. *et al.* High-Throughput Screening of Enzyme Inhibitors: Automatic Determination of Tight-Binding Inhibition Constants. *Analytical Biochemistry* **281**, 62-67, doi:10.1006/abio.2000.4501 (2000).

227 Seefried, F. *et al.* CiRCus: A Framework to Enable Classification of Complex High-Throughput Experiments. *Journal of Proteome Research* **18**, 1486-1493, doi:10.1021/acs.jproteome.8b00724 (2019).

228 Ferdinandusse, S. *et al.* Clinical, biochemical, and mutational spectrum of peroxisomal acyl-coenzyme A oxidase deficiency. *Hum Mutat* **28**, 904-912, doi:10.1002/humu.20535 (2007).

229 Oaxaca-Castillo, D. *et al.* Biochemical characterization of two functional human liver acyl-CoA oxidase isoforms 1a and 1b encoded by a single gene. *Biochem Biophys Res Commun* **360**, 314-319, doi:10.1016/j.bbrc.2007.06.059 (2007).

230 Oh, E.-T. & Park, H. J. Implications of NQO1 in cancer therapy. *BMB Rep* **48**, 609-617, doi:10.5483/bmbrep.2015.48.11.190 (2015).

231 Srijiwangsa, P., Ponnikorn, S. & Na-Bangchang, K. Effect of β-Eudesmol on NQO1 suppression-enhanced sensitivity of cholangiocarcinoma cells to chemotherapeutic agents. *BMC Pharmacol Toxicol* **19**, 32-32, doi:10.1186/s40360-018-0223-4 (2018).

232 Missner, E. *et al.* Off-Target Decoding of a Multitarget Kinase Inhibitor by Chemical Proteomics. *ChemBioChem* **10**, 1163-1174, doi:10.1002/cbic.200800796 (2009).

233 Daver, N., Schlenk, R. F., Russell, N. H. & Levis, M. J. Targeting FLT3 mutations in AML: review of current knowledge and evidence. *Leukemia* **33**, 299-312, doi:10.1038/s41375-018-0357-9 (2019).

234 Jakimiec, M., Paprocka, J. & Śmigiel, R. CDKL5 Deficiency Disorder-A Complex Epileptic Encephalopathy. *Brain Sci* **10**, 107, doi:10.3390/brainsci10020107 (2020).

235 Matsuoka, H., Obama, H., Kelly, M. L., Matsui, T. & Nakamoto, M. Biphasic functions of the kinase-defective Ephb6 receptor in cell adhesion and migration. *J Biol Chem* **280**, 29355-29363, doi:10.1074/jbc.M500010200 (2005).

236 Byrne, D. P., Foulkes, D. M. & Eyers, P. A. Pseudokinases: update on their functions and evaluation as new drug targets. *Future Medicinal Chemistry* **9**, 245-265, doi:10.4155/fmc-2016-0207 (2017).

237 Litchfield, D. W. *et al.* Functional specialization of CK2 isoforms and characterization of isoform-specific binding partners. *Molecular and Cellular Biochemistry* **227**, 21-29, doi:10.1023/A:1013188101465 (2001).

238 Trembley, J. H. *et al.* Emergence of protein kinase CK2 as a key target in cancer therapy. *Biofactors* **36**, 187-195, doi:10.1002/biof.96 (2010).

239 Ruzzene, M. & Pinna, L. A. Addiction to protein kinase CK2: A common denominator of diverse cancer cells? *Biochimica et Biophysica Acta (BBA) - Proteins and Proteomics* **1804**, 499-504, doi:10.1016/j.bbapap.2009.07.018 (2010).

240 Litchfield, D. W. Protein kinase CK2: structure, regulation and role in cellular decisions of life and death. *Biochem J* **369**, 1-15, doi:10.1042/bj20021469 (2003).

241 Dowling, J. E. *et al.* Potent and Selective CK2 Kinase Inhibitors with Effects on Wnt Pathway Signaling in Vivo. *ACS Med Chem Lett* **7**, 300-305, doi:10.1021/acsmedchemlett.5b00452 (2016).

242 Kim, H. *et al.* Identification of a Novel Function of CX-4945 as a Splicing Regulator. *PLoS One* **9**, e94978, doi:10.1371/journal.pone.0094978 (2014).

243 Vassilev, L. T. *et al.* Selective small-molecule inhibitor reveals critical mitotic functions of human CDK1. *Proc Natl Acad Sci U S A* **103**, 10660-10665, doi:10.1073/pnas.0600447103 (2006).

244 Chen, S. *et al.* Synthesis and activity of quinolinyl-methylene-thiazolinones as potent and selective cyclin-dependent kinase 1 inhibitors. *Bioorg Med Chem Lett* **17**, 2134-2138, doi:10.1016/j.bmcl.2007.01.081 (2007).

245 Llorens, F. *et al.* The N-terminal domain of the human eIF2beta subunit and the CK2 phosphorylation sites are required for its function. *Biochem J* **394**, 227-236, doi:10.1042/bj20050605 (2006).

246 Kobayashi, T., Nakamura, S., Taniguchi, T. & Yamamura, H. Purification and characterization of a cytosolic protein-tyrosine kinase from porcine spleen. *Eur J Biochem* **188**, 535-540, doi:10.1111/j.1432-1033.1990.tb15433.x (1990).

247 Sada, K., Takano, T., Yanagi, S. & Yamamura, H. Structure and Function of Syk Protein-Tyrosine Kinase1. *The Journal of Biochemistry* **130**, 177-186, doi:10.1093/oxfordjournals.jbchem.a002970 (2001).

248 Braegelmann, C. *et al.* Spleen tyrosine kinase (SYK) is a potential target for the treatment of cutaneous lupus erythematosus patients. *Experimental Dermatology* **25**, 375-379, doi:10.1111/exd.12986 (2016).

249 Masuda, E. S. & Schmitz, J. Syk inhibitors as treatment for allergic rhinitis. *Pulmonary Pharmacology & Therapeutics* **21**, 461-467, doi:10.1016/j.pupt.2007.06.002 (2008).

250 Gómez-Puerta, J. A. & Bosch, X. Spleen tyrosine kinase inhibitors—novel therapies for RA? *Nature Reviews Rheumatology* **7**, 134-136, doi:10.1038/nrrheum.2011.8 (2011).

251 Sharman, J. *et al.* An open-label phase 2 trial of entospletinib (GS-9973), a selective spleen tyrosine kinase inhibitor, in chronic lymphocytic leukemia. *Blood* **125**, 2336-2343, doi:10.1182/blood-2014-08-595934 (2015).

252 Lam, B. *et al.* Discovery of TAK-659 an orally available investigational inhibitor of Spleen Tyrosine Kinase (SYK). *Bioorg Med Chem Lett* **26**, 5947-5950, doi:10.1016/j.bmcl.2016.10.087 (2016).

253 Markham, A. Fostamatinib: First Global Approval. *Drugs* **78**, 959-963, doi:10.1007/s40265-018-0927-1 (2018).

254 Weinblatt, M. E. *et al.* Treatment of rheumatoid arthritis with a syk kinase inhibitor: A twelve-week, randomized, placebo-controlled trial. *Arthritis & Rheumatism* **58**, 3309-3318, doi:10.1002/art.23992 (2008).

255 Gross, O. *et al.* Card9 controls a non-TLR signalling pathway for innate anti-fungal immunity. *Nature* **442**, 651-656, doi:10.1038/nature04926 (2006).

256 Sahan-Firat, S. *et al.* NF-κB activation mediates LPS-or zymosan-induced hypotension and inflammation reversed by BAY61-3606, a selective Syk inhibitor, in rat models of septic and non-septic shock. *Clinical and Experimental Pharmacology and Physiology* **46**, 173-182, doi:10.1111/1440-1681.13045 (2019).

257 Mukai, H. *et al.* PKN3 is the major regulator of angiogenesis and tumor metastasis in mice. *Sci Rep* **6**, 18979, doi:10.1038/srep18979 (2016).

258 Aleku, M. *et al.* Atu027, a liposomal small interfering RNA formulation targeting protein kinase N3, inhibits cancer progression. *Cancer Res* **68**, 9788-9798, doi:10.1158/0008-5472.Can-08-2428 (2008).

259 Schultheis, B. *et al.* First-in-human phase I study of the liposomal RNA interference therapeutic Atu027 in patients with advanced solid tumors. *J Clin Oncol* **32**, 4141-4148, doi:10.1200/jco.2013.55.0376 (2014).

260 Browne, C. M. *et al.* A Chemoproteomic Strategy for Direct and Proteome-Wide Covalent Inhibitor Target-Site Identification. *Journal of the American Chemical Society* **141**, 191-203, doi:10.1021/jacs.8b07911 (2019).

261 Samaras, P. *et al.* ProteomicsDB: a multi-omics and multi-organism resource for life science research. *Nucleic Acids Research*, doi:10.1093/nar/gkz974 (2019).

262 Björkblom, B. *et al.* c-Jun N-terminal kinase phosphorylation of MARCKSL1 determines actin stability and migration in neurons and in cancer cells. *Mol Cell Biol* **32**, 3513-3526, doi:10.1128/MCB.00713-12 (2012).

263 Graff, J. M., Rajan, R. R., Randall, R. R., Nairn, A. C. & Blackshear, P. J. Protein kinase C substrate and inhibitor characteristics of peptides derived from the myristoylated alanine-rich C kinase substrate (MARCKS) protein phosphorylation site domain. *J Biol Chem* **266**, 14390-14398 (1991).

264 Shu, J. *et al.* BTBD7 Downregulates E-Cadherin and Promotes Epithelial-Mesenchymal Transition in Lung Cancer. *Biomed Res Int* **2019**, 5937635, doi:10.1155/2019/5937635 (2019).

265 Luo, F. Y. *et al.* Association of BTBD7 with Metastasis and Poor Prognosis in Non-Small-Cell Lung Cancer Patients. *J Cancer* **6**, 477-481, doi:10.7150/jca.11715 (2015).

266 Dittus, L., Werner, T., Muelbaier, M. & Bantscheff, M. Differential Kinobeads Profiling for Target Identification of Irreversible Kinase Inhibitors. *ACS Chemical Biology* **12**, 2515-2521, doi:10.1021/acschembio.7b00617 (2017).

267 Markham, A. Brigatinib: First Global Approval. *Drugs* **77**, 1131-1135, doi:10.1007/s40265-017-0776-3 (2017).

268 Markham, A. & Keam, S. J. Peficitinib: First Global Approval. *Drugs* **79**, 887-891, doi:10.1007/s40265-019-01131-y (2019).

269 Lin, A. *et al.* Identification of a dual specificity kinase that activates the Jun kinases and p38-Mpk2. *Science* **268**, 286-290, doi:10.1126/science.7716521 (1995).

270 Xue, Z. *et al.* MAP3K1 and MAP2K4 mutations are associated with sensitivity to MEK inhibitors in multiple cancer models. *Cell Research* **28**, 719-729, doi:10.1038/s41422-018-0044-4 (2018).

271 Davis, S. J. *et al.* Analysis of the mitogen-activated protein kinase kinase 4 (MAP2K4) tumor suppressor gene in ovarian cancer. *BMC Cancer* **11**, 173, doi:10.1186/1471-2407-11-173 (2011).

272 Ding, L., Yu, L.-L., Han, N. & Zhang, B.-T. miR-141 promotes colon cancer cell proliferation by inhibiting MAP2K4. *Oncol Lett* **13**, 1665-1671, doi:10.3892/ol.2017.5653 (2017).

273 Hanson, S. M. *et al.* What Makes a Kinase Promiscuous for Inhibitors? *Cell Chem Biol* **26**, 390-399.e395, doi:10.1016/j.chembiol.2018.11.005 (2019).

274 Zheng, Y. & Jiang, Y. mTOR Inhibitors at a Glance. *Mol Cell Pharmacol* **7**, 15-20 (2015).

275 Bhagwat, S. V. *et al.* Preclinical characterization of OSI-027, a potent and selective inhibitor of mTORC1 and mTORC2: distinct from rapamycin. *Mol Cancer Ther* **10**, 1394-1406, doi:10.1158/1535-7163.Mct-10-1099 (2011).

276 Huang, P., Cai, Y., Zhao, B. & Cui, L. Roles of NUCKS1 in Diseases: Susceptibility, Potential Biomarker, and Regulatory Mechanisms. *BioMed research international* **2018**, 7969068-7969068, doi:10.1155/2018/7969068 (2018).

277 Cortez, D., Glick, G. & Elledge, S. J. Minichromosome maintenance proteins are direct targets of the ATM and ATR checkpoint kinases. *Proc Natl Acad Sci U S A* **101**, 10078-10083, doi:10.1073/pnas.0403410101 (2004).

278 Doukas, J. *et al.* Isoform-selective PI3K inhibitors as novel therapeutics for the treatment of acute myocardial infarction. *Biochemical Society Transactions* **35**, 204-206, doi:10.1042/bst0350204 (2007).

279 Sabini, E., Ort, S., Monnerjahn, C., Konrad, M. & Lavie, A. Structure of human dCK suggests strategies to improve anticancer and antiviral therapy. *Nature Structural & Molecular Biology* **10**, 513-519, doi:10.1038/nsb942 (2003).

280 Knezevic, C. E. *et al.* Proteome-wide Profiling of Clinical PARP Inhibitors Reveals Compound-Specific Secondary Targets. *Cell Chemical Biology* **23**, 1490-1503, doi:10.1016/j.chembiol.2016.10.011 (2016).

281 Poddar, S. *et al.* Development and preclinical pharmacology of a novel dCK inhibitor, DI-87. *Biochem Pharmacol* **172**, 113742, doi:10.1016/j.bcp.2019.113742 (2020).

282 Mortensen, D. S. *et al.* CC-223, a Potent and Selective Inhibitor of mTOR Kinase: In Vitro and In Vivo Characterization. *Mol Cancer Ther* **14**, 1295-1305, doi:10.1158/1535-7163.Mct-14-1052 (2015).

283 Mortensen, D. S. *et al.* Discovery of Mammalian Target of Rapamycin (mTOR) Kinase Inhibitor CC-223. *Journal of Medicinal Chemistry* **58**, 5323-5333, doi:10.1021/acs.jmedchem.5b00626 (2015).

284 Tröster, A. *et al.* NVP-BHG712: Effects of Regioisomers on the Affinity and Selectivity toward the EPHrin Family. *ChemMedChem* **13**, 1629-1633, doi:10.1002/cmdc.201800398 (2018).

285 Abo, M. & Weerapana, E. A Caged Electrophilic Probe for Global Analysis of Cysteine Reactivity in Living Cells. *Journal of the American Chemical Society* **137**, 7087-7090, doi:10.1021/jacs.5b04350 (2015).

286 Seda, V. & Mraz, M. B-cell receptor signalling and its crosstalk with other pathways in normal and malignant cells. *Eur J Haematol* **94**, 193-205, doi:10.1111/ejh.12427 (2015).

287 Bond, D. A. & Woyach, J. A. Targeting BTK in CLL: Beyond Ibrutinib. *Curr Hematol Malig Rep* **14**, 197-205, doi:10.1007/s11899-019-00512-0 (2019).

288 Rai, K. R. & Jain, P. Chronic lymphocytic leukemia (CLL)-Then and now. *Am J Hematol* **91**, 330-340, doi:10.1002/ajh.24282 (2016).

289 Wu, J., Liu, C., Tsui, S. T. & Liu, D. Second-generation inhibitors of Bruton tyrosine kinase. *J Hematol Oncol* **9**, 80, doi:10.1186/s13045-016-0313-y (2016).

290 Zhao, Z., Liu, Q., Bliven, S., Xie, L. & Bourne, P. E. Determining Cysteines Available for Covalent Inhibition Across the Human Kinome. *Journal of medicinal chemistry* **60**, 2879-2889, doi:10.1021/acs.jmedchem.6b01815 (2017).

291 Wu, H. *et al.* Ibrutinib selectively and irreversibly targets EGFR (L858R, Del19) mutant but is moderately resistant to EGFR (T790M) mutant NSCLC Cells. *Oncotarget* **6**, 31313-31322, doi:10.18632/oncotarget.5182 (2015).

292 Dubovsky, J. A. *et al.* Ibrutinib is an irreversible molecular inhibitor of ITK driving a Th1-selective pressure in T lymphocytes. *Blood* **122**, 2539-2549, doi:10.1182/blood-2013-06-507947 (2013).

293 Ferrer, G. & Montserrat, E. Critical molecular pathways in CLL therapy. *Mol Med* **24**, 9-9, doi:10.1186/s10020-018-0001-1 (2018).

294 Shi, Y. *et al.* Ibrutinib inactivates BMX-STAT3 in glioma stem cells to impair malignant growth and radioresistance. *Science translational medicine* **10**, eaah6816, doi:10.1126/scitranslmed.aah6816 (2018).

295 Rauf, F. *et al.* Ibrutinib inhibition of ERBB4 reduces cell growth in a WNT5A-dependent manner. *Oncogene* **37**, 2237-2250, doi:10.1038/s41388-017-0079-x (2018).

296 Backus, K. M. *et al.* Proteome-wide covalent ligand discovery in native biological systems. *Nature* **534**, 570-574, doi:10.1038/nature18002 (2016).

297 Daryaee, F. *et al.* A quantitative mechanistic PK/PD model directly connects Btk target engagement and in vivo efficacy. *Chemical science* **8**, 3434-3443, doi:10.1039/c6sc03306g (2017).

298 Traut, T. W. Physiological concentrations of purines and pyrimidines. *Mol Cell Biochem* **140**, 1-22, doi:10.1007/bf00928361 (1994).

299 Gribble, F. M. *et al.* A novel method for measurement of submembrane ATP concentration. *J Biol Chem* **275**, 30046-30049, doi:10.1074/jbc.M001010200 (2000).

300 Imamura, H. *et al.* Visualization of ATP levels inside single living cells with fluorescence resonance energy transfer-based genetically encoded indicators. *Proc Natl Acad Sci U S A* **106**, 15651-15656, doi:10.1073/pnas.0904764106 (2009).

301 Becher, I. *et al.* Affinity Profiling of the Cellular Kinome for the Nucleotide Cofactors ATP, ADP, and GTP. *ACS Chemical Biology* **8**, 599-607, doi:10.1021/cb3005879 (2013).

302 Stefaniak, J. & Huber, K. V. M. Importance of Quantifying Drug-Target Engagement in Cells. *ACS Medicinal Chemistry Letters*, doi:10.1021/acsmedchemlett.9b00570 (2020).

303 Golkowski, M. *et al.* Kinome chemoproteomics characterization of pyrrolo[3,4-c]pyrazoles as potent and selective inhibitors of glycogen synthase kinase 3. *Mol Omics* **14**, 26-36, doi:10.1039/c7mo00006e (2018).

304 Cross, D. A. *et al.* AZD9291, an irreversible EGFR TKI, overcomes T790M-mediated resistance to EGFR inhibitors in lung cancer. *Cancer Discov* **4**, 1046-1061, doi:10.1158/2159-8290.Cd-14-0337 (2014).

305 Paquet, T. *et al.* Antimalarial efficacy of MMV390048, an inhibitor of Plasmodium phosphatidylinositol 4-kinase. *Sci Transl Med* **9**, doi:10.1126/scitranslmed.aad9735 (2017).

306 Frejno, M. *et al.* Pharmacoproteomic characterisation of human colon and rectal cancer. *Molecular Systems Biology* **13**, 951, doi:10.15252/msb.20177701 (2017).

307 Bunnage, M. E., Chekler, E. L. P. & Jones, L. H. Target validation using chemical probes. *Nature Chemical Biology* **9**, 195-199, doi:10.1038/nchembio.1197 (2013).

308 Filippakopoulos, P. *et al.* Selective inhibition of BET bromodomains. *Nature* **468**, 1067-1073, doi:10.1038/nature09504 (2010).

309 Cheng, F. In Silico Oncology Drug Repositioning and Polypharmacology. *Methods Mol Biol* **1878**, 243-261, doi:10.1007/978-1-4939-8868-6_15 (2019).

310 Janssen, A. P. A. *et al.* Drug Discovery Maps, a Machine Learning Model That Visualizes and Predicts Kinome-Inhibitor Interaction Landscapes. *J Chem Inf Model* **59**, 1221-1229, doi:10.1021/acs.jcim.8b00640 (2019).

311 Workman, P., Clarke, P. A., Raynaud, F. I. & van Montfort, R. L. M. Drugging the PI3 Kinome: From Chemical Tools to Drugs in the Clinic. *Cancer Research* **70**, 2146-2157, doi:10.1158/0008-5472.Can-09-4355 (2010).

312 Rauch, J., Volinsky, N., Romano, D. & Kolch, W. The secret life of kinases: functions beyond catalysis. *Cell Communication and Signaling* **9**, 23, doi:10.1186/1478-811X-9-23 (2011).

313 Kung, J. E. & Jura, N. Structural Basis for the Non-catalytic Functions of Protein Kinases. *Structure* **24**, 7-24, doi:10.1016/j.str.2015.10.020 (2016).

314 Popow, J. *et al.* Highly Selective PTK2 Proteolysis Targeting Chimeras to Probe Focal Adhesion Kinase Scaffolding Functions. *Journal of Medicinal Chemistry* **62**, 2508-2520, doi:10.1021/acs.jmedchem.8b01826 (2019).

315 Holch, J. W. *et al.* Universal Genomic Testing: The next step in oncological decision-making or a dead end street? *Eur J Cancer* **82**, 72-79, doi:10.1016/j.ejca.2017.05.034 (2017).

316 Vasconcellos, V. F., Colli, L. M., Awada, A. & de Castro Junior, G. Precision oncology: as much expectations as limitations. *Ecancermedicalscience* **12**, ed86-ed86, doi:10.3332/ecancer.2018.ed86 (2018).

317 Bode, A. M. & Dong, Z. Recent advances in precision oncology research. *NPJ Precis Oncol* **2**, 11-11, doi:10.1038/s41698-018-0055-0 (2018).

318 Horak, P. *et al.* Precision oncology based on omics data: The NCT Heidelberg experience. *International Journal of Cancer* **141**, 877-886, doi:10.1002/ijc.30828 (2017).

319 Riedmann, K., Bassermann, F. & Jost, P. J. Kinaseinhibitoren in der Onkologie. *Der Internist* **60**, 540-544, doi:10.1007/s00108-019-0577-8 (2019).

320 Siehl, J. & Thiel, E. C-kit, GIST, and imatinib. *Recent Results Cancer Res* **176**, 145-151, doi:10.1007/978-3-540-46091-6_12 (2007).

321 Babina, I. S. & Turner, N. C. Advances and challenges in targeting FGFR signalling in cancer. *Nat Rev Cancer* **17**, 318-332, doi:10.1038/nrc.2017.8 (2017).

322 Wang, D. *et al.* A deep proteome and transcriptome abundance atlas of 29 healthy human tissues. *Molecular systems biology* **15**, e8503-e8503, doi:10.15252/msb.20188503 (2019).

323 Gholami, A. M. *et al.* Global proteome analysis of the NCI-60 cell line panel. *Cell Rep* **4**, 609-620, doi:10.1016/j.celrep.2013.07.018 (2013).

324 Schmidt, T. *et al.* ProteomicsDB. *Nucleic Acids Res* **46**, D1271-d1281, doi:10.1093/nar/gkx1029 (2018).

Abbreviations

ABPP	Activity-based protein profiling
ACN	Acetonitrile
ADP	Adenosine triphosphate
AGC	Automatic gain control
ATP	Adenosine triphosphate
BRET	Bioluminescence resonance energy transfer
C-lobe	C-terminal lobe
C-spine	Catalytic spine
CATDS	Concentration and target dependent selectivity
CETSA	Cellular thermal shift assay
CK2	Casein kinase 2
DDA	Data dependent acquisition
DMSO	Dimethylsufoxide
DMF	Dimethylformamide
DTT	Dithiothreitol
EC_{50}	Effective concentration for half maximal inhibition
ESI	Electrospray ionization
FA	Formic acid
FBS	Fetal bovine serum
FC	Fold change
FDA	Food and Drug Administration
FDR	False discovery rate
FECH	Ferrochelatase
GSK	GlaxoSmithKline
HCD	Higher energy collision dissociation
IC_{50}	Inhibitory concentration for half maximal inhibition
IMAC	Immobilized metal ion affinity chromatography
ITDR	Isothermal dose response assay
K_d^{app}	Apparent dissociation constant
KB	Kinobeads
KCGS	Kinome chemogenomic set
LC	Liquid chromatography
LFQ	Label-free quantification
MS	Mass spectrometry
MS/MS	Tandem mass spectrometry
MTA	Molecular targeting agent
m/z	Mass-to-charge ratio

N-lobe	N-terminal lobe
NCE	Normalized collision energy
NHS	N-hydroxysuccinimide
PAL	Photoaffinity labeling
PBS	Phosphate buffered saline
PI3K	Phosphoinositide-3-kinase
PIK	Phosphoinositide-3-kinase family
PIKK	PI3K-related kinase family
PKIS	Published kinase inhibitor set
PSM	Peptide spectrum match
PTM	Post translational modification
PROTAC	Proteolysis targeting chimeras
qPCR	Real-time quantitative polymerase chain reaction
R-spine	Regulatory spine
RP	Reverse phase
SDS	Sodium dodecyl sulfate
SGC	Structure genomic consortium
siRNA	Small interfering ribonucleic acid
TBS	Tri Buffered Saline
TFA	Trifluoroacetic acid
TK	Tyrosine kinase group
TKL	Tyrosine kinase like group
TMT	Tandem mass tag
WT	Wild type

Proteins and gene names are based on UniProt and HUGO nomenclature.

Acknowledgements

Endlich geschafft! Nach über vier Jahren, knapp 4.000 Kinobeads pulldowns, vielen Höhen und Tiefen ist es vollbracht. Kaum zu glauben, dass die fertige Arbeit nun wirklich vor mir liegt. Diesen Weg bis hierher bin ich aber nicht alleine gegangen, sondern viele wunderbare Menschen haben mich begleitet und unterstützt. Ohne euch wäre ich niemals an diesem Punkt meines Lebens angekommen.

Zuallererst möchte ich meinem Doktorvater danken. Danke Bernhard, dass Du mir die Möglichkeit gegeben hast, meine Doktorarbeit bei Dir am Lehrstuhl zu schreiben! Du bist der beste Chef, den man sich wünschen kann, fachlich sowie menschlich. Du gibst einem die wissenschaftliche Freiheit und bist immer da, wenn man Deine Hilfe braucht. Du spornst mich nicht nur wissenschaftlich an, dass beste aus mir rauszuholen, sondern auch sportlich...

Ich möchte mich zudem bei den Mitgliedern meines Prüfungskommittes, Prof. Dr. Knapp und Prof. Dr. Jost für die Bereitschaft bedanken meine Arbeit zu begutachten und bei Prof. Dr. Angelika Schnieke, die sich als Prüfungsvorsitzende zur Verfügung gestellt hat. Außerdem bedanke ich mich bei meinen externen Kollaborationspartnern für die konstruktive Zusammenarbeit.

Ein ganz großer Dank geht außerdem an das gesamte „Terrific TUM Team“ (inkl. der Ehemaligen). Ihr seid die aller besten Arbeitskollegen die man sich vorstellen kann. Viele von euch sind im Laufe der Zeit zu richtig guten Freunden geworden, die ich nicht mehr missen möchte. Danke euch allen für die tolle Arbeitsatmosphäre, die wissenschaftliche Hilfe, die tollen Gespräche, die lustigen TGTIFs, die unzähligen Mittagspausen, Grillparties.... Ohne euch wären die letzten vier Jahr nicht annäherend so schön gewesen.

Ein besonderer Dank gilt Steffi und Mathias. Danke euch beiden für die großartige Unterstützung während der letzten vier Jahre! Besondern Du Steffi, mit deiner immer positiven Art hast mir doch oft geholfen und mich aufgemuntert. Ich danke Dir von ganzem Herzen! Außerdem möchte ich mich bei Guillaume bedanken für die wissenschafliche Hilfe in jeglicher Hinsicht, insbesondere bei unserem Kinobeads Paper! Polina, danke auch Dir für deine tollen Gespräche und das Du immer ein offenes Ohr für mich hast. Ein großer Dank geht an die Bond Girls. Julia, Jana und Anna: Ich habe es sehr genossen, mit euch ein Büro zu teilen. Danke für die tollen fachlichen und auch die nicht so fachlichen Gespräche. Ein großer Dank gilt auch Andrea, Micha, Andy und Martina für die großartige Hilfe im Labor sowie Julia für die gefühlt 1000000 Kinobeads Proben die wir gemeinsam auf der HF gemessen haben.

Auch meinen Studenten, Felix, Marvin, Stephan und Doil möchte ich ganz herzlich danken. Ihr habt einen wichtigen Beitrag zu dieser Dissertation geleistet.

Meinen Freunden aus Grevenbrück sowie aus München/Freising möchte ich ein ganz großen Dank aussprechen. Ihr zeigt mir immer wieder, was wirklich wichtig ist und das sich nicht immer alles nur um die Arbeit dreht.

Mama und Papa: Danke euch beiden! Ihr seid immer für mich da, ihr gebt mir halt und habt mich die ganze Zeit über unterstützt. Ihr habt mich immer aufgebaut und euch mit mir gefreut. Mein Dank geht auch an den Rest meiner wunderbaren Familie. Auch ihr zeigt mir immer wieder, was wirklich zählt im Leben. Meinem Opa Hajo möchte ich noch besonders danken, er würde jetzt wahrscheinlich vor Stolz platzen.

Zu allerletzt danke ich Dir Christian. Du musstest in letzter Zeit einiges ertragen. Danke, dass Du mich immer unterstützt, immer für mich da bist und einfach der wunderbarste und wichtigste Mensch für mich bist.

Danke!

List of Publications

Main Publications of this thesis:

- **Reinecke M***, Ruprecht B*, Poser S, Wiechmann S, Wilhelm M, Heinzlmeir S, Kuster B, Médard G, (2017) Chemoproteomic Selectivity Profiling of PIKK and PI3K Kinase Inhibitors. ACS Chem Bio. 14 (4), 655-664. doi:10.1021/acschembio.8b01020

Additional publications during PhD:

- **Reinecke M***, Heinzlmeir S*, Wilhlem M, Médard G, Klaeger S, Kuster B, (2020) Kinobeads: A Chemical Proteomic Approach for Kinase Inhibitor Selectivity Profiling and Target Discovery. In *Target Discovery and Validation, A.T. Plowright (Ed.)*, pp 97-130.

- Bian Y, Zheng R, Bayer FP, Wong C, Chang YC, Meng C, Zolg DP, **Reinecke M**, Zecha J, Wiechmann S, Heinzlmeir S, Scherr J, Hemmer B, Baynham M, Gingras AC, Boychenko O, Kuster B, (2020) Robust, reproducible and quantitative analysis of thousands of proteomes by micro-flow LC-MS/MS. *Nat Commun. 11* (1), 157. doi: 10.1038/s41467-019-13973-x

- Le P, Kunold E, Macsics R, Rox K, Jennings MC, Ugur I, **Reinecke M**, Chaves-Moreno D, Hackl MW, Fetzer C, Mandl FAM, Lehmann J, Korotkov VS, Hacker SM, Kuster B, Antes I, Pieper DH, Rohde M, Wuest WM, Medina E, Sieber SA, (2019) Repurposing human kinase inhibitors to create an antibiotic active against drug-resistant Staphylococcus aureus, persisters and biofilms. Nat Chem. 12(2):145-158. doi: 10.1038/s41557-019-0378-7.

- Samaras P, Schmidt T, Frejno M, Gessulat S, **Reinecke M**, Jarzab A, Zecha J, Mergner J, Giansanti P, Ehrlich HC, Aiche S, Rank J, Kienegger H, Krcmar H, Kuster B, Wilhelm M, (2019) ProteomicsDB: a multi-omics and multi-organism resource for life science research. Nucleic Acids Res. 48(D1):D1153-D1163. doi: 10.1093/nar/gkz974.

- Seefried F, Schmidt T, **Reinecke M**, Heinzlmeir S, Kuster B, Wilhelm M (2019) CiRCus: A Framework to Enable Classification of Complex High-Throughput Experiments. J Proteome Res. 18(4):1486-1493. doi: 10.1021/acs.jproteome.8b00724.

- Mulder C, Prust N, van Doorn S, **Reinecke M**, Kuster B, van Bergen En Henegouwen P, Lemeer S (2018) Adaptive Resistance to EGFR-Targeted Therapy by Calcium Signaling in NSCLC Cells. Mol Cancer Res. 16(11):1773-1784. doi: 10.1158/1541-7786.MCR-18-0212.

- Klaeger S*, Heinzlmeir S*, Wilhelm M*, Polzer H, Vick B, König PA, **Reinecke M**, Ruprecht B, Petzoldt S, Meng C, Zecha J, Reiter K, Qiao H, Helm D, Koch H, Schoof M, Canevari G, Casale E, Re Depaolini S, Feuchtinger A, Wu Z, Schmidt T, Rueckert L, Becker W, Huenges J, Garz A, Gohlke B, Zolg DP, Kayser G, Vooder T, Preissner R, Hahne H, Tonisson N, Kramer K, Götze K, Bassermann F, Schlegl J, Ehrlich H, Aiche S, Walch A, Greif P, Schneider S, Felder ER, Ruland J, Médard G, Jeremias I, Spiekermann K, Kuster B, (2017) The target landscape of clinical kinase drugs. Science. 358(6367). pii: eaan4368

* Authors contributed equally to this work

Appendix

Table of contents

1 Supplementary Figures

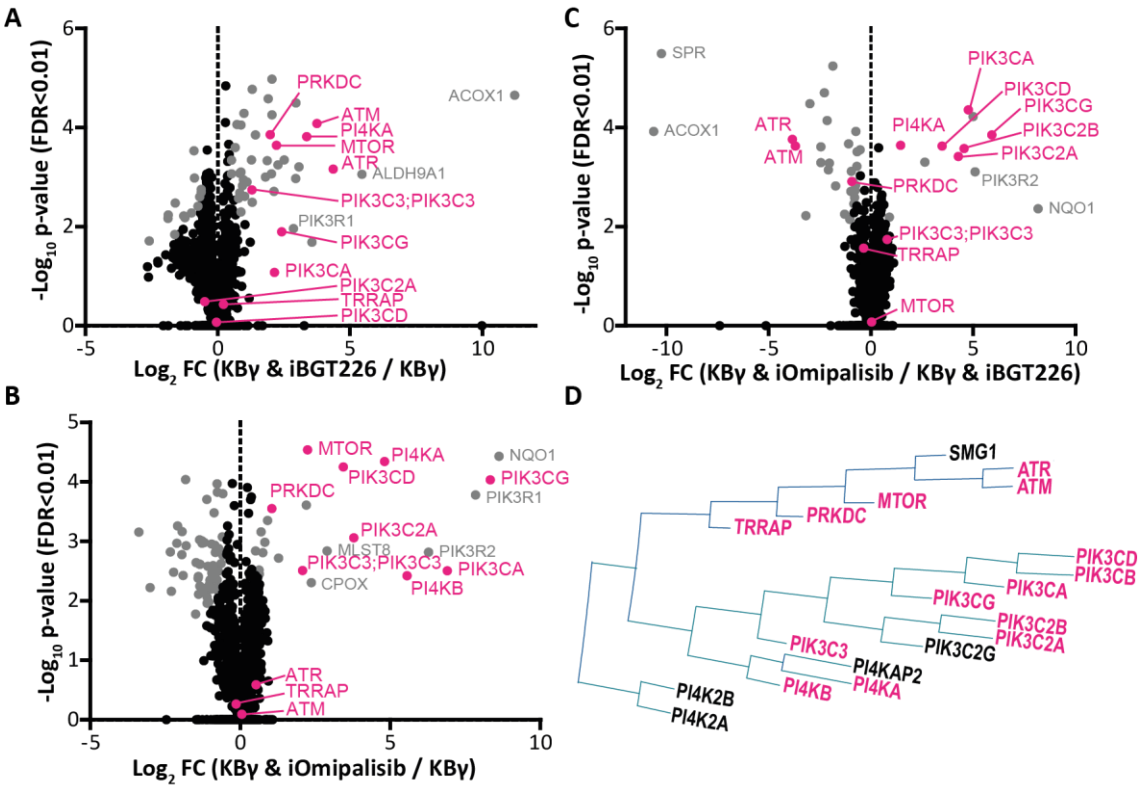

Figure S 1 | Systematic evaluation of new PIKK and PI3K affinity probes. (A-C) Nature and intensity of proteins captured by different bead mixtures (KBγ & iBGT226, KBγ & iOmipalisib or KBγ) were determined by triplicate pulldown experiments using a five cell line mixture and tested for significant differences in a two-sided t-test (S0=0.1, 1 % FDR). ATR and ATM were specifically enriched by iBGT226 whereas most of the PI3K family members were significantly enriched by iOmipalisib. PIKKs and PI3Ks are labeled in pink. Proteins exhibiting significant differences are colored in grey. D) Part of the kinome tree showing the PIK and PIKK families. Kinases that have been enriched and competed using Kinobeads ε are marked in pink.

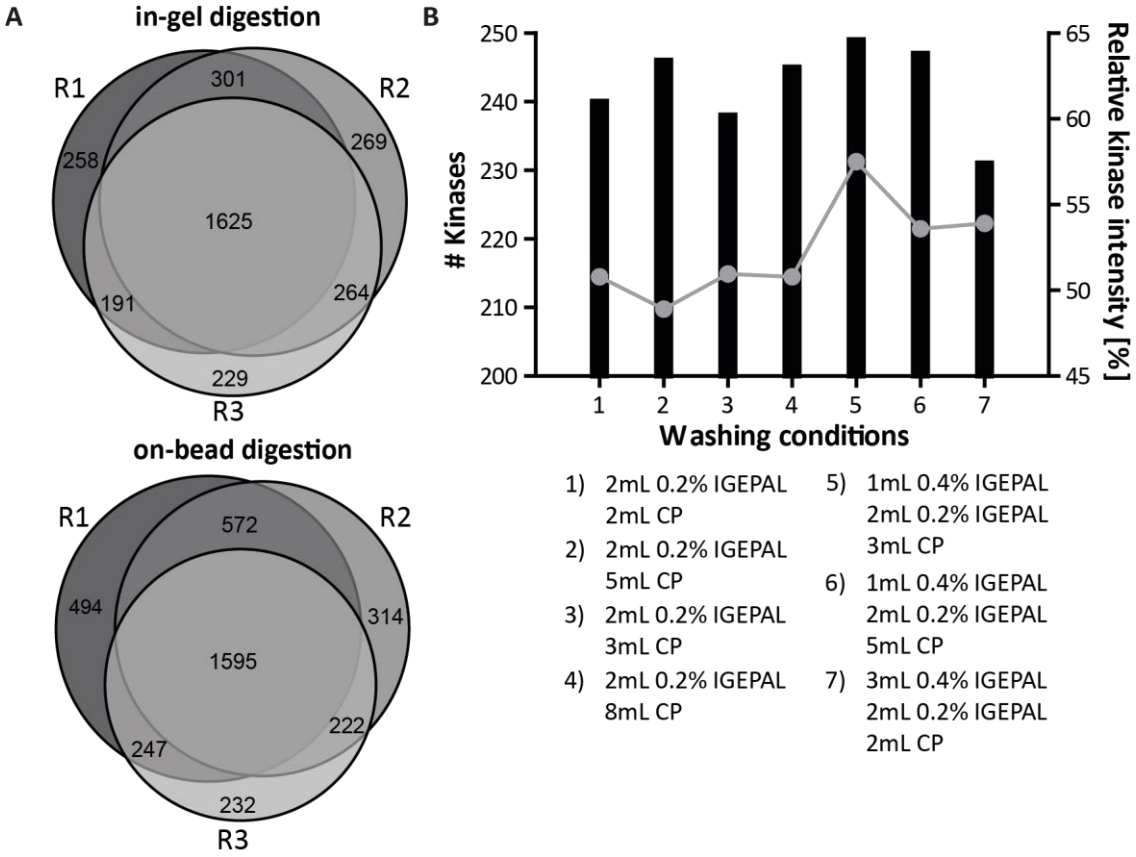

Figure S2 | Comparison of digestion protocols. (A) Number kinase peptides of triplicate Kinobeads pulldown experiments. Proteins were either digested in-gel or on-bead. The overlap was triplicates pulldowns is slightly higher for the in-gel digestion workflow. (B) Number of identified kinases relative intensity of kinases using different washing conditions after Kinobeads incubation. Washing condition 5 (1 ml 0.4 % IGPAL, 2 ml 0.2 % IGPAL, 3 ml CP buffer) leads to the highest number of identified kinases.

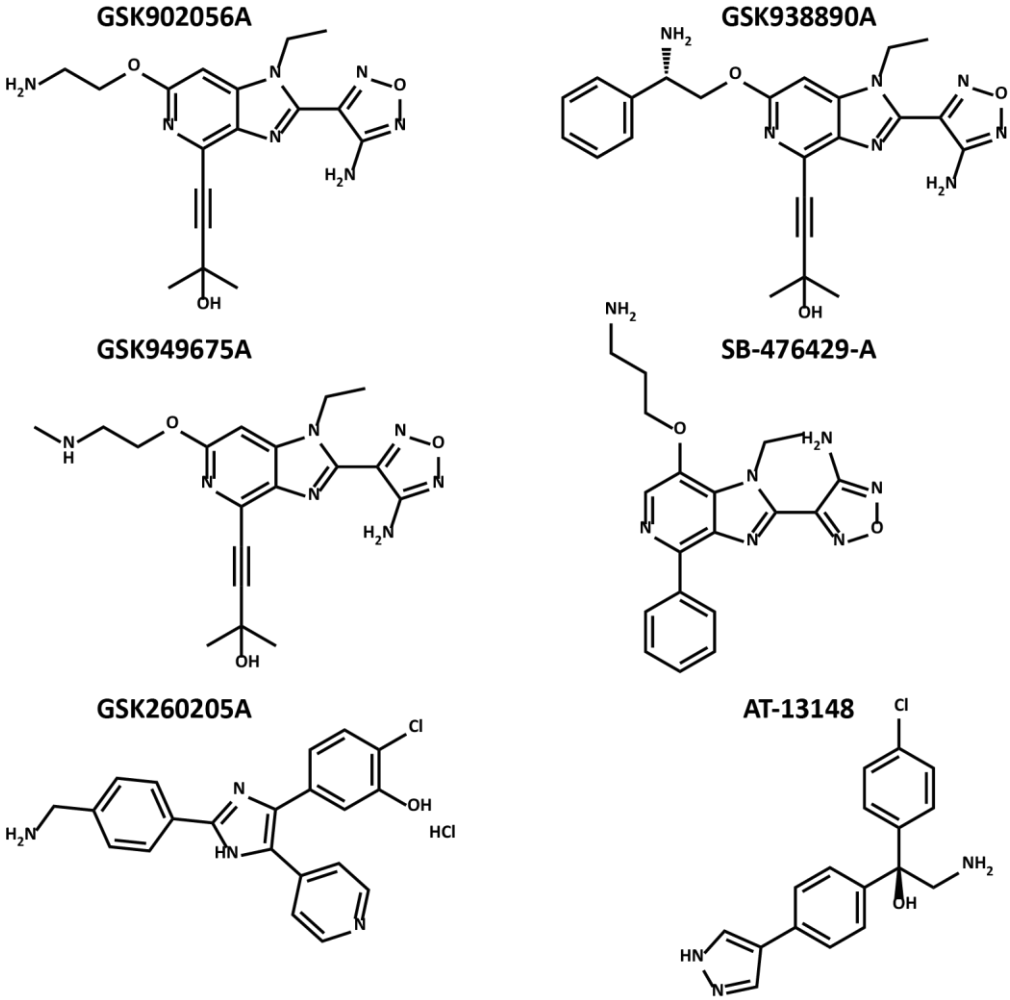

Figure S 3 | Chemical structure of tool compounds targeting PKN3.

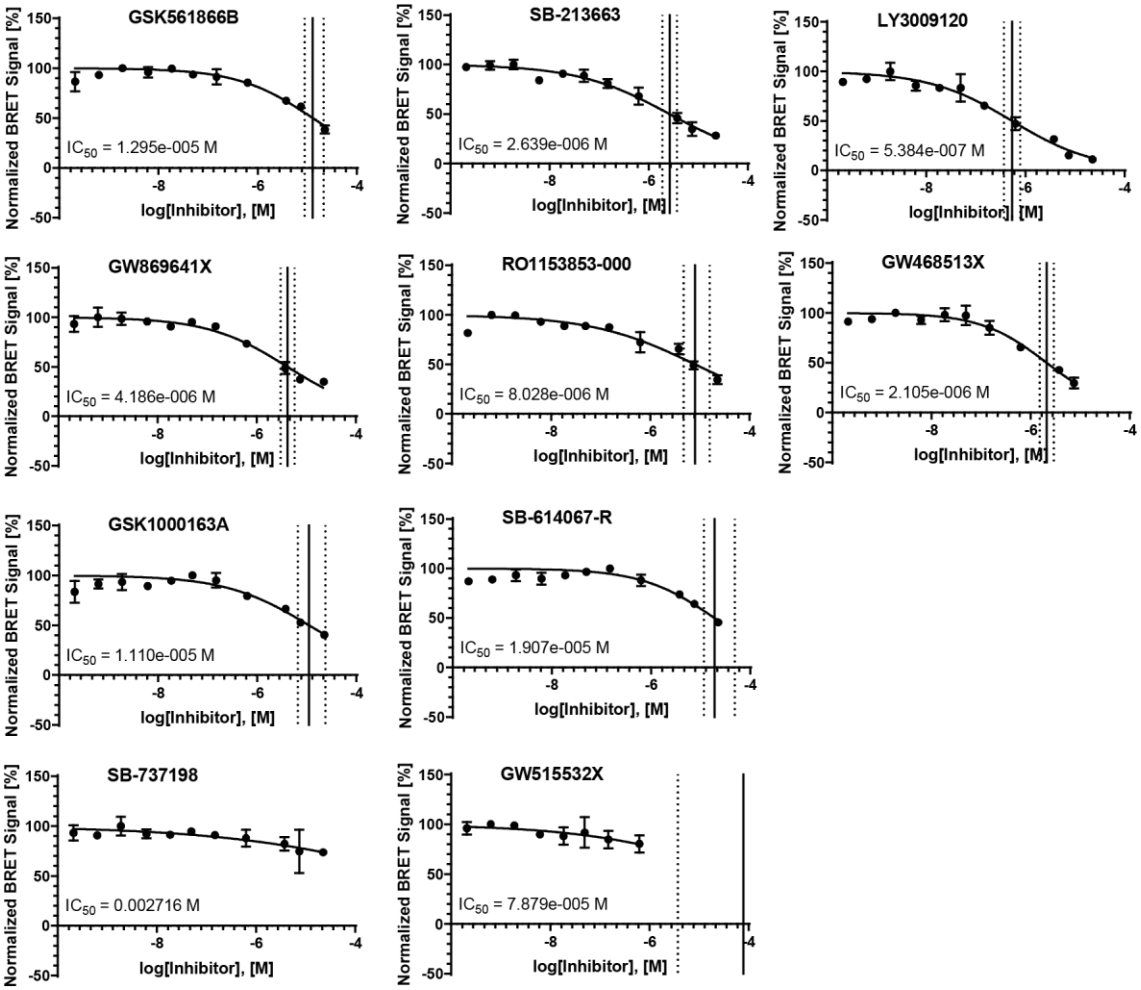

Figure S 4 | PKN3 target engagement in cells. Dose dependent reduction of the BRET signal with increasing inhibitor concentrations were observed for eight compounds indicating PKN3 target engagement in cells. Experiments were performed by Benedict-Tillmann Berger under supervision of Dr. Susanne Mueller-Knapp at the Goethe University in Frankfurt.

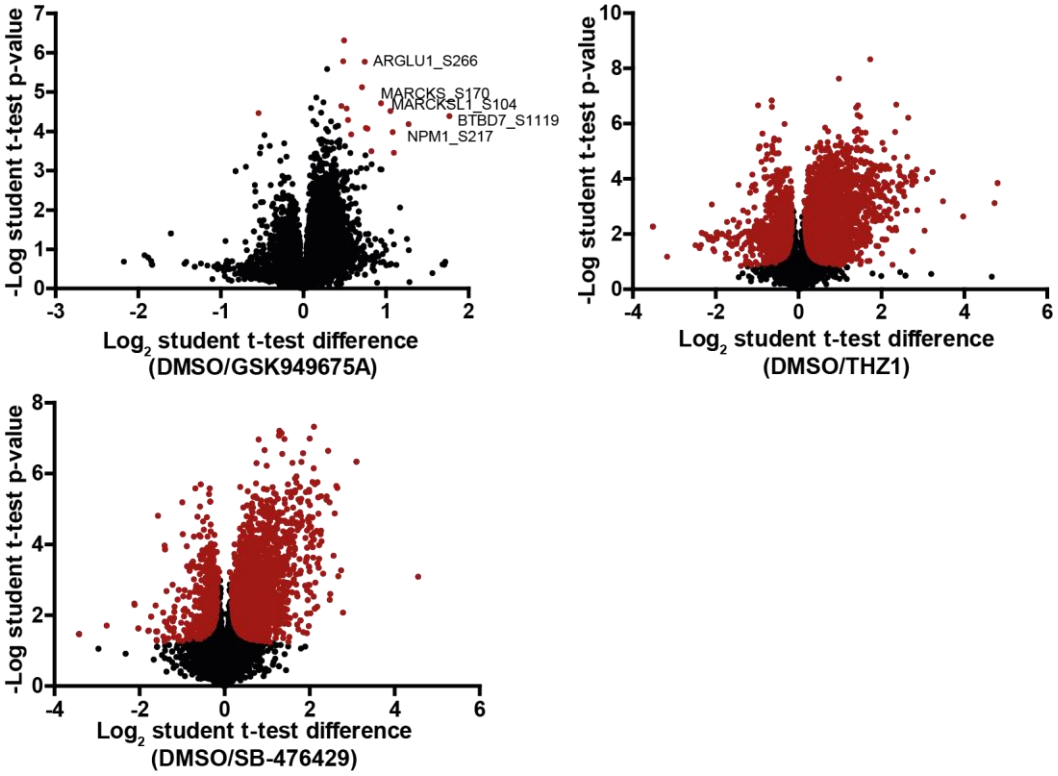

Figure S 5 | PKN3 inhibitor perturbed phosphoproteome. Volcano plots showing log2 fold changes of quantified phosphorylation sites after treating RKO cells with 1 µM GSK949675A, 1 µM THZ1, 1 µM SB-476429 or DMSO as control for 30 min. Phosphorylation sites exhibiting significant changes are colored in red (FDR of 1 %, S0 of 0.036, 0.04, 0.037, 0.068 and 0.049 for GSK949675A, GSK902056A, SB-476429-A, THZ1 and siRNA).

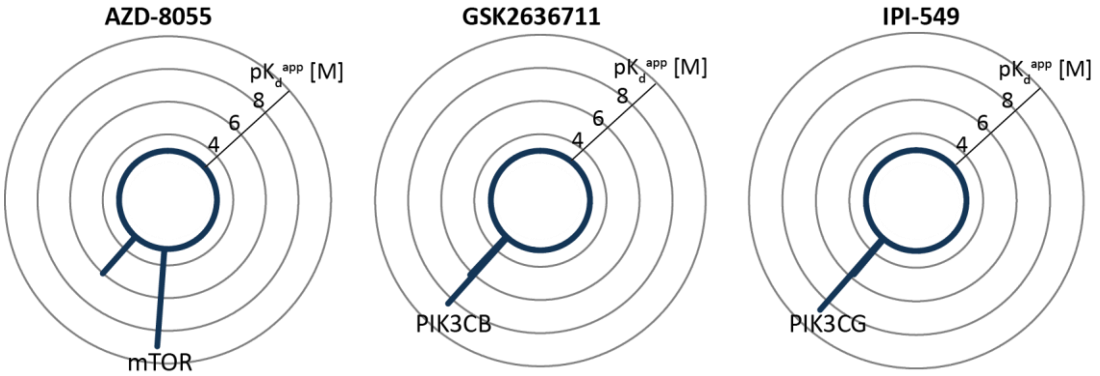

Figure S 6 | Target space of selective mTOR and PI3K inhibitors. Radarplots depicting the targets of the selective mTOR inhibitor AZD-8055, the selective PIK3CB inhibitor GSK2636711 and the selective PIK3CG inhibitor IPI-549. Each spike represents one target and the length of the spike depicts the affinity of the interaction.

2 Supplementary Tables

Table S1 | List of analyzed kinase Inhibitors in Results and Discussion Chapter 2

Compound	Library	SMILES
Abemaciclib	Clinical KIs	CCN1CCN(Cc2ccc(Nc3ncc(F)c(n3)c4cc(F)c5nc(C)n(C(C)C)c5c4)nc2)CC1
Afatinib	Clinical KIs	CN(C)C\C=C\C(=O)Nc1cc2c(Nc3ccc(F)c(Cl)c3)ncnc2cc1O[C@H]4CCOC4
AH20685XX	PKIS2	C1(N=CC=NN12)=NC=C2C3=CC=CC=C3
AH2635	PKIS2	NC1=NC=NC2=C1N=CN2C3=CC=C(Cl)C=C3
AH5015_KCGS	KCGS	Nc1ncnc2[nH]c(nc12)-c1ccccc1
Alectinib	Clinical KIs	CCc1cc2C(=O)c3c([nH]c4cc(ccc34)C#N)C(C)(C)c2cc1N5CCC(CC5)N6CCOCC6
Apatinib	Clinical KIs	O=C(Nc1ccc(cc1)C2(CCCC2)C#N)c3cccnc3NCc4ccncc4
AT-13148	Clinical KIs	NC[C@@](O)(c1ccc(Cl)cc1)c2ccc(cc2)c3cn[nH]c3
AT-9283	Clinical KIs	O=C(NC1CC1)Nc2c[nH]nc2c3nc4cc(CN5CCOCC5)ccc4[nH]3
Axitinib	Clinical KIs	CNC(=O)c1ccccc1Sc2ccc3c(\C=C\c4ccccn4)n[nH]c3c2
Baricitinib	Clinical KIs	CCS(=O)(=O)N1CC(CC#N)(C1)n2cc(cn2)c3ncnc4[nH]ccc34
BI00007366	KCGS	N1(CCC(CC1)Oc3c(cc2ncnc(c2c3)Nc4cc(ccc4)C#C)OC)C
BI00009348	KCGS	S(=O)(=O)(CCN1CCOCC1)c2cc(ccc2)Nc3nc4c(cn3)N(C(=O)CN4C(C)C)C
BI00036838	KCGS	N2c1c(cc(cc1)C(=O)C)C(=C(NN(C)C)CC)C2=O
BI00047804	KCGS	Clc1c(cccc1)-c2nc-3c(cn2)CCc4nc(sc4-3)NC(=O)N5C[C@@H](CC5)NC(=O)C(C)C
BI00113608	KCGS	Fc1c(cccc1Nc2ncnc3c2cc(c(c3)OC)O[C@@H]5CC[C@@]4(NCCNC4=O)CC5)Cl
BI00133844	KCGS	Fc1c(cccc1Nc2ncnc3c2cc(c(c3)OC)O[C@@H]4CC[C@H](CC4)[C@@H]5NCCNC5=O)Cl
BI00601000	KCGS	Fc1c(ccc(c1)F)Nc2cc3c(cc2)N(C(=O)N3)CC4CCCCC4
BI00604564	KCGS	s2c1nc(cc(c1c3ncnc(c32)N)CCC)N4CCN(CCC4)C
BI00614644	KCGS	O=C(C1=CC2=C(C=C1)C=C3N2CC(CN)CNC3=O)NC4=CC=CN=C4
BI00645435	KCGS	O=C(C1=CC2=C(C=C1)C=C3N2[C@H](C)CCNC3=O)NC4=NC5=CC=CC=C5N4CCCN(C)C
BI00801818	KCGS	Brc1c(ccc(c1)C(=O)NCCC)Nc2nc(c(cn2)C(F)(F)F)Nc3c(cccc3)C(=O)C
BI00865461	KCGS	Fc1c(c(ccc1NS(=O)(=O)CCC)F)-n2nnc(c2)-c3cncc(c3)OC
BI01125081	KCGS	N1(CCOCC1)c2ncc(cc2)-c4cc3ncccc3c(c4)OCc5ncccc5C(=O)N
BI2536	KCGS	O=C1[C@H](N(C2=C(N1C)C=NC(NC3=CC=C(C(NC4CCN(C)CC4)=O)C=C3OC)=N2)C5CCCC5)CC
BIBF0846CL	KCGS	N4c1c(cc(c(c1)OC)OC)C(=C(Nc2ccccc2)c3cc(ccc3)CN)C4=O
BIBW3133BS	KCGS	Fc1c(cc(cc1)Nc2ncnc3c2cc(c(c3)OC)O[C@@H]4CC[C@H](CC4)N)Cl
Binimetinib	Clinical KIs	Cn1cnc2c(F)c(Nc3ccc(Br)cc3F)c(cc12)C(=O)NOCCO
BIRB0876BS	KCGS	n1(nc(cc1NC(=O)Nc2ccc(cc2)OCCN3CCOCC3)C(C)(C)C)-c4ccc(cc4)C
BIRZ0518XX	KCGS	FC(F)(F)OC1=CC=CC=C1CNC2=NC=C([N+]([O-])=O)C(NCC3CCC(CN)CC3)=N2
BMX-IN-1	KCGS	CS(NC1=CC=C(C2=CC=C(N=CC(C=C3)=C4N(C5=CC(NC(C=C)=O)=C(C)C=C5)C3=O)C4=C2)C=C1)(=O)=O
Bosutinib	Clinical KIs	COc1cc(Nc2c(cnc3cc(OCCCN4CCN(C)CC4)c(OC)cc23)C#N)c(Cl)cc1Cl
Brigatinib	Clinical KIs	CN1CCN(CC1)C2CCN(CC2)C3=CC(=C(C=C3)NC4=NC=C(C(=N4)NC5=CC=CC=C5P(=O)(C)C)Cl)OC
CA93.0	KCGS	COC1=C(OC)C(OC)=CC(NC2=C3C(C=CC(Br)=C3)=NC=C2)=C1
Cabozantinib	Clinical KIs	COc1cc2nccc(Oc3ccc(NC(=O)C4(CC4)C(=O)Nc5ccc(F)cc5)cc3)c2cc1OC

Compound	Library	SMILES
CCT241533	KCGS	FC1=CC(C3=NC2=CC(OC)=C(OC)C=C2C(N[C@H]4[C@H]([C@](C)(O)C)CNC4)=N3)=C(O)C=C1.Cl.Cl
CCT244747	KCGS	C[C@](OC1=NC(NC(C=C2OC)=NC=C2C(C=N3)=CN3C)=CN=C1C#N)([H])CN(C)C
CCT251545	KCGS	O=C(NCC1)C1(CC2)CCN2C3=C(C4=CC=C(C5=CN(C)N=C5)C=C4)C=NC=C3Cl
CCT251921	KCGS	O=C1NCCC12CCN(C3=C(Cl)C(N)=NC=C3C4=CC5=C(N(C)N=C5)C=C4)CC2
Ceritinib	Clinical KIs	CC(C)Oc1cc(C2CCNCC2)c(C)cc1Nc3ncc(Cl)c(Nc4ccccc4S(=O)(=O)C(C)C)n3
Cobimetinib	Clinical KIs	OC1(CN(C1)C(=O)c2ccc(F)c(F)c2Nc3ccc(I)cc3F)[C@@H]4CCCCN4
Copanlisib	Clinical KIs	COc1c(OCCCN2CCOCC2)ccc3C4=NCCN4C(=Nc13)NC(=O)c5cnc(N)nc5
Crizotinib	Clinical KIs	C[C@@H](Oc1cc(cnc1N)c2cnn(c2)C3CCNCC3)c4c(Cl)ccc(F)c4Cl
D2202-1	KCGS	Cc1cn(cn1)c1cc(cc(c1)NC(c1ccc2c(CN(C[C@@H]2C)c2cncnc2)c1)=O)C(F)(F)F
Dabrafenib	Clinical KIs	CC(C)(C)c1nc(c2cccc(NS(=O)(=O)c3c(F)cccc3F)c2F)c(s1)c4ccnc(N)n4
Danusertib	Clinical KIs	CO[C@@H](C(=O)N1Cc2n[nH]c(NC(=O)c3ccc(cc3)N4CCN(C)CC4)c2C1)c5ccccc5
Dasatinib	Clinical KIs	Cc1nc(Nc2ncc(s2)C(=O)Nc3c(C)cccc3Cl)cc(n1)N4CCN(CCO)CC4
DDR1-in-1	KCGS	CC1=C(OC4=CC(CC(N5)=O)=C5C=C4)C=C(NC(C2=CC=C(CN3CCN(CC)CC3)C(C(F)(F)F)=C2)=O)C=C1.Cl.Cl
Enzastaurin	Clinical KIs	Cn1cc(C2=C(C(=O)NC2=O)c3cn(C4CCN(Cc5ccccn5)CC4)c6ccccc36)c7ccccc17
ERK5-IN-1	KCGS	O=C1C2=CC=CC=C2N(C3CCCC3)C4=NC(NC5=CC=C(C(N6CCC(N7CCN(C)CC7)CC6)=O)C=C5OCC)=NC=C4N1C
Fasudil	Clinical KIs	O=S(=O)(N1CCCNCC1)c2cccc3cnccc23
FM-381	KCGS	N(C)(C)C(C(\C#N)=C\C(=CC=C1C2N(C(C(N=2)=C2)=C(C(=N2)N2)C=C2)C(C2)CCCC2)O1)=O
Fostamatinib	Clinical KIs	COc1cc(Nc2ncc(F)c(Nc3ccc4OC(C)(C)C(=O)N(COP(=O)(O)O)c4n3)n2)cc(OC)c1OC
Gefitinib	Clinical KIs	COc1cc2ncnc(Nc3ccc(F)c(Cl)c3)c2cc1OCCCN4CCOCC4
GI230329A	PKIS2	COC1=CC2=NC=NC(NC3=CC=CC(Br)=C3)=C2C=C1OC.Cl
GI261520A	PKIS1	Cl.COc1ccc2ncnc(Nc3ccc(OCc4ccccc4)cc3)c2c1
GI261590A	PKIS2	COC1=CC2=C(C=C1OC)C(NC3=CC=C(C(Cl)=C3)OCC4=CC=CC=C4Br)=NC=N2.Cl
GI261656A	PKIS2	COC1=C(OC)C=C2C(N=CC=C2NC3=CC=C(OC4=CC=CC=C4)C=C3)=C1.Cl
GI262866A	PKIS2	OC1=CC2=C(N=CN=C2NC3=CC=C(C=C3)OCC4=CC=CC=C4)C=C1.Cl
GNF-5	KCGS	C1=CC(=CC(=C1)C(=O)NCCO)C2=CC(=NC=N2)NC3=CC=C(C=C3)OC(F)(F)F
GR105659X	PKIS1	Oc1ccc2c(CC\C2=C2\C(=O)Nc3ccccc23)c1
GR269666A	PKIS1	Cl.C(c1nc2ccc(Nc3ncnc4ccccc34)cc2[nH]1)c1ccccc1
GSK1000163A	PKIS1	CCn1c(nc2c(nc(CN3CCCC3)cc12)C#CC(C)(C)O)-c1nonc1N
GSK1007102B	PKIS1	OC(=O)C(F)(F)F.CCn1c(nc2c(nc(O[C@@H](CN)c3ccccc3)cc12)C#CC(C)(C)O)-c1nonc1N
GSK1010829B	PKIS2	O=C(C1=C(F)C=CC=C1F)NC2=CC=CC(C(N=C3N4C=CC=C3)=C4C5=CC=NC(NC6=CC=C(CCN(C)C7)C7=C6)=N5)=C2.Cl
GSK1014915A	PKIS2	O=C(NC(C=C1)=CC=C1C)NC2=CC(C(C)(C)C)=NN2C3=CC=CC=C3
GSK1023156A	PKIS1	NC(=O)c1sc(cc1OCc1ccccc1Br)-n1cnc2ccccc12
GSK1024304A	PKIS2	NC(C(S1)=C(C=C1N2C=NC3=C2C=CC=C3)OCC4=CC=C(OC)C=C4)=O
GSK1024306A	PKIS2	NC(C(S1)=C(C=C1N2C=NC3=C2C=CC=C3)OCC4=CC=CC=C4F)=O
GSK1030058A	PKIS1	COC(=O)c1sc(cc1OCc1ccccc1C(F)(F)F)-n1cnc2cc(OC)c(OC)cc12
GSK1030059A	PKIS1	COc1cc2ncn(-c3cc(OCc4ccccc4C(F)(F)F)c(s3)C(C)=O)c2cc1OC
GSK1030061A	PKIS1	CNC(=O)c1sc(cc1OCc1ccccc1C(F)(F)F)-n1cnc2cc(OC)c(OC)cc12
GSK1030062A	PKIS1	COc1cc2ncn(-c3cc(OCc4ccccc4C(F)(F)F)c(s3)C(=O)N(C)C)c2cc1OC
GSK1033723A	PKIS2	O=C1NC=C(C2=CC=C(O)C=C2)C3=C1C=C(C4=CC=NC=C4)S3

Compound	Library	SMILES
GSK1034945A	PKIS2	NC1=NNC2=CC(C3=NC(N)=NC=C3)=CC=C21
GSK1070916	KCGS	CCN1C=C(C(=N1)C2=CC=C(C=C2)NC(=O)N(C)C)C3=C4C=C(NC4=NC=C3)C5=CC(=CC=C5)CN(C)C
GSK1122999D	PKIS2	C1(C2=CC=CC=C2)=C(OC3CCNCC3)C=C(C=NC=C4)C4=C1.C5(C6=CC=CC=C6)=C(OC7CCNCC7)C=C(C=NC=C8)C8=C5.Cl.Cl
GSK114	KCGS	COC1=CC2=NC=NC(N(C3=C(N(C)C)C=CC(S(=O)(N(C)[H])=O)=C3)[H])=C2C=C1OC
GSK1173862A	PKIS1	CCCN1CCCC(C1)c1ccc(Nc2nc(Nc3cc(F)ccc3C(N)=O)c3cc[nH]c3n2)c(OC)c1
GSK1220512A	PKIS1	COc1cc(ccc1Nc1nc(Nc2ccc(F)cc2C(N)=O)c2cc[nH]c2n1)N1CCN(CC1)C(C)C
GSK1229496A	PKIS2	O=C(NC1=CC=C(C=C1)C2=NC(NC(C=C3)=CC=C3OC)=NC=C2)C4=CC5=CC(F)=CC=C5N4
GSK1229782A	PKIS2	O=C(NC1=CC=CC(C2=NC(NC(C=C3)=CC=C3OC)=NC=C2)=C1)C4=CC5=CC(F)=CC=C5N4
GSK1229959A	PKIS2	O=C(NC(CN)C1=CC=CC=C1)C2=CC(C3=C4C=CNC4=NC=C3)=CS2.O=C(NC(CN)C5=CC=CC=C5)C6=CC(C7=C8C=CNC8=NC=C7)=CS6.Cl.Cl
GSK1269851A	PKIS2	O=C(NC(S1)=CC(Br)=C1C2=C(C=CN3)C3=NC=C2)C(CN)C4=CC=CC=C4.O=C(NC(S5)=CC(Br)=C5C6=C(C=CN7)C7=NC=C6)C(CN)C8=CC=CC=C8.Cl.Cl
GSK1287544A	PKIS2	O=C(NC(C1=CC=CC=C1)CCCN)C(S2)=CC(Br)=C2C3=C(C=CN4)C4=NC=C3.OC(C(F)(F)F)=O.O=C(NC(C5=CC=CC=C5)CCCN)C(S6)=CC(Br)=C6C7=C(C=CN8)C8=NC=C7.OC(C(F)(F)F)=O
GSK1292139B	PKIS2	NCCNC1=NC=C(C(N)=O)C(NC2=CC(C)=CC=C2)=N1
GSK1307810A	PKIS2	NCCC(NC(C1=CC(Br)=C(C2=C(C=CN3)C3=NC=C2)S1)=O)C4=CC=CC=C4.OC(C(F)(F)F)=O.NCCC(NC(C5=CC(Br)=C(C6=C(C=CN7)C7=NC=C6)S5)=O)C8=CC=CC=C8.OC(C(F)(F)F)=O
GSK1321565A	PKIS2	NCC(C1=CC=CC=C1)NCC2=CC=C(C3=C4C=CNC4=NC=C3)S2.NCC(C5=CC=CC=C5)NCC6=CC=C(C7=C8C=CNC8=NC=C7)S6.Cl.Cl
GSK1322949A	PKIS2	O=C(NCC(C1=CC=CC=C1)N)C2=CC(Br)=C(C3=C4C=CNC4=NC=C3)S2.O=C(NCC(C5=CC=CC=C5)N)C6=CC(Br)=C(C7=C8C=CNC8=NC=C7)S6.Cl.Cl
GSK1323434A	PKIS2	NCC(C1=CC=CC=C1)NC(C2=CC(C3=CN=CC=C3)=C(C4=CC=NC5=C4C=CN5)S2)=O.NCC(C6=CC=CC=C6)NC(C7=CC(C8=CN=CC=C8)=C(C9=CC=NC%10=C9C=CN%10)S7)=O.Cl.Cl
GSK1325775A	PKIS2	NCC(C1=CC=CC=C1)NC(C(S2)=CC(C3=CNN=C3)=C2C4=CC=NC5=C4C=CN5)=O.OC(C(F)(F)F)=O.NCC(C6=CC=CC=C6)NC(C(S7)=CC(C8=CNN=C8)=C7C9=CC=NC%10=C9C=CN%10)=O.OC(C(F)(F)F)=O
GSK1326180A	PKIS2	O=C(C1=C(F)C=CC=C1)C2=CNC(C(NC3=C(F)C=CC=C3F)=O)=C2
GSK1326255A	PKIS1	CCCN1CCC(CC1)c1ccc(Nc2nc(Nc3cc(F)ccc3C(N)=O)c3cc[nH]c3n2)c(OC)c1
GSK1379706A	PKIS2	O=C(NCC1=CC=C(OC)C=C1)NC2CN(CC2)C3=NC(NC(C=C4)=CC=C4F)=NC=C3
GSK1379708A	PKIS2	O=C(C1=CC(C#N)=CC=C1)NC2CN(CC2)C3=NC(NC4=CC=C(F)C=C4)=NC=C3
GSK1379710A	PKIS2	O=C(NC1=CC=CC(C(C)=O)=C1)NC2CN(CC2)C3=NC(NC(C=C4)=CC=C4F)=NC=C3
GSK1379712	KCGS	COC(=O)C(NC(=O)NC1CCN(C1)c1ccnc(Nc2ccc(F)cc2)n1)c1ccccc1
GSK1379713A	PKIS2	O=C(C(C)C1=CC=C(Cl)C=C1)NC2CN(CC2)C3=NC(NC(C=C4)=CC=C4F)=NC=C3
GSK1379714A	PKIS2	O=C(NC(CC1=CC=CC=C1)C(OC)=O)NC2CN(CC2)C3=NC(NC4=CC=C(F)C=C4)=NC=C3
GSK1379715A	PKIS2	O=S(NC1CN(CC1)C2=NC(NC3=CC=C(F)C=C3)=NC=C2)(C(C=C4)=CC=C4CCC)=O
GSK1379716A	PKIS2	O=C(NC1CN(CC1)C2=NC(NC3=CC=C(F)C=C3)=NC=C2)C4=CC5=CC=CC=C5S4
GSK1379717A	PKIS2	O=C(NC1CN(CC1)C2=NC(NC3=CC=C(F)C=C3)=NC=C2)C4=CN=CN4C
GSK1379720A	PKIS2	O=C(NC1=C(C)C=CC(C)=C1)NC2CN(CC2)C3=NC(NC4=CC=C(F)C=C4)=NC=C3
GSK1379721A	PKIS2	O=C(NC1=CC(OC)=CC=C1)NC2CN(CC2)C3=NC(NC(C=C4)=CC=C4F)=NC=C3
GSK1379722A	PKIS2	O=C(NC1=CC=CC=C1F)NC2CN(CC2)C3=NC(NC(C=C4)=CC=C4F)=NC=C3
GSK1379723A	PKIS2	O=C(NCC1=CC=CC(OC)=C1)NC2CN(CC2)C3=NC(NC4=CC=C(F)C=C4)=NC=C3

Compound	Library	SMILES
GSK1379724A	PKIS2	O=C(NC1=CC=C2OCOC2=C1)NC3CN(CC3)C4=NC(NC(C=C5)=CC=C5F)=NC=C4
GSK1379725A	PKIS2	O=C(NC1=CC=CC(C(OC)=O)=C1)NC2CN(CC2)C3=NC(NC4=CC=C(F)C=C4)=NC=C3
GSK1379727A	PKIS2	O=C(NCC1=CC=C(OC)C=C1)NC2CN(CC2)C3=NC(NC4=CC=C(OC)C=C4)=NC=C3
GSK1379729A	PKIS2	O=S(NC1CN(CC1)C2=NC(NC3=CC=C(OC)C=C3)=NC=C2)(C(C=C4)=CC=C4NC(C)=O)=O
GSK1379730A	PKIS2	O=C(C1=CC(C#N)=CC=C1)NC2CN(CC2)C3=NC(NC(C=C4)=CC=C4OC)=NC=C3
GSK1379731A	PKIS2	O=C(NC1=CC=CC(C(C)=O)=C1)NC2CN(CC2)C3=NC(NC4=CC=C(OC)C=C4)=NC=C3
GSK1379732A	PKIS2	O=C(C1=CC(NC(C)=O)=CC=C1)NC2CN(CC2)C3=NC(NC4=CC=C(OC)C=C4)=NC=C3
GSK1379735A	PKIS2	O=C(C(C)C1=CC=C(Cl)C=C1)NC2CN(CC2)C3=NC(NC4=CC=C(OC)C=C4)=NC=C3
GSK1379737A	PKIS2	O=S(NC1CN(CC1)C2=NC(NC(C=C3)=CC=C3OC)=NC=C2)(C(C=C4)=CC=C4CCC)=O
GSK1379738A	PKIS2	O=C(NC1CN(CC1)C2=NC(NC(C=C3)=CC=C3OC)=NC=C2)C4=CC5=CC=CC=C5S4
GSK1379741A	PKIS2	O=C(NC1=C(C)C=CC(C)=C1)NC2CN(CC2)C3=NC(NC(C=C4)=CC=C4OC)=NC=C3
GSK1379742A	PKIS2	O=C(NC1=CC(OC)=CC=C1)NC2CN(CC2)C3=NC(NC4=CC=C(OC)C=C4)=NC=C3
GSK1379745A	PKIS2	O=C(NC1=CC=C2OCOC2=C1)NC3CN(CC3)C4=NC(NC5=CC=C(OC)C=C5)=NC=C4
GSK1379746A	PKIS2	O=C(NC1=CC=CC(C(OC)=O)=C1)NC2CN(CC2)C3=NC(NC(C=C4)=CC=C4OC)=NC=C3
GSK1379748A	PKIS2	O=C(NCC1=CC=C(OC)C=C1)NC2CN(CC2)C3=NC(NC4=CC(OC)=C(OC)C(OC)=C4)=NC=C3
GSK1379751A	PKIS2	O=C(C1=CC(C#N)=CC=C1)NC2CN(CC2)C3=NC(NC4=CC(OC)=C(C(OC)=C4)OC)=NC=C3
GSK1379753A	PKIS2	O=C(NC1=CC=CC(C(C)=O)=C1)NC2CN(CC2)C3=NC(NC4=CC(OC)=C(OC)C(OC)=C4)=NC=C3
GSK1379754A	PKIS2	O=C(C1=CC(NC(C)=O)=CC=C1)NC2CN(CC2)C3=NC(NC4=CC(OC)=C(OC)C(OC)=C4)=NC=C3
GSK1379757A	PKIS2	O=C(C(C)C1=CC=C(Cl)C=C1)NC2CN(CC2)C3=NC(NC4=CC(OC)=C(OC)C(OC)=C4)=NC=C3
GSK1379760A	PKIS2	O=C(NC1CN(CC1)C2=NC(NC3=CC(OC)=C(C(OC)=C3)OC)=NC=C2)C4=CC5=CC=CC=C5S4
GSK1379761A	PKIS2	O=C(NC1CN(CC1)C2=NC(NC3=CC(OC)=C(OC)C(OC)=C3)=NC=C2)C4OC5=CC=CC=C5OC4
GSK1379762	KCGS	COc1cc(Nc2nccc(n2)N2CCC(C2)NC(=O)Nc2cc(C)ccc2C)cc(OC)c1OC
GSK1379763A	PKIS2	O=C(NC1=CC(OC)=CC=C1)NC2CN(CC2)C3=NC(NC4=CC(OC)=C(OC)C(OC)=C4)=NC=C3
GSK1379766A	PKIS2	O=C(NC1=CC=C2OCOC2=C1)NC3CN(CC3)C4=NC(NC5=CC(OC)=C(C(OC)=C5)OC)=NC=C4
GSK1379767A	PKIS2	O=C(NC1=CC=CC(C(OC)=O)=C1)NC2CN(CC2)C3=NC(NC4=CC(OC)=C(C(OC)=C4)OC)=NC=C3
GSK1379788A	PKIS2	O=C(NCC1=CC=C(OC)C=C1)NC2CCN(CC2)C3=NC(NC(C=C4)=CC=C4F)=NC=C3
GSK1379800A	PKIS2	O=C(NC1=CC=CC=C1F)NC2CCN(CC2)C3=NC(NC(C=C4)=CC=C4F)=NC=C3
GSK1379812A	PKIS2	O=C(C(C)C1=CC=C(Cl)C=C1)NC2CCN(CC2)C3=NC(NC4=CC=C(OC)C=C4)=NC=C3
GSK1379825A	PKIS2	O=S(NC1CCN(CC1)C2=NC(NC3=CC(OC)=C(C(OC)=C3)OC)=NC=C2)(C(C=C4)=CC=C4NC(C)=O)=O
GSK1379859A	PKIS2	O=C(NC1=CC=C2OCOC2=C1)NC3CCN(CC3)C4=NC(NCC5=CC=C(C=C5)F)=NC=C4
GSK1379860A	PKIS2	O=C(NC1=CC=CC(C(OC)=O)=C1)NC2CCN(CC2)C3=NC(NCC4=CC=C(F)C=C4)=NC=C3
GSK1379874A	PKIS2	O=C(NCCNC1=NC(NC2=CC=C(F)C=C2)=NC=C1)C3=CC4=CC=CC=C4S3
GSK1379878A	PKIS2	FC1=CC=C(C=C1)NC2=NC=CC(NCCNC(NC3=C(C)C=CC(C)=C3)=O)=N2
GSK1379879A	PKIS2	FC1=CC=C(C=C1)NC2=NC=CC(NCCNC(NC3=CC(OC)=CC=C3)=O)=N2

Compound	Library	SMILES
GSK1379880A	PKIS2	FC1=CC=C(C=C1)NC2=NC=CC(NCCNC(NC3=CC=CC=C3F)=O)=N2
GSK1379882A	PKIS2	FC1=CC=C(C=C1)NC2=NC=CC(NCCNC(NC3=CC=C4OCOC4=C3)=O)=N2
GSK1379883A	PKIS2	FC1=CC=C(C=C1)NC2=NC=CC(NCCNC(NC3=CC=CC(C(OC)=O)=C3)=O)=N2
GSK1379896A	PKIS2	O=C(NCCNC1=NC(NC(C=C2)=CC=C2OC)=NC=C1)C3=CC4=CC=CC=C4S3
GSK1379899A	PKIS2	O=C(NC1=C(C)C=CC(C)=C1)NCCNC2=NC(NC(C=C3)=CC=C3OC)=NC=C2
GSK1379901A	PKIS2	O=C(NC1=CC=CC=C1F)NCCNC2=NC(NC3=CC=C(OC)C=C3)=NC=C2
GSK1379944A	PKIS2	O=C(NCCNC1=NC(NCC2=CC=C(F)C=C2)=NC=C1)C3=CC4=CC=CC=C4S3
GSK1383280A	PKIS2	BrC1=C(C2=C3C=CNC3=NC=C2)SC(C(NC(CNCC)CC4=CC=CC=C4)=O)=C1.BrC5=C(C6=C7C=CNC7=NC=C6)SC(C(NC(CNCC)CC8=CC=CC=C8)=O)=C5.Cl.Cl
GSK1383281A	PKIS2	BrC1=C(C2=C3C=CNC3=NC=C2)SC(C(NC(CNC(C)C)CC4=CC=CC=C4)=O)=C1.BrC5=C(C6=C7C=CNC7=NC=C6)SC(C(NC(CNC(C)C)CC8=CC=CC=C8)=O)=C5.Cl.Cl
GSK1389063A	PKIS2	O=C(N[C@H](CN)CC1=CC=C(OC)C=C1)C2=CC(Br)=C(C3=C4C=CNC4=NC=C3)S2.O=C(N[C@H](CN)CC5=CC=C(OC)C=C5)C6=CC(Br)=C(C7=C8C=CNC8=NC=C7)S6.Cl.Cl
GSK1392956A	PKIS1	COc1cc(ccc1Nc1nc(Nc2ccc(F)cc2C(=O)NC[C@@H](O)CO)c2cc[nH]c2n1)N1CCN(CC1)C(C)C
GSK1398460A	PKIS2	O=C(NC1=CC=NC=C1)C(C=C2)=CC=C2C3=C(C)C=CC(NC(C4=CC=C(C(Cl)=C4)Cl)=O)=C3
GSK1398463A	PKIS2	O=C(NC1=CC=NC=C1)C(C=C2)=CC=C2C3=C(C)C=CC(NC(C4=CC(C#N)=CC=C4)=O)=C3
GSK1398467A	PKIS2	O=C(NC1=CC=NC=C1)C(C=C2)=CC=C2C3=C(C)C=CC(NC(C4=CC=C(Cl)C=C4)=O)=C3
GSK1398468A	PKIS2	O=C(NC1=CC=NC=C1)C(C=C2)=CC=C2C3=C(C)C=CC(NC(NC4=CC=CC(Cl)=C4)=O)=C3
GSK1398470A	PKIS2	O=C(NC1=CC(C2=CC=C(C=C2)C(NC3=CC=NC=C3)=O)=C(C)C=C1)NC4=CC(C(F)(F)F)=C(Cl)C=C4
GSK1398471A	PKIS2	O=C(NC1=CC=NC=C1)C(C=C2)=CC=C2C3=C(C)C=CC(NC(NC4=CC=CC=C4)=O)=C3
GSK1398472A	PKIS2	O=C(NC1=CC=NC=C1)C(C=C2)=CC=C2C3=C(C)C=CC(NC(NC(C=C4)=CC=C4Cl)=O)=C3
GSK1398473A	PKIS2	O=C(NC1=CC=NC=C1)C(C=C2)=CC=C2C3=C(C)C=CC(NC(NC4=C(C)C=CC(C)=C4)=O)=C3
GSK1398474A	PKIS2	O=C(NC1=CC=NC=C1)C(C=C2)=CC=C2C3=C(C)C=CC(NC(NC4=CC(OC)=CC=C4)=O)=C3
GSK1398475A	PKIS2	O=C(NC1=CC=NC=C1)C(C=C2)=CC=C2C3=C(C)C=CC(NC(NC4=CC=C(OC)C=C4)=O)=C3
GSK1398477	KCGS	Cc1ccc(NC(=O)Nc2ccccc2F)cc1-c1ccc(cc1)C(=O)Nc1ccncc1
GSK1440913A	PKIS2	N#CC1=CC=CC(NC2=NC=CC(C3=CC(C)=C(C(C)=C3)O)=N2)=C1
GSK1487252A	PKIS2	O=C(N[C@H](CN)CC1=CC=C(C(F)(F)F)C=C1)C2=CC(Br)=C(C3=C(C=CN4)C4=NC=C3)S2.O=C(N[C@H](CN)CC5=CC=C(C(F)(F)F)C=C5)C6=CC(Br)=C(C7=C(C=CN8)C8=NC=C7)S6.Cl.Cl
GSK1511931A	PKIS1	COc1cc(ccc1Nc1nc(Nc2cccc3ncccc23)c2cc[nH]c2n1)N1CCN(CC1)C(C)C
GSK1520489A	PKIS2	CNC(C1=CC=CC=C1NC2=NC(NC3=CC=CC(CS(=O)(C)=O)=C3)=NC=C2C)=O.OC=O
GSK1535721A	PKIS2	O=S(C1=CC=CC(C2=CC=C(N=CC(N3CCOCC3)=N4)C4=C2)=C1)(N)=O
GSK1558669A	PKIS2	N#CC1=CN=C(N=C1NC2=CC=CC=C2C(N)=O)NC3=CC(N4CCN(C)CC4)=C(OC)C=C3.Cl
GSK1576028A	PKIS2	O=C(NC)C1=CC=CC=C1NC2=NC(NC3=CC=C(N4CCOCC4)C=C3)=NC=C2Cl.Cl
GSK1581427A	PKIS2	O=C(N[C@H](CN)CC1CCCCC1)C2=CC(Br)=C(C3=C4C(NC=C4)=NC=C3)S2.O=C(N[C@H](CN)CC5CCCCC5)C6=CC(Br)=C(C7=C8C(NC=C8)=NC=C7)S6.Cl.Cl
GSK1581428A	PKIS2	O=C(N[C@H](CN)CC1CCCCC1)C2=CC=C(C3=C4C(NC=C4)=NC=C3)S2.O=C(N[C@H](CN)CC5CCCCC5)C6=CC=C(C7=C8C(NC=C8)=NC=C7)S6.Cl.Cl

Compound	Library	SMILES
GSK1627798A	PKIS2	NC1=NC=C(C2=CC3=C(N=CC=C3C4=CC=NC=C4)C=C2)C=C1S(N5CCOCC5)(=O)=O
GSK1645872A	PKIS2	CC(N(CC1)CCN1C2=NC=C(NC3=NC(C(SC(C(C)C)=N4)=C4C5=CC(NS(C6=CC=CC=C6)(=O)=O)=CC=C5)=CC=N3)C=C2)=O
GSK1645895A	PKIS2	O=S(N(C)C1=CC=CC(C2=C(C3=CC=NC(NC4=CC=C(N5CCN(C(C)=O)CC5)N=C4)=N3)SC(CC)=N2)=C1)(C6=CC=CC=C6)=O
GSK1649598A	PKIS2	O=S(C1=CC=CC=C1)(NC2=CC=CC(C3=C(SC(C(C)C)=N3)C4=CC=NC(NC5=CC=C6C(CN(C)CC6)=C5)=N4)=C2)=O
GSK1653537A	PKIS2	CC1=NC(NC2=CC(C#N)=CC=C2)=NC(N3CCC(NS(=O)(C4=CC=C(F)C=C4)=O)CC3)=C1.OC(C(F)(F)F)=O
GSK1653539A	PKIS2	COC1=CC=C(S(=O)(NC2CCN(C3=NC(NC4=CC(C#N)=CC=C4)=NC(C)=C3)CC2)=O)C=C1.OC(C(F)(F)F)=O
GSK1660437A	PKIS2	O=S(NC1=CC=CC(C2=C(C3=CC=NC(NC4=CC=C(N5CCN(C(C)=O)CC5)N=C4)=N3)SC(C(C)C)=N2)=C1)(C6=CC=CC(Cl)=C6)=O
GSK1660450B	PKIS2	NC1=C(OC[C@H](CC2=CNC3=C2C=CC=C3)N)C=C(C4=CC(C(C)=NN5)=C5C=N4)C(C6=C(C)OC=C6)=N1
GSK1669917A	PKIS2	O=S(N1CCOCC1)(C(C=C2)=CC=C2NC3=NC(C)=CC(N4CC5=C(C=CC=C5)C4)=N3)=O.Cl
GSK1669921A	PKIS2	NC1=NC=C(C=C1S(=O)(N(C)C)=O)C(C=C23)=CC=C3N=CC=C2C4=CC(S(N)(=O)=O)=CC=C4
GSK1693850A	PKIS2	NC1=NC=C(C2=CC3=C(N=CC=C3C4=CC=NC=C4)C=C2)C=C1S(N5CCCCC5)(=O)=O
GSK1713088A	PKIS1	CCCN1CCC(CC1)Oc1cc(Nc2nc(Nc3cccc(F)c3C(N)=O)c3cc[nH]c3n2)c(OC)cc1Cl
GSK1723980B	PKIS2	O=S(NC1=CC=CC(C2=C(C3=CC=NC(NC4=CC=C(N5CCOCC5)N=C4)=N3)SC(C(C)C)=N2)=C1)(C6=C(F)C=CC=C6F)=O.Cl
GSK1751853A	PKIS1	COc1cc2CCN(C(=O)CN3CCN(CC3)C(C)C)c2cc1Nc1nc(Nc2cccc(F)c2C(N)=O)c2cc[nH]c2n1
GSK175726A	PKIS2	ClC1=CC(Cl)=CC(NC2=CC=NC(NC3=CC(Cl)=CC(Cl)=C3)=N2)=C1
GSK1804250A	PKIS2	O=S(NC1=C(F)C=CC(C2=C(C3=CC=NC(NC4=CC=C(N5CCOCC5)N=C4)=N3)SC(C(C)C)=N2)=C1)(C6=C(F)C=CC=C6F)=O
GSK180736A	PKIS1	CC1=C(C(NC(=O)N1)c1ccc(F)cc1)C(=O)Nc1ccc2[nH]ncc2c1
GSK1819799A	PKIS1	COc1cc(ccc1Nc1nc(Nc2cccc(F)c2C(O)=O)c2cc[nH]c2n1)N1CCN(CC1)C(C)C
GSK182497A	PKIS1	CN(C)C(=O)O[C@H]1CN[C@@H](C1)C#Cc1cc2ncnc(Nc3ccc(OCc4cccc(F)c4)c(Cl)c3)c2s1
GSK1838705	KCGS	CNC(C1=C(NC2=NC(NC3=C(OC)C=C4CCN(C(CN(C)C)=O)C4=C3)=NC5=C2C=CN5)C=CC=C1F)=O
GSK189015A	PKIS2	CC(S1)=CC=C1C2=NC3=CC=CC=C3C(NC4=CC=NC=C4)=N2
GSK1904529	KCGS	O=C(NC1=C(F)C=CC=C1F)C2=CC(C3=C(C4=NC(NC5=CC(CC)=C(N6CCC(N7CCN(S(=O)(C)=O)CC7)CC6)C=C5OC)=NC=C4)N8C=CC=CC8=N3)=CC=C2OC
GSK190937A	PKIS2	O=C(NCCC1=C(Cl)C=C(Cl)C=C1)C2=CN=CC(/C=C/C3=C(N)N=CC(C)=C3)=C2.Cl
GSK1917008A	PKIS2	O=C(C1=CC(N2CCCCC2)=CC=C1)NC3=CC(C(C=C4)=CC=C4C(NCC5CC5)=O)=C(C=C3)C
GSK192082A	PKIS1	CCNC(=O)O[C@H]1CN[C@@H](C1)C#Cc1cc2ncnc(Nc3ccc(OCc4cccc(F)c4)c(Cl)c3)c2s1
GSK198271A	PKIS2	O=C(C1=C(F)C=CC=C1F)NC2=CC=CC(C3=NN4N=CC=CC4=C3C5=CC=NC(NC6=CC=CC=C6)=N5)=C2
GSK200398A	PKIS1	Cl.O=C(O[C@H]1CN[C@@H](C1)C#Cc1cc2ncnc(Nc3ccc4n(Cc5ccccc5)ncc4c3)c2s1)N1CCOCC1
GSK2008607A	PKIS2	O=S(NC1=CC=CC(C2=C(C3=CC=NC(NC4=CN=C(N5CCOCC5)C=C4)=N3)SC(C(C)C)=N2)=C1F)(C6=C(F)C=CC=C6F)=O
GSK204559A	PKIS2	NC(C1=C(OCC2CCCCC2)C=C(S1)N3C=NC(C=C4OC)=C3C=C4OC)=O
GSK204607A	PKIS2	NC(C(SC(N1C=NC(C=C2OC)=C1C=C2OC)=C3)=C3OCC4CCCO4)=O

Compound	Library	SMILES
GSK204919	KCGS	COc1ccc2nc(nc(Nc3ccncc3)c2c1)-c1cccc(C)n1
GSK204925A	PKIS1	COc1cc2ncn(-c3cc(OCCc4ccccc4)c(s3)C(N)=O)c2cc1OC
GSK205189A	PKIS2	NC(C1=C(OCCCC2=CC=CC=C2)C=C(N3C=NC(C=C4OC)=C3C=C4OC)S1)=O
GSK2110236A	PKIS1	COc1cc2CCCN(C(=O)CN(C)C)c2cc1Nc1nc(Nc2ccsc2C(N)=O)c2cc[nH]c2n1
GSK2137462A	PKIS2	N#CC1=CC=C(C=C1)CCNC2=NC=CC(C3=CC=CC(CN4CCNCC4)=C3)=N2.N#CC5=CC=C(C=C5)CCNC6=NC=CC(C7=CC=CC(CN8CCNCC8)=C7)=N6.Cl.Cl.Cl
GSK2163632A	PKIS1	COc1cc2c(cc1Nc1nc(Nc3ccsc3C(N)=O)c3cc[nH]c3n1)N(CCC2(C)C)C(=O)CN(C)C
GSK2177277A	PKIS2	O=C1C2=C(NC3=CC=C(S(N4CCOCC4)(=O)=O)C=C3)N=C(N[C@H]5CNCCC5)N=C2C=CN1.OC(C(F)(F)F)=O.O=C6C7=C(NC8=CC=C(S(N9CCOCC9)(=O)=O)C=C8)N=C(N[C@H]%10CNCCC%10)N=C7C=CN6.OC(C(F)(F)F)=O
GSK2181306A	PKIS2	O=C1C2=C(NC3=CC=C(CCS4(=O)=O)C4=C3)N=C(N[C@@H]5CCNC5)N=C2C=CN1.OC(C(F)(F)F)=O
GSK2186269A	PKIS1	COc1cc2CCN(C(=O)CN(C)C)c2cc1Nc1nc(N2CCc3ccccc23)c2cc[nH]c2n1
GSK2188764A	PKIS2	O=C1C2=C(C=CN1)N=C(N[C@H]3CNCC3)N=C2NC4=CC(Cl)=CC(Cl)=C4.OC(C(F)(F)F)=O
GSK2189892A	PKIS2	NC1=NNC2=CC(C3=CC=CC=N3)=CC=C21.Cl
GSK2192730A	PKIS2	NC1=NNC2=CC(C3=CC=CC(N)=N3)=CC=C21
GSK2193613A	PKIS2	NC1=NNC2=CC(C3=CC=CC(N)=C3)=CC=C21
GSK2197149A	PKIS2	CC1=CC(NC2=C(C(N)=O)C=NC(N[C@H]3CCNC3)=N2)=CC=C1.Cl
GSK2206003A	PKIS2	NC1=NNC2=C1C=CC(C3=CC=NC(NC)=N3)=C2
GSK2213727A	PKIS1	COc1cc(C)c(NC(=O)CN(C)C)cc1Nc1nc(Nc2cccc(F)c2C(N)=O)c2cc[nH]c2n1
GSK2219329A	PKIS2	NC1=NC(C2=CC3=C(C=C2)C(N)=NN3)=CC(N(C)C)=N1
GSK2219385	KCGS	COc1cc(C)c(cc1Nc1nc(Nc2cccc(F)c2C(N)=O)c2cc[nH]c2n1)N(C)C(=O)CN(C)C
GSK2220400A	PKIS1	CNC(=O)c1ncccc1Nc1nc(Nc2cc3N(CCCc3cc2OC)C(=O)CN(C)C)nc2[nH]ccc12
GSK2221681A	PKIS2	NC1=NC(C2=CC3=C(C=C2)C(N)=NN3)=CC(NC(C)C)=N1
GSK2224810A	PKIS2	NC1=NC(C2=CC3=C(C=C2)C(N)=NN3)=CC(NC)=N1
GSK2225749A	PKIS2	NC1=NC(C2=CC(NN=C3N)=C3C=C2)=CC(NC4=CC=CC=C4)=N1
GSK2227430A	PKIS2	NC1=NC(C2=CC3=C(C=C2)C(N)=NN3)=CC(N4CCCC4)=N1
GSK2228768A	PKIS2	NC1=NC(C2=CC3=C(C=C2)C(N)=NN3)=CC(N4CCCCC4)=N1
GSK223675A	PKIS2	CC1=NC(C2=NC3=CC=CC=C3C(NC4=CC=NC=C4)=C2)=CC=C1
GSK223810A	PKIS2	COC(C(OCCCN1CCOCC1)=C2)=CC3=C2N=CN=C3NC4=CC(NC(C5=CC=CC=C5)=O)=CC=C4
GSK2250882A	PKIS2	CC(C)C1=NC(N)=NC(C2=CC(NN=C3N)=C3C=C2)=C1
GSK2258759A	PKIS2	C[C@H](CCCC1)N1C2=NC(N)=NC(C3=CC(NN=C4N)=C4C=C3)=C2
GSK2269557	KCGS	CC(C)N1CCN(Cc2cnc(o2)-c2cc(cc3[nH]ncc23)-c2cccc3[nH]ccc23)CC1
GSK2269905A	PKIS2	CC1=CC=CC=C1CN2C=CN3C(C=C(N4CCOCC4)N=C32)=O
GSK2276055A	PKIS2	O=C1NC=C(C2=CC=C(N3CCOCC3)C=C2)C4=C1C=C(C5=CNN=C5)S4
GSK2283293	KCGS	C[C@H]1CC[C@H](CN1c1cc(nc(N)n1)-c1ccc2c(N)n[nH]c2c1)C(=O)Nc1ccccc1
GSK2286062A	PKIS2	NC1=NC(C2=CC(NN=C3N)=C3C=C2)=CC(N4[C@H](C)CC[C@@H](C(NC5=CC=CC=C5)=O)C4)=N1
GSK2286096A	PKIS2	O=C(OC(C)(C)C)NC1CN(C2=NC(N)=NC(C3=CC=C4C(NN=C4N)=C3)=C2)CCC1
GSK2286295A	PKIS2	O=C1N(C=CN2CC3=CC=CC(Cl)=C3Cl)C2=NC(N4CCOCC4)=C1
GSK2286775B	PKIS2	NC1=NC(C2=CC=C3C(NN=C3N)=C2)=CC(N4CC(NC(C5=CC=CC=C5)=O)CCC4)=N1
GSK2288359A	PKIS2	O=C(NC1=CC=CC=C1)[C@H]2CN(C3=NC(N)=NC(C4=CC(NN=C5N)=C5C=C4)=C3)CCC2.OC(C(F)(F)F)=O.O=C(NC6=CC=CC=C6)[C@H]7CN(C8=NC(N)=NC(C9=CC(NN=C%10N)=C%10C=C9)=C8)CCC7.OC(C(F)(F)F)=O

Compound	Library	SMILES
GSK2289044B	PKIS2	O=C1C=C(N2CCOCC2)N=C3N1C=CN3C([2H])([2H])C4=C(C)C(C(F)(F)F)=CC=C4
GSK2291363A	PKIS2	NC1=NC(C2=CC(NN=C3N)=C3C=C2)=CC(N4[C@H](C)CC[C@H](C(NC5CCCCC5)=O)C4)=N1
GSK2292767	KCGS	COc1ncc(cc1NS(C)(=O)=O)-c1cc(-c2ncc(CN3C[C@H](C)O[C@H](C)C3)o2)c2cn[nH]c2c1
GSK2296823A	PKIS2	O=C1N(C=CN2CC3=CC=CC(Cl)=C3)C2=NC(N4CCOCC4)=C1
GSK2297099A	PKIS2	O=C1N(C=CN2CC3=CC=C(F)C(Cl)=C3)C2=NC(N4CCOCC4)=C1
GSK2297428A	PKIS2	O=C1N(C=CN2CC3=CC=CC=C3F)C2=NC(N4CCOCC4)=C1
GSK2297430A	PKIS2	O=C1N(C=CN2CC3=CC=CC(F)=C3)C2=NC(N4CCOCC4)=C1
GSK2297542A	PKIS2	O=C1N(C=CN2CC3=CC=CC(C)=C3)C2=NC(N4CCOCC4)=C1
GSK2297543A	PKIS2	O=C1N(C=CN2CC3=CC=CC(C(F)(F)F)=C3)C2=NC(N4CCOCC4)=C1
GSK2298859A	PKIS2	C[C@H]1N(C2=NC(NC)=NC(C3=CC(NN=C4N)=C4C=C3)=C2)C[C@@H](C(NC5=CC=CC=C5)=O)CC1
GSK2299009A	PKIS2	O=C1N(C2=C(C=CC=C2)N3CC4=CC=CC(Cl)=C4Cl)C3=NC(N5CCOCC5)=C1
GSK2306394A	PKIS2	O=C1N(C2=C(C=CC=C2)N3CC4=CC=CC(C(F)(F)F)=C4C)C3=NC(N5CCOCC5)=C1
GSK2328680	KCGS	Cc1c(C)n2c(nc(cc2=O)N2CCOCC2)n1Cc1cccc(c1C)C(F)(F)F
GSK2333389A	PKIS2	O=C1N(C=CN2CC3=CC=CC4=CC=CC=C34)C2=NC(N5CCOCC5)=C1
GSK2334006A	PKIS2	O=C1N(C=C(C)N2CC3=CC=CC(Cl)=C3Cl)C2=NC(N4CCOCC4)=C1
GSK2334470	KCGS	O=C([C@@H]1CN(C2=NC(NC)=NC(C3=CC4=C(C=C3)C(N)=NN4)=C2)[C@H](C)CC1)NC5CCCCC5
GSK2336394A	PKIS2	O=C1N2C(N(CC3=C(C)C(C(F)(F)F)=CC=C3)C=C2)=CC(N4CCOCC4)=N1
GSK2342769A	PKIS2	O=C1N(N=C(C)N2CC3=CC=CC(Cl)=C3Cl)C2=NC(N4CCOCC4)=C1
GSK2344444A	PKIS2	O=C1N2C(N(CC3=CC=CC(C(F)(F)F)=C3C)C(C)=N2)=NC(N4CCOC(C)C4)=C1
GSK2347225A	PKIS2	O=C1C=C(N2CCOCC2)N=C3N1N=C(SC)N3CC4=CC=CC(Cl)=C4Cl
GSK2358994A	PKIS2	O=C1N(N=C(C2CC2)N3CC4=CC=CC(Cl)=C4Cl)C3=NC(N5CCOCC5)=C1
GSK2363608B	PKIS2	O=C1C=C(N2CCOCC2)N=C3N1N=C(SC)N3C([2H])([2H])C4=CC=CC(C(F)(F)F)=C4C.OC(C(F)(F)F)=O
GSK2373690A	PKIS2	O=C1N2C(N(CC3=CC=CC(C(F)(F)F)=C3C)C(C)=N2)=NC(N4CCO[C@H](C)C4)=C1
GSK2373693A	PKIS2	O=C1N2C(N(CC3=CC=CC(Cl)=C3Cl)C(C)=N2)=NC(N4CCO[C@H](C)C4)=C1
GSK2375584A	PKIS2	C[C@H]1N(C2=NC(NC)=NC(C3=CC(NN=C4N)=C4C=C3)=C2)C[C@@H](C(NC5CCCCC5)=O)OC1
GSK2376236A	PKIS2	CNC1=NC(C2=CC=C3C(NN=C3N)=C2)=CC(N4[C@H](CC)CO[C@H](C(NC5=CC=CC=C5)=O)C4)=N1
GSK237700A	PKIS1	COc1cc2ncn(-c3cc(O[C@@H](C)c4ccccc4Cl)c(s3)C(N)=O)c2cc1OC
GSK237701A	PKIS1	COc1cc2ncn(-c3cc(O[C@H](C)c4ccccc4Cl)c(s3)C(N)=O)c2cc1OC
GSK238063A	PKIS1	CN(C)C(=O)O[C@@H]1CN[C@H](C1)C#Cc1cc2ncnc(Nc3ccc(OCc4cccc(F)c4)c(Cl)c3)c2s1
GSK238583A	PKIS1	OC(=O)C(F)(F)F.O=C(O[C@H]1CN[C@@H](C1)C#Cc1cc2ncnc(Nc3ccc(Cc4ccccc4)cc3)c2s1)N1CCOCC1
GSK248233A	PKIS1	CCn1c(nc2cnc(Oc3cccc(NC(=O)c4ccc(cc4)N(C)C)c3)cc12)-c1nonc1N
GSK2576924A	PKIS2	NC1=C2C(SC=C2C3=CC(CCN4C(CC5=CC=CC=C5)=O)=C4C=C3)=CC=N1
GSK2578215	KCGS	FC1=NC=CC(C2=CC=C(OCC3=CC=CC=C3)C(C(NC4=CC=CN=C4)=O)=C2)=C1
GSK257997A	PKIS2	CC1=CC(NC2=CC=NC=C2)=NC(C3=CC=CC(C)=N3)=N1
GSK2587663A	PKIS2	NC1=C2C(SC=C2C3=CC(CCN4C(CC5=C(F)C=CC(F)=C5)=O)=C4C=C3)=CC=N1
GSK259178A	PKIS1	OC(=O)C(F)(F)F.Fc1ccc(F)c(Cn2ccc3cc(Nc4ncnc5cc(sc45)C#C[C@@H]4C[C@H](CN4)OC(=O)N4CCOCC4)ccc23)c1

Appendix

Compound	Library	SMILES
GSK2592465A	PKIS2	O=C(CC1=CC=CC=C1)N2CCC3=C2C=CC(C4=CSC5=C(C6=CC=NC=C6)C=NC(N)=C54)=C3
GSK2593067A	PKIS2	O=C(CC1=CC=CC=C1)N2CCC3=C2C=CC(C4=CSC5=C(C6=CNN=C6)C=NC(N)=C54)=C3
GSK2593074A	PKIS2	O=C(CC1=CC=CC=C1)N2CCC3=C2C=CC(C4=CSC5=C(C6=CN(C)N=C6)C=NC(N)=C54)=C3
GSK260205A	PKIS2	NC1=NON=C1C2=NC3=C(C4=CC=CC=C4)N=CC(OCCCN)=C3N2CC.OC(C(F)(F)F)=O.NC5=NON=C5C6=NC7=C(C8=CC=CC=C8)N=CC(OCCCN)=C7N6CC.OC(C(F)(F)F)=O
GSK2603346A	PKIS2	NC1=NC=NC2=C1C(C3=CC(CCN4C(CC5=CC=CC=C5C)=O)=C4C=C3)=CN2C
GSK2603358A	PKIS2	NC1=NC=NC2=C1C(C3=CC(CCN4C(CC5=CC=CC(F)=C5)=O)=C4C=C3)=CN2C
GSK2606414A	PKIS2	NC1=NC=NC2=C1C(C3=CC(CCN4C(CC5=CC(C(F)(F)F)=CC=C5)=O)=C4C=C3)=CN2C
GSK2606590A	PKIS2	NC1=NC=NC2=C1C(C3=CC(CCN4C(CC5=CC(Cl)=CC=C5)=O)=C4C=C3)=CN2C
GSK2608885A	PKIS2	NC1=NC=NC2=C1C(C3=CC(CCN4C(CC5=CC=CC=C5Cl)=O)=C4C=C3)=CN2C
GSK2608899A	PKIS2	NC1=NC=NC2=C1C(C3=CC(CCN4C(CC5=CC(OC)=CC=C5)=O)=C4C=C3)=CN2C
GSK2634140A	PKIS2	NC1=NC=NC2=C1C(C3=CC(CCN4C(CC5=CC(F)=CC(F)=C5F)=O)=C4C=C3)=CN2C
GSK2634758A	PKIS2	NC1=NC=NC2=C1C(C3=CC(CCN4C(CC5=CC=C(C)C=C5)=O)=C4C=C3)=CN2C
GSK2635225A	PKIS2	NC1=NC=NC2=C1C(C3=CC(CCN4C(CC5=CC(C(F)(F)F)=CC(F)=C5)=O)=C4C=C3)=CN2C
GSK2645446A	PKIS2	NC1=NC=NC2=C1C(C3=CC=C4C(CCN4C(CC5=CC(F)=CC=C5F)=O)=C3)=CO2
GSK2656157	KCGS	NC1=NC=NC2=C1C(C3=CC=C4C(CCN4C(CC5=NC(C)=CC=C5)=O)=C3F)=CN2C
GSK269962B	PKIS1	Cl.CCn1c(nc2cnc(Oc3cccc(NC(=O)c4ccc(OCCN5CCOCC5)cc4)c3)cc12)-c1nonc1N
GSK270822A	PKIS1	CC1=C(C(CC(=O)N1)c1ccc2ccccc2c1)C(=O)Nc1ccc2[nH]ncc2c1
GSK2850163	KCGS	O=C(N(CCC1)C[C@]21CCN(CC3=CC=C(Cl)C(Cl)=C3)C2)NCC4=CC=C(C)C=C4
GSK292658A	PKIS2	O=C(C1=C(C=CC=C1F)F)NC2=CC=CC(C3=NN4C=CC=CC4=C3C5=CC=NC(NC6=CC(C(F)(F)F)=CC=C6)=N5)=C2
GSK299115A	PKIS1	CC1=C(C(CC(=O)N1)c1ccc(Cl)c(Cl)c1)C(=O)Nc1ccc2[nH]ncc2c1
GSK299495A	PKIS2	O=C(C1=C(F)C=CC=C1F)NC2=CC=CC(C3=NN4N=CC=CC4=C3C5=CC=NC(NC6=CC=CC(C(F)(F)F)=C6)=N5)=C2
GSK300014A	PKIS1	CS(=O)(=O)CCNCc1cc(cs1)-c1cc2c(Nc3ccc(OCc4cccc(F)c4)c(Cl)c3)ncnc2s1
GSK300657X	KCGS	NS(=O)(=O)c1ccc(N\N=C2/C(=O)Nc3ccc(cc23)C(=O)NCc2ccncc2)cc1
GSK301329A	PKIS2	COC(C(OCCCN1CCOCC1)=C2)=CC3=C2N=CN=C3NC4=CC=C(NC(C5=CC=CC=C5)=O)C=C4
GSK301362A	PKIS2	O=C(N)C1=C(NC=C2C3CCNCC3)C2=CC(C4=CC=CC=C4)=C1
GSK306886A	PKIS2	ClC1=C(S(C2=CC(F)=CC=C2)(=O)=O)C=CC(NC3=C(SC(Br)=C4)C4=NC=N3)=C1.Cl
GSK312879A	PKIS2	O=C(C1=C(F)C=CC=C1F)NC2=CC=CC(C3=NN4N=CC=CC4=C3C5=CC=NC(NC6=CN=CC=C6)=N5)=C2.Cl
GSK312948A	PKIS1	COc1cc2ncn(-c3cc(OCc4cccs4)c(s3)C(N)=O)c2cc1OC
GSK317315A	PKIS1	COc1ccc2ncn(-c3cc(O[C@H](C)c4ccccc4C(F)(F)F)c(s3)C(N)=O)c2c1
GSK317354A	PKIS1	CC1=C(C(N=C(N1)c1ccc(nc1)C(F)(F)F)c1ccc(F)cc1)C(=O)Nc1ccc2[nH]ncc2c1
GSK319347A	PKIS1	COc1cc2ncn(-c3cc(OCc4ccccc4S(C)(=O)=O)c(s3)C#N)c2cc1OC
GSK323521A	PKIS2	O=C(C1=C(F)C=CC=C1F)NC2=CC=CC(C3=NN(C=CC=C4)C4=C3C5=CC=NC(NC6=CC(OC)=C(OC)C(OC)=C6)=N5)=C2
GSK323543A	PKIS2	O=C(C1=C(F)C=CC=C1F)NC2=CC=CC(C3=NN(C=CC=C4)C4=C3C5=CC=NC(NC6=CC=C(CS(C)(=O)=O)C=C6)=N5)=C2
GSK326090A	PKIS1	C[C@@H](Oc1cc(sc1C(N)=O)-n1cnc2ccc(OCC3CCN(C)CC3)cc12)c1ccccc1C(F)(F)F

Compound	Library	SMILES
GSK326180A	PKIS2	O=C(C1=C(F)C=CC=C1F)NC2=CC=CC(C3=NN4C(C=CC=N4)=C3C5=CC=NC(NC6=CC(S(=O)(CC)=O)=CC=C6OC)=N5)=C2
GSK327238A	PKIS2	O=C(C1=C(F)C=CC=C1F)NC2=CC=CC(C3=NN4C(C=CC=N4)=C3C5=CC=NC(NC6=CC(OC)=C(OC)C(OC)=C6)=N5)=C2
GSK336313A	PKIS2	NC(C(SC(N1C=NC(C=C2OC)=C1C=C2OC)=C3)=C3OCC4=CC=NC=C4)=O
GSK336735A	PKIS2	O=C(C1=C(F)C=CC=C1F)NC2=CC=CC(C3=NN(C=CC=C4)C4=C3C5=CC=NC(NC6=CC=CC(CCS(=O)(N)=O)=C6)=N5)=C2
GSK346294A	PKIS2	C[C@@H](OC1=C(C(N)=O)SC(N2C=NC3=C2C=C(NC(NC(C)(C)C)=O)C=C3)=C1)C4=CC=CC=C4Cl
GSK350559A	PKIS2	CS(CC1=CC=C(NC2=NC(C3=C4N(N=C3C5=CC(NC(C6CCCCC6)=O)=CC=C5)N=CC=C4)=CC=N2)C=C1)(=O)=O
GSK357952A	PKIS2	O=C(C1=C(F)C=CC(F)=C1Cl)NC2=CC=CC(C3=NN4C=CC=CC4=C3C5=CC=NC(NC6=CC(F)=CC=C6)=N5)=C2
GSK361061A	PKIS2	O=C(C1=C(F)C(C)=CC=C1F)NC2=CC=CC(C3=NN4C(C=CC=C4)=C3C5=CC=NC(NC6=CC(F)=CC=C6)=N5)=C2
GSK361065A	PKIS2	O=C(C1=C(OC)C=CC=C1OC)NC2=CC=CC(C3=NN4C(C=CC=C4)=C3C5=CC=NC(NC6=CC(F)=CC=C6)=N5)=C2
GSK364507A	PKIS2	O=C(C(C=CC=C1)=C1C)C2=CNC(C(NCC(C=CC=C3)=C3OC)=O)=C2
GSK398099A	PKIS2	O=S(C1=CC=C(NC(/C2=C\NC3=CC(S(=O)(N)=O)=CC=C3)=O)C2=C1)(CC4=C(Cl)C=CC=C4Cl)=O
GSK429286A	PKIS2	O=C(CC1C2=CC=C(C=C2)C(F)(F)F)NC(C)=C1C(NC3=C(F)C=C(NN=C4)C4=C3)=O
GSK448459A	PKIS2	COC1=C(OC)C=C2N=CN(C3=CC(OCC4=C(Cl)C=CS4)=C(C(N)=O)S3)C2=C1
GSK461364	KCGS	O=C(C1=C(O[C@@H](C2=CC=CC=C2C(F)(F)F)C)C=C(N3C=NC4=CC=C(CN5CCN(C)CC5)C=C34)S1)N
GSK466314A	PKIS1	Cc1n[nH]c2ccc(NC(=O)C3=C(C)NC(=O)CC3c3ccc(cc3)C(F)(F)F)cc12
GSK466317A	PKIS1	CC1=C(C(CC(=O)N1)c1ccc(cc1)C(F)(F)F)C(=O)Nc1cc(Cl)c2[nH]ncc2c1
GSK479719A	PKIS2	C[C@H](C1=CC=CC=C1Cl)OC2=C(C(N)=O)SC(N3C=NC4=CC(C5=CC=NC=C5)=CC=C43)=C2
GSK481	KCGS	O=C(C1=NOC(CC2=CC=CC=C2)=C1)N[C@H]3COC4=CC=CC=C4N(C)C3=O
GSK483724A	PKIS2	C[C@H](C1=CC=CC=C1Cl)OC2=C(C(N)=O)SC(N3C=NC4=CC=C(C5=CC=NC=C5)C=C43)=C2
GSK507274A	PKIS2	NC1=NON=C1C2=NC(C(C#CC(C)(O)C)=NC=C3OCCCCN)=C3N2CC.OC(C(F)(F)F)=O.NC4=NON=C4C5=NC(C(C#CC(C)(O)C)=NC=C6OCCCCN)=C6N5CC.OC(C(F)(F)F)=O
GSK507358A	PKIS2	CC1=NNC(C=C2)=C1C=C2C3=C(N=CC(OC[C@@H](N)CC4=CC=CC=C4)=C3)C5=COC=C5.OC(C(F)(F)F)=O.CC6=NNC(C=C7)=C6C=C7C8=C(N=CC(OC[C@@H](N)CC9=CC=CC=C9)=C8)C%10=COC=C%10.OC(C(F)(F)F)=O
GSK534911A	PKIS2	CC1=C(C(C2=C(F)C=C(Cl)C=C2)N=C(C3=CC(OC)=NC=C3)N1)C(NC4=CC=C(NN=C5)C5=C4)=O.OC(C(F)(F)F)=O
GSK534913A	PKIS2	CC(N1)=C(C(C2=C(F)C=C(Cl)C=C2)N=C1C3=CN=C(OC)C=C3)C(NC4=CC=C(NN=C5)C5=C4)=O.OC(C(F)(F)F)=O
GSK554170A	PKIS1	OC(=O)C(F)(F)F.CCn1c(nc2c(ncc(OCC3CCNCC3)c12)C#CC(C)(C)O)-c1nonc1N
GSK561866B	PKIS1	OC(=O)C(F)(F)F.CCn1c(nc2c(ncc(OCCCN)c12)C#CCN)-c1nonc1N
GSK562689A	PKIS2	N[C@@H](CC1=CNC2=C1C=CC=C2)COC3=CC(C4=CC5=C(C=C4)NN=C5C)=C(N=C3)C6=COC=C6.OC(C(F)(F)F)=O.N[C@@H](CC7=CNC8=C7C=CC=C8)COC9=CC(C%10=CC%11=C(C=C%10)NN=C%11C)=C(N=C9)C%12=COC=C%12.OC(C(F)(F)F)=O.OC(C(F)(F)F)=O
GSK571989A	PKIS1	C[C@@H](Oc1cc(sc1C(N)=O)-n1cnc2ccc(OCC3CCN(C)CC3)cc12)c1ccccc1Cl
GSK579289A	PKIS1	C[C@@H](Oc1cc(sc1C(N)=O)-n1cnc2ccc(OC3CCN(C)CC3)cc12)c1ccccc1Cl

Compound	Library	SMILES
GSK580432A	PKIS2	C[C@H](C1=CC=CC=C1Cl)OC2=C(C(N)=O)SC(N3C=NC4=CC(C5=CN(C)N=C5)=CC=C43)=C2
GSK581271A	PKIS2	O=S(NC(C=C1)=CC=C1NC2=NC(NC3=CC=CC4=C3C=NN4)=CC=N2)(C5=CC=C(C)C=C5)=O
GSK583	KCGS	CC(C)(C)S(=O)(=O)C1=CC2=C(C=CN=C2C=C1)NC3=NNC4=C3C=C(C=C4)F
GSK586581A	PKIS1	CS(=O)(=O)Nc1ccc(cc1)-c1cc(cc(C(N)=O)c1N)-c1ccccc1
GSK605714A	PKIS1	COc1ccc(cc1C(N)=O)-c1ccncc1
GSK614526A	PKIS1	OC(=O)C(F)(F)F.CCn1c(nc2c(ncc(OC[C@@H]3CCCN3)c12)C#CC(C)(C)O)-c1nonc1N
GSK619487A	PKIS1	OC(=O)C(F)(F)F.CCn1c(nc2c(ncc(OC3CCNCC3)c12)C#CC(C)(C)O)-c1nonc1N
GSK620503A	PKIS1	NC(=O)c1cc(cc(-c2ccncc2)c1N)-c1ccc(F)cc1
GSK625137A	PKIS1	NC(=O)c1cc(cc(-c2ccccc2)c1N)-c1ccncc1
GSK641502A	PKIS2	C[C@@H](OC1=C(C(N)=O)SC(N2C3=C(C=C(C4=CC=NC(N5CCN(C)CC5)=C4)C=C3)N=C2)=C1)C6=CC=CC=C6Cl
GSK683281A	PKIS2	NC1=C2C(SC=C2C3=CC(CCN4C(CC5=CC=CC=C5)=O)=C4C=C3)=C(C6=CC=CN=C6)C=N1
GSK711701A	PKIS1	COc1c(cc(cc1-c1ccc(cc1)S(N)(=O)=O)-c1ccc(Cl)cc1)C(N)=O
GSK840	KCGS	O=C(OC(C)(C)C)CC1=CC=C(N2C3=CC=C(C(NC)=O)C=C3N=C2)C=C1
GSK843	KCGS	NC1=NC=C(C2=CC(C)=NN2C)C3=C1C(C4=CC=C(SC=N5)C5=C4)=CS3
GSK846226A	PKIS2	O=S(C1=CC=C(C=C1)C2=CC=NC3=C2C=CN3)(N4CCCC4)=O
GSK872	KCGS	O=S(C1=CC=C2N=CC=C(NC3=CC=C(SC=N4)C4=C3)C2=C1)(C(C)C)=O
GSK902056A	PKIS2	CCN1C2=CC(OCCN)=NC(C#CC(C)(O)C)=C2N=C1C3=NON=C3N.CCN4C5=CC(OCCN)=NC(C#CC(C)(O)C)=C5N=C4C6=NON=C6N.Cl.Cl
GSK907232A	PKIS2	C[C@H](C1=CC=CC=C1Cl)OC2=C(C(N)=O)SC(N3C4=C(C=C(C5=CC=NC(NCCS(C)(=O)=O)=C5)C=C4)N=C3)=C2
GSK938890A	PKIS1	CCn1c(nc2c(nc(OC[C@@H](N)c3ccccc3)cc12)C#CC(C)(C)O)-c1nonc1N
GSK943949A	PKIS1	CCn1c(nc2c(nc(OC[C@H](N)c3ccccc3)cc12)C#CC(C)(C)O)-c1nonc1N
GSK949675A	PKIS1	Cl.CCn1c(nc2c(nc(OCCNC)cc12)C#CC(C)(C)O)-c1nonc1N
GSK953913A	PKIS1	NS(=O)(=O)c1ccc(cc1)-c1cc2ccncc2cc1OCc1ccccc1
GSK955403A	PKIS2	O=C(NC1=CC=C(C)C=C1)NC2=CC=CC(C(F)(F)F)=C2
GSK969786A	PKIS1	Fc1cccc(COc2ccc(Nc3ncnc4sc(cc34)-c3ccco3)cc2Cl)c1
GSK977617A	PKIS2	O=S(C1=CC=C(C2=CC=NC3=C2C=CN3)C=C1)(NCCN)=O
GSK977620A	PKIS2	O=S(C1=CC=C(C2=CC=NC3=C2C=CN3)C=C1)(NCCN(C)C)=O
GSK978744A	PKIS1	C[C@@H](Oc1cc(sc1C(N)=O)-n1cnc2ccc(OC[C@@H](O)CO)cc12)c1ccccc1Cl
GSK980961A	PKIS1	NS(=O)(=O)c1cccc(c1)-c1cc2ccncc2cc1OCc1ccccc1
GSK986310C	PKIS2	O=C(N)C1=C(NC2=CC(C)=CC=C2)N=C(N[C@@H]3[C@H](N)CCCC3)N=C1.Cl
GSK993273A	PKIS2	O=S(NC1=CC=C(C=C1)C2=C3C(NC=C3)=NC=C2)(C)=O
GSK994854A	PKIS1	CCCN1CCC=C(C1)c1ccc(Nc2nc(Nc3ccccc3C(N)=O)c3cc[nH]c3n2)c(C)c1
GW2429374A	KCGS	Cl.Oc1c(Br)cc(C=C2C(=O)Nc3ccc(cc23)-c2cccnc2)cc1Br
GW271431X	PKIS2	C1(C2=NNC=C2C3=C4C(C=CC=C4)=NC=C3)=CC=CC=N1
GW272142A	PKIS2	C1(CN2C=NC3=C2C=CC(NC4=C5C(C=CC=C5)=NC=N4)=C3)=CC=CC=C1.Cl
GW273749A	PKIS2	C1(CN2N=CC3=C2C=CC(NC4=C5C(C=CC=C5)=NC=N4)=C3)=CC=CC=C1.Cl
GW275568A	PKIS2	C1(CN2C=CC3=CC(NC4=NC=NC5=C4C=CC=C5)=CC=C23)=CC=CC=C1.Cl
GW275616X	PKIS1	NS(=O)(=O)c1cccc(N\C=C2/C(=O)Nc3ccccc23)c1
GW275944X	PKIS1	Cc1ccc2NC(=O)\C(c2c1)=N/Nc1ccc(cc1)S(N)(=O)=O
GW276655	KCGS	NS(=O)(=O)c1ccc(N\N=C2/C(=O)Nc3ccc(cc23)-c2cnco2)cc1

Compound	Library	SMILES
GW278681X	PKIS1	CS(=O)(=O)Nc1ccc(N\C=C2/C(=O)Nc3ccccc23)cc1
GW279320X	PKIS1	Cc1cc(Cl)cc2C(=NNc3ccc(cc3)S(N)(=O)=O)C(=O)Nc12
GW280670X	PKIS1	NS(=O)(=O)c1ccc(N\N=C2/C(=O)Nc3ccc(Cl)cc23)cc1
GW281179X	PKIS2	CN1C=NC=C1C2=CC3=C(N=CN=C3C=N2)NC4=CC=C(OCC5=CC=CC=C5)C=C4
GW282449A	PKIS1	Cl.COc1cc2ncnc(Nc3ccc4n(Cc5ccccc5)ncc4c3)c2cc1OC
GW282450A	PKIS2	COC1=CC2=NC=NC(NC3=CC4=C(N=C(C5=CC=CC=C5)N4)C=C3)=C2C=C1OC.Cl
GW282536X	PKIS1	Cc1cccc2c1NC(=O)\C2=N/Nc1ccc(cc1)S(N)(=O)=O
GW282974X	PKIS1	CN(C)c1cc2c(Nc3ccc4n(Cc5ccccc5)ncc4c3)ncnc2cn1
GW284372X	PKIS1	C(Oc1ccc(Nc2ncnc3ccc(cc23)-c2ccco2)cc1)c1ccccc1
GW284408X	PKIS1	O=C1Nc2ccccc2\C1=C\Nc1ccc2[nH]c(=O)[nH]c2c1
GW284543A	PKIS2	COC1=CC2=C(C=C1OC)C(NC3=CC(OC4=CC=CC=C4)=CC=C3)=CC=N2.Cl
GW290597X	PKIS1	NS(=O)(=O)c1ccc(N\N=C2/C(=O)Nc3ccc(cc23)C(=O)NCCCn2ccnc2)cc1
GW296115X	PKIS1	COc1ccc2[nH]c3c4[nH]c5ccc(OC)cc5c4c4C(=O)NC(=O)c4c3c2c1
GW297361X	PKIS1	NS(=O)(=O)c1ccc(N\C=C2/C(=O)Nc3ccc4ncsc4c23)cc1
GW300653X	PKIS1	CC(C)c1ccc2c(NC(=O)\C2=N\Nc2ccc(cc2)S(N)(=O)=O)c1
GW300660X	PKIS1	NS(=O)(=O)c1ccc(N\N=C2/C(=O)Nc3ccc(cc23)C(=O)NCCc2c[nH]cn2)cc1
GW301784X	PKIS1	CC(C)(CO)CNC(=O)c1ccc2NC(=O)\C(c2c1)=N/Nc1ccc(cc1)S(N)(=O)=O
GW301789X	PKIS1	O=C1Nc2ccccc2\C1=C\Nc1ccc(cc1)-n1cncn1
GW301888X	PKIS1	CN(C)c1cc2c(Nc3ccc4nc(Cc5ccccc5)[nH]c4c3)ncnc2cn1
GW305074X	PKIS1	Oc1c(Br)cc(C=C2C(=O)Nc3ccc(I)cc23)cc1Br
GW305178X	PKIS1	NS(=O)(=O)c1ccc(N\N=C2/C(=O)Nc3ccc4ncccc4c23)cc1
GW320571X	PKIS2	CN1C=NC=C1C2=CC3=C(NC4=CC=C(OCC5=CC=CC=C5)C=C4)N=CN=C3C=C2
GW335962X	PKIS1	C\C(Nc1ccc(cc1)S(N)(=O)=O)=C1\C(=O)Nc2ccccc12
GW345098X	PKIS2	CCN1C=NC2=C1N=CN=C2N
GW352430A	PKIS1	Cl.NS(=O)(=O)c1ccc(N\N=C2/C(=O)Nc3cccc(CCc4ccncc4)c23)cc1
GW396574X	PKIS1	CC(C)=Cc1cccc2NC(=O)\C(c12)=N/Nc1ccc(cc1)S(N)(=O)=O
GW405841X	PKIS1	COC(=O)c1ccc2NC(=O)C(=Cc3cc(Br)c(O)c(Br)c3)c2c1
GW406108X	PKIS1	Oc1c(Cl)cc(C=C2C(=O)Nc3ccc(cc23)C(=O)c2ccco2)cc1Cl
GW406731X	PKIS1	COC(=O)c1cncc(\C=C\c2c(C)cc(O)cc2C)c1
GW407034X	PKIS2	C1(NC2=C3C(C=CC(C4=NC=CC=C4)=C3)=NC=C2)=CC=C(OC5=CC=CC=C5)C=C1
GW407323A	PKIS1	Cl.Nc1nc(cs1)-c1ccc2NC(=O)C(=Cc3cc(Br)c(O)c(Br)c3)c2c1
GW410563A	PKIS1	Cl.COc1cc2ncnc(Nc3ccc(C)c(O)c3)c2cc1OC
GW412617A	PKIS2	C[C@@H](C1=CC=CC=C1)N[C@@H]2CCC3=CC(C4=CN=C(C(C)=C4)N)=CC=C3C2.C[C@@H](C5=CC=CC=C5)N[C@@H]6CCC7=CC(C8=CN=C(C(C)=C8)N)=CC=C7C6.Cl.Cl
GW416469X	PKIS1	CN(C)c1ccc2NC(=O)\C(=C/Nc3ccc(cc3)S(N)(=O)=O)c2c1
GW416981X	PKIS1	CC(C)COC(=O)c1ccc2NC(=O)\C(=C/Nc3ccc(cc3)S(N)(=O)=O)c2c1
GW424170A	PKIS2	FC1=CC=CC=C1COC2=CC=C(C=C2Cl)NC3=C4C(C=CC(C5=NN=C(C(F)(F)F)O5)=C4)=NC=N3.Cl
GW427984X	PKIS1	CN(C)C(=O)c1cncc(\C=C\c2c(C)cc(O)cc2C)c1
GW432441X	PKIS1	CNC(=O)Oc1cc(C)c(\C=C\c2cncc(c2)C(=O)NC)c(C)c1
GW434756X	PKIS1	Fc1ccc(cc1)-c1nn2ccccc2c1-c1ccncc1
GW435821X	PKIS1	Cc1cc(O)cc(C)c1\C=C\c1cncc(c1)C(N)=O
GW439255X	PKIS1	Cc1cc(O)cc(C)c1\C=C\c1cncc(c1)C(=O)OC(C)(C)C

Compound	Library	SMILES
GW440132A	PKIS2	COC1=CC2=C(C=C1OC)C(NC3=CC=C(C(O)=C3)NC(C4=CC=C(C=C4)C)=O)=CC=N2.Cl
GW440135A	PKIS2	COC1=CC2=C(C=C1OC)C(NC3=CC=C(C=C3)OCC4=CC=C(NC(C)=O)C=C4)=CC=N2.Cl
GW440137A	PKIS2	C1(NC2=CC=NC3=C2C=CC(C4=NC=CC=C4)=C3)=CC5=C(NN=C5)C=C1.Cl
GW440138A	PKIS2	C1(NC2=CC=NC3=C2C=CC(C4=NC=CC=C4)=C3)=CC5=C(NC=C5)C=C1.Cl
GW440139A	PKIS1	Cl.Cc1ccc(O)cc1Nc1ccnc2cc(ccc12)-c1ccccn1
GW440146A	PKIS2	CC1=CC=C(C(NC2=CC=C(C=C2O)NC3=CC=NC4=C3C=CC(C5=NC=CC=C5)=C4)=O)C=C1.Cl
GW440148A	PKIS2	CC(NC1=CC=C(COC2=CC=C(NC3=CC=NC4=C3C=CC(C5=NC=CC=C5)=C4)C=C2)C=C1)=O.Cl
GW441756X	PKIS1	Cn1cc(C=C2C(=O)Nc3cccnc23)c2ccccc12
GW441806A	PKIS1	Cl.Cc1cc(O)cc(C)c1\C=C\c1cncc(c1)-c1nn[nH]n1
GW442130X	PKIS1	COc1ccccc1-c1cc(\C=C2/C(=O)Nc3ncc(Br)cc23)cc(Br)c1O
GW445012X	PKIS1	CNC(=O)c1cncc(\C=C\c2c(C)cccc2C)c1
GW445014X	PKIS1	CNC(=O)c1cncc(\C=C\c2c(Cl)cccc2Cl)c1
GW445015X	PKIS1	CNC(=O)c1cncc(\C=C\c2ccccc2C)c1
GW445017X	PKIS1	CNC(=O)c1cncc(\C=C\c2ccccc2Cl)c1
GW450241X	PKIS1	CCc1cccc(CC)c1\C=C\c1cncc(c1)C(=O)NC
GW457859A	PKIS2	CC1=CC2=C(C(C3=CC=C(F)C=C3)=NN2C=C1)C4=CC=NC=C4.Cl
GW458344A	PKIS1	Cl.Cc1cc(cc(C)c1\C=C\c1cncc(c1)-c1nn[nH]n1)-c1ccco1
GW458787A	PKIS1	Cl.CS(=O)(=O)CCNCc1ccc(o1)-c1ccc2ncnc(Nc3ccc(OCc4ccccc4)cc3)c2c1
GW459057A	PKIS1	Cl.Cc1cc(cc(C)c1\C=C\c1cncc(c1)-c1nn[nH]n1)-c1ccccn1
GW459135A	PKIS2	COCCOC1=CC2=NC=NC(NC3=CC=CC(C#C)=C3)=C2C=C1OCCOC.Cl
GW461104A	PKIS1	Cl.CS(=O)(=O)CCNCc1nc(cs1)-c1ccc2ncnc(Nc3ccc(F)c(Cl)c3)c2c1
GW461484A	PKIS2	CC1=CN2N=C(C(C3=CC=NC=C3)=C2C=C1)C4=CC=C(C=C4)F.Cl
GW461487A	PKIS2	CC1=CC=CC2=C(C(C3=CC=C(F)C=C3)=NN12)C4=CC=NC=C4.Cl
GW466413A	PKIS2	CC1=C(C=CC=C1NC2=C3C(C=CC(C(F)(F)F)=C3)=NC=C2)O.Cl
GW468513X	PKIS2	COC1=CC=CC2=C(C(C3=CC=C(F)C=C3)=NN12)C4=CC=NC=C4
GW475620X	PKIS2	FC1=CC=CN2N=C(C(C3=CC=NC=C3)=C12)C4=CC=C(F)C=C4
GW482059X	PKIS2	OC1=CC=C(C(C)C)C(NC2=CC=NC3=CC=C(C(F)(F)F)C=C32)=C1
GW493036X	PKIS2	CC1=C(NC(C2=CC=NC=C2)=C1C(C)=O)C3=CC=NC=C3
GW494601A	PKIS2	OC1=CC=CC(NC2=C3C(C=C(C4=CC=NC=C4)C=C3)=NC=C2)=C1.Cl
GW494610A	PKIS2	COC1=C(OC)C(OC)=CC(NC2=C3C(C=C(C4=CC=NC=C4)C=C3)=NC=C2)=C1.Cl
GW494702A	PKIS2	OC1=C(NC(C2=CC=C(C)C=C2)=O)C=CC(NC3=C4C(C=C(C5=NC=CS5)C=C4)=NC=C3)=C1.Cl
GW497681X	PKIS2	FC(F)(F)C(C=C1)=CC=C1CNC2=NC(C)=CC(NCC(C3=CC=CC=C3)C4=CC=CC=C4)=N2
GW513184X	PKIS1	COc1cc(C=NNc2ncnc3n(ncc23)-c2ccccc2)ccc1O
GW514784X	PKIS2	FC(C=C1)=CC=C1C2=NN3C(OCC(F)(F)F)=CC=CC3=C2C4=CC=NC=C4
GW514786X	PKIS2	FC1=CC=C(C2=NN3C(C=CC=C3SC)=C2C4=NC=NC=C4)C=C1
GW515532X	PKIS2	FC1=CC=C(C=C1)C2=NN(C(C)=CC=C3)C3=C2C4=CC=NC=N4
GW525701	KCGS	Cn1ccc(n1)-c1cccc(Nc2ccnc3cc(ccc23)-c2nccs2)c1
GW548057X	PKIS2	NC1=NC(C2=CC=CC=N2)=C(C3=C(C=CC=C4)C4=NC=C3)S1
GW549390X	PKIS1	N(c1ncc(o1)-c1ccccc1)c1ccccc1
GW551191X	PKIS2	FC1=CC(Cl)=CC=C1NC2=C(C=CC(I)=C3)C3=NC=C2

Compound	Library	SMILES
GW552771X	PKIS2	OC1=CC(NC2=C(C=CC(I)=C3)C3=NC=C2)=CC=C1F
GW554060X	PKIS2	NC1=NNC2=C1C(C3=CC=CC=C3)=C(N=N2)C4=CC=CC=C4
GW557777X	PKIS2	CC1=CC=C(O)C=C1NC2=CC=NC3=CC(C4=CC=C(O4)CN5CCCCC5)=CC=C23
GW559768X	PKIS1	Cc1ccc(O)cc1Nc1ccnc2ccc(cc12)S(C)(=O)=O
GW560106X	PKIS2	FC1=C(NC2=C(C=CC(C3=CC=C(CN4CCSCC4)O3)=C5)C5=NC=C2)C=CC(Cl)=C1
GW560109X	PKIS2	FC1=C(NC2=C(C=CC(C3=CC=C(CN4CCOCC4)O3)=C5)C5=NC=C2)C=CC(Cl)=C1
GW560116X	PKIS2	FC1=C(NC2=C(C=CC(C3=CC=C(CN4CCCCC4)O3)=C5)C5=NC=C2)C=CC(Cl)=C1
GW560459X	PKIS2	FC1=CC=CC=C1C2=C(C3=CC=NC4=CC=CC=C43)SC(N)=N2
GW561436X	PKIS1	Fc1ccc(cc1)-c1nn2cc(ccc2c1-c1ccnc(NC2CC2)n1)C#N
GW566221B	PKIS1	CS(=O)(=O)CCNCc1coc(c1)c2ccc3ncnc(Nc4ccc(OCc5ccccc5)cc4)c3c2
GW567140X	PKIS2	CN(CC1)CCN1CC2=CC=C(O2)C3=CC4=NC=CC(NC5=CC=C(OC6=NC=CC=C6)C=C5)=C4C=C3
GW567142A	PKIS2	C12=NC=CC(NC3=CC=C(OC4=NC=CC=C4)C=C3)=C1C=CC(C5=CC=C(CN6CCNCC6)O5)=C2.C78=NC=CC(NC9=CC=C(OC%10=NC=CC=C%10)C=C9)=C7C=CC(C%11=CC=C(CN%12CCNCC%12)O%11)=C8.Cl.Cl.Cl
GW567143X	PKIS2	C12=NC=CC(NC3=CC=C(OC4=NC=CC=C4)C=C3)=C1C=CC(C5=CC=C(CN6CCCCC6)O5)=C2
GW567145X	PKIS2	C12=NC=CC(NC3=CC=C(OC4=NC=CC=C4)C=C3)=C1C=CC(C5=CC=C(CNCCN6CCOCC6)O5)=C2
GW567148X	PKIS2	CN(C)CC1=CC=C(O1)C2=CC3=NC=CC(NC4=CC=C(OC5=NC=CC=C5)C=C4)=C3C=C2
GW567808A	PKIS1	Cl.CS(=O)(=O)CCNCc1ccc(o1)-c1ccc2ncnc(Nc3ccc(OCc4cccc(c4)C(F)(F)F)cc3)c2c1
GW568326X	PKIS1	Nc1nccc(n1)-c1c(nn2cc(ccc12)C(F)(F)F)-c1ccc(F)cc1
GW569293E	PKIS1	OC(=O)\C=C\C(O)=O.OCCCNc1nccc(n1)-c1c(nn2cc(ccc12)C(F)(F)F)-c1ccc(F)cc1
GW569716A	PKIS2	CS(CCNCC1=NC(C2=CC=C(N=CN=C3NC4=CC(C=NN5CC6=CC=CC=C6)=C5C=C4)C3=C2)=CS1)(=O)=O.CS(CCNCC7=NC(C8=CC=C(N=CN=C9NC%10=CC(C=NN%11CC%12=CC=CC=C%12)=C%11C=C%10)C9=C8)=CS7)(=O)=O.Cl.Cl
GW572399X	PKIS1	NS(=O)(=O)c1ccc(Nc2ncc(o2)-c2ccccc2)cc1
GW572401X	PKIS1	CCN(CC)S(=O)(=O)c1ccc(OC)c(Nc2ncc(o2)-c2ccccc2)c1
GW572738X	PKIS1	Fc1ccccc1C(=O)Nc1sc2CCCCc2c1C#N
GW574782A	PKIS1	Cl.CS(=O)(=O)CCNCc1ccc(o1)-c1ccc2ncnc(Nc3ccc(OCc4ccccc4)c(c3)C(F)(F)F)c2c1
GW574783B	PKIS1	Cl.CS(=O)(=O)CCNCc1ccc(o1)-c1ccc2ncnc(Nc3ccc(OCc4ccccc4)c(Cl)c3)c2c1
GW574783B	PKIS2	CS(CCNCC1=CC=C(C2=CC=C(N=CN=C3NC4=CC(Cl)=C(OCC5=CC=CC=C5)C=C4)C3=C2)O1)(=O)=O.CS(CCNCC6=CC=C(C7=CC=C(N=CN=C8NC9=CC(Cl)=C(OCC%10=CC=CC=C%10)C=C9)C8=C7)O6)(=O)=O.Cl.Cl
GW575533A	PKIS1	Cl.COc1ccc(Nc2ncc(o2)-c2ccccc2)cc1OC
GW575808A	PKIS1	Cl.Cc1ccc(Nc2ccnc(Nc3cccc(c3)C(N)=O)n2)cc1O
GW576484X	PKIS1	CS(=O)(=O)CCNCc1ccc(o1)-c1ccc2ncnc(Nc3ccc(OCc4cccc(F)c4)c(c3)C(F)(F)F)c2c1
GW576604X	PKIS2	C1(C2=NC=CC(C3=CNN=C3C4=CC=CC=N4)=C2)=CC=CC=C1
GW576609A	PKIS1	OC(=O)C(F)(F)F.Fc1cccc(COc2ccc(Nc3ncnc4ccc(cc34)-c3ccc(CN4CCS(=O)CC4)o3)cc2Cl)c1
GW576924A	PKIS1	Cl.Fc1cc(Nc2ncnc3ccc(cc23)-c2ccc(CN3CCS(=O)CC3)o2)ccc1OCc1ccccc1
GW577382X	PKIS2	COC1=C(OC)C=C(C=C1OC)NC2=CC=NC3=CC=C(C(F)(F)F)C=C23
GW577921A	PKIS1	Cl.COc1ccccc1Nc1ncc(o1)-c1ccccc1

Compound	Library	SMILES
GW578342X	PKIS2	CN1CCN(CC2=CC(C3=CC=C4C(N=CC=C4NC5=CC=C(OC6=CC=CC=C6)C=C5)=C3)=CC=C2)CC1
GW578748X	PKIS1	COc1cc(\C=N\Nc2ncnc3[nH]ncc23)ccc1O
GW579362A	PKIS2	CC(C=C1)=C(O)C=C1NC2=NC(NC3=CC(CS(C4)(=O)=O)=C4C=C3)=NC=C2.Cl
GW580509X	PKIS1	CCS(=O)(=O)c1ccc(OC)c(Nc2ncc(o2)-c2cccc(OC)c2)c1
GW581744X	PKIS1	NC(=O)c1ccc2c(c(nn2c1)-c1ccc(F)cc1)-c1ccnc(NCCCO)n1
GW582764A	PKIS2	CS(CCNCC1=NC(C2=CC=C(N=CN=C3NC4=CC=C(OCC5=CC=CC=C5)C(Cl)=C4)C3=C2)=CS1)(=O)=O.CS(CCNCC6=NC(C7=CC=C(N=CN=C8NC9=CC=C(OCC%10=CC=CC=C%10)C(Cl)=C9)C8=C7)=CS6)(=O)=O.Cl.Cl
GW582868A	PKIS2	OC1=C(C)C=CC(NC2=NC(NC3=CC=C(C)C(F)=C3)=NC=C2)=C1.Cl
GW583340C	PKIS2	ClC1=CC(NC2=NC=NC3=CC=C(C4=CSC(CNCCS(C)(=O)=O)=N4)C=C32)=CC=C1OCC5=CC(F)=CC=C5.Cl
GW583373A	PKIS1	Cl.Clc1cc(Nc2ncnc3ccc(cc23)-c2ccc(CN3CCS(=O)CC3)o2)ccc1OCc1ccccc1
GW589933X	PKIS1	NS(=O)(=O)c1ccc(NC=C2C(=O)Nc3ccc4ncsc4c23)cc1
GW589961A	PKIS1	Cl.COC(=O)Nc1nc2ccc(Oc3ccc(NC(=O)Nc4cccc(Cl)c4)cc3)cc2[nH]1
GW591947A	PKIS2	O=S(C1=CC=C(OC)C(NC(O2)=NC=C2C3=CC=C(F)C=C3)=C1)(CC)=O.Cl
GW595885X	PKIS2	CC1=NN=C(C2=CC=C(C)C(C3=CC=C(C(NC4=CC=C(OC)C=C4)=O)C=C3)=C2)O1
GW599550X	PKIS2	FC(F)(F)C(C=C1)=CC=C1C2=NC=CC(C3=CNN=C3C4=CC=CC=N4)=C2
GW607049C	PKIS1	OS(O)(=O)=O.COC(=O)Nc1nc2ccc(Sc3ccc(NC(=O)Nc4cc(ccc4F)C(F)(F)F)cc3)cc2[nH]1
GW607117X	PKIS1	Cc1nnc(o1)-c1ccc(C)c(c1)-c1ccc(cc1)C(=O)Nc1cccc(c1)C#N
GW608005X	PKIS2	CC1=NN=C(C2=CC=C(C)C(C3=CC=C(C(O)=O)C=C3)=C2)O1
GW612286X	PKIS1	COc1cc(Nc2nccc(Nc3ccc4c(C)n[nH]c4c3)n2)cc(OC)c1OC
GW615311X	PKIS1	Fc1cccc(COc2ccc(Nc3ncnc4ccc(cc34)-c3ccc(COCCS(=O)(=O)c4ccccc4)o3)cc2Cl)c1
GW616030X	PKIS1	CS(=O)(=O)CCN(CC#N)Cc1ccc(o1)-c1ccc2ncnc(Nc3ccc(OCc4cccc(F)c4)c(Cl)c3)c2c1
GW618013A	PKIS1	CS(O)(=O)=O.CN(C)CCCNc1nccc(n1)-c1c(nn2cc(ccc12)C(F)(F)F)-c1ccc(F)cc1
GW620972X	PKIS1	O=C(Nc1sc2CCCCc2c1C#N)c1cccc2ccccc12
GW621431X	PKIS1	CCS(=O)(=O)c1ccc(OC)c(Nc2ncc(o2)-c2cccc(c2)C(C)=O)c1
GW621581X	PKIS2	FC(C=C1)=CC=C1C2=NN3C=C(C(F)(F)F)C=CC3=C2C4=CC=NC(NCCCN5CCN(C)CC5)=N4
GW621823A	PKIS1	Cl.CCCN(CCS(C)(=O)=O)Cc1ccc(o1)-c1ccc2ncnc(Nc3ccc(OCc4cccc(F)c4)c(Cl)c3)c2c1
GW621970X	PKIS1	CCS(=O)(=O)c1ccc(OC)c(Nc2ncc(o2)-c2cccc(F)c2)c1
GW622055X	PKIS1	CCS(=O)(=O)c1ccc(OC)c(Nc2ncc(o2)-c2ccccc2Cl)c1
GW622475X	PKIS2	O=C(N)C1=CN2N=C(C3=CC=C(F)C=C3)C(C4=CC=NC(NCCCN5CCN(C)CC5)=N4)=C2C=C1
GW627512B	PKIS1	COc1cc(Nc2ncc(o2)-c2ccccc2)cc(OC)c1OC
GW627834A	PKIS1	Cl.N#Cc1cccc(Nc2ncc(o2)-c2ccccc2)c1
GW630813X	PKIS2	FC(F)(F)C1=CN2C(C=C1)=C(C3=CC=NC(NCCCO)=N3)C(C4=CC(C(F)(F)F)=CC=C4)=N2
GW630823A	PKIS2	FC(C1=CC(NC2=C(C)C=CC(O)=C2)=C3C(C=CC(C4=CC=NC=C4)=C3)=N1)(F)F.Cl
GW631581B	PKIS1	COc1cc(Nc2ncc(o2)-c2ccccc2)cc(OC)c1
GW632046X	PKIS1	Cc1cccc(Nc2ncc(o2)-c2ccccc2)c1
GW632580X	PKIS1	COc1ccc(COc2ccc(Cc3cnc(N)nc3N)cc2OC)cc1

Compound	Library	SMILES
GW633459A	PKIS1	Cl.Fc1cccc(COc2ccc(Nc3ncnc4ccc(cc34)-c3ccc(CNCCS(=O)(=O)c4ccccc4)o3)cc2Cl)c1
GW635815X	PKIS2	O=C(C1=CSC=C1)NC2=NC(C=C3CN4CCN(S(=O)(C(C)C)=O)CC4)=C(C=C3)N2C[C@H](O)C5=CC=CC=C5
GW639905A	PKIS2	N#CCC1=CC=C(C=C1)NC2=NC=CC(NC3=CC=C(OC4=CC=CC=C4)C=C3)=N2.Cl
GW641155A	PKIS1	Cl.N(c1ncc(o1)-c1ccccc1)c1ccc(Oc2ccccc2)cc1
GW642125X	PKIS1	COc1ccc(cc1)-c1coc2ncnc(N)c12
GW642138X	PKIS1	COc1ccc(cc1)-c1cc2c(N)ncnc2o1
GW643971X	PKIS1	COc1cc(C=NNc2ncnc3n(Cc4ccccc4)ncc23)ccc1O
GW644007X	PKIS1	COc1cc(ccc1O)\C=N\Nc1ncnc2n(ncc12)C(C)C
GW651576X	PKIS1	Fc1cccc(COc2ccc(Nc3ncncc3C#Cc3ccccc3)cc2Cl)c1
GW654607A	PKIS2	O=C(OC)NC1=NC2=CC=C(OC3=CC=C(NC(NC4=C(F)C=CC(C(F)(F)F)=C4)=O)C=C3)C=C2N1.Cl
GW654652C	PKIS1	Cl.CCS(=O)(=O)c1ccc(OC)c(Nc2nccc(n2)N(C)c2ccc3c(C)n[nH]c3c2)c1
GW659008A	PKIS2	O=C(N)C1=CC(NC2=NC=CC(NC3=CC=C(OC4=CC=CC(Cl)=C4)C(Cl)=C3)=N2)=CC=C1.Cl
GW659009A	PKIS2	O=C(N)C1=CC(NC2=NC=CC(NC3=CC=C(OC4=C(Cl)C=CC=C4Cl)C(Cl)=C3)=N2)=CC=C1.Cl
GW659386A	PKIS1	Cl.COC(=O)Nc1nc2cc(Oc3cccc(NC(=O)Nc4cc(ccc4F)C(F)(F)F)c3)ccc2[nH]1
GW659893X	PKIS1	Nc1ccc(cc1)C#Cc1cncnc1Nc1ccc(OCc2cccc(F)c2)c(Cl)c1
GW663929X	PKIS2	O=C(NCCCN1CCOCC1)C2=CC=CC(NC3=NC=CC(NC4=CC=C(C=C4)OC5=CC=CC=C5)=N3)=C2
GW664114X	PKIS2	N#CC1=CN=C2C(C=CC(C3=CN=C(CNCCN4CCOCC4)S3)=C2)=C1NC5=CC=C(OC6=CC=CC=C6)C=C5
GW673715X	PKIS1	CCc1cccc(NC(=O)Nc2ccc(Oc3ccc4nc(NC(=O)OC)[nH]c4c3)cc2)c1
GW678313X	PKIS1	CCS(=O)(=O)c1ccc(OC)c(Nc2ncc(o2)-c2cccc(c2)-c2ccccc2F)c1
GW679395X	PKIS2	CC1=CC=CC(C2=NC=CC(C3=CNN=C3C4=CC=CC=N4)=C2)=C1
GW679396X	PKIS2	FC(F)(F)C1=C(C=CC=C1)C2=NC=CC(C3=CNN=C3C4=CC=CC=N4)=C2
GW679410X	PKIS1	COc1ccc(cc1)-c1cc(ccn1)-c1c[nH]nc1-c1ccccn1
GW679662X	PKIS2	CC1=NN=C(C2=CC=C(C)C(C3=CC=C(C(NCC4CC4)=O)C=C3)=C2)O1
GW680061X	PKIS2	CC1=C(C=CC=C1)C2=NC=CC(C3=CNN=C3C4=CC=CC=N4)=C2
GW680191X	PKIS1	CS(=O)(=O)CCNCCCCOc1ccc2ncnc(Nc3cccc(c3)C#C)c2c1
GW680338X	PKIS2	COC1=CC=CC(C2=NC=CC(C3=CNN=C3C4=CC=CC=N4)=C2)=C1
GW680903X	PKIS2	O=C(OC)NC1=NC2=C(C=C(OC3=CC=C(CC(NC4=CC(C(F)(F)F)=CC=C4F)=O)C=C3)C=C2)N1
GW680908A	PKIS1	Cl.COC(=O)Nc1nc2ccc(cc2[nH]1)S(=O)(=O)c1ccc(NC(=O)Nc2cc(ccc2F)C(F)(F)F)cc1
GW680975X	PKIS1	Fc1ccc(cc1)-c1cc(ccn1)-c1c[nH]nc1-c1ccccn1
GW681170A	PKIS2	O=C(OC)NC1=NC(C=C(OC2=CC=C(NC(NC3=CC(C(F)(F)F)=CC=C3F)=O)C=N2)C=C4)=C4N1.O=C(OC)NC5=NC(C=C(OC6=CC=C(NC(NC7=CC(C(F)(F)F)=CC=C7F)=O)C=N6)C=C8)=C8N5.Cl.Cl
GW681251X	PKIS2	ClC1=CC=C(C=C1)C2=NC=CC(C3=CNN=C3C4=CC=CC=N4)=C2
GW682569X	PKIS2	CC1=NNC2=C1C=CC(NC3=NC(NC4=CC(CN5CCOCC5)=CC=C4)=NC=C3)=C2
GW682841X	PKIS1	CC(C)c1ccc(cc1)-c1cc(ccn1)-c1c[nH]nc1-c1ccccn1
GW683003X	PKIS1	FC(F)(F)CNc1nccc(n1)-c1cnn2ncccc12
GW683109X	PKIS1	C(CNc1nccc(n1)-c1cnn2ncccc12)CN1CCOCC1
GW683134A	KCGS	Cl.Fc1ccc(cc1NC(=O)Nc1ccc(Oc2ccc3[nH]c(NC(=O)c4ccco4)nc3c2)cc1)C(F)(F)F

Compound	Library	SMILES
GW683768X	PKIS1	CCc1nn2ncccc2c1-c1ccnc(NC2CC2)n1
GW684083X	PKIS2	NC1=NC(C2=CC=CN=C2)=C(S1)C3=CC=NC4=CC=CC=C34
GW684088X	PKIS2	CC1=CC=C(C=C1)C2=CC(C3=CNN=C3C4=CC=CC=N4)=CC=N2
GW684374X	PKIS2	CCCCC1=NN2N=CC=CC2=C1C3=CC=NC(NC4CC4)=N3
GW684626B	PKIS1	Fc1cccc(COc2ccc(Nc3ncnc4sc(cc34)-c3cccs3)cc2Cl)c1
GW684941X	PKIS2	CN(CC1)CCN1C(C=C2)=CC=C2NC3=NC=CC(C4=C(C=CC=N5)N5N=C4CCCC)=N3
GW689066X	PKIS2	ClC1=CC(NC2=NC=NC3=NN4C=CC=CC4=C32)=CC=C1OCC5=CC=CC(F)=C5
GW692089A	PKIS2	FC(F)(F)C1=CC(NC(NC2=CC=C(OC3=CC=C(N=C(NC(OC)=O)N4C)C4=C3)C=C2)=O)=C(F)C=C1.Cl
GW693028X	PKIS2	N#CC1=CC=C(C=C1)C2=CC(C3=CNN=C3C4=CC=CC=N4)=CC=N2
GW693481X	PKIS1	Nc1nc(c(s1)-c1ccc2ncccc2n1)-c1ccccn1
GW693542X	PKIS2	NC1=NC(C2=NC=CS2)=C(S1)C3=CC=NC4=CC=CC=C34
GW693881A	PKIS1	Cl.Fc1cccc(COc2ccc(Nc3ncnc4cc(sc34)-c3ccc[nH]3)cc2Cl)c1
GW693917A	PKIS1	Cl.COC(=O)Nc1nc2ccc(Oc3ccc(NC(=O)Nc4cc(ccc4F)C(F)(F)F)cc3)cc2s1
GW694077X	PKIS2	C1(C2=CC=CC=N2)=NNC=C1NC3=CC=NC4=CC=CC=C34
GW694234A	PKIS1	Cl.COC(=O)Nc1nc2cc(Oc3ccc(NC(=O)Nc4cccc(Br)c4)cc3)ccc2[nH]1
GW694590A	PKIS1	Cl.COC(=O)Nc1nc2cc(Oc3ccc(NC(=O)Nc4ccccc4)cc3)ccc2[nH]1
GW695874X	PKIS1	C(CN1CCOCC1)Oc1ccc(cc1)-c1cc(ccn1)-c1c[nH]nc1-c1ccccn1
GW696155X	PKIS2	CN(CC1)CCN1C(C=C2)=CC=C2NC3=NC(C4=C5C=CC(OC(C)C)=NN5N=C4)=CC=N3
GW697465A	PKIS2	O=C(OC)NC1=NC(C=C(OC2=CC=C(NC(NC3=CC(C(F)(F)F)=CC=C3Cl)=O)C=C2)C=C4)=C4N1.Cl
GW697999A	PKIS2	O=C(OC)NC1=NC2=CC(OC3=CC=C(NC(NC4=CC=CC(SC)=C4)=O)C=C3)=CC=C2N1.Cl
GW700494A	PKIS1	Cl.CN1CCN(CCCNc2nc3ccc(Oc4ccc(NC(=O)Nc5cc(ccc5F)C(F)(F)F)cc4)cc3[nH]2)CC1
GW701032X	PKIS1	COc1ccc(CNC(=O)c2ccc(cc2)-c2cc(ccc2C)-c2nnc(C)o2)cc1
GW701424A	PKIS2	O=C(OC)NC1=NC(C=C(OC2=CC=C(NC(NC3=CC(F)=CC=C3F)=O)C=C2)C=C4)=C4N1.Cl
GW701427A	PKIS1	Cl.COC(=O)Nc1nc2cc(Oc3ccc(NC(=O)Nc4cccc(c4)C(O)=O)cc3)ccc2[nH]1
GW702865X	PKIS2	CC(C=CC(C1=NN=C(C)O1)=C2)=C2C3=CC=C(C(NC4=CC=C(NS(=O)(C)=O)C=C4)=O)C=C3
GW703087X	PKIS1	CC(=O)Nc1cccc(c1)C#Cc1cncnc1Nc1ccc(OCc2cccc(F)c2)c(Cl)c1
GW707818B	PKIS2	ClC1=CC(NC2=NC=NC3=C2C=C(C4=CC=CN4)S3)=CC=C1OCC5=CC(F)=CC=C5
GW708336X	PKIS1	C1CC1Nc1nccc(n1)-c1cnn2nc(ccc12)N1CCOCC1
GW708893X	PKIS1	Cc1nnc(o1)-c1ccc(C)c(c1)-c1ccc(cc1)C(=O)NCc1ccc(Cl)cc1
GW709042A	PKIS1	Cl.Fc1ccc(cc1NC(=O)Nc1ccc(Oc2ccc3[nH]c(NC(=O)c4ccccc4)nc3c2)cc1)C(F)(F)F
GW709199X	PKIS2	FC(F)(F)C(C=C1)=CC=C1/C=C/C2=CN=CN=C2NC3=CC(N=C(CC4=CC=CC=C4)N5)=C5C=C3
GW709213X	PKIS2	C1(NCC2=CC=C(C3=NC=CC(C4=CNN=C4C5=CC=CC=N5)=C3)C=C2)CCOCC1
GW711782X	PKIS1	C(Cn1ccnc1)Oc1ccc(cc1)-c1cc(ccn1)-c1c[nH]nc1-c1ccccn1
GW734508X	PKIS1	Cc1nnc(o1)-c1cccc(c1)-c1ccc(cc1)C(=O)NCC1CC1
GW743024X	PKIS1	Cc1ccc(NC(=O)c2ccoc2)cc1-c1ccc(cc1)C(=O)NCC1CC1
GW759710A	PKIS1	Cl.NC(=O)c1cccc(Nc2nccc(Nc3cccc(F)c3)n2)c1
GW767488X	PKIS2	CN(C)CC(O)COC(C=C1)=CC=C1NC2=NC(C3=C(C=CC(N4CCOCC4)=N5)N5N=C3)=CC=N2

Compound	Library	SMILES
GW768504A	PKIS2	CN(CC1)CCN1CCNC2=NC(C=C(OC3=CC=C(NC(NC4=CC(C(F)(F)F)=CC=C4F)=O)C=C3)C=C5)=C5N2.CN(CC6)CCN6CCNC7=NC(C=C(OC8=CC=C(NC(NC9=CC(C(F)(F)F)=CC=C9F)=O)C=C8)C=C%10)=C%10N7.Cl.Cl
GW768505A	PKIS1	Cl.COc1ccc(cc1)-c1oc2ncnc(N)c2c1-c1ccc(NC(=O)Nc2cc(ccc2F)C(F)(F)F)cc1
GW769076X	PKIS1	Cc1ccc(NC(=O)c2ccnc(c2)N2CCCC2)cc1-c1ccc(cc1)C(=O)NCC1CC1
GW770220A	PKIS1	Cl.CN(c1ccc2c(C)nn(C)c2c1)c1ccnc(Nc2cccc(c2)S(N)(=O)=O)n1
GW770249A	PKIS1	Nc1ncnc2occ(-c3ccc(NC(=O)Nc4cc(ccc4F)C(F)(F)F)cc3)c12
GW771127A	PKIS1	Cl.CN(c1ccc2c(C)n(C)nc2c1)c1ccnc(Nc2cccc(c2)S(N)(=O)=O)n1
GW772405X	PKIS1	CNC(=O)c1cccc(c1)C#Cc1cncnc1Nc1ccc(OCc2cccc(F)c2)c(Cl)c1
GW775604X	PKIS2	O=C(NCC1CC1)C2=CC=C(C3=C(C)C=CC(NC(C4=CC(N5CCN(C)CC5)=NC=C4)=O)=C3)C=C2
GW775608X	PKIS1	Cc1ccc(NC(=O)c2ccnc(c2)N2CCOCC2)cc1-c1ccc(cc1)C(=O)NCC1CC1
GW775610X	PKIS2	O=C(NCC1CC1)C2=CC=C(C3=C(C)C=CC(NC(C4=CC(N5CCCCC5)=NC=C4)=O)=C3)C=C2
GW776245A	PKIS2	N1(CC2=CC=C(C3=NC=CC(C4=CNN=C4C5=CC=CC=N5)=C3)C=C2)CCOCC1.Cl
GW777257X	PKIS2	CC1=C2C(C=CC(C3=C(C4=CC=CC=N4)N=C(N)S3)=N2)=NC=C1
GW778894X	PKIS1	N#Cc1cccc(Nc2nccc(n2)-c2cnn3ncccc23)c1
GW779439X	PKIS1	CN1CCN(CC1)c1ccc(Nc2nccc(n2)-c2cnn3ncccc23)cc1C(F)(F)F
GW780056X	PKIS1	CCN(CC)Cc1ccc(Nc2nccc(n2)-c2cnn3ncccc23)cc1
GW780159X	PKIS1	Nc1nc(c(s1)-c1ccc2ncccc2n1)-c1cccc(Cl)c1
GW781483X	PKIS2	ClC1=C(F)C=CC(NC2=NC=NC3=C2C=C(NC(C=C)=O)C(OCCCN4CCOCC4)=C3)=C1
GW781673X	PKIS1	Clc1ccc(CNc2nccc(n2)-c2cnn3ncccc23)cc1
GW782612X	PKIS1	NC(=O)c1cccc(Nc2nccc(Nc3cccc4[nH]ncc34)n2)c1
GW782907X	PKIS1	Cc1ccc(cc1-c1ccc(cc1)C(=O)NCC1CC1)C(=O)NC1CCCCC1
GW782912X	PKIS1	Cc1ccc(cc1-c1ccc(cc1)C(=O)NCC1CC1)C(=O)NC1CCC1
GW784041A	PKIS2	CC1=C(NC2=NC(NC3=CC=C(C4=CN=CN4)C=C3)=NC=C2)C=C(OC)C=C1.Cl
GW784307A	PKIS1	Cl.COc1cccc(c1)-n1ncc2c(N\N=C\c3ccc(cc3)C(=O)NCCN(C)C)ncnc12
GW784684X	PKIS1	CN1CCN(Cc2ccc(o2)-c2cc3ncnc(Nc4ccc(OCc5cccc(F)c5)c(Cl)c4)c3s2)CC1
GW784752X	PKIS1	COc1cccc(c1)-n1ncc2c(N\N=C\c3ccncc3)ncnc12
GW785404X	PKIS1	CCn1c(nc2ccc(F)cc12)-c1nonc1N
GW785804X	PKIS1	Nc1nc(c(s1)-c1ccc2ncccc2n1)-c1ccc(F)cc1
GW785974X	PKIS1	CC(C)NC(=O)c1ccc(C)c(c1)-c1ccc(cc1)C(=O)NCC1CC1
GW786460X	PKIS1	Cc1cccc(n1)-c1n[nH]cc1-c1ccc2ncccc2n1
GW787226A	PKIS2	CC1=C(C=C2)C(C=C2N(C)C3=NC(NC4=CC(S(=O)(N)=O)=CC=C4)=NC=C3)=NN1CC5=CC=CC=C5.CC6=C(C=C7)C(C=C7N(C)C8=NC(NC9=CC(S(=O)(N)=O)=CC=C9)=NC=C8)=NN6CC%10=CC=CC=C%10.Cl.Cl
GW789449X	PKIS2	NC(C1=C(NC(N)=O)SC(C(C=C2)=CC=C2F)=C1)=O
GW792479X	PKIS2	O=C(N1CCCC1)C2=CC=C(C=C2)C3=NC=CC(C4=CNN=C4C5=CC=CC=N5)=C3
GW794607X	PKIS1	CCCNc1cccc(c1)-n1ncc2c(N\N=C\c3ccncc3)ncnc12
GW794726X	PKIS1	CC(=O)Nc1cccc(n1)C#Cc1cncnc1Nc1ccc(OCc2cccc(F)c2)c(Cl)c1
GW795486X	PKIS1	Nc1ncnc2occ(-c3ccc(NC(=O)Nc4cc(cc(c4)C(F)(F)F)C(F)(F)F)cc3)c12
GW795493X	PKIS1	Nc1ncnc2occ(-c3ccc(NC(=O)Nc4cccc(c4)C(F)(F)F)cc3)c12
GW796920X	PKIS1	Cc1ccc(NC(=O)CC2CC2)cc1-c1ccc(cc1)C(=O)NCC1CC1
GW796921X	PKIS1	CCC(=O)Nc1ccc(C)c(c1)-c1ccc(cc1)C(=O)NCC1CC1
GW799251X	PKIS1	Nc1nccc(n1)C#Cc1cncnc1Nc1ccc(OCc2cccc(F)c2)c(Cl)c1

Appendix

Compound	Library	SMILES
GW800172X	PKIS2	O=C(C1=CC=C(C2=CC(C(NC3CCCC3)=O)=CC=C2C)C=C1)NCC4CC4
GW801372X	PKIS1	COc1cc(Nc2nccc(n2)-c2cnn3ncccc23)cc(OC)c1
GW804482X	PKIS1	COc1cccc(COc2cc(sc2C(N)=O)-n2cnc3ccccc23)c1
GW805758X	PKIS1	CC(C)c1ccc(Nc2nccc(n2)-c2cnn3ncccc23)cc1
GW806290X	PKIS1	C1COc2cc(Nc3nccc(n3)-c3cnn4ncccc34)ccc2O1
GW806742X	PKIS1	CN(c1ccc(NC(=O)Nc2ccc(OC(F)(F)F)cc2)cc1)c1ccnc(Nc2cccc(c2)S(N)(=O)=O)n1
GW806776X	PKIS1	O=C(NCC1CC1)c1ccc(cc1)-c1cccc(c1)C(=O)NC1CC1
GW807930X	PKIS1	CC(=O)NCc1cccc(c1)C#Cc1cncnc1Nc1ccc(OCc2cccc(F)c2)c(Cl)c1
GW807982X	PKIS1	CCOc1ccc2c(cnn2n1)-c1ccnc(Nc2cc(OC)cc(c2)C(F)(F)F)n1
GW809885X	PKIS1	COc1cccc(c1)-n1nc(C)c2c(N\N=C(/C)c3ccncc3)ncnc12
GW809893X	PKIS2	CN(C1=CC=C(NC(NC2=CC(C(F)(F)F)=CC=C2F)=O)C=C1)C3=NC(NC4=CC=C(S(N)(=O)=O)C=C4)=NC=C3
GW809897X	PKIS1	CN(c1ccc(NC(=O)Nc2c(Cl)cccc2Cl)cc1)c1ccnc(Nc2cccc(CS(C)(=O)=O)c2)n1
GW810083X	PKIS2	O=C(N(C)C1CCOCC1)C2=CC=C(C=C2)C3=NC=CC(C4=CNN=C4C5=CC=CC=N5)=C3
GW810372X	PKIS1	COc1ccc2c(cnn2n1)-c1ccnc(Nc2cccc(OC(F)(F)F)c2)n1
GW810437X	PKIS2	O=C(C1=COC=C1)NC2=CC(C3=CC=C(C(NCC4CC4)=O)C=C3)=C(OC)C=C2
GW810445X	PKIS2	O=C(NCC1CC1)C2=CC=C(C3=C(F)C=CC(C(NC4CC4)=O)=C3)C=C2
GW810576X	PKIS1	COc1cccc(Nc2nccc(n2)-c2cnn3ncccc23)c1
GW810578X	PKIS2	BrC1=CC(NC2=NC=CC(C3=C4C=CC=NN4N=C3)=N2)=CC(C(F)(F)F)=C1
GW811168X	PKIS1	COc1cccc(c1)-n1ncc2c(N\N=C\c3ccc(cc3)S(C)(=O)=O)ncnc12
GW811603A	PKIS2	CN(C1=CC=NC(NC2=CC=C(CS(C)(=O)=O)C=C2)=N1)C3=CC=C4N(C)C(NCC5=CC=CC=C5)=NC4=C3.Cl
GW811761X	PKIS1	CCOc1ccc2c(cnn2n1)-c1ccnc(Nc2cccc(c2)C(F)(F)F)n1
GW812171X	PKIS2	O=C(N1CCOCC1)C2=CC=C(C=C2)C3=CC(C4=CNN=C4C5=CC=CC=N5)=CC=N3
GW813244A	PKIS2	CN1C(NCC2=CC=C(F)C=C2)=NC3=CC(N(C4=CC=NC(NC5=CC=C(CS(C)(=O)=O)C=C5)=N4)C)=CC=C13.Cl
GW813349X	PKIS2	NC(C(SC(N1C=NC2=C1C=CC(Cl)=C2)=C3)=C3OCC4=CC=CC=C4C)=O
GW813360X	PKIS1	COc1cccc(c1)-n1cnc2c(N\N=C\c3ccncc3)ncnc12
GW814408X	PKIS1	COc1cccc(c1)-c1c[nH]c2c(N\N=C\c3ccncc3)ncnc12
GW817394X	PKIS1	COc1cccc(c1)-n1ncc2c(N\N=C\c3cccc(F)c3)ncnc12
GW817396X	PKIS1	COc1cccc(c1)-n1ncc2c(N\N=C\c3ccc(F)cc3)ncnc12
GW818933X	PKIS2	O=C(NCCC)NC1=CC=C(N(C2=CC=NC(NC3CC3)=N2)C)C=C1
GW818941X	PKIS2	C(C=C1)(C2=CC=CC=C2)=NN3C1=C(C4=NC(NC5=CC=C(OCCO6)C6=C5)=NC=C4)C=N3
GW819077X	PKIS1	FC(F)(F)c1cccc(Nc2nccc(n2)-c2cnn3nc(ccc23)-c2ccccc2)c1
GW819230X	PKIS1	Cc1ccc(cc1)-c1cc2c(NC(=O)C3CC3)ncnc2o1
GW819776X	PKIS2	CC1=NN2N=CC(C3=NC(NC4=CC=C(C(F)(F)F)C=C4)=NC=C3)=C2C=C1
GW820759X	PKIS1	Cc1ccc(cc1-c1ccc2[nH]ncc2c1)C(=O)NC1CC1
GW823670X	PKIS2	O=C(C1=CNC(C(NCC2=CC=CS2)=O)=C1)C(C(Cl)=CC=C3)=C3Cl
GW824645A	PKIS2	O=S(C1=CC(NC2=CC(C3=CC=C(F)C=C3)=NN2)=CC=C1)(N)=O.Cl
GW827102X	PKIS1	FC(F)(F)c1cccc(c1)-c1nn2ncccc2c1-c1ccnc(Nc2ccc3OCCOc3c2)n1
GW827105X	PKIS1	COc1ccc(cc1)-c1nn2ncccc2c1-c1ccnc(Nc2cccc(c2)C(F)(F)F)n1
GW827106X	PKIS1	COc1ccc(cc1)-c1nn2ncccc2c1-c1ccnc(Nc2ccc3OCCOc3c2)n1
GW827396X	PKIS1	COc1ccc(cc1)-c1nn2ncccc2c1-c1ccnc(Nc2ccc(F)c(F)c2)n1

Compound	Library	SMILES
GW827654A	PKIS2	O=C(NC1=CC=C(CN2CCN(C)CC2)C=C1)NC3=CC=C(N(C4=CC=NC(NC5=CC=C(CS(C)(=O)=O)C=C5)=N4)C)C=C3.Cl
GW828205X	PKIS2	FC(F)(F)C1=CC=CC(NC2=NC=CC(C3=C4C=CC=NN4N=C3C5=CC=C(C(F)(F)F)C=C5)=N2)=C1
GW828206X	PKIS2	FC(F)(F)C1=CC=C(C2=NN3N=CC=CC3=C2C4=NC(NC5=CC=CC=C5)=NC=C4)C=C1
GW828525X	PKIS1	FC(F)(F)c1ccc(cc1)-c1nn2ncccc2c1-c1ccnc(Nc2ccc3OCCOc3c2)n1
GW828529X	PKIS1	Fc1ccc(Nc2nccc(n2)-c2c(nn3ncccc23)-c2ccc(cc2)C(F)(F)F)cc1F
GW829055X	PKIS1	Clc1ccc(cc1)-c1nn2ncccc2c1-c1ccnc(Nc2ccccc2)n1
GW829058X	PKIS2	ClC(C=C1)=CC=C1C2=NN3N=CC=CC3=C2C4=CC=NC(NC5=CC(F)=C(F)C=C5)=N4
GW829115X	PKIS1	COc1ccc(cc1)-c1nn2ncccc2c1-c1ccnc(Nc2ccc(Cl)c(c2)C(F)(F)F)n1
GW829116X	PKIS2	ClC(C=C1)=CC=C1C2=NN3N=CC=CC3=C2C4=CC=NC(NC5=CC(OCCO6)=C6C=C5)=N4
GW829350X	PKIS2	FC(F)(F)C1=CC=C(C2=NN3N=CC=CC3=C2C4=NC(NC5=CC(C(F)(F)F)=C(Cl)C=C5)=NC=C4)C=C1
GW829351X	PKIS2	ClC1=CC=C(C2=NN3N=CC=CC3=C2C4=NC(NC5=CC(C(F)(F)F)=C(Cl)C=C5)=NC=C4)C=C1
GW829874X	PKIS1	COc1cccc(\C=N\Nc2ncnc3n(ncc23)-c2cccc(OC)c2)c1
GW829877X	PKIS1	COc1cccc(c1)-n1ncc2c(N\N=C\c3ccc(C)cc3)ncnc12
GW829906X	PKIS1	Cc1ccc2c(c(nn2n1)-c1ccccc1)-c1ccnc(Nc2cccc(c2)C(F)(F)F)n1
GW830263A	PKIS1	Cl.CN(c1ccc(NC(=O)Nc2ccc(cc2)C(=O)N2CCN(C)CC2)cc1)c1ccnc(Nc2ccc(CS(C)(=O)=O)cc2)n1
GW830365A	PKIS1	Cl.CN(c1ccc(NC(=O)NCCN2CCOCC2)cc1)c1ccnc(Nc2ccc(CS(C)(=O)=O)cc2)n1
GW830707A	PKIS2	CN(C1=CC=C(NC(NC2=CC=CC(Cl)=C2)=O)C=C1)C3=NC(N)=NC=C3.Cl
GW830899A	PKIS2	CN(C1=CC=C(NC(N2CCN(CCCN3CCOCC3)CC2)=O)C=C1)C4=NC(NC5=CC=C(CS(C)(=O)=O)C=C5)=NC=C4.Cl
GW830900A	PKIS1	Cl.CN(C)CCNC(=O)Nc1ccc(cc1)N(C)c1ccnc(Nc2ccc(CS(C)(=O)=O)cc2)n1
GW831091X	PKIS1	NS(=O)(=O)c1ccc(Nc2cc(n[nH]2)-c2ccc(O)c(F)c2)cc1
GW832467X	PKIS1	Cc1ccc2c(c(nn2n1)-c1ccc(cc1)C(F)(F)F)-c1ccnc(Nc2ccc3OCCOc3c2)n1
GW832476X	KCGS	NS(=O)(=O)c1ccc(Nc2cc(n[nH]2)-c2cccc(O)c2)cc1
GW833373X	PKIS1	Cc1ccc2c(c(nn2n1)-c1ccc(F)cc1)-c1ccnc(Nc2ccccc2)n1
GW835314X	PKIS2	CN(C)CCOC1=CC=C(C2=NC=CC(C3=CNN=C3C4=CC=CC=N4)=C2)C=C1
GW837331X	PKIS1	COc1cc(Nc2ncc3c(C)nc(-c4cccc(c4)C(F)(F)F)n3n2)cc(OC)c1OC
GW839464X	PKIS2	O=C(NC1=CC(C(C)(C)C)=NN1C2=CC=C(C)C=C2)NC3=C(C=CC=C4)C4=C(OCCN5CCOCC5)C=C3
GW843682X	PKIS1	COc1cc2ncn(-c3cc(OCc4ccccc4C(F)(F)F)c(s3)C(N)=O)c2cc1OC
GW846105X	PKIS1	O=C(Nc1sc2N(CCCc2c1C#N)C(=O)C1CC1)c1cccc2ccccc12
GW852849X	PKIS1	COc1cc2ncn(-c3cc(OCc4ccccc4Cl)c(s3)C(N)=O)c2cc1OC
GW853606X	PKIS1	NC(=O)c1sc(cc1OCc1ccccc1Br)-n1cnc2ccc(cc12)C(F)(F)F
GW853609X	PKIS1	NC(=O)c1sc(cc1OCc1ccccc1Br)-n1cnc2cc(ccc12)C(F)(F)F
GW854278X	PKIS2	NC(C(SC(N1C=NC2=C1C=C(OC)C(OC)=C2)=C3)=C3OCC4=C(Br)C=NC=C4)=O
GW855857X	PKIS2	CC1=NC(C2=NC3=CC=CC=C3C(NC4=CC=NC=C4)=N2)=CC=C1
GW856795X	PKIS2	OC1=CC(NC2=C3C(C=CC(C(C)(C)C)=C3)=NC=C2)=CC=C1
GW856804X	PKIS1	Nc1ncc(-c2cccc(c2)S(N)(=O)=O)c2scc(-c3ccc(F)c(Cl)c3)c12
GW856805X	PKIS2	CC(C)(C)C1=CC2=C(NC3=C(C)C=CC(O)=C3)C=CN=C2C=C1
GW857175X	PKIS2	CC1=NC(C2=NC3=CC=CC=C3C(NC4=CC5=C(NN=C5)C=C4)=N2)=CC=C1
GW861893X	PKIS1	COc1cc(Nc2ncc3c(C)nc(-c4cccc(Oc5ccccc5)c4)n3n2)cc(OC)c1OC

Appendix

Compound	Library	SMILES
GW867253X	PKIS2	NS(C1=CC=CC(C2=CC=C3N=CC=C(C4=CC=CC(S(N)(=O)=O)=C4)C3=C2)=C1)(=O)=O
GW867587X	PKIS2	CC1=NC(C2=NC3=CC=CC=C3C(NC4=CC(N=NN5)=C5C=C4)=N2)=CC=C1
GW867588X	PKIS2	CC1=NC(C2=NC3=CC=CC=C3C(NC4=CC(SC=N5)=C5C=C4)=N2)=CC=C1
GW868318X	PKIS2	COCCNC(C1=CC=C(C2=C(C)C(F)=CC(C(NC3CC3)=O)=C2)C=C1)=O
GW869516X	PKIS2	CC1=C2C=NC(NC3=CC(OC)=C(OC)C(OC)=C3)=NN2C(C4=CC(C=CC=C5)=C5N4)=N1
GW869640X	PKIS2	CC1=CSC(C2=NC3=CC=CC=C3C(NC4=CC=NC=C4)=N2)=N1
GW869641X	PKIS2	CC1=NC(C(N=C2NC3=CC=NC=C3)=NC4=C2SC=C4)=CC=C1
GW869810X	PKIS1	Fc1cccc(COc2ccc(Nc3ncnc4cc(sc34)C#C[C@@H]3C[C@H](CN3)OC(=O)N3CCOCC3)cc2Cl)c1
GW869979X	PKIS2	NC(C(SC(N1C=NC(C=C2OC)=C1C=C2OC)=C3)=C3OCC4=CC=C(S(C)(=O)=O)C=C4)=O
GW872411X	PKIS2	CC1=NC(C2=NC3=CC=CC=C3C(NC4=CC(C)=NC=C4)=N2)=CC=C1
GW873004X	PKIS2	ClC1=CC(C2=NC3=CC=CC=C3C(NC4=CC=NC=C4)=N2)=CC=C1
GW874091X	PKIS1	Cc1nc(-c2ccccc2)n2nc(NCCCN3CCOCC3)ncc12
GW876019X	PKIS2	CC1=NC(C2=NC3=CC=CC=C3C(NC4=CC=CC(C(N)=O)=C4)=N2)=CC=C1
GW876731X	PKIS2	CN1N=CC2=C1C=CC(NC3=NC(C4=CC=CC(C)=N4)=NC5=CC=CC=C35)=C2
GW876790X	PKIS1	CCn1c(nc2cncc(C(=O)NCCNC)c12)-c1nonc1N
HG-10-102-01	KCGS	O=C(C1=CC(OC)=C(NC2=NC=C(Cl)C(NC)=N2)C=C1)N3CCOCC3
HTH-01-015	KCGS	O=C1N(C)C2=C(N=C(NC3=CN(C4CCNCC4)N=C3)N=C2C)N(C)C5=CC6=CC=CC=C6C=C51
Ibrutinib	Clinical KIs	Nc1ncnc2c1c(nn2[C@@H]3CCCN(C3)C(=O)C=C)c4ccc(Oc5ccccc5)cc4
Icotinib	Clinical KIs	C#Cc1cccc(Nc2ncnc3cc4OCCOCCOCCOc4cc23)c1
Idelalisib	Clinical KIs	CC[C@H](Nc1ncnc2[nH]cnc12)C3=Nc4cccc(F)c4C(=O)N3c5ccccc5
Imatinib	Clinical KIs	CN1CCN(Cc2ccc(cc2)C(=O)Nc3ccc(C)c(Nc4nccc(n4)c5cccnc5)c3)CC1
JH-II-127	KCGS	CNC1=C2C(NC=C2Cl)=NC(NC3=CC=C(C(N4CCOCC4)=O)C=C3OC)=N1
JNK-IN-7	KCGS	O=C(NC1=CC=C(NC2=NC=CC(C3=CC=CN=C3)=N2)C(C)=C1)C4=CC=CC(NC(/C=C/CN(C)C)=O)=C4
K05908	KCGS	COC1=CC(C2=CN=CC(C3=CN(C4CCNCC4)N=C3)=C2)=CC(OC)=C1OC
Lapatinib	Clinical KIs	CS(=O)(=O)CCNCc1oc(cc1)c2ccc3ncnc(Nc4ccc(OCc5cccc(F)c5)c(Cl)c4)c3c2
Lenvatinib	Clinical KIs	COc1cc2nccc(Oc3ccc(NC(=O)NC4CC4)c(Cl)c3)c2cc1C(=O)N
Midostaurin	Clinical KIs	CO[C@@H]1[C@@H](C[C@H]2O[C@]1(C)n3c4ccccc4c5c6CNC(=O)c6c7c8cccc8n2c7c35)N(C)C(=O)c9ccccc9
Neratinib	Clinical KIs	CCOc1cc2ncc(C#N)c(Nc3ccc(OCc4ccccn4)c(Cl)c3)c2cc1NC(=O)\C=C\CN(C)C
Nilotinib	Clinical KIs	Cc1cn(cn1)c2cc(NC(=O)c3ccc(C)c(Nc4nccc(n4)c5cccnc5)c3)cc(c2)C(F)(F)F
Nintedanib	Clinical KIs	COC(=O)c1ccc2\C(=C(\Nc3ccc(cc3)N(C)C(=O)CN4CCN(C)CC4)/c5ccccc5)\C(=O)Nc2c1
NVP-2	KCGS	ClC1=CN=C(N[C@H]2CC[C@H](N[C@H](C)COC)CC2)C=C1C3=CC=CC(NCC4(C#N)CCOCC4)=N3
NVS-PAK1-1	KCGS	O=C(N1C[C@@H](NC2=NC3=CC(F)=CC=C3N(CC(F)F)C4=CC=C(Cl)C=C42)CC1)NC(C)C
Osimertinib	Clinical KIs	COc1cc(N(C)CCN(C)C)c(NC(=O)C=C)cc1Nc2nccc(n2)c3cn(C)c4ccccc34
Pazopanib	Clinical KIs	CN(c1ccc2c(C)n(C)nc2c1)c3ccnc(Nc4ccc(C)c(c4)S(=O)(=O)N)n3
PFE-PKIS_1	KCGS	O=C1C(Br)=C(OCC2=C(F)C=C(F)C=C2)C=C(C)N1C3=CC(C(NCC(N)=O)=O)=CC=C3C
PFE-PKIS_12	KCGS	O=C(NCCCN1CCOC1=O)C2=CN=C(NCC3=C(Cl)C=CC(Cl)=C3)N=C2NC4CCCC4

Compound	Library	SMILES
PFE-PKIS_21	KCGS	FC1=C(F)C=CC(C(NOC[C@H](O)CO)=O)=C1NC2=CC=C(I)C=C2F
PFE-PKIS_29	KCGS	COC(N=C1)=CC=C1C2=CC3=C(C)N=C(N)N=C3N([C@H]4CC[C@H](OCCO)CC4)C2=O
PFE-PKIS_3	KCGS	COC1=CC(C2=CC3=CN=C(N)N=C3N=C2NC(NC(C)(C)C)=O)=CC(OC)=C1
PFE-PKIS_32	KCGS	CC(C1=CN=C(NC2=NC=C(N3CCNCC3)C=C2)N=C1N4C5CCCC5)=C(C(C)=O)C4=O
PFE-PKIS_34	KCGS	CN([C@H]1CN(C(CO)=O)CC[C@H]1C)C2=C3C(NC=C3)=NC=N2
PFE-PKIS_39	KCGS	CN(N=C1)C=C1C(C=C2)=NN3C2=NN=C3[C@@H](C)C4=CC=C(N=CC=C5)C5=C4
PFE-PKIS_40	KCGS	O=C1N([C@@H]2CC[C@@H](O)CC2)C3=NC(N)=NC(C)=C3C=C1C4=CC=C(OC)N=C4
PFE-PKIS_41	KCGS	CC1=CC(OCC2=C(F)C=C(F)C=C2)=C(Br)C(N1C3=C(C)C=CC(C(NC)=O)=C3)=O
PFE-PKIS_44	KCGS	CC(C1=CN=C(NC2=NN(C)C=C2)N=C1N3C4CCCC4)=C(C(C)=O)C3=O
Ponatinib	Clinical KIs	CN1CCN(Cc2ccc(NC(=O)c3ccc(C)c(c3)C#Cc4cnc5cccnn45)cc2C(F)(F)F)CC1
R-547	Clinical KIs	COc1ccc(F)c(F)c1C(=O)c2cnc(NC3CCN(CC3)S(=O)(=O)C)nc2N
Rapamycin	Clinical KIs	CO[C@@H]1C[C@H](C[C@@H](C)[C@@H]2CC(=O)[C@H](C)\C=C(/C)\[C@@H](O)[C@@H](OC)C(=O)[C@H](C)C[C@H](C)\C=C\C=C\C=C(/C)\[C@H](C[C@@H]3CC[C@@H](C)[C@@](O)(O3)C(=O)C(=O)N4CCCC[C@H]4C(=O)O2)OC)CC[C@H]1O
Regorafenib	Clinical KIs	CNC(=O)c1cc(Oc2ccc(NC(=O)Nc3ccc(Cl)c(c3)C(F)(F)F)c(F)c2)ccn1
Ribociclib	Clinical KIs	CN(C)C(=O)c1cc2cnc(Nc3ccc(cn3)N4CCNCC4)nc2n1C5CCCC5
RO0117162-000	Roche	[O-][N+](=O)c1ccc2Nc3n[nH]cc3N=C(c4ccccc4Cl)c2c1
RO0150463-000	Roche	Nc1n[nH]c2nc(cc(c12)C(F)(F)F)c3cccs3
RO0271528-000	Roche	Cn1cc(C2=C(C(=O)NC2=O)c3cn(C)c4ncccc34)c5ccccc15
RO0272148-000	Roche	Fc1ccc2NC(=O)\C(=C/c3ccc[nH]3)\c2c1
RO0272159-000	Roche	COc1cc[nH]c1\C=C\2/C(=O)Nc3ccccc23
RO0274406-000	Roche	Cc1[nH]nc2Nc3ccc(cc3C(=Nc12)c4ccccc4Cl)[N+](=O)[O-]
RO0274710-000	Roche	CC(C)c1[nH]nc2Nc3ccc(cc3C(=Nc12)c4ccccc4Cl)[N+](=O)[O-]
RO0275062-000	Roche	Cc1[nH]nc2Nc3ccc(cc3C(=Nc12)c4ccccc4F)C#N
RO0281498-000	Roche	COc1ccc2Nc3n[nH]c(C)c3N=C(c4ccccc4Cl)c2c1
RO0281567-000	Roche	COc1cc[nH]c1\C=C\2/C(=O)Nc3ccc(F)c(I)c23
RO0281601-001	Roche	Cl.CNCC#Cc1c(F)ccc2NC(=O)\C(=C/c3[nH]ccc3OC)\c12
RO0281752-000	Roche	CC(=O)Nc1ccc2Nc3n[nH]c(C)c3N=C(c4ccccc4Cl)c2c1
RO0282586-000	Roche	Cc1[nH]nc2Nc3ccc(cc3C(=Nc12)c4ccccc4F)C(=O)N
RO0282986-001	Roche	Cl.COc1cc[nH]c1\C=C\2/C(=O)Nc3ccc(F)c(C#CC4(O)CCNCC4)c23
RO0283049-001	Roche	Cl.CN[C@@H](CO)C#Cc1c(F)ccc2NC(=O)\C(=C/c3[nH]ccc3OC)\c12
RO0283120-000	Roche	COc1cc[nH]c1\C=C\2/C(=O)Nc3ccc(F)c(C#C[C@@H](O)[C@@H](N)[C@@H](C)O)c23
RO0316045-000	Roche	CN1C(=O)C(=C(C1=O)c2c[nH]c3ccccc23)c4c[nH]c5ccccc45
RO0316233-000	Roche	O=C1NC(=O)C(=C1c2c[nH]c3ccccc23)c4c[nH]c5ccccc45
RO0316849-000	Roche	O=C1NC(=O)C(=C1c2ccccc2)c3c[nH]c4ccccc34
RO0316873-000	Roche	OC1NC(=O)C(=C1c2c[nH]c3ccccc23)c4c[nH]c5ccccc45
RO0317208-000	Roche	Cn1cc(C2=C(C(=O)NC2=O)c3cn(C)c4ccccc34)c5ccccc15
RO0317253-000	Roche	Cn1cc(C2=C(C(=O)NC2=O)c3cccc4ccccc34)c5ccccc15
RO0317254-000	Roche	Cn1cc(C2=C(C(=O)NC2=O)c3ccc4ccccc4c3)c5ccccc15
RO0317257-000	Roche	COc1ccc(cc1)C2=C(C(=O)NC2=O)c3cn(C)c4ccccc34
RO0317302-000	Roche	COc1ccc2c(cn(C)c2c1)C3=C(C(=O)NC3=O)c4cn(C)c5ccccc45

Compound	Library	SMILES
RO0317328-000	Roche	Cn1cc(C2=C(C(=O)NC2=O)c3ccsc3)c4ccccc14
RO0317340-000	Roche	CSc1c(C2=C(C(=O)NC2=O)c3cn(C)c4ccccc34)c5ccccc5n1C
RO0317365-000	Roche	Cn1cc(C2=C(C(=O)NC2=O)c3cn(C)c4ccc(N)cc34)c5ccccc15
RO0317373-001	Roche	Cl.Cn1cc(C2=C(C(=O)NC2=O)c3ccc(N)cc3)c4ccccc14
RO0317377-000	Roche	Cn1cc(C2=C(C(=O)NC2=O)c3cn(CCCO)c4ccccc34)c5ccccc15
RO0317379-000	Roche	CS(=O)c1c(C2=C(C(=O)NC2=O)c3cn(C)c4ccccc34)c5ccccc5n1C
RO0317432-000	Roche	Cn1cc(C2=C(C(=O)NC2=O)c3cn(C)c4ccc(OCc5ccccc5)cc34)c6ccccc16
RO0317452-000	Roche	Cn1cc(C2=C(C(=O)NC2=O)c3cn(C)c4c(cccc34)[N+](=O)[O-])c5ccccc15
RO0317471-000	Roche	Cn1cc(C2=C(C(=O)NC2=O)c3cccc(N)c3)c4ccccc14
RO0317474-000	Roche	Cn1cc(C2=C(C(=O)NC2=O)c3cccc(c3)[N+](=O)[O-])c4ccccc14
RO0317476-000	Roche	Cn1cc(C2=C(C(=O)NC2=O)c3cccc(Cl)c3)c4ccccc14
RO0317482-000	Roche	Cn1cc(C2=C(C(=O)NC2=O)c3cn(C)c4c(N)cccc34)c5ccccc15
RO0317494-000	Roche	COc1cccc2c1c(cn2C)C3=C(C(=O)NC3=O)c4cn(C)c5ccccc45
RO0317510-000	Roche	Cc1ccc2c(c1)c(cn2C)C3=C(C(=O)NC3=O)c4cn(C)c5ccccc45
RO0317511-000	Roche	Cn1cc(C2=C(C(=O)NC2=O)c3cn(C)c4cc(N)ccc34)c5ccccc15
RO0317549-002	Roche	Cl.Cn1cc(C2=C(C(=O)NC2=O)c3cn(CCCN)c4ccccc34)c5ccccc15
RO0317596-000	Roche	CC(=O)Nc1ccc2c(cn(C)c2c1)C3=C(C(=O)NC3=O)c4cn(C)c5ccccc45
RO0317597-000	Roche	Cn1cc(C2=C(C(=O)NC2=O)c3cn(C)c4cc(Cl)ccc34)c5ccccc15
RO0317612-000	Roche	Cc1ccccc1C2=C(C(=O)NC2=O)c3cn(C)c4ccccc34
RO0317621-000	Roche	Cn1cc(C2=C(C(=O)NC2=O)c3cn(C)c4ccc(Cl)cc34)c5ccccc15
RO0317625-000	Roche	Cn1cc(C2=C(C(=O)NC2=O)c3cccc(Br)c3)c4ccccc14
RO0317699-000	Roche	Cc1ccc(C)c(c1)C2=C(C(=O)NC2=O)c3cn(C)c4ccccc34
RO0317717-000	Roche	Cn1cc(C2=C(C(=O)NC2=O)c3ccccc3C(F)(F)F)c4ccccc14
RO0317753-000	Roche	Cn1cc(C2=C(C(=O)NC2=O)c3ccccc3[N+](=O)[O-])c4ccccc14
RO0317777-000	Roche	Cc1c(C2=C(C(=O)NC2=O)c3cn(C)c4ccccc34)c5ccccc5n1C
RO0317843-000	Roche	Cn1cc(C2=C(C(=O)NC2=O)c3cn(CCCCCN)c4ccccc34)c5ccccc15
RO0317884-000	Roche	Cn1cc(C2=C(C(=O)NC2=O)c3c[nH]c4ccccc34)c5ccccc15
RO0317886-000	Roche	Cn1cc(C2=C(C(=O)NC2=O)c3cccnc3)c4ccccc14
RO0317888-000	Roche	Cn1cc(C2=C(C(=O)NC2=O)c3cn(CCCCN)c4ccccc34)c5ccccc15
RO0318036-000	Roche	Cn1cc(C2=C(C(=O)NC2=O)c3cn(CCO)c4ccccc34)c5ccccc15
RO0318044-001	Roche	Cl.CNCCCn1cc(C2=C(C(=O)NC2=O)c3cn(C)c4ccccc34)c5ccccc15
RO0318045-000	Roche	Cn1cc(C2=C(C(=O)NC2=O)c3cn(CCN)c4ccccc34)c5ccccc15
RO0318053-000	Roche	Cn1cc(C2=C(C(=O)NC2=O)c3cn(CCCCCO)c4ccccc34)c5ccccc15
RO0318069-000	Roche	Cn1cc(C2=C(C(=O)NC2=O)n3ccc4ccccc34)c5ccccc15
RO0318161-000	Roche	Cn1cc(C2=C(C(=O)NC2=O)c3cn(CCCN\C(=N\[N+](=O)[O-])\N)c4ccccc34)c5ccccc15
RO0318220-000	Roche	Cn1cc(C2=C(C(=O)NC2=O)c3cn(CCCSC(=N)N)c4ccccc34)c5ccccc15
RO0318259-000	Roche	Cn1cc(C2=C(C(=O)NC2=O)c3c4CCCCn4c5ccccc35)c6ccccc16
RO0318352-000	Roche	Cn1cc(C2=C(C(=O)NC2=O)c3cn(CCCNC(=N)N)c4ccccc34)c5ccccc15
RO0318365-001	Roche	Cl.Cn1cc(C2=C(C(=O)NC2=O)c3c4CNCCn4c5ccccc35)c6ccccc16
RO0318425-001	Roche	Cl.Cn1cc(C2=C(C(=O)NC2=O)c3c4CC(CN)CCn4c5ccccc35)c6ccccc16
RO0318549-000	Roche	CCCn1cc(C2=C(C(=O)NC2=O)c3cn(C)c4ccccc34)c5ccccc15
RO0318564-000	Roche	Cn1cc(C2=C(C(=O)NC2=O)c3cn(c4ccccc4)c5ccccc35)c6ccccc16
RO0318649-000	Roche	COc1cccc(c1)C2=C(C(=O)NC2=O)c3cn(C)c4ccccc34

Compound	Library	SMILES
RO0318676-000	Roche	CNCC1CCn2c(C1)c(C3=C(C(=O)NC3=O)c4cn(C)c5ccccc45)c6ccccc26
RO0318830-000	Roche	CN(C)CC1CCn2c(C1)c(C3=C(C(=O)NC3=O)c4cn(C)c5ccccc45)c6ccccc26
RO0318987-000	Roche	Cn1cc(C2=C(C(=O)NC2=O)c3c4CCCCCn4c5ccccc35)c6ccccc16
RO0319317-000	Roche	Cn1cc(C2=C(C(=O)NC2=O)c3cn(C)c4cc(ccc34)C(=O)N)c5ccccc15
RO0319318-000	Roche	Cn1cc(C2=C(C(=O)NC2=O)c3cn(C)c4cc(ccc34)C(=O)O)c5ccccc15
RO0319371-000	Roche	Cn1cc(C2=C(C(=O)NC2=O)c3c4CCC(CN)CCn4c5ccccc35)c6ccccc16
RO0319377-000	Roche	Cn1cc(C2=C(C(=O)NC2=O)c3c4CN(CCn4c5ccccc35)C(=S)N)c6ccccc16
RO0320234-001	Roche	Cl.CN1C[C@@H]2Cc3c(C4=C(C(=O)NC4=O)c5cn(C)c6ccccc56)c7ccccc7n3C[C@H]2C1
RO0320344-000	Roche	O=C1OC(=O)C(=C1c2c[nH]c3ccccc23)c4c[nH]c5ccccc45
RO0320346-000	Roche	ON1C(=O)C(=C(C1=O)c2c[nH]c3ccccc23)c4c[nH]c5ccccc45
RO0320432-000	Roche	CN(C)C[C@H]1CCn2c(C1)c(C3=C(C(=O)NC3=O)c4cn(C)c5ccccc45)c6ccccc26
RO0320557-001	Roche	Cl.CN1C[C@@H]2Cc3c(C4=C(C(=O)NC4=O)c5cn(C)c6ccccc56)c7ccccc7n3C[C@H]2C1
RO0324253-000	Roche	CC(=O)N[C@@H](Cc1ccc(OP(=O)(O)O)cc1)C(=O)N[C@H]2CCC(=O)N3CCC[C@H](N3C2=O)C(=O)NCc4ccccc4
RO0324381-000	Roche	CC(=O)N[C@@H](Cc1ccc(OP(=O)(O)O)cc1)C(=O)N[C@H]2CCC(=O)N3CCC[C@H](N3C2=O)C(=O)NCc4ccc(O)cc4
RO0324438-000	Roche	CC(=O)N[C@@H](Cc1ccc(OP(=O)(O)O)cc1)C(=O)N[C@H]2CCC(=O)N3CCC[C@H](N3C2=O)C(=O)NC4CCc5ccccc45
RO0324476-000	Roche	CC(=O)N[C@@H](Cc1ccc(OP(=O)(O)O)cc1)C(=O)N[C@H]2CCC(=O)N3CCC[C@H](N3C2=O)C(=O)NCc4cccc5ccccc45
RO0324694-000	Roche	CCCCCNC(=O)[C@@H]1CCCN2N1C(=O)[C@H](CCC2=O)NC(=O)[C@H](Cc3ccc(OP(=O)(O)O)cc3)NC(=O)C
RO0325308-000	Roche	CC(=O)N[C@@H](Cc1ccc(OP(=O)(O)O)cc1)C(=O)N[C@H]2CCC(=O)N3CCC[C@H](N3C2=O)C(=O)NCc4ccc(Cl)cc4
RO0325851-000	Roche	CCNC(=O)[C@@H]1CCCN2N1C(=O)[C@H](CCC2=O)NC(=O)[C@H](Cc3ccc(OP(=O)(O)O)cc3)NC(=O)C
RO0480500-002	Roche	Cl.COc1ccc(O)c(C(=O)c2ccc(cc2)C(=O)O[C@@H]3CCCNC[C@H]3NC(=O)c4ccncc4)c1F
RO0504985-000	Roche	COc1cc[nH]c1\C=C\2/C(=O)Nc3ccc(c(N4CC[C@@H](O)C4)c23)[N+](=O)[O-]
RO0505124-000	Roche	CN1CCN(CC1)c2ccc(Nc3nc(N)c(s3)C(=O)c4ccc5OCCOc5c4)cc2
RO0506220-000	Roche	COc1cccc(c1)C(=O)c2sc(Nc3ccc(cc3)N4CCN(CC4)C(C)C)nc2N
RO1150868-000	Roche	O=C(c1ccccc1)c2cnn(c3ccccc3)c2C#N
RO1151080-000	Roche	Cc1nn(c(O)c1C(=O)c2ccccc2)c3ccccc3
RO1151246-000	Roche	Nc1c(cnn1c2ccc(F)cc2)C(=O)c3ccccc3
RO1151248-000	Roche	Cc1ccccc1n2ncc(C(=O)c3ccccc3)c2N
RO1153136-000	Roche	Nc1c(cnn1c2ccc(F)cc2)C(=O)c3ccc(cc3)C#CCN4CCOCC4
RO1153198-000	Roche	Nc1c(cnn1c2ccc(F)cc2)C(=O)c3ccc(cc3)C#N
RO1153320-001	Roche	Cl.Nc1c(cnn1c2ccc(F)cc2)C(=O)c3cccc(c3)C#CCN4CCOCC4
RO1153321-000	Roche	Nc1c(cnn1c2ccc(F)cc2)C(=O)c3cccc(c3)C#N
RO1153427-001	Roche	Cl.Nc1c(cnn1c2ccc(F)cc2)C(=O)c3ccc(CCCN4CCOCC4)cc3
RO1153583-001	Roche	Cl.Nc1c(cnn1c2ccc(F)cc2)C(=O)c3cccc(CCCN4CCOCC4)c3
RO1153836-000	Roche	Nc1c(cnn1c2ccc(F)cc2)C(=O)c3cccc(c3)C#CCO
RO1153853-000	Roche	Fc1ccc(cc1)c2c([nH]c3cccnc23)c4ccncc4
RO1154309-001	Roche	Cl.CN1CCN(CC#Cc2cccc(c2)C(=O)c3cnn(c3N)c4ccc(F)cc4)CC1
RO1154461-001	Roche	Cl.Nc1c(cnn1c2ccc(F)cc2)C(=O)c3cccc(c3)C#CCN4CCCCC4

Compound	Library	SMILES
RO1154507-000	Roche	Fc1ccc(cc1)c2c(c3ccncc3)n(CCN4CCOCC4)c5cccnc25
RO1154641-001	Roche	Cl.CN(C)CC#Cc1cccc(c1)C(=O)c2cnn(c2N)c3ccc(F)cc3
RO1155240-000	Roche	Cn1c(c2ccncc2)c(c3ccc(F)cc3)c4ncccc14
RO1155697-000	Roche	Fc1ccc(cc1)c2c([nH]c3nccnc23)c4ccncc4
RO1155798-000	Roche	OCCn1c(c2ccncc2)c(c3ccc(F)cc3)c4ncccc14
RO1160347-001	Roche	Cl.CN1CCN(CCc2cccc(c2)C(=O)c3cnn(c3N)c4ccc(F)cc4)CC1
RO1162009-000	Roche	Nc1c(cnn1c2ccc(F)cc2)C(=O)c3cccc(CCS(=O)(=O)N)c3
RO1162529-002	Roche	Cl.Nc1c(cnn1c2ccc(F)cc2)C(=O)c3cccc(c3)c4cccnc4
RO1163374-000	Roche	CO\N=C(/c1ccccc1)\c2cnn(c2N)c3ccccc3
RO1164194-001	Roche	Cl.Nc1c(cnn1c2ccc(F)cc2F)C(=O)c3cccc(c3)c4cccnc4
RO1165037-001	Roche	Cl.Nc1c(cnn1c2ccc(F)cc2)C(=O)c3cccc(c3)c4ccncc4
RO1166259-000	Roche	Nc1c(cnn1c2ccc(F)cc2F)C(=O)c3cccc(c3)c4ccc[n+]([O-])c4
RO1166300-001	Roche	Cl.Nc1c(cnn1c2ccc(F)cc2F)C(=O)c3cccc(c3)c4ccncc4
RO3200567-000	Roche	Nc1c(cnn1c2ccc(F)cc2)C(=O)c3cccc(c3)C(O)CO
RO3200934-000	Roche	Nc1c(cnn1c2ccc(F)cc2)C(=O)c3cccc(CCC4(O)CCCC4)c3
RO3200935-000	Roche	CC(C)(O)CCc1cccc(c1)C(=O)c2cnn(c2N)c3ccc(F)cc3
RO3201196-000	Roche	Nc1c(cnn1c2ccc(F)cc2)C(=O)c3cccc(OC[C@H](O)CO)c3
RO3201331-000	Roche	CS(=O)(=O)CCc1cccc(c1)C(=O)c2cnn(c2N)c3ccc(F)cc3
RO3201790-000	Roche	Nc1c(cnn1c2ccc(F)cc2)C(=O)c3cccc(c3)C(O)(CO)CO
RO3202002-001	Roche	Cl.Nc1c(cnn1c2ccc(F)cc2)C(=O)c3ccc(cc3)c4cccnc4
RO3202312-001	Roche	Cl.CC(CO)Nc1cc(ccn1)c2[nH]c3cccnc3c2c4ccc(F)cc4
RO3206145-001	Roche	Cl.C[C@H](O)CNc1cc(ccn1)c2[nH]c3cccnc3c2c4ccc(F)cc4
RO3206173-000	Roche	Cn1cc(C2=C(C(=O)NC2=O)c3cccc(OC[C@H](O)CO)c3)c4ccccc14
RO3206363-000	Roche	COc1ccc(cc1OC)C2=C(C(=O)NC2=O)c3cn(C)c4ccccc34
RO3208546-000	Roche	Cn1cc(C2=C(C(=O)NC2=O)c3ccc(OC[C@@H](O)CO)cc3)c4ccccc14
RO3245084-000	Roche	COc1ccc(OC)c(c1)C2=C(C(=O)NC2=O)c3cn(C)c4ccccc34
RO3300167-000	Roche	COc1cccc(c1)C2=C(C(=O)NC2=O)c3c(C)n(C)c4ccccc34
RO3300230-000	Roche	COc1cccc(c1)C2=C(C(=O)NC2=O)c3cn(C)c4ccc(Cl)cc34
RO3300896-000	Roche	COc1cccc(c1)C2=C(C(=O)NC2=O)c3cn(C)c4cc(F)ccc34
RO3300953-000	Roche	COc1cccc(c1)C2=C(C(=O)NC2=O)c3cn(C)c4cccc(OC)c34
RO3301011-000	Roche	Cn1cc(C2=C(Sc3ccccc3)C(=O)NC2=O)c4ccccc14
RO3301012-000	Roche	COc1cccc(c1)C2=C(C(=O)NC2=O)c3cn(C)c4c(C)cccc34
RO3301277-000	Roche	Cn1cc(C2=C(Oc3ccccc3)C(=O)NC2=O)c4ccccc14
RO3301767-000	Roche	Cn1cc(C2=C(Nc3ccccc3)C(=O)NC2=O)c4ccccc14
RO3303031-000	Roche	Cn1cc(C2=C(N3CCOCC3)C(=O)NC2=O)c4ccccc14
RO3303470-000	Roche	CN1C(=O)C(=Cc2cnc(NC3CCOCC3)nc12)c4ccccc4Cl
RO3303724-001	Roche	Cl.Cn1cc(C2=C(C(=O)NC2=O)c3cccc(NCC(O)CO)c3)c4cc(Cl)ccc14
RO3304757-001	Roche	Cl.CN1C(=O)C(=Cc2cnc(NC3CCOCC3)nc12)Oc4ccccc4
RO3304774-001	Roche	Cl.CN1C(=O)C(=Cc2cnc(NC3CCOCC3)nc12)Oc4cccc(F)c4
RO3304805-001	Roche	Cl.CN1C(=O)C(=Cc2cnc(NC3CCOCC3)nc12)Oc4ccccc4F
RO3304806-000	Roche	CN1C(=O)C(=Cc2cnc(NC3CCOCC3)nc12)Oc4ccc(F)cc4F
RO3304882-001	Roche	Cl.CN1C(=O)C(=Cc2cnc(NC3CCOCC3)nc12)Oc4ccc(F)cc4
RO3305377-001	Roche	Cl.CN1C(=O)C(=Cc2cnc(NC3CCOCC3)nc12)Cc4ccccc4F

Compound	Library	SMILES
RO3305411-001	Roche	Cl.CN1C(=O)C(=Cc2cnc(NC(C)(C)CO)nc12)Oc3ccc(F)cc3F
RO3305413-001	Roche	Cl.CN1C(=O)C(=Cc2cnc(N[C@@H]3CC[C@@H](O)CC3)nc12)Oc4ccc(F)cc4F
RO3308271-001	Roche	Cl.CN1C(=O)C(=Cc2cnc(NC3CCS(=O)(=O)CC3)nc12)Oc4ccc(F)cc4F
RO3308757-001	Roche	Cl.CN1C(=O)C(=Cc2cnc(NC3CCOCC3)nc12)Cc4ccc(F)cc4F
RO3308967-001	Roche	Cl.CN1C(=O)C(=Cc2cnc(NCC(C)(C)O)nc12)Oc3ccc(F)cc3F
RO3309180-001	Roche	Cl.CC(C)Nc1ncc2C=C(Oc3ccc(F)cc3F)C(=O)N(C)c2n1
RO3309294-001	Roche	Cl.CN1C(=O)C(=Cc2cnc(NCCS(=O)(=O)C)nc12)Oc3ccc(F)cc3F
RO3310123-001	Roche	Cl.CN1C(=O)C(=Cc2cnc(NC(CO)CO)nc12)Oc3ccc(F)cc3F
RO3310867-000	Roche	Fc1ccc(OC2=Cc3cnc(NC4CCOCC4)nc3NC2=O)c(F)c1
RO3311017-001	Roche	Cl.CN1C(=O)C(=Cc2cnc(N[C@H]3CCOC3)nc12)Oc4ccc(F)cc4F
RO4241967-000	Roche	Cc1cc(C)c2c(n1)sc3c(N)ncnc23
RO4241984-000	Roche	Cc1nc2sc3c(N)ncnc3c2c(C)c1C
RO4367438-000	Roche	CCN1C(=O)C(=Cc2cnc(NC3CCOCC3)nc12)Oc4ccc(F)cc4F
RO4367842-001	Roche	Cl.COc1ccc(O)c(C(=O)c2ccc(cc2)C(=O)N[C@@H]3CCCNC[C@H]3NC(=O)c4ccncc4)c1F
RO4383596-000	Roche	COc1ccc(cc1)N2Cc3cnc(Nc4ccccc4)nc3N([C@@H]5CC[C@@H](O)C5)C2=O
RO4399247-000	Roche	Fc1ccc(OC2=Cc3cnc(NC4CCOCC4)nc3N(C5CC5)C2=O)c(F)c1
RO4442080-000	Roche	O=C1N=C(NCc2ccccc2)S/C/1=C\c3ccc4ncccc4c3
RO4442245-000	Roche	OCCCN1C(=O)C(=Cc2cnc(NC3CCOCC3)nc12)Oc4ccc(F)cc4F
RO4493940-000	Roche	O=C1N=C(Nc2ccccc2)S/C/1=C\c3ccc4ncccc4c3
RO4493941-000	Roche	O=C1N=C(NCCCc2ccccc2)S/C/1=C\c3ccc4ncccc4c3
RO4493944-000	Roche	CCc1c(C)nc2sc3c(N)ncnc3c2c1C
RO4498476-000	Roche	COc1ccc(CCNC2=NC(=O)\C(=C\c3ccc4ncccc4c3)\S2)cc1
RO4498479-000	Roche	Clc1ccc(CCNC2=NC(=O)\C(=C\c3ccc4ncccc4c3)\S2)cc1
RO4498483-000	Roche	Fc1ccccc1CCNC2=NC(=O)\C(=C\c3ccc4ncccc4c3)\S2
RO4498484-000	Roche	Clc1ccccc1CCNC2=NC(=O)\C(=C\c3ccc4ncccc4c3)\S2
RO4503314-000	Roche	CCOc1ccccc1CCNC2=NC(=O)\C(=C\c3ccc4ncccc4c3)\S2
RO4503315-000	Roche	COc1ccccc1CNC2=NC(=O)\C(=C\c3ccc4ncccc4c3)\S2
RO4503316-000	Roche	COc1ccccc1CCNC2=NC(=O)\C(=C\c3ccc4ncccc4c3)\S2
RO4503319-000	Roche	OC[C@H](Cc1ccccc1)NC2=NC(=O)\C(=C\c3ccc4ncccc4c3)\S2
RO4506917-000	Roche	Clc1ccccc1CNC2=NC(=O)\C(=C\c3ccc4ncccc4c3)\S2
RO4506918-000	Roche	Brc1ccccc1CNC2=NC(=O)\C(=C\c3ccc4ncccc4c3)\S2
RO4508334-000	Roche	Brc1ccc(CCNC2=NC(=O)\C(=C\c3ccc4ncccc4c3)\S2)cc1
RO4508340-000	Roche	Fc1ccc(CCNC2=NC(=O)\C(=C\c3ccc4ncccc4c3)\S2)cc1
RO4508344-000	Roche	Fc1cccc(CCNC2=NC(=O)\C(=C\c3ccc4ncccc4c3)\S2)c1
RO4508346-000	Roche	O=C1N=C(NCCc2ccccn2)S/C/1=C\c3ccc4ncccc4c3
RO4508348-000	Roche	O=C1N=C(NCCc2cccs2)S/C/1=C\c3ccc4ncccc4c3
RO4509200-000	Roche	OC[C@@H](Cc1ccccc1)NC2=NC(=O)\C(=C\c3ccc4ncccc4c3)\S2
RO4509201-000	Roche	Clc1cccc(CCNC2=NC(=O)\C(=C\c3ccc4ncccc4c3)\S2)c1
RO4509407-000	Roche	NC1=NC(=N)\C(=C\c2ccc3ncccc3c2)\S1
RO4514610-000	Roche	COc1ccccc1C(=O)c2cnc(NC3CCN(CC3)S(=O)(=O)C)nc2N
RO4517872-000	Roche	COc1ccc(F)cc1C(=O)c2cnc(NC3CCN(CC3)S(=O)(=O)C)nc2N
RO4554339-000	Roche	OC[C@@H](NC1=NC(=O)\C(=C\c2ccc3ncccc3c2)\S1)c4ccccc4
RO4554340-000	Roche	OC[C@H](NC1=NC(=O)\C(=C\c2ccc3ncccc3c2)\S1)c4ccccc4

Compound	Library	SMILES
RO4569139-000	Roche	NC1=NC(=O)\C(=C\c2ccc3ncccc3c2)\S1
RO4582641-000	Roche	OCC(CNC1=NC(=O)\C(=C\c2ccc3ncccc3c2)\S1)c4ccccc4
RO4595655-000	Roche	COc1cc(F)c(F)cc1C(=O)c2cnc(NC3CCN(CC3)S(=O)(=O)C)nc2N
RO4595946-000	Roche	COC[C@H](NC1=NC(=O)\C(=C\c2ccc3ncccc3c2)\S1)c4ccccc4
RO4595949-000	Roche	CNC1=NC(=O)\C(=C\c2ccc3ncccc3c2)\S1
RO4600445-000	Roche	Clc1cccc(Cl)c1CNC2=NC(=O)\C(=C\c3ccc4ncccc4c3)\S2
RO4600703-000	Roche	COc1cc(F)c(F)c(F)c1C(=O)c2cnc(NC3CCN(CC3)S(=O)(=O)C)nc2N
RO4602005-000	Roche	COc1cccc(F)c1C(=O)c2cnc(NC3CCN(CC3)S(=O)(=O)C)nc2N
RO4603632-000	Roche	O=C1NC(=O)\C(=C\c2ccc3ncccc3c2)\S1
RO4607009-000	Roche	C\C(=C/1\SC(=NC1=O)NCc2cccs2)\c3ccc4ncccc4c3
RO4613269-000	Roche	CONC1=NC(=O)\C(=C\c2ccc3ncccc3c2)\S1
RO4624208-000	Roche	O=C1N=C(NCc2cccs2)O/C/1=C\c3ccc4ncccc4c3
RO4629078-000	Roche	O=C1N=C(NCc2cccs2)SC1Cc3ccc4ncccc4c3
RO4874953-001	Roche	Cl.O=C1N=C(NCc2ccccn2)S/C/1=C\c3ccc4ncccc4c3
RO4915610-000	Roche	O=C1N=C(N[C@@H]2C[C@H]2c3ccccc3)S/C/1=C\c4ccc5ncccc5c4
RO4930481-000	Roche	CS(=O)(=O)N1CCC(CC1)Nc2ncc(C(=O)c3c(F)cccc3F)c(N)n2
RO4944065-000	Roche	CN1C(=O)C(=Cc2cnc(NC3CCOCC3)nc12)Sc4ccccc4F
RO5027956-000	Roche	CS(=O)(=O)CCN1C(=O)C(=Cc2cnc(NC3CCOCC3)nc12)Oc4ccc(F)cc4F
RO5033700-000	Roche	CS(=O)(=O)CCCN1C(=O)C(=Cc2cnc(NC3CCOCC3)nc12)Oc4ccc(F)cc4F
RO5036538-000	Roche	Fc1ccc(OC2=Cc3cnc(NC4CCOCC4)nc3N(C5CCS(=O)(=O)CC5)C2=O)c(F)c1
RO5036558-000	Roche	CC(C)(O)CN1C(=O)C(=Cc2cnc(NC3CCOCC3)nc12)Oc4ccc(F)cc4F
RO5040027-000	Roche	Fc1ccc(OC2=Cc3cnc(NC4CCOCC4)nc3N(CC#N)C2=O)c(F)c1
RO5043011-000	Roche	CN1C(=O)C(=Cc2cnc(NC3CCN(CC3)C(=O)C)nc12)Oc4ccc(F)cc4F
RO5043312-000	Roche	C[C@H](CS(=O)(=O)C)Nc1ncc2C=C(Oc3ccc(F)cc3F)C(=O)N(C)c2n1
RO5044198-000	Roche	C[C@@H](CS(=O)(=O)C)Nc1ncc2C=C(Oc3ccc(F)cc3F)C(=O)N(C)c2n1
RO5045977-000	Roche	CS(=O)(=O)N1CCC(CC1)N2C(=O)C(=Cc3cnc(NC4CCOCC4)nc23)Oc5ccc(F)cc5F
RO5067310-000	Roche	C[C@@H](Cn1ncnn1)Nc2ncc3C=C(Oc4ccc(F)cc4F)C(=O)N(C)c3n2
RO5068760-000	Roche	C[C@H]([C@H](N1C(=O)N[C@@H](C1=O)c2ccc(OC[C@H](O)CO)cc2)C(=O)Nc3ccc(I)cc3F)c4ccccc4
RO5083957-000	Roche	CNc1ncc2C=C(Oc3ccc(F)cc3F)C(=O)N(C)c2n1
RO5198354-000	Roche	Cn1cc(C2=C(C(=O)NC2=O)c3cccc(OCC(O)CO)c3)c4ccccc14
RO5301104-000	Roche	Nc1c(cnn1c2ccc(F)cc2)C(=O)c3cccc(OCCN4CCOCC4)c3
Ruxolitinib	Clinical KIs	N#CC[C@H](C1CCCC1)n2cc(cn2)c3ncnc4[nH]ccc34
SB-202620	PKIS2	FC1=CC=C(C=C1)C(N=C2C3=CC=C(C(O)=O)C=C3)=C(N2)C4=CC=NC=C4
SB-210313	PKIS1	Fc1ccc(cc1)-c1ncn(CCCN2CCOCC2)c1-c1ccncc1
SB-210486	PKIS2	FC1=CC=C(C=C1)C2=C(C3=CC=NC=C3)N(CCCNCC4=CC=CC=C4)C=N2
SB-211742	PKIS2	FC1=CC=C(C=C1)C2=C(C3=NC=CC=C3)N(CCCN4CCOCC4)C=N2
SB-211743	PKIS2	FC1=CC=C(C=C1)C2=C(C3=CN=CC=C3)N(CCCN4CCOCC4)C=N2
SB-213663	PKIS2	FC1=CC=C(C=C1)C2=C(C3=CC=NC=C3)NC(C4=C(S(C)(=O)=O)C=CC=C4)=N2
SB-216385	PKIS1	Nc1nccc(n1)-c1c(ncn1CCCN1CCOCC1)-c1ccc(F)cc1
SB-217146-A	PKIS2	CSC1=NC=CC(C(N(CCCN2CCOCC2)C=N3)=C3C4=CC=C(F)C=C4)=N1.Cl
SB-217360	PKIS2	FC1=CC=C(C=C1)C(N=CN2)=C2C3=CC=NC=C3
SB-217780	PKIS2	FC(F)(F)C1=CC=C(C=C1)C2=C(C3=CC=NC=C3)N(CCCN4CCOCC4)C=N2
SB-219952	PKIS2	NC1=NC(C(N(C=N2)C(CC3)CCN3C(OCC)=O)=C2C4=CC=C(F)C=C4)=CC=N1

Compound	Library	SMILES
SB-219980	PKIS2	NC1=NC(C(N(C=N2)C(CC3)CCN3CC4=CC=CC=C4)=C2C5=CC=C(F)C=C5)=CC=N1
SB-220025-A	PKIS1	Cl.Nc1nccc(n1)-c1c(ncn1C1CCNCC1)-c1ccc(F)cc1
SB-220455	PKIS1	CN1CCC(CC1)n1cnc(c1-c1ccnc(N)n1)-c1ccc(F)cc1
SB-221466	PKIS1	CC1(C)CC(CC(C)(C)N1)n1cnc(c1-c1ccnc(N)n1)-c1ccc(F)cc1
SB-222516	PKIS2	CNC1=NC=CC(C(N(CCCN2CCOCC2)C=N3)=C3C4=CC=C(F)C=C4)=N1
SB-222517	PKIS2	CC1=CC(C(N(CCCN2CCOCC2)C=N3)=C3C4=CC=C(F)C=C4)=NC(N)=N1
SB-222903	PKIS2	CNC1=NC(C(N2C(CC3)CCN3C)=C(N=C2)C(C=C4)=CC=C4F)=CC=N1
SB-223132	PKIS2	NC1=NC(C(N(C=N2)C(CC3)CCN3C(C)C)=C2C4=CC=C(F)C=C4)=CC=N1
SB-223133	PKIS1	Nc1nccc(n1)-c1c(ncn1C1CCC(O)CC1)-c1ccc(F)cc1
SB-226605	PKIS2	FC1=CC=C(C=C1)C(N=C2)=C(C3=NC(NCC)=NC=C3)N2C(CC4)CCN4C
SB-226879	PKIS1	CN1CCC(CC1)n1cnc(c1-c1ccnc(NCCO)n1)-c1ccc(F)cc1
SB-229482	PKIS2	FC1=CC=C(C=C1)C(N=C2)=C(C3=NC(NC4CCNCC4)=NC=C3)N2C(CC5)CCN5C
SB-236560	PKIS2	NC1=NC=CC(C(N(C=N2)C(CC3)CCN3CC(F)(F)F)=C2C4=CC=C(F)C=C4)=N1
SB-236687	PKIS1	CN1CCC(CC1)n1cnc(c1-c1ccnc(Nc2ccccc2)n1)-c1ccc(F)cc1
SB-238039-R	PKIS2	FC1=CC=C(C=C1)C(N=C2)=C(C3=NC(NC4=CC=CC=C4)=NC=C3)N2C5CCNCC5.FC6=CC=C(C=C6)C(N=C7)=C(C8=NC(NC9=CC=CC=C9)=NC=C8)N7C%10CCNCC%10.Cl.Cl.Cl
SB-239272	PKIS1	Fc1ccc(cc1)-c1ncn(C2CCNCC2)c1-c1ccnc(Oc2ccccc2)n1
SB-242717	PKIS1	Fc1ccc(Oc2nccc(n2)-c2c(ncn2C2CCNCC2)-c2ccc(F)cc2)cc1
SB-242718	PKIS1	NC(=O)c1ccc(Oc2nccc(n2)-c2c(ncn2C2CCNCC2)-c2ccc(F)cc2)cc1
SB-242719	PKIS1	CCc1ccc(Oc2nccc(n2)-c2c(ncn2C2CCNCC2)-c2ccc(F)cc2)cc1
SB-242721	PKIS1	Fc1ccc(cc1)-c1ncn(C2CCNCC2)c1-c1ccnc(Oc2ccc(cc2)C#N)n1
SB-245391	PKIS2	FC1=CC=C(C=C1)C(N=C2)=C(C3=NC(OC4=CC=C(C5=CC=CC=C5)C=C4)=NC=C3)N2C6CCNCC6
SB-245392	PKIS1	Fc1ccc(cc1)-c1ncn(C2CCNCC2)c1-c1ccnc(Oc2ccc(Oc3ccccc3)cc2)n1
SB-249175	PKIS2	FC1=CC=C(C=C1)C(N=C2)=C(C3=NC(OCC)=NC=C3)N2C4CCNCC4
SB-250715	PKIS1	Fc1ccc(cc1)-c1ncn(C2CCNCC2)c1-c1ccnc(Oc2ccc3OCOc3c2)n1
SB-251505	PKIS1	Fc1ccc(cc1)-c1ncn(C2CCNCC2)c1-c1ccnc(Oc2cccc(F)c2)n1
SB-251527	PKIS1	COc1ccccc1Oc1nccc(n1)-c1c(ncn1C1CCNCC1)-c1ccc(F)cc1
SB-253226	PKIS1	Fc1ccc(cc1)-c1ncn(C2CCNCC2)c1-c1ccnc(Oc2cccc(c2)C(F)(F)F)n1
SB-253228	PKIS1	Fc1ccc(cc1)-c1ncn(C2CCNCC2)c1-c1ccnc(Oc2ccc(F)c(F)c2)n1
SB-254169	PKIS1	CS(=O)(=O)c1ccc(Oc2nccc(n2)-c2c(ncn2C2CCNCC2)-c2ccc(F)cc2)cc1
SB-264865	PKIS1	NC(=O)Cc1ccccc1Oc1nccc(n1)-c1c(ncn1C1CCNCC1)-c1ccc(F)cc1
SB-264866	PKIS1	NC(=O)CCc1ccccc1Oc1nccc(n1)-c1c(ncn1C1CCNCC1)-c1ccc(F)cc1
SB-278538	PKIS1	CC(C)(C)c1ccc(Oc2nccc(n2)-c2c(ncn2C2CCNCC2)-c2ccc(F)cc2)cc1
SB-278539	PKIS1	Fc1ccc(cc1)-c1ncn(C2CCNCC2)c1-c1ccnc(Oc2ccc(Cl)cc2)n1
SB-282852	PKIS2	COC1=NC=CC(C(N(CCCN2CCOCC2)C=N3)=C3C4=CC=C(F)C=C4)=N1
SB-282975-A	PKIS2	CC1=NC=CC(C(N(CCCN2CCOCC2)C=N3)=C3C(C=C4)=CC=C4F)=N1.Cl
SB-284847-BT	PKIS1	OC(=O)C(F)(F)F.Cc1cccc(Oc2nccc(n2)-c2c(ncn2C2CCNCC2)-c2ccc(F)cc2)c1C
SB-284851-BT	PKIS2	FC1=CC=C(C=C1)C(N=C2)=C(C3=NC(OC4=CC(C)=CC(C)=C4)=NC=C3)N2C5CCNCC5.OC(C(F)(F)F)=O.FC6=CC=C(C=C6)C(N=C7)=C(C8=NC(OC9=CC(C)=CC(C)=C9)=NC=C8)N7C%10CCNCC%10.OC(C(F)(F)F)=O.OC(C(F)(F)F)=O
SB-284852-BT	PKIS2	FC1=CC=C(C=C1)C(N=C2)=C(C3=NC(OC4=C(C)C=CC(C)=C4)=NC=C3)N2C5CCNCC5.OC(C(F)(F)F)=O.FC6=CC=C(C=C6)C(N=C7)=C(C8=NC(OC9=C(C)C=CC(C)=C9)=NC=C8)N7C%10CCNCC%10.OC(C(F)(F)F)=O.OC(C(F)(F)F)=O

Compound	Library	SMILES
SB-285234-W	PKIS1	[Li+].[O-]C(=O)c1ccc(Oc2nccc(n2)-c2c(ncn2C2CCNCC2)-c2ccc(F)cc2)cc1
SB-300079	PKIS2	O=C(N1C)C(C2=CC=CC=C2)=C(NC3=CC=CC=C3)C1=O
SB-317651	PKIS2	O=C(N1)C(C(C=C2)=CC=C2Cl)=C(C1=O)NC3=CC(Cl)=CC=C3
SB-317658	PKIS2	O=C(N1)C(C(C=C2)=CC=C2Cl)=C(C1=O)NC(C=C3)=CC=C3SC
SB-317661	PKIS2	O=C(N1)C(C(C=C2)=CC=C2Cl)=C(C1=O)NC3=CC=CC=C3
SB-326892	PKIS2	O=C(N1)C(C(C=C2)=CC=C2OC)=C(C1=O)NC3=CC=CC(Cl)=C3
SB-331032	PKIS2	O=C(N1)C(C2=CC(OC)=CC=C2)=C(C1=O)NC(C=C3)=CC=C3SC
SB-333612	PKIS1	Clc1ccc(cc1)C1=C(N2CCc3ccccc23)C(=O)NC1=O
SB-333613	PKIS2	O=C(N1)C(C(C=C2)=CC=C2Cl)=C(C1=O)NC3=CC(O)=CC=C3
SB-334860	PKIS2	O=C(N1)C(C2=CC=CC=C2)=C(C1=O)N(C)C3=CC=CC=C3
SB-334865	PKIS2	O=C(N1)C(C2=CC(OC)=CC=C2)=C(C1=O)N(C)C3=CC=CC=C3
SB-340867	PKIS2	O=C(N1)C(C(C=C2)=CC=C2Cl)=C(C1=O)NC3=CC=C(O)C=C3
SB-341528	PKIS2	O=C(N1)C(C2=CC(Cl)=CC=C2)=C(C1=O)NC(C=C3)=CC=C3SC
SB-341556	PKIS2	O=C(N1)C(C2=CC(OC)=CC=C2)=C(C1=O)NC3=CC=CC(Cl)=C3
SB-342409	PKIS2	O=C(N1)C(C2=C(Cl)C=CC=C2)=C(C1=O)NC3=CC(Cl)=CC=C3
SB-342411	PKIS2	O=C(N1)C(C2=C(Cl)C=CC=C2)=C(C1=O)NC(C=C3)=CC=C3SC
SB-347804	PKIS1	Fc1ccc(cc1)C(=O)Nc1sc2CCCCc2c1C#N
SB-358518	PKIS1	Oc1c(Cl)cc(NC2=C(C(=O)NC2=O)c2cccc(c2)N(=O)=O)cc1Cl
SB-360737	PKIS2	O=C(N1)C(C(C=C2)=CC=C2Cl)=C(C1=O)NC3=CC=CC(C(O)=O)=C3
SB-360741	PKIS1	OC(=O)c1cc(NC2=C(C(=O)NC2=O)c2ccc(Cl)cc2)ccc1Cl
SB-361058	PKIS1	COc1ccc(cc1)C1=C(N2CCc3ccccc23)C(=O)NC1=O
SB-373598	PKIS2	O=C(N1)C(N(CC2)C3=C2C=CC=C3)=C(C1=O)C4=C(Cl)C=CC=C4
SB-376715	PKIS2	O=C(N1)C(C2=C(Cl)C=CC=C2)=C(C1=O)NC3=CC=CC=C3
SB-376719	PKIS1	COc1ccccc1C1=C(Nc2ccccc2)C(=O)NC1=O
SB-381891	PKIS2	O=C(N1)C(C2=C(OC)C=CC=C2)=C(C1=O)NC3=CC(O)=CC=C3
SB-381904	PKIS2	O=C(N1)C(C2=C(OC)C=CC=C2)=C(C1=O)NC(C=C3)=CC(Cl)=C3O
SB-386023-B	PKIS2	OC1=CC(C(N=C2C3=CC=CC=C3)=C(N2)C4=CC=NC=C4)=CC=C1Cl.OC5=CC(C(N=C6C7=CC=CC=C7)=C(N6)C8=CC=NC=C8)=CC=C5Cl.Cl.Cl
SB-390523	PKIS1	Oc1c(Cl)cc(NC2=C(C(=O)NC2=O)c2ccccc2Cl)cc1Cl
SB-390526	PKIS2	O=C(N1)C(C2=C(Cl)C=CC=C2)=C(C1=O)NC3=CC=CC(C(O)=O)=C3
SB-390527	PKIS1	Oc1cccc(NC2=C(C(=O)NC2=O)c2ccccc2Cl)c1
SB-390530	PKIS2	O=C(N1)C(C2=CC=CC=C2)=C(C1=O)NC3=CC(Cl)=C(O)C(Cl)=C3
SB-390532	PKIS2	O=C(N1)C(C2=CC=CC=C2)=C(C1=O)NC3=CC=C(Cl)C(C(O)=O)=C3
SB-390534	PKIS2	O=C(N1)C(NC2=CC=CC(O)=C2)=C(C1=O)C3=CC=CC=C3
SB-390765	PKIS2	O=C(N1)C(C(C=C2)=CC=C2OC)=C(C1=O)NC3=CC=CC(C(O)=O)=C3
SB-390766	PKIS2	O=C(N1)C(C(C=C2)=CC=C2OC)=C(C1=O)NC3=CC=CC(O)=C3
SB-390767	PKIS2	O=C(N1)C(NC2=CC(Cl)=C(O)C(Cl)=C2)=C(C1=O)C3=CC(OC)=CC=C3
SB-390769	PKIS2	O=C(N1)C(C2=CC(OC)=CC=C2)=C(C1=O)NC3=CC=C(Cl)C(C(O)=O)=C3
SB-390770	PKIS2	O=C(N1)C(C2=CC(OC)=CC=C2)=C(C1=O)NC3=CC=CC(C(O)=O)=C3
SB-390771	PKIS2	O=C(N1)C(C2=CC(OC)=CC=C2)=C(C1=O)NC3=CC=CC(O)=C3
SB-400868-A	PKIS1	Cl.C1Cc2nc(c(-c3ccc4OCOc4c3)n2C1)-c1ccccn1
SB-404290	PKIS2	O=C(N1C)C(C(C=C2)=CC=C2Cl)=C(C1=O)NC(C=C3)=CC(C(O)=O)=O)=C3Cl
SB-404321	PKIS2	O=C(N1C)C(C(C=C2)=CC=C2Cl)=C(NC(C=C3Cl)=CC(Cl)=C3O)C1=O
SB-405367	PKIS2	O=C(N1)C(C(C=C2)=CC=C2Cl)=C(C1=O)NC3=CC=C(O)C(Cl)=C3

Compound	Library	SMILES
SB-408010	PKIS2	O=C(N1)C(N(CC2)C3=C2C=CC=C3)=C(C1=O)C4=CC(Cl)=CC=C4
SB-409513	PKIS1	OC(=O)c1cc(NC2=C(C(=O)NC2=O)c2cccc(Cl)c2)ccc1Cl
SB-409514	PKIS1	Oc1ccc(NC2=C(C(=O)NC2=O)c2cccc(Cl)c2)cc1Cl
SB-428218-A	PKIS2	OC1=CC=C(C=C1)C(N=C2C3=CC=CC=C3)=C(N2)C4=CC=NC=C4.Cl
SB-431533	PKIS1	OCc1ccc(cc1)-c1nc(c([nH]1)-c1ccc2OCOc2c1)-c1ccccn1
SB-431542-A	PKIS1	Cl.NC(=O)c1ccc(cc1)-c1nc(c([nH]1)-c1ccc2OCOc2c1)-c1ccccn1
SB-437013	PKIS1	COc1ccc2cc(ccc2c1)-c1c(nc(-c2ccc(cc2)S(C)=O)n1C)-c1ccncc1
SB-476429-A	PKIS1	Cl.NCc1ccc(cc1)-c1nc(c([nH]1)-c1ccncc1)-c1ccc(Cl)c(O)c1
SB-477794-AAA	PKIS2	OC1=CC(C(N=C2C(C)(C)CN)=C(N2)C3=CC=NC=C3)=CC=C1Cl.OC(C(F)(F)F)=O
SB-517081	PKIS2	Nc1n[nH]c2ncc(cc12)-c1ccccc1
SB-517389	PKIS2	NC1=NNC(N=N2)=C1C=C2C3=CC=CC=C3
SB-548492	PKIS2	CC(NC1=NNC2=NC=C(C3=CC=CC=C3)C=C21)=O
SB-589132	PKIS2	NC1=NC=NC2=C1C(C(C=C3)=CC=C3OC)=C(C4=CC=C(OC)C=C4)O2
SB-590885	KCGS	CN(C)CCOC1=CC=C(C2=NC(C3=CC=C4/C(CCC4=C3)=N\O)=C(C5=CC=NC=C5)N2)C=C1
SB-590885-AAD	PKIS1	O.Cl.CN(C)CCOc1ccc(cc1)-c1nc(c([nH]1)-c1ccc2c(CC\C2=N/O)c1)-c1ccncc1
SB-601273	PKIS2	O=C1C(C2=C(Cl)C=CC=C2Cl)=CC3=CN=C(NC(C=C4)=CC=C4OCCN(CC)CC)N=C3N1C
SB-601436	PKIS2	O=C(CCC)NC1=NNC2=NC=CC=C12
SB-610250	PKIS2	COC1=CC(C(N=C2C3=CC=CC=C3)=C(N2)C4=CC=NC=C4)=CC=C1
SB-610251-B	PKIS1	Cl.Oc1cccc(c1)-c1nc([nH]c1-c1ccncc1)-c1ccccc1
SB-614067-R	PKIS1	Cl.ON=C1CCc2cc(ccc12)-c1nc([nH]c1-c1ccncc1)C1CCNCC1
SB-625086-M	PKIS2	CN1C(C2=CC3=CC=C(OC)C=C3C=C2)=C(C4=CC=NC=C4)N=C1C(C=C5)=C(C)C=C5SC.OC(C(F)(F)F)=O
SB-627772-A	PKIS2	O=C(CCCN(C)C)NC1=NNC2=NN=C(C3=CC=CC=C3)C=C21.Cl
SB-630812	PKIS1	COc1ccc2cc(ccc2c1)-c1c(nc(-c2ccc(cc2C)S(C)=O)n1C)-c1ccncc1
SB-633825	PKIS1	COc1ccc2cc(ccc2c1)-c1c(nc(-c2ccc(cc2C)S(C)(=O)=O)n1C)-c1ccncc1
SB-642057	PKIS2	O=C(CCC)NC1=NNC2=NC=C(C3=C(C=CC=C4)C4=CC=C3)C=C21
SB-642124-AAA	PKIS2	NC1=NNC2=CN=C(C3=CC=CC=C3)C=C21
SB-657836-AAA	PKIS1	OC(=O)C(O)=O.O=C(CN1CCOCC1)Nc1sc2CCCCc2c1C#N
SB-660566	PKIS2	CC(C)C1=C(C=CC=C1)C2=NC(C3=CC4=CC=C(OC)C=C4C=C3)=C(C5=CC=NC=C5)N2
SB-675259-M	PKIS1	OC(=O)C(F)(F)F.O=C(Nc1n[nH]c2nnc(cc12)-c1cccnc1)C1CC1
SB-678557-A	PKIS1	Cl.CN1CCC(CC1)C(=O)Nc1n[nH]c2nnc(cc12)-c1ccccc1
SB-682330-A	PKIS1	Cl.CN(C)CCOc1ccc(cc1)-c1cc(c(o1)-c1ccncc1)-c1ccc2C(CCc2c1)=NO
SB-684387-B	PKIS2	OC1=CC(C(C=C2C(C=C3)=CC=C3OCCN(C)C)=C(N2)C4=CC=NC=C4)=CC=C1Cl.OC5=CC(C(C=C6C(C=C7)=CC=C7OCCN(C)C)=C(N6)C8=CC=NC=C8)=CC=C5Cl.Cl.Cl
SB-686709-A	PKIS1	Cl.CCN1CCC(CC1)C(=O)Nc1n[nH]c2nnc(cc12)-c1cccc(F)c1F
SB-693162	PKIS2	NC1=NON=C1C2=NC3=C(C=CC=C3)N2CC
SB-693578	PKIS2	C1(C(C2=CC=CC=C2)=CC=N3)=C3NC=C1
SB-698596-AC	PKIS1	O[C@H]([C@@H](O)C(O)=O)C(O)=O.CCN1CCC(CC(=O)Nc2n[nH]c3nnc(cc23)-c2cccc(F)c2F)CC1
SB-708998	PKIS2	BrC1=C(C2=CC=CC=C2)N=C3C(C(NC(C4CC4)=O)=NN3)=C1
SB-708999	PKIS2	O=C(C1CC1)NC2=NNC3=NC(C4=CC=CC=C4)=CC=C32
SB-710363	PKIS2	O=C(C1CC1)NC2=NNC3=NC(C(C=C4)=CC=C4O)=CC=C32
SB-710397	KCGS	CN(C)CCN(C)C(=O)c1cc(c(o1)-c1ccc(Cl)c(O)c1)-c1ccncc1

Compound	Library	SMILES
SB-710397-B	PKIS2	OC1=CC(C(OC(C(N(C)CCN(C)C)=O)=C2)=C2C3=CC=NC=C3)=CC=C1Cl.OC4=CC(C(OC(C(N(C)CCN(C)C)=O)=C5)=C5C6=CC=NC=C6)=CC=C4Cl.Cl.Cl
SB-710903	PKIS2	O=C(C1CC1)NC2=NNC3=C2C=CC(C4=CC(OC)=CC=C4)=N3
SB-711237	PKIS1	COc1ccc(cc1)-c1ccc2c(NC(=O)C3CC3)n[nH]c2n1
SB-711239	PKIS2	COc1ccccc1-c1ccc2c(NC(=O)C3CC3)n[nH]c2n1
SB-711805	PKIS2	O=C(C1CC1)NC2=NNC3=C2C=CC(C4=CC(O)=CC=C4)=N3
SB-711880	PKIS2	O=C(C1CC1)NC2=NNC3=C2C=CC(C4=C(O)C=CC=C4)=N3
SB-725317	PKIS1	Oc1ccc(cc1)-c1nc2[nH]nc(NC(=O)C3CC3)c2cc1Br
SB-731254-M	PKIS2	NC1=C2C(C(C=C3)=CC=C3NC(CC4=CC(F)=CC=C4F)=O)=CSC2=NC=N1.OC(C(F)(F)F)=O
SB-731284	PKIS2	O=C(C1CC1)NC2=NNC3=CC(C4=CC=CS4)=CC=C32
SB-731579	PKIS2	BrC1=C(C(C=C2)=CC=C2O)N=C3C(C(NC(CCCN(CC4)CCN4CC)=O)=NN3)=C1
SB-732881	PKIS1	CN1CCC(CC1)C(=O)Nc1n[nH]c2nc(-c3ccc(O)cc3)c(Br)cc12
SB-732881-H	PKIS1	OC(=O)\C=C/C(O)=O.CN1CCC(CC1)C(=O)Nc1n[nH]c2nc(-c3ccc(O)cc3)c(Br)cc12
SB-732932	PKIS2	O=C(Nc1n[nH]c2cc(ccc12)-c1ccsc1)C1CC1
SB-732941	PKIS1	O=C(Nc1n[nH]c2cc(ccc12)-c1ccccc1)C1CC1
SB-733371	PKIS2	O=C(C1CC1)NC2=NNC3=CC(C4=CC=CC=C4F)=CC=C32
SB-733416	PKIS2	CCN1C(C2=CC=CC=C2)=NC3=CN=CC=C13
SB-733887	PKIS2	CCN1C(C2=COC=C2)=NC3=CN=CC=C13
SB-733894	PKIS2	O=C(C1CC1)NC2=NNC3=CC(C4=CC=CC(F)=C4F)=CC=C32
SB-734117	PKIS1	Nc1nonc1-c1nc2cnccc2n1C1CCCCC1
SB-734909	PKIS2	ClC1=C(C2=CC=CC=C2)N=C3C(C(NC(C4CC4)=O)=NN3)=C1
SB-735216	PKIS2	CCN1C(C2=CC=NC=C2)=NC3=CN=CC=C13
SB-735297	PKIS2	BrC1=C(C2=CC=CS2)N=C3C(C(NC(C4CC4)=O)=NN3)=C1
SB-735464	PKIS2	O=C(C1CC1)NC2=NNC3=C2C=CC(C4=CC(F)=CC=C4)=C3
SB-735465	PKIS1	Fc1ccc(F)c(c1)-c1ccc2c(NC(=O)C3CC3)n[nH]c2c1
SB-735467	PKIS1	Fc1ccc(cc1)-c1ccc2c(NC(=O)C3CC3)n[nH]c2c1
SB-736290	PKIS1	Cn1c(nc2cnccc12)-c1nonc1N
SB-736302	PKIS1	Nc1nonc1-c1nc2cnccc2n1C1CC1
SB-736398	PKIS2	CCN1C(C2=CC=CC=N2)=NC3=CN=CC=C13
SB-736715	PKIS2	CCN1C(C2=C(O)N=CC=C2)=NC3=CN=CC=C13
SB-737198	PKIS1	CCOc1nccc2n(CC)c(nc12)-c1nonc1N
SB-737447	PKIS2	O=C(C1CC1)NC2=NNC3=CC(C4=CC=CO4)=CC=C32
SB-737856	PKIS2	NC1=NOC(C)=C1C2=NC3=CN=CC=C3N2CC
SB-738004	PKIS2	BrC1=C2N(CC)C(C3=NON=C3N)=NC2=CN=C1
SB-738481	PKIS2	O=C(C1CC1)NC2=NNC3=CC(C4=COC=C4)=CC=C32
SB-738482	PKIS1	NS(=O)(=O)c1ccc(cc1)-c1ccc2c(NC(=O)C3CC3)n[nH]c2c1
SB-738561	PKIS1	CCn1c(nc2ccncc12)-c1nonc1N
SB-739245-AC	PKIS1	O[C@H]([C@@H](O)C(O)=O)C(O)=O.CCN1CCC(CC(=O)Nc2n[nH]c3nc(-c4cccs4)c(Br)cc23)CC1
SB-739452	PKIS1	Brc1cc2c(NC(=O)C3CC3)n[nH]c2nc1-c1ccco1
SB-741905	PKIS1	NS(=O)(=O)c1cccc(c1)-c1ccc2c(NC(=O)C3CC3)n[nH]c2c1
SB-742034-AC	PKIS2	BrC1=C(C2=CC=CO2)N=C3C(C(NC(C(CC4)CN4CC5=CC=CC=C5)=O)=NN3)=C1.O[C@@H](C(O)=O)[C@H](C(O)=O)O
SB-742251	PKIS2	BrC1=C(C2=NC=CS2)N=C3C(C(NC(C4CC4)=O)=NN3)=C1

Compound	Library	SMILES
SB-742352-AC	PKIS2	BrC1=C(C2=CC=CO2)N=C3C(C(NC(C(C=C4)=CC=C4CN5CCCC5)=O)=NN3)=C1.O[C@@H](C(O)=O)[C@H](C(O)=O)O
SB-742609	PKIS2	BrC1=C(C2=NC=CS2)N=C3C(C(NC(C4CCCC4)=O)=NN3)=C1
SB-742864	PKIS1	CS(=O)(=O)Nc1cccc(c1)-c1ccc2c(NC(=O)C3CC3)n[nH]c2c1
SB-742865	PKIS1	CS(=O)(=O)Nc1ccc(cc1)-c1ccc2c(NC(=O)C3CC3)n[nH]c2c1
SB-743341	PKIS2	BrC1=C(C2=CC=CS2)N=C3C(C(NC(C4CCCC4)=O)=NN3)=C1
SB-743899	PKIS1	O=C(Nc1n[nH]c2nc(ccc12)-c1ccco1)C1CC1
SB-744941	PKIS1	CCn1c(nc2c(nccc12)N1CCCC1)-c1nonc1N
SB-747651A	KCGS	NC1=NON=C1C(N2CC)=NC3=C2C(CNC4CCNCC4)=CN=C3
SB-750140	PKIS1	NCc1ccc(cc1)-n1c(nc2cnccc12)-c1nonc1N
SB-750250-M	PKIS2	CN1N=C(C(C=C2)=CC(F)=C2NC(NC3=CC=C4C(C=CC=C4)=C3)=O)C(C=N5)=C1N=C5NCCN6CCOCC6.OC(C(F)(F)F)=O
SB-751148	PKIS1	CCc1nccc2n(CC)c(nc12)-c1nonc1N
SB-751399-B	PKIS1	CN(C)CCCn1c(nc2cnccc12)-c1nonc1N
SB-759335-B	PKIS1	Cl.CCn1c(nc2cncc(C(=O)N3CCNCC3)c12)-c1nonc1N
SB-772077-B	PKIS1	Cl.CCn1c(nc2cncc(C(=O)N3CC[C@H](N)C3)c12)-c1nonc1N
SB-814597	PKIS1	Fc1ccc(C(=O)Nc2sc3CCCCc3c2C#N)c2ccccc12
SGC-AAK1-1	KCGS	O=S(N(CC)CC)(NC1=CC(C2=CC3=C(C(NC(C4CC4)=O)=NN3)C=C2)=CC=C1)=O
SKF-104365	PKIS2	FC1=CC=C(C=C1)C(N(CCS2)C2=N3)=C3C4=NC=CC=C4
SKF-104493-B2	PKIS2	COC1=CC=C(C=C1)C2=C(C3=CC=NC=C3)N(CCC4)C4=N2.OS(O)(=O)=O.COC5=CC=C(C=C5)C6=C(C7=CC=NC=C7)N(CCC8)C8=N6.OS(O)(=O)=O
SKF-105561	PKIS2	CSC1=CC=C(C=C1)C2=C(C3=CC=NC=C3)N(CCC4)C4=N2
SKF-105942	PKIS2	CS(C1=CC=C(C=C1)C2=C(C3=CC=NC=C3)N(CCC4)C4=N2)(=O)=O
SKF-106164-A2	PKIS2	CCSC1=CC=C(C=C1)C2=C(C3=CC=NC=C3)N(CCC4)C4=N2.CCSC5=CC=C(C=C5)C6=C(C7=CC=NC=C7)N(CCC8)C8=N6.Cl.Cl
SKF-12778	PKIS2	NC1=NC(N)=NC(N2)=C1N=C2C3=CC=CC=C3
SKF-18267	PKIS2	NC1=NC=NC2=C1C=NN2C
SKF-18355	PKIS2	CNC1=NC=NC2=C1C=NN2
SKF-31736	PKIS2	CN(C)C1=NC=NC2=C1NC=N2
SKF-62604	PKIS1	O=C1NC(=O)C(=C1Nc1ccccc1)c1ccccc1
SKF-86002-A2	PKIS1	Cl.Fc1ccc(cc1)-c1nc2SCCn2c1-c1ccncc1
SKF-86055	PKIS1	Fc1ccc(cc1)-c1c(nc2SCCn12)-c1ccncc1
SKF-96418	PKIS2	CCN1C2=C(N=C1)C(NCC3=CC=CC=C3)=NC=N2
SKF-97184	PKIS2	NC1=NC=NC2=C1N=CN2C3=CC=CC4=C3C=CC=C4
SKF-97236	PKIS2	NC1=NC=NC2=C1N=CN2C(C=C3)=CC=C3OC
SKF-97255	PKIS2	NC1=NC=NC2=C1N=C(CCCCC)N2CCCCC
SKF-97263	PKIS2	NC1=NC=NC2=C1N=CN2C(C=C3)=CC=C3C(C)(C)C
SKF-97293	PKIS2	NC1=NC=NC2=C1N=C(C3=CC=CC=C3)N2C4=CC=CC=C4
SKF-97359	PKIS2	NC1=NC=NC2=C1N=CN2C(C)(C)C
SKF-97416	PKIS2	NC1=NC=NC2=C1N=CN2C3=CC=CC(OC)=C3
SKF-97510	PKIS2	CC1=C(C=CC=C1)N(C=N2)C3=C2C(N)=NC=N3
SKF-97560	PKIS2	NC1=NC=NC2=C1N=CN2C3=CC(F)=CC=C3
SKF-97620	PKIS2	CCC(CC)(CC)N(C=N1)C2=C1C(N)=NC=N2
SKF-97623	PKIS2	NC1=NC=NC2=C1N=CN2C
Sorafenib	Clinical KIs	CNC(=O)c1cc(Oc2ccc(NC(=O)Nc3ccc(Cl)c(c3)C(F)(F)F)cc2)ccn1

Appendix

Compound	Library	SMILES
Sunitinib	Clinical KIs	CCN(CC)CCNC(=O)c1c(C)[nH]c(\C=C\2/C(=O)Nc3ccc(F)cc23)c1C
TH257	KCGS	O=C(N(CCCC)CC1=CC=CC=C1)C(C=C2)=CC=C2S(NC3=CC=CC=C3)(=O)=O
THZ1	KCGS	ClC1=CN=C(N=C1C2=CNC3=CC=CC=C23)NC4=CC=CC(NC(C5=CC=C(NC(/C=C/CN(C)C)=O)C=C5)=O)=C4
THZ531	KCGS	CN(C)C\C=C\C(=O)NC1=CC=C(C=C1)C(=O)N1CCC[C@H](C1)NC1=NC=C(Cl)C(=N1)C1=CNC2=CC=CC=C12
Tivozanib	Clinical KIs	COc1cc2nccc(Oc3ccc(NC(=O)Nc4cc(C)on4)c(Cl)c3)c2cc1OC
Tofacitinib	Clinical KIs	C[C@@H]1CCN(C[C@@H]1N(C)c2ncnc3[nH]ccc23)C(=O)CC#N
TPKI-100	KCGS	COC(=O)C1=C(C2=CC=CC=C2)C2=CC(Br)=CC=C2C(=O)N1CC1=CC=C(C=C1)S(C)(=O)=O
TPKI-105	KCGS	CCC(=O)C1=C(C2=CC=CC=C2)C2=CC(Cl)=CC=C2C(=O)N1CC1=NN(CC(N)=O)C(=C1)S(C)(=O)=O
TPKI-106	KCGS	CCC1=NC(=C(S1)C1=CC=NC=C1)C1=CC(C)=CC=C1
TPKI-16	KCGS	Cn1c2ncn(OC[C@H](O)CO)c(=O)c2c(Nc3ccc(I)cc3F)c(F)c1=O
TPKI-24	KCGS	COc1cc(ccc1Nc2ncc3N(C)C(=O)C(F)(F)CN(C4CCCC4)c3n2)C(=O)NC5CCN(C)CC5
TPKI-26	KCGS	CC[C@]1(F)CN(C2CCCC2)c3nc(Nc4ccc(cc4OC)C(=O)NC5CCN(C)CC5)ncc3N(C)C1=O
TPKI-39	KCGS	O=C(NC1=CC=CC=C1)NC1=CC=CC(OC2=NN3C=CN=C3C=C2)=C1
TPKI-58	KCGS	CC(C)(C)C1=CC=C(C=C1)C(=O)NC1=CN2C=C(C=CC2=N1)C1=CC=CN=C1
TPKI-69	KCGS	CN1C=CC2=C1C(OC1=CC=C(NC(=O)NC3=CC=CC=C3)C=C1)=NC=N2
TPKI-72	KCGS	CN1C=CC2=C1C(OC1=CC=C(NC3=NC4=C(N3)C=CC=C4)C=C1)=NC=N2
TPKI-85	KCGS	CC1=NN=C(N1)C1=CC=C2OC=C(C2=C1)C1=CC=C(C=C1)S(C)=O
TPKI-91	KCGS	COC1=CC=C(CSC2=NN=C(O2)C2=CC3=C(C=C2)N=CS3)C=C1C(F)(F)F
TPKI-97	KCGS	COC(=O)C1=C(C2=CC=CC=C2)C2=CC(OC)=CC=C2C(=O)N1CC1=CC=CC=C1
Trametinib	Clinical KIs	CN1C(=O)C(=C2N(C(=O)N(C3CC3)C(=O)C2=C1Nc4ccc(I)cc4F)c5cccc(NC(=O)C)c5)C
TX-85-1	KCGS	CC(=O)N1CCN(CC1)C2CCC(CC2)N3C4=C(C(=N3)C5=CC(=C(C=C5)OC6=CC=CC=C6)NC(=O)C=C)C(=NC=N4)N
UNC-AA-1-0017	KCGS	O=S(N(C)CC)(NC1=CC(C2=CC3=C(C(NC(C4CC4)=O)=NN3)C=C2)=CC=C1)=O
Vandetanib	Clinical KIs	COc1cc2c(Nc3ccc(Br)cc3F)ncnc2cc1OCC4CCN(C)CC4
VE-821	KCGS	NC1=C(C(N([H])C2=CC=CC=C2)=O)N=C(C3=CC=C(S(=O)(C)=O)C=C3)C=N1
VE-822	KCGS	CC(C)S(=O)(=O)C1=CC=C(C=C1)C2=CN=C(C(=N2)C3=CC(=NO3)C4=CC=C(C=C4)CNC)N
Vemurafenib	Clinical KIs	CCCS(=O)(=O)Nc1ccc(F)c(C(=O)c2c[nH]c3ncc(cc23)c4ccc(Cl)cc4)c1F
Vertex11e	KCGS	[H]N1C(C(N[C@H](CO)C2=CC=CC(Cl)=C2)=O)=CC(C3=NC(NC4=C(Cl)C=C(F)C=C4)=NC=C3C)=C1
WZ4003	KCGS	CN(CC3)CCN3C(C=C2)=CC(OC)=C2NC1=NC=C(Cl)C(OC4=CC(NC(CC)=O)=CC=C4)=N1
XMD-17-51	KCGS	CN(C1=CN=C(NC2=CN(C3CCNCC3)N=C2)N=C1N(C)C4=C5C=CC=C4)C5=O
XMD8-87	KCGS	O=C1C2=C(C=CC=C2)N(C)C3=NC(N(C4=C(OC)C=C(N5CCN(C)CC5)C=C4)[H])=NC=C3N1
XMD8-92	KCGS	O=C1N(C)C2=CN=C(NC3=CC=C(N4CCC(O)CC4)C=C3OCC)N=C2N(C)C5=CC=CC=C15

Table S2 | List of analyzed clinical kinase inhibitors in in Results and Discussion Chapter 3. Clinical phase as of (March 2020)

Compound	Clinical Phase (March 2020)	Designated Target	PubChemCID	Supplier	Order #
Acalabrutinib	approved	BTK	71226662	Selleckchem	S8116
Amcasertib	Phase II	stemness kinases	25190990	MedChemExpress	HY-17602
AMG-337	Phase I	MET	44181686	Selleckchem	S8167
Anlotinib	Phase III	VEGFR2	25017411	Selleckchem	S8726
Asciminib	Phase III	ABL	72165228	MedChemExpress	HY-104010
Atuveciclib	Phase I	PTEFb, CDK9	71618220	Selleckchem	S8727
Avapritinib	approved	PDGFRa, KIT	118023034	Selleckchem	S8553
AZD3759	Phase II/III	EGFR	78209992	Selleckchem	S7971
BAY1125976	Phase I	AKT1/2	70817911	MedChemExpress	HY-100018
BAY1251152	Phase I	CDK9	74767009	MedChemExpress	HY-103019
BGB324	Phase II	AXL	46215462	Selleckchem	S2841
BGJ398	Phase III	FGFR1/2/3	53235510	Selleckchem	S2183
BMS-582949	Phase II	MAPK14	10409068	Selleckchem	S8124
Brigatinib	approved	ALK, ROS1	68165256	Selleckchem	S7000
CC-223	Phase II	MTOR	58298316	Selleckchem	S7886
CEP-37440	Phase I	FAK, ALK	71721648	Medchem Express	HY-15841
CFI-402257	Phase I/II	TTK, Mps1	118086034	MedChemExpress	HY-101340
CH5132799	Phase I	PIK3CA	49784945	Selleckchem	S2699
Derazantinib	Phase II	FGFR	46834118	MedChemExpress	HY-19981
Duvelisib	approved	PIK3CD, PIK3CG	50905713	Selleckchem	S7028
Entospletinib	Phase II	SYK	59473233	Selleckchem	S7523
Erdafitinib	approved	FGFR	67462786	Selleckchem	S8401
Evobrutinib	Phase II	BTK	71479709	MedChemExpress	HY-101215
Fenebrutinib	Phase II	BTK	86567195	MedChemExpress	HY-19834
Fruquintinib	Phase III	VEGFR	44480399	APExBIO	B5864
GDC-0349	Phase I	MTOR	59239165	Selleckchem	S8040
GDC-0623	Phase I	MEK1	42642654	Selleckchem	S7553
GSK2256098	Phase II	FAK	46214930	Medchem Express	HY-100498
Ipatasertib	Phase III	AKT	24788740	Selleckchem	S2808
IPI-549	Phase I	PIKCG	91933883	Medchem Express	HY-100716
Itacitinib	Phase III	JAK1	53380437	Medchem Express	HY-16997
JI-101	Phase I/II	VEGFR2, PDGFRb, EPHB4	11691242	Medchem Express	HY-16265
Larotrectinib	approved	TRK	46188928	Selleckchem	S7960
Leniolisib	Phase II/III	PIK3CD	57495353	MedChemExpress	HY-17635
Lorlatinib	approved	ALK, ROS1	71731823	MedChem Express	HY-12215
LY2090314	Phase II	GSK3	10029385	Selleckchem	S7063
LY3009120	Phase I	RAF	71721540	Selleckchem	S7842

Appendix

Compound	Clinical Phase (March 2020)	Designated Target	PubChemCID	Supplier	Order #
LY3023414	Phase II	PI3K, mTOR, PRKDC	57519748	Medchem Express	HY-12513
Olmutinib	Phase II	EGFR	54758501	MedChem Express	HY-19730
ONO-4059	Phase II	BTK	71571562	Medchem Express	HY-15771A
Palomid529	Phase I	MTORC1/2	11998575	Selleckchem	S2238
Peficitinib	approved (Japan)	JAK	57928435	Selleckchem	S7650
PIM447	Phase I	PIM	44814409	Medchem Express	HY-19322
PLX8394	Phase I/II	RAF	90116675	Medchem Express	HY-18972
Pyrotinib	Phase III	EGFR, HER2	51039030	MedChemExpress	HY-104065
Radotinib	Phase III	BCR-ABL1	16063245	Selleckchem	S8134
Rogaratinib	Phase II/III	FGFR	71611869	MedChemExpress	HY-100019
Selonsertib	Phase III	MAP3K5	71245288	Selleckchem	S8292
Semaxanib	Phase III	VEGFR	5329098	Selleckchem	S2845
Sulfatinib	Phase III	VEGFR, FGFR, CSF1R	52920501	MedChemExpress	HY-12297
TAK659	Phase II	SYK	53252276	MedChemExpress	HY-100867A
Taselisib	Phase III	PIK3	51001932	Selleckchem	S7103
Upadacitinib	approved	JAK	58557659	MedChemExpress	HY-19569
Zanubrutinib	approved	BTK	121413432	MedChemExpress	HY-101474A
ZSTK474	Phase I	PIK3	11647372	Selleckchem	S1072